IJERT

AMASE-2016

National Conference On Advances In Mathematics And Its Applications To Science And Engineering

22nd January, 2016

Organized by :

University College Of Engineering, Pattukkottai
Department Of Mathematics

Conference Proceedings

Published By

International Journal of Engineering Research and Technology
(www.ijert.org)

Effect of Corrosion Inhibitor on the Durability Properties of Hardened Self Compacting Concrete

R. Dharmaraj*
Department of Civil Engineering,
University College of Engineering Panruti,
Panruti-607106, Tamil Nadu, India.

R. Malathy
Department of Civil Engineering,
Sona College of Technology,
Salem-636005, Tamil Nadu, India.

***Abstract*— This paper presents the results of an experimental study on the durability properties of self compacting concrete (SCC) mixes. Self compacting concrete mixes with a higher cement replacement at 40% of cement with fly ash, are designed and their performance is compared with conventional concrete mixes (CC) of equivalent M25 strength grade. The durability properties are evaluated in terms of chloride-ion permeability as measured by RCPT tests. The results indicate that the SCC mixes would have lesser permeable voids than the conventional concrete mixes of comparable strengths. The experimental results also show that improvements against chloride penetration can be realized with self compacting concrete mixes additionally inhibitors with Hexamine and Diethanolamine.**

Keywords*— *Self compacting concrete; fly ash; chloride permeability; corrosion inhibitor; Durability.

I. INTRODUCTION

The development of a special form of concrete specifically self compacted concrete provides an opportunity to the contractors and changed the options open to the construction industry. The wide ranching interest in the development of self compacting concrete highlights the significance of this new type of concrete to modern day construction. The advances in admixture technology are refusal doubt helping the concrete producers towards achieve their target with ease. Apart from increasing the quality of concrete structures, the make use of self compacting concrete reduces the construction cost, all the way through minimizing the compaction effort and reducing the construction time.

The self compacting concrete differs as of conventional concrete in the following three characteristic features, that is to say, appropriate flow ability, non segregation, and no blocking tendency. An increase in the flow ability of concrete is well known to increase the risk of segregation. Therefore it is essential to have proper mix design.

Durability of concrete possibly will be defined as the ability of concrete to resist weathering action, chemical attack and abrasion while maintaining its looked-for engineering properties. Corrosion of reinforcing steel is a major problem facing the concrete infrastructures. Many structures in adverse environments have experienced unacceptable loss in serviceability of safety earlier than predictable due to the corrosion of reinforcing steel and thus need replacement, rehabilitation or strengthening.

Corrosion can be prohibited by chemical technique by using certain corrosion inhibiting chemical and coating to reinforcement. According to National Association of Corrosion Engineers (NACE) inhibitors are substances which when added to an environment, decrease the rate of attack on a metal. Corrosion inhibitors function by forming a passive layer around the reinforcing steel an prevent outside agents and reduce the corrosion current. Corrosion inhibitors are becoming an accepted method of getting your strength back durability of reinforced concrete in chloride laden environments.

II. EXPERIMENTAL DETAILS

A. Objective

The objectives of the current research work to study the durability properties of M25 grade of self compacting concrete with different optimum percentages of addition of organic corrosion inhibitors H2% and DA3% at 7 and 28 days compare with 0% at 7 and 28 days.

B. Materials used

Cement

Ordinary Portland cement of available in local market is used in the investigation. The Cement used has been tested for various proportions as per IS: 4031 and found to be confirming to various specifications of I.S- 8112- 1989. The specific gravity was 3.15 and fineness was 5.0% and standard consistency 29 %.

Fine aggregate

In this study, the use of fine aggregate was instrumented about the whole work comprising natural river sand of maximum size 4.75mm. By IS 383-1970, it is ratified to grading zone-II against specific gravity of 2.60 and fineness modulus of 2.25 was applied in this investigation.

Coarse aggregate

Coarse aggregate obtained from nearby granite quarry has been used for this study. it consisted of machine crushed stone angular in shape and the maximum size of aggregate is 12.5 mm with specific gravity 2.80, and fineness modulus 6.23 was used.

Table 1. Materials required per $1m^3$ of SCC

Mix	Grade of Concrete	Cement	Fly ash	FA	CA	Water	SP
SCC	M25	330.72	220.48	907.68	713.18	220.48	2.76

Fly ash

Class F fly ash from Mettur Thermal Power Station, Tamil Nadu was used as cement replacement material. The properties fly ash are confirming to I.S. 3812 – 2003 of Indian Standard Specification for Fly Ash for use as Pozzolanic and Admixture. The specific gravity was 2.15.

Mixing water

For casting the concrete specimen potable water has been used. Also the water has been had a water-soluble Chloride content of 140 mg/lit. The permissible limit for chloride is 500 mg/lit as per IS 456 – 2000. Therefore the amount of chloride present is very less than the permissible limit.

Admixture

Sulphonated Naphthalene Polymers (Conplast SP430) based super plasticizer which is brown colour and free flowing and having relative density 1.20 super plasticizer confirming to IS: 9103-1999. To give high water reduction up to 25% without loss of workability or to produce high quality of concrete that reduces permeability it is formulated Conplast SP430.

Corrosion inhibitor

Hexamine is Hexamethylenetetramine which is a heterocyclic organic compound with the molecular formula $(CH2)_6N4$.

Diethanolamine (DEA) is an organic compound with chemical formula $C_4H_11NO_2$. DEA is used as a surfactant and a corrosion inhibitor.

Mix proportions

The concrete mix design was proposed by using IS 10262:2009. The grade of concrete used was M-25 with water to cement ratio of 0.40. Proportion of concrete should be selected to make the most economical use of available materials to produce concrete of required quality. The standard concrete mix proportions were modified as per EFNARC specifications and different trial mixture proportions. Varying percentage inorganic corrosion inhibitor (Hexamine and Diethanolamine) from 0% to 5% i.e., 0%, 1%, 0.1%, 2%, 3%,4% and 5% to the total volume of cement content. The details of mix proportions are given in Table 1 for 1m3 of concrete.

III. PREPARATION OF SPECIMEN

The program consists of specimens were cured under water along with moulds after 24 hours of casting. After 28 days of curing, permeability test were conducted.

A. Rapid chloride permeability test

Corrosion is mainly caused by the ingress of chloride ions into concrete annulling the original passivity present. Standardized testing procedures are in ASTM C 1202. The RCPT is performed by monitoring the amount of electrical current that passes through a sample 50 mm thick by 100 mm in diameter in 6 hours using the apparatus and the cell arrangement is shown in Fig - 1 and Fig - 3 shows the experimental set up for RCPT and Fig - 2 concrete discs. Readings are taken every 30 minutes. This sample is typically cut as a slice of a core or cylinder. A voltage of 60V DC is maintained across the ends of the sample throughout the test. One lead is immersed in a 3% sodium chloride (NaCl) solution and the other in a 0.3M sodium hydroxide (NaOH) solution. At the end of 6 hours the sample is removed from the cell and the amount of coulombs passed through the specimens is calculated.

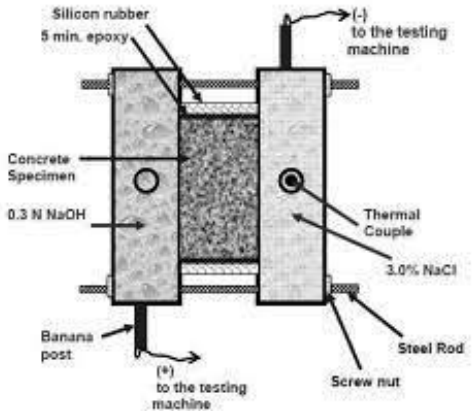

Fig. 1. Schematic diagram of RCPT (ASTM C1202-94)

Charge Passed (Coulombs)	Chloride Permeability
> 4,000	High
2,000 - 4,000	Moderate
1,000 - 2,000	Low
100 - 1,000	Very Low
< 100	Negligible

Table 2. Chloride permeability base on charge passed

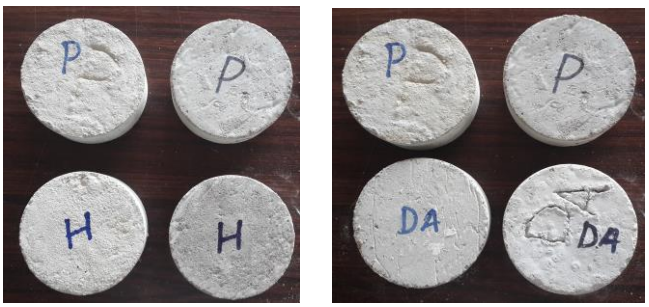

Fig.2. Typical M25 grade SCC concrete disc with different optimum % of organic corrosion inhibitors

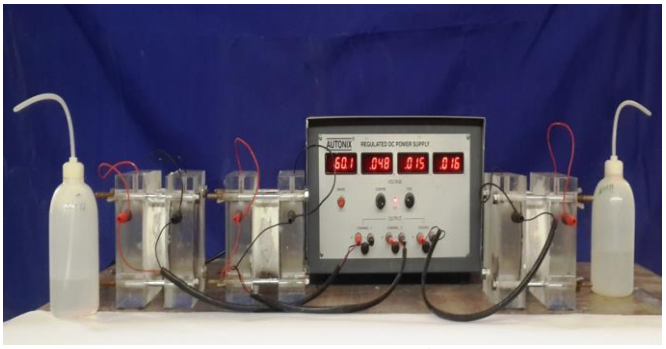

Fig. 3. Experimental set up of RCPT

Grade of concrete	Optimum % of Corrosion Inhibitor	Charge passed (Coulombs)		Chloride permeability as per ASTM C1202	
		7	28	7	28
M 25	CC 0%	484.65	543.60	Very Low	Very Low
	H 2%	567.45	448.65	Very Low	Very Low
	DA 3%	1161	1559.70	Low	Low

Table 4. Rapid chloride permeability test for SCC with and without corrosion inhibitors

IV. TESTING OF SPECIMENS

The specimens were fit in the chamber with the required brass as well as rubber oaring. The record time is set as 30 minutes and also the log time as 6 hours and 30 minutes and the current of 60 V is passed continuously. The data logger records the reading of corresponding cells at the every record time with its initial readings. At the end of log time the system halts after taking the final reading.

Average current flowing through one cell is calculated by,

$$Q=900\times(I0+2I_{30}+2I_{60}+2I_{90}+2I_{120}+2I_{150}+2I_{180}+2I_{210}+2I_{240}+2I_{270}+2I_{300}+2I_{330}+I_{360})$$

Q	Current flowing through one cell (Coulombs)
I_0	Initial current reading in mA
I_{30}	Current reading at 30 minutes in mA
I_{60}	Current reading at 60 minutes in mA
I_{90}	Current reading at 90 minutes in mA
I_{120}	Current reading at 120 minutes in mA
I_{150}	Current reading at 150 minutes in mA
I_{180}	Current reading at 180 minutes in mA
I_{210}	Current reading at 210 minutes in mA
I_{240}	Current reading at 240 minutes in mA
I_{270}	Current reading at 270 minutes in mA
I_{300}	Current reading at 300 minutes in mA
I_{330}	Current reading at 330 minutes in mA
I_{360}	Current reading at 360 minutes in mA

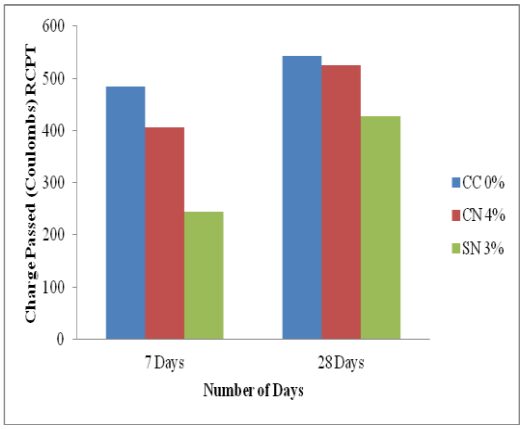

Fig. 4. Average values of rapid chloride permeability test

IV. CONCLUSION

Rapid Chloride ion Penetration Test (RCPT) is essentially a measure of concrete's electrical conductivity which depends on both pore structure characteristics and pore solution chemistry Chloride diffusion is one of the major reasons for causing corrosion to steel reinforcement inside concrete. Therefore it is necessary to study concrete for its chloride ion permeability.

- Rapid Chloride permeability of Self Compacting concrete shows less permeability of chlorides into concrete resulting into reduction the cracks causing interconnecting voids to be minimum.
- The high volume fly ash SCC mixes showed significantly lower chloride ion permeability than conventional concrete mixes.
- Considering strength as well as durability criteria, the optimum percentage of Hexamine and Diethanolamine to be added in self compacting concrete containing fly ash as cementitious material is 40% for delaying corrosion and to increase the strength and other durability characteristics.
- Addition of the organic corrosion inhibitors to fly ash replaced self compacting concrete, offered very good resistance against chemical attack and increases corrosion resistance by forming thin oxide layer to prevent outside agents and protecting the anodic sites.

REFERENCES

[1] Yahia A, Tamawara m, Shimbukuro A, and Shimoyama Y," Effect of Rheological Parameters on Self Compatibility of Concrete Containing Various Mineral Admixture, proceeding of the first RILEM. International Symposium on self compacting concrete, Stockholm, 1999.

[2] Bilek v, Sehmid P,"Properties of self compacting concrete with different fine admixtures andtheir comparision with properties of usual concrete, proceeding of the International Conference held at the University of Dundee, Scotland, UK on July 2005, pp 21-260.

[3] Emerging Technology Series on Self Consolidating Concrete, ACI 237, ACI International, Farmington Hills, MI, http://www.concrete.org.

[4] Berke N.S. Hicks, M.C.Predicting, "Long-Term Durability of Steel Reinforced Concrete with Calcium Nitrite Corrosion Inhibitor". Cement & Concrete Composites. 26, pp 191-198, 2004.

[5] De. Schutterg.Luol, "Effect of corrosion Inhibiting Admixture on Concrete Properties", Construction And Building Materials, pp 483-489, 2004.

[6] Michael C.Brown, Richard E.Weyers, and Michael M.Sprinkel. "Effect of Corrosion Inhibiting Admixtures on Material Properties of Concrete". ACI Material Journal, Vol.98. No.3, May - June 2001.

[7] Standard test method for electrical indication of concrete's ability to resist chloride ion penetration, ASTMC 1202-97, Annual book of ASTM standards, Vol.04.02, pp 639-644.

[8] D.Whiting, "Rapid Determination of the chloride Permeability of concrete," Report No. FHWA/RD-81/119, August 1981, Federal Highway Administration, Office of Research & Development, Washington, DC.

Coloring Edge Connectivity of Fuzzy Graph

S. Sarulatha
Department of Mathematics,
TRP Engineering College (SRM Group),
Trichy-621105, Tamil Nadu, India.

***Abstract*— Fuzzy graphs were introduced by Rosenfeld in 1975. Fuzzy graph theory has numerous applications in modern science and technology, especially in the fields of information theory, neural networks, expert systems, cluster analysis, medical diagnosis, control theory etc. In this paper, we deal with coloring of the edge connectivity of a fuzzy graph to obtain the better result in diagnosis of cancer cells.**

***Keywords*— Fuzzy graphs; fuzzy bonds; Fuzzy k-coloring; Fuzzy edge connectivity**.

I. INTRODUCTION

The fuzzy graph approach is more powerful in cluster analysis than the usual graph-theoretic approach due to its ability to handle the strengths of edges effectively. As in graphs, connectivity concepts play a key role in applications related with fuzzy graphs [1]. Fuzzy graphs were introduced by Rosenfeld [2] and Yeh and Bang [3] independently in 1975. Rosenfeld in his paper "Fuzzy Graphs" presented the basic structural and connectivity concepts while Yeh and Bang introduced different connectivity parameters of a fuzzy graph and discussed their applications in the paper titled "Fuzzy relations, Fuzzy graphs and their applications to clustering analysis" [3]. In [4] the authors have defined the concepts of strong arcs and strong paths. Also, in modern fuzzy graph theory, we have the notions of strong as well as strongest path [4] between any pair of vertices and a fuzzy edge cut can be viewed as a set of strong edges whose removal from G reduces the strength of connectedness between some pair of vertices of G, at least one of them differing from the end vertices of edges in the cut. The edges which are not strong need not be considered because the flow through such edges can be redirected through a different path having more strength. In the same manner we have to coloring the edge connectivity to diagnosis the cancer cells for better result.

II. FUZZY GRAPH

Definition 2.1. *Let V be a non-empty set, A fuzzy graph is a pair of functions* $G:(\sigma,\mu)$ *where* σ *is a fuzzy subset of V and* μ *is a symmetric fuzzy relation on* σ*. i.e.,* $\sigma: V \to [0,1]$ *and* $\mu: V \times V \to [0,1]$ *such that* $\sigma(u) \wedge \sigma(v) \geq \mu(u,v)$ *for all u, v in V.*

Definition 2.2. *The fuzzy graph* $H:(\tau,\nu)$ *is called a partial fuzzy sub graph of* $G:(\sigma,\mu)$ *if* $\tau \leq \sigma$ *and* $\nu \leq \mu$*. In particular, we call* $H:(\tau,\nu)$ *a fuzzy sub graph of* $G:(\sigma,\mu)$ *if* $\tau(u) = \sigma(u) \forall u \in \tau^*$ *and* $V(u,v) = \mu(u,v) \forall (u,v) \in \nu^*$.

Definition 2.3. *A fuzzy graph* $G:(\sigma,\mu)$ *is strong if* $\sigma(u) \wedge \sigma(v) = \mu(u,v) \forall u,v \in \mu^*$ *and is complete if* $\sigma(u) \wedge \sigma(v) = \mu(u,v) \forall u,v \in \sigma^*$.

Note that every complete fuzzy graph is strong but not conversely.

Also if $G:(\sigma,\mu)$ is a complete fuzzy graph than $G^*:(\sigma^*,\mu^*)$ is a complete graph.

Definition 2.4. *A path P in a fuzzy graph* $G:(\sigma,\mu)$ *is a sequence of distinct vertices* $u_0, u_1, u_2, ..., u_n$ *such that* $\mu(u_{i-1}, u_i) > 0,\ 1 \leq i \leq n.$

Here $n \geq 1$ is called the length of the path P. A single vertex u may also be considered as a path. In this case the path is of length 0. The consecutive pairs (u_{i-1}, u_i) are called edges of the path. We call P a cycle if $u_0 = u_n$ and $n \geq 3.$

Definition 2.5. *The strength of a path P is defined as* $\bigwedge_{i=1}^{n} \mu(u_{i-1}, u_i)$. *In other words, the strength of a path is defined to be the degree of membership of a weakest edge of the path. If the path has length 0, it is convenient to define its strength to be* $\sigma(u_0)$.

Definition 2.6. *Let* $G:(\sigma,\mu)$ *be a fuzzy graph. The strong degree of a vertex* $v \in \sigma^*$ *is defined as the sum of membership values of all strong edges incident at* v. *It is denoted by* $D_s(v)$. *Also if* $n_s(v)$ *denote the set of all strong neighbours of* v, *then* $D_s(v) = \sum_{u \in n_s(v)} \mu(u,v)$.

Example-2.7.

$\sigma(u_1) = 0.7, \sigma(u_2) = 1, \sigma(u_3) = 0.6,$
$\sigma(u_4) = 0.8, \sigma(u_5) = 0.9$ *and*
$\mu(u_1,u_2) = 0.3, \mu(u_1,u_3) = 0.4, \mu(u_2,u_3) = 0.2,$
$\mu(u_2,u_4) = 0.7, \mu(u_2,u_5) = 0.8,$
$\mu(u_3,u_5) = 0.5, \mu(u_4,u_5) = 0.6.$

Since the values satisfy $\mu(u,v) \le \sigma(u) \wedge \sigma(v)$ which is a fuzzy graph a strongest path joining u_2 *and* u_5 is the path

$P: u_2, u_4, u_5$ with $\mu^\infty(u_2,u_5) = 0.6$

$\mu^\infty(u_1,u_2) = \mu^\infty(u_1,u_4) = \mu^\infty(u_1,u_5) = \mu^\infty(u_1,u_3) = 0.3$

$\mu^\infty(u_2,u_3) = 0.2, \mu^\infty(u_2,u_4) = 0.7, \mu^\infty(u_2,u_5) = 0.6$

$\mu^\infty(u_3,u_5) = 0.5$ *and* $\mu^\infty(u_4,u_5) = 0.6.$

III. FUZZY EDGE CONNECTIVITY

In [3], the notion of edge connectivity of a fuzzy graph if defined as given below. As mentioned in the introduction this definition is more close to a graph rather than a fuzzy graph since, in a fuzzy graph the concept of strength of connectedness plays a crucial role.

Definition 3.1. *Let G be a fuzzy graph and* $\{V_1, V_2\}$ *be a partition of its vertex set. The set of edges joining vertices of* V_1 *and vertices of* V_2 *is called a cut-set of G, denoted by* (V_1, V_2) *relative to the partition* $\{V_1, V_2\}$. *The weight of the cut-set* (V_1, V_2) *is defined as* $\sum_{u \in V_1, v \in V_2} \mu(u,v)$.

Definition 3.2. *Let G be a fuzzy graph. The edge connectivity of G denoted by* $\lambda(G)$ *is defined to be the minimum weight of cut-sets of G.*

Definition 3.3. *A one fuzzy edge connectivity is called a fuzzy bond.*

Remark 3.4. Note that fuzzy bonds are special type of fuzzy bridges. Note all fuzzy bridges are fuzzy bonds.

Example 3.5.

Let $G: (\sigma, \mu)$ be with $\sigma^* = \{a, b, c, d, e\}$ with

$\mu(a,b) = 0.4, \mu(a,c) = 0.2, \mu(b,c) = 0.3,$

$\mu(c,d) = 0.5, \mu(d,a) = 0.7, \mu(a,e) = 0.6,$.

$\mu(b,e) = 0.5$

There are four fuzzy bonds in this fuzzy graph namely edges (a, d), (a, e), (d, c) and (e, b).

IV. COLORING FUZZY EDGE CONNECTIVITY

In a crisp graph G = (V, E), a coloring function C assigns an integer value $c(i)$ to each vertex $i \in V$ in such a way that the extremes of any edge $(i, j) \in E$ cannot share the same color,

i.e., $c(i) \ne c(j)$. In a fuzzy graph $G = (V, \mu)$, its chromatic number is the fuzzy number $\chi(G) = \{(x, v(x)) / x \in X\}$ where $X = \{1, ..., |v|\}, v(x) = \sup\{\alpha \in I / x \in A_\alpha\} \forall x \in X$ and $A_\alpha = \{1, ..., \chi_\alpha\} \forall \alpha \in I.$

Definition 4.1. *A family* $\Gamma = \{\gamma_1, \gamma_2, ..., \gamma_k\}$ *of fuzzy sets on X is called a k-fuzzy coloring of* $G = (X, \sigma, \mu)$ *if*

(i) $\vee\Gamma = \sigma,$

(ii) $\gamma_i \wedge \gamma_j = 0,$

(iii) *for every strong edge xy of G,* $\min\{\gamma_i(x), \gamma_i(y)\} = 0 \ \ (1 \le i \le k).$

The least value of k for which G has a k-fuzzy coloring, denoted by $\chi_F(G)$, is called the fuzzy chromatic number of G.

Definition 4.2. *A family* $\Gamma = \{\gamma_1, \gamma_2, ..., \gamma_k\}$ *of fuzzy sets on* $X \cup E$ *is called a k-fuzzy total coloring of* $G = (V, \sigma, \mu)$ *if*

(i) $\max_i \{\gamma_i(x)\} = \sigma(x)$ *for all* $x \in X$ *and* $\max_i \{\gamma_i(xy)\} = \mu(xy)$ *for all edges* $xy \in E.$

(ii) $\gamma_i \wedge \gamma_j = 0,$

(iii) *For every adjacent vertices x, y of* $\min\{\gamma_i(y_j y_k) / y_j y_k\} = 0,$ *(are set of incident edges from the vertex* x_j*)* $j = 1, 2, ..., |x|.$

Definition 4.3. *Let G be a fuzzy graph. The coloring edge connectivity of G denoted by* $\lambda_F(G)$ *is defined to be the minimum weight of cut-sets of G. Given a fuzzy graph* $G = (V, \sigma_F, \mu_F)$ *its edge chromatic number in fuzzy number* $\lambda_F(G) = \{x_\alpha, \alpha\}$ *where* x_α *is the edge connectivity chromatic number of* G_α *and* $\propto$ *values are the different membership value of vertex and edge of graph G.*

IV. ILLUSTRATION: CANCER DETECTION PROBLEM

In our human body, based on the location of the cells in the low magnification image of a tissue sample, surgically removed from a patient, it is possible to construct a graph with G with vertices as cells, called cell graph [5]. By analyzing the physical features of the cells; for example color and size, we can assign a membership value to the vertices of G. This value will range over (0, 1] depending of the nature of the cell; that is healthy, inflammatory or cancerous. Also, edges of G can assign a membership value based on the distances between the cells. Thus the cell graph can be converted to a fuzzy graph in this manner.

Applying the above clustering procedure to such a fuzzy graph, the cancerous cell clusters can be detected at the

cellular level in principle. This process, classifies cell clusters in a tissue into different phases of cancer, depending of the distribution, density and fuzzy connectivity of the cell clusters within the tissue using coloring the edge connectivity.

Assume that the vertices with weights more than 0.6 represent cancerous cells, edges with weights between 0.3 and 0.5 inflammatory cells and between 0 and 0.4 healthy cells. Let the vertex set of G be $\{v_1, v_2, v_3, v_4, v_5\}$

Let $G:(\sigma,\mu)$ be an fuzzy graph with

$$\sigma^* = \{v_1, v_2, v_3, v_4, v_5\} \text{ with}$$

and

$$\sigma(v_1) = \sigma(v_2) = \sigma(v_3) = \sigma(v_4) = \sigma(v_5) = 0.8$$

$$\mu(a,b) = \mu(a,c) = 0.4,$$

$$\mu(b,d) = \mu(d,e) = \mu(c,e) = 0.6$$

$$\mu(b,c) = 0.3,\ \mu(c,d) = 0.5$$

using coloring edge connectivity

$$\sigma(x_i) = 0.8 \text{ for } i = 1,...,5$$

$$\mu(x_i, y_j) = \begin{cases} 0.4 \text{ for } ij = 12,13 \\ 0.6 \text{ for } ij = 24,45,35 \\ 0.3 \text{ for } ij = 23 \\ 0.4 \text{ for } ij = 34 \end{cases}$$

Level	Maximal edge connectivity	Clusters
(0, 0.6]	{1, 2, 3}	C_1={1, 2, 3}
[0.6, 1]	{2}, {4}, {5}	C_2={2}, C_3={4}, C_4={5}

After applying the coloring edge connectivity of fuzzy graph G is $\lambda_F(G)$=0.6. Using the Yeh and Bang procedure in coloring we obtain the level as given below

From the above clusters corresponding to $\lambda_F(G)$=0.6, it is observed that {4, 5} is a cell cluster which is affected seriously by cancer whereas its neighbouring area containing the cells {2} and {3} can be found inflammatory. Note that the cell {1} is healthy.

REFERENCES

[1] J.N.Moderson, P.S.Nair, Fuzzy Graphs and FuzzyHypergraphs, Physica-Verlog, 2000.

[2] A.Rosenfeld, Fuzzy Graphs,in: L.A. Zadeh, K.S.Fu, M.Shimura(Eds), Fuzzy sets and their applications to cognitive and Decision processes, Academic Press, New York, 1975, pp 77-95.

[3] R.T.Yeh, S.Y.Bang, Fuzzy relations, fuzzy graphs and their applications to clustering analysis, in: L.A.Zadeh, K.S.Fu, M.Shimura, Fuzzy sets and their applications, Academic Press, 1975, pp 125-149.

[4] K.R. Bhutani, A.Rosenfeld, Strong arcs in fuzzy graphs, information sciences 152(2003) 319-322.

[5] B.Yenes, C.Gunduz, S.H.Gultekin, The cell graphs of cancer, Bio informatics 20(1) 2004, 145-151.

Accident Prediction Model: A Comparison of Conventional And Advanced Modeling Methods

L. Vinoth Kumar*
Department of Civil Engineering
College of Engineering Guindy,
Anna University,
Chennai, India.

G. Umadevi
Department of Civil Engineering,
College of Engineering Guindy,
Anna University,
Chennai, India.

***Abstract*—Primary objective of any transportation infrastructure is to facilitate mobility and accidents pose an unwarranted by products of the system, which need to be controlled in order to achieve the objective. Especially in India, there is a need to do a lot more to minimize the number of accidents. According to National Crime Records Bureau (NCRB) report, 51 cases of road accidents took place every one hour during 2014.In the above back drop of the accidents scenario it is imperative to reduce the level of road accidents through some sort of advanced methodology since the conventional methods lack to prevent the accident occurrences and reduce the severity. Hence, system dynamic (SD) model and conventional model were compared to establish the inadequacy in conventional modeling ensure Road Safety through accurate accident prediction.**

Keywords— Accident Prediction, System Dynamic (SD) Model, Conventional Model, Road Safety.

I. INTRODUCTION

Transport Sector in India is a very extensive system, comprising different modes of transport like roads, railways, aviation, inland waterways, and shipping that facilitates easy and efficient conveyance of goods and people across the country. The backbone of economic development of India depends on its transportation. Road Transport is the primary mode of transport, which plays an important role in conveyance of goods and passengers and linking the centers of production, consumption, and distribution. An efficient transport system is a pre- requisite for sustained economic development. It plays a significant role in promoting national integration, which is particularly important in a large country like India.

According to National Crime Records Bureau (NCRB) reports, during 2014 a total of 4,50,898 cases of Road Accidents were reported which rendered 4,77,731 persons injured and 1,41, 526 deaths. Deaths due to Road Accidents in the country have increased by 2.9% during 2014 (1,41,526) over 2013 (1,37,423). In Tamil Nadu, 67250 cases has been reported out of those 15190 were fatalities. The maximum fatalities in traffic accidents was reported in Delhi City (2,199 deaths) followed by Chennai (1,046 deaths) and Jaipur (844 deaths). [5]

II. OBJECTIVES

- To review various accidents prediction models established earlier locally and globally.
- To develop mathematical and simulation model for accident prediction and establish the inadequacy in conventional modeling.
- To suggest appropriate preventive measures to reduce the number of accidents through accident prediction to ensure road safety.

III. METHODOLOGY

The flow chart of this study has shown in Fig.1. The literature regarding various accident prediction models has been studied. Then, data related for model has been collected from various sources and the study stretch has been selected. Model was formulated in both conventional and system dynamic model. For conventional model, Smeed's formula and for SD model, STELLA software has been used. Various scenarios analysis like Do minimum scenario, Partial scenario and Desirable scenario has been developed.

IV. DATA COLLECTION

The accident data has been collected and analyzed for observing the current trend of accidents in India. The secondary data are collected from various sources like Population census, NCRB, MORTH (Ministry of Road Transport and Highways), etc. The secondary data collected includes details like total number of accidents and registered motor vehicles in India. [6, 7, 8, 9]

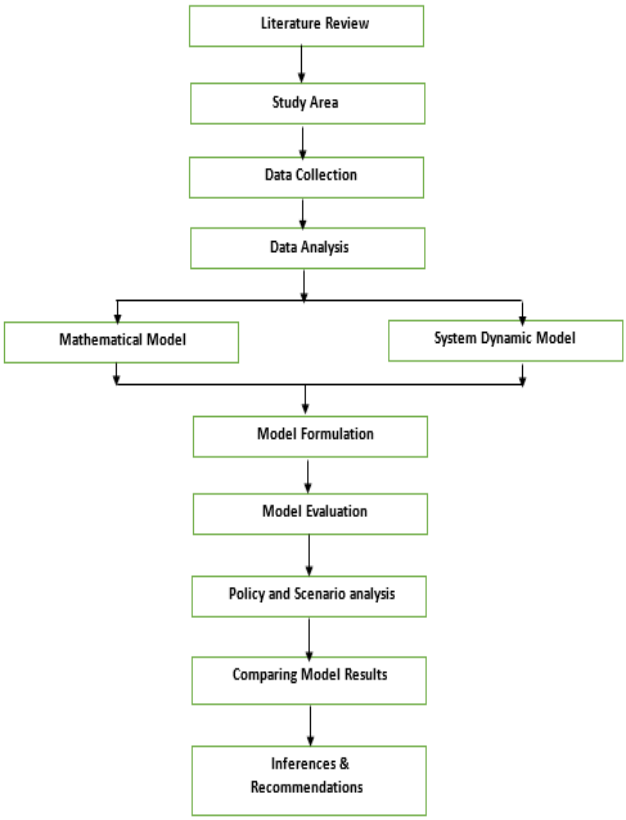

Fig .1. Methodology of the study

MODEL DEVELOPMENT

A. *Smeed's Model*

Smeed's examined the relationship on a number of Road fatalities with those of motor vehicles and the populations of 20 countries in 1938 in the following form

$$D / N = 0.0003 (N / P)^{-0.67}$$

Where D, N, P are deaths, motor vehicles, and population respectively.

P. Pramada Valli (2004), [1] the regression analysis was carried out using Smeed's model for the years (1970-2001) for india following equations are derived:

$$C / N = 0.0008 (N / P)^{-0.75} \quad (1)$$

$$F / N = 0.0003 (N / P)^{-0.58} \quad (2)$$

$$I / N = 0.0014 (N / P)^{-0.57} \quad (3)$$

In this study, development of relationships among the parameters namely road accidents, the number of registered motor vehicles and population. [4]

where C/N = Number of total accidents

Where **C/N** = Number of total accidents per vehicular population, **F/N** = Number of fatalities per vehicular population, **I/N** = Number of injuries per vehicular population and **N/P** = Number of registered motor vehicles per population.

B. . *System Dynamic Model*

It is a methodology whereby complex, dynamic, and nonlinear interactions in social systems can be understood and analyzed and new structures and policies can be designed to improve the system behavior.

The Road Accident model has been developed in this study, using the System Dynamics Simulation Software "STELLA". The STELLA is object oriented simulation software, which allows the development of any complex, dynamic and nonlinear systems with significantly less effort than using traditional programming languages. It has a user-friendly graphical interface and supports modular program development. [2]

The system dynamics modeling tool has four basic building blocks**.**

- Stocks or levels are used to represent anything that accumulates.
- Flows or rates represent activities that increase and decrease stocks. An example of flow includes birth rate or death rate.
- Connectors are used to establish the relationship among variables in the model, which is represented as arrows graphically in the model. They carry information, which can be a quantity, constants, an algebraic relationship, or a graphical relationship.
- Converters transform input into output. Converters can accept input in the form of algebraic relationships, graphs, and Tables.

Fig .2. Represents flow diagramming symbols, which are used in System Dynamics.

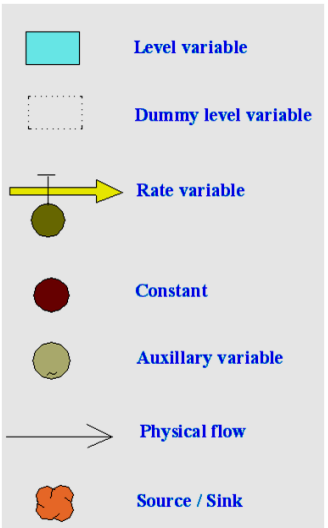

Fig .2. Flow Diagramming Symbols

V. DATA ANALYSIS

In this work SD model for human population and vehicle population were developed as shown in Fig 3 and 4 respectively. First, growth rate of human and vehicle population of previous years were obtained. Based on this trend, populations has been predicted. For both population, 2011 was taken as base year value. Then it has predicted up to horizon year 2020.

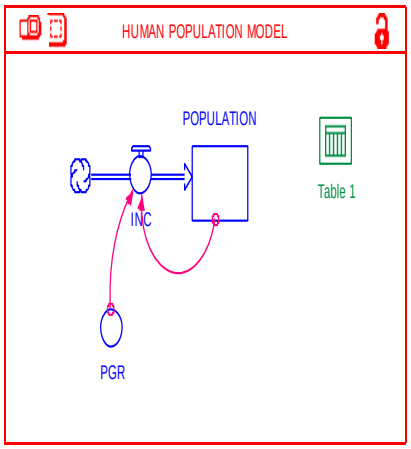

Fig .3. Model for Human Population

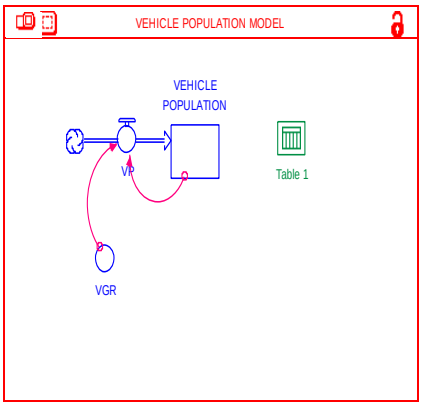

Fig .4. Model for Vehicle Population

The accident model is similar to above Population model and accident has been predicted with existing trends. This is also called as "Do minimum Scenario". Developed accident model as illustrated in Fig 5

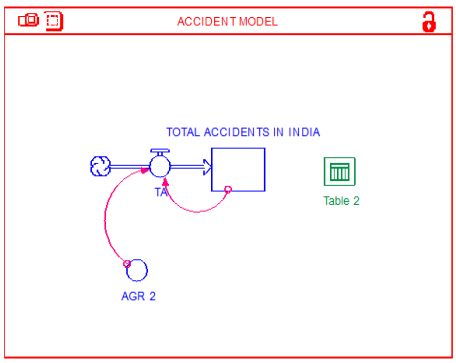

Fig .5.Accident Model for India

Years	Population	Vehicle Population
2011	1,210,193,422	141,866,000
2012	1,230,040,594	155,967,480
2013	1,250,213,260	171,470,648
2014	1,270,716,757	188,514,830
2015	1,291,556,512	207,253,205
2016	1,312,738,039	227,854,173
2017	1,334,266,943	250,502,878
2018	1,356,148,921	275,402,864
2019	1,378,389,763	302,777,909
2020	1,400,995,355	332,874,033

TABLE 1. PREDICTED HUMAN POPULATION AND VEHICLE POPULATION FOR INDIA

Years	Population	Vehicle Population	Total Accidents in Smeed's Model	Total Accidents in SD Model
2011	1,210,193,422	141,866,000	566,501	497,686
2012	1,230,040,594	155,967,480	587,203	508,137
2013	1,250,213,260	171,470,648	608,661	518,808
2014	1,270,716,757	188,514,830	630,903	529,703
2015	1,291,556,512	207,253,205	653,959	540,827
2016	1,312,738,039	227,854,173	677,857	552,184
2017	1,334,266,943	250,502,878	702,628	563,780
2018	1,356,148,921	275,402,864	728,304	575,620
2019	1,378,389,763	302,777,909	754,918	587,708
2020	1,400,995,355	332,874,033	782,506	600,050

TABLE 2. PREDICTED ACCIDENTS FOR INDIA IN SMEED'S MODEL AND SD MODEL

VI. PREDICTED ROAD ACCIDENTS

Total accidents increased from 566,501 to 782,506 in Smeed's model and 497,686 to 600,050 in system dynamic model during 2011 to 2020 as shown in Table II

VII. COMPARISON OF CONVENTIONAL AND SYSTEM DYNAMICS (SD) MODEL

After the total accidents has been predicted in both models, predicted values are compared with existing values, which is given in government records. Comparison of Smeed's and Stella model with total accidents for India as given in Table III. Percentage difference in Smeed's model is 19.74 % whereas Stella model 3.62% in the year 2012. So comparing both models, SD has accurate results when compared to Conventional model.

Years	Total Accidents in Smeed's Model	Total Accidents inSD Model	Total Accidents	% Differences in Smeed's Model	% Differences in SD Model
2012	587,203	508,137	490,383	19.74	3.62
2013	608,661	518,808	486,476	25.11	6.64

TABLE 3. COMPARISON OF CONVENTIONAL AND SYSTEM DYNAMICS (SD) MODEL

VIII. SCENARIO ANALYSIS

Scenario analysis is a process of analyzing possible future events by considering alternative possible outcomes. There are three types of scenarios. They are Do minimum scenario, Partial scenario and Desirable scenario.

A. Partial Scenario

Partial Scenario Here the values of total accidents getting reduced when compared to do minimum scenario. This is done by providing training to drivers, create awareness among peoples and enforcement of rules. In Fig 5 depicts that enforcement and training are outflow. Table shows that the Partial scenario total number of accidents in 2020 was 277,084 which is less when compared to do minimum scenario.

B. Partial Scenario

Partial Scenario Here the values of total accidents getting reduced when compared to do minimum scenario. This is done by providing training to drivers, create awareness among peoples and enforcement of rules. In Fig 5 depicts that enforcement and training are outflow. Table shows that the Partial scenario total number of accidents in 2020 was 277,084 which is less when compared to do minimum scenario.

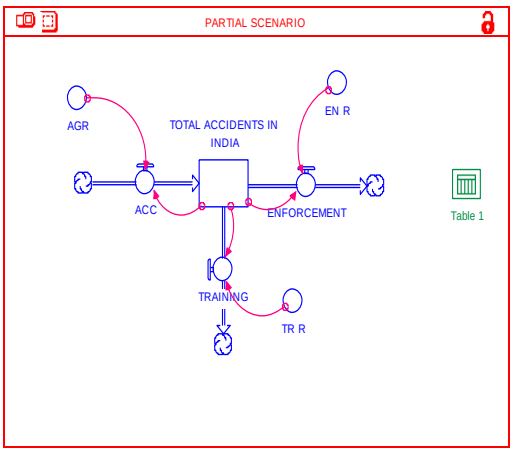

Fig .6. Partial Scenario Model

C. Desirable Scenario

In the "Desirable Scenario" has done to calibrate the model to achieve nil/ very minimum accidents in the future years. The Desirable scenario achieves an accident reduction in the horizon year 2020, which is in 148,101 numbers when compared to do minimum scenario. Here also accidents was reduced by providing training to drivers and enforcement of rules but efforts taken to achieve this will be more when compare to Dominium and Partial Scenarios. The results of all scenarios are consolidated and tabulated in Table IV

IX. RESULTS AND INFERENCE

- The total number of predicted accidents had been developed from Smeed's Model as well as System Dynamic Model for the years 2011 to 2020.
- It shows that System Dynamic Model gives accurate results.
- System Dynamic model can be used to perform any scenario whereas Conventional model is cumbersome to perform scenario like partial and desirable scenario.
- Comparing both System Dynamic and Conventional models, SD is the best and accurate Model.

ACKNOWLEDGMENT

The first author thanks Professor Dr. Umadevi. G of Anna University, who provided insight and expertise that greatly assisted his research. He also thanks Mr. S. Satheesh and his friends from Anna University for their help for developing this paper.

REFERENCES

[1] Pramada VALLI.P (2004) 'Road Accident Models for Large Metropolitan Cities of India', Central Road Research Institute, Delhi.
[2] Naveen Kumar.S, Umadevi.G (2011), 'Application of System Dynamic Simulation Modeling in Road Safety', College of Engineering, Guindy, Chennai.
[3] Nachimuthu.K, Partheeban.P (2013), 'Development of A Road Accident Prediction Model Based on System Dynamic Approach', Sathyabama University, Chennai.
[4] Sandip Chakraborty and Sudip K.Roy (2005), 'Traffic Accidents Characteristics of Kolkata', Transport and Communication Bulletin for Asia and the Pacific.
[5] www.ncrb.gov.in
[6] www.censusindia.gov.in
[7] www.morth.nic.in
[8] www.mospi.nic.in
[9] www.tn.gov.in

Stochastic Models on Time to Recruitment in a Two Grade Manpower System using Univariate Recruitment Policy

P. Saranya*
Department of Mathematics,
TRP Engineering College (SRM Group),
Trichy-621105, Tamil Nadu, India.

A. Srinivasan
PG & Research Department of Mathematics,
Bishop Heber College,
Trichy -620017, Tamil Nadu, India.

***Abstract*— In this paper for a two grade manpower system involving optional and mandatory exponential thresholds, the analytical results for some performance measures related to time to recruitment are obtained using a univariate policy of recruitment by considering different forms of inter-decision times and loss of manpower in the system.**

Keywords*— *Two grade manpower system; loss of manpower; Univariate policy of recruitment, geometric process; Correlated random variables and Mean time to recruitment.

I. INTRODUCTION

In any organization, depletion of manpower is quite common whenever policy decisions are announced .Frequent recruitment to compensate this depletion is costlier and hence suitable policy decision on recruitment has to be designed. In this context, several authors have obtained performance measures namely mean and variance of time to recruitment using different policies of recruitment based on shock mode approach. Employing the univariate recruitment policy, the expected time to recruitment is obtained under different conditions for several models in [1], [2] and [3].In [5],for a single grade man-power system with a mandatory exponential threshold for the loss of manpower ,the authors have obtained the system performance measures when the inter-decision times form an order statistics .In [2] ,for a single grade manpower system, the author has considered a new recruitment policy involving two thresholds for the loss of man-power in the organization in which one is optional and the other is mandatory and obtained the mean time to recruitment under different conditions on the nature of thresholds ,inter -decision times and loss of man-hours . In [6-9] the authors have extended the results in [2] for a two-grade system according as the thresholds are exponential random variables or extended exponential random variables or SCBZ property possessing random variables or geometric random variables. In [10],the authors have obtained performance measures by assuming that the inter-decision times for the two grades form same geometric process .In [11-19], the authors have extended the results in [5] for a two-grade system involving two thresholds by assuming different distributions for thresholds under different condition of inter-decision time and wastage. The objective of the present paper is to obtain performance measures for a two grade manpower system with exponential thresholds by considering different forms of loss of manpower and inter decision times.

II. MODEL DESCRIPTION AND ANALYSIS OF MODEL –I

Consider an organization taking decisions at random epoch in $(0, \infty)$ and at every decision epoch a random number of persons quit the organization. There is an associated loss of man-hours if a person quits. It is assumed that the loss of man-hours are linear and cumulative. Let Y_1, Y_2 (Z_1, Z_2) denotes the optional (mandatory) thresholds for the loss of man-hours in grades 1 and 2, with parameters $\theta_1, \theta_2, \alpha_1, \alpha_2$ respectively, where $\theta_1, \theta_2, \alpha_1, \alpha_2$ are positive. It is assumed that $Y_1 < Z_1$and $Y_2 < Z_2$. Write $Y = \text{Max}(Y_1, Y_2)$ and $Z=\text{Max}(Z_1, Z_2)$, where Y (Z) is the optional (mandatory) threshold for the loss of man-hours in the organization. The loss of man- hours, optional and mandatory thresholds are assumed as statistically independent. Let T be the time to recruitment in the organization with cumulative distribution function L (.), probability density function l (.), mean E (T) and variance V (T). Let $F_k(.)$ be the k fold convolution of F(.). Let $l^*(.)$ and $f^*(.)$, be the Laplace transform of l (.) and f (.), respectively. Let $V_k(t)$ be the probability that there are exactly k decision epochs in (0, t]. It is known from Renewal theory that $V_k(t) = F_k(t) - F_{k+1}(t)$ with $F_0(t) = 1$.Let p be the probability that the organization is not going for recruitment whenever the total loss of man-hours crosses optional threshold Y. The Univariate recruitment policy employed in this paper is as follows: If the total loss of man-hours exceeds the optional threshold Y, the organization may or may not go for recruitment. But if the total loss of man-hours exceeds the mandatory threshold Z, the recruitment is necessary.

III. MAIN RESULTS

$$P(T > t) = \sum_{k=0}^{\infty} V_k(t) P\left(\sum_{i=1}^{k} X_i \le Y\right) + p \sum_{k=0}^{\infty} V_k(t) P\left(\sum_{i=1}^{k} X_i > Y\right) \times P\left(\sum_{i=1}^{k} X_i < Z\right) \quad (1)$$

We now obtain some performance measures related to time to recruitment for different forms of wastage and inter-decision times.

Case (i): Let X_i be the loss of man hours due to the i^{th} decision epoch , i=1,2,3… forming a sequence of independent and identically distributed exponential random variables with mean $\frac{1}{c}$ (c>0), probability density function g(.),U_i are exchangeable and constantly correlated exponential random variables denoting inter-decision time between $(i-1)^{th}$ and i^{th} decision, i=1,2, 3….k. with cumulative distribution function F(.), probability density function f(.) and mean u .

Using law of total probability

$$P\left(\sum_{i=1}^{k} X_i < Y\right) = \int_0^{\infty} (1 - P(Y \le x)) g_k(x) dx = \int_0^{\infty} (1 - H(x)) g_k(x) dx \quad (2)$$

Since the distribution of thresholds follow exponential distribution it can be shown that

$$P\left(\sum_{i=1}^{k} X_i < Y\right) = \int_0^{\infty} \left(e^{-\theta_1 x} + e^{-\theta_2 x} - e^{-(\theta_1 + \theta_2)x} \right) g_k(x) dx \quad (3)$$

Similarly,

$$P\left(\sum_{i=1}^{k} X_i < Z\right) = \int_0^{\infty} \left(e^{-\alpha_1 x} + e^{-\alpha_2 x} - e^{-(\alpha_1 + \alpha_2)x} \right) g_k(x) dx \quad (4)$$

Using (3) and (4) in (1) and on further simplification we get,

$$\begin{aligned} P(T > t) = {} & \sum_{k=0}^{\infty} [F_k(t) - F_{k+1}(t)] \left(g^*(\theta_1) \right)^k + \left(g^*(\theta_2) \right)^k - \left(g^*(\theta_1 + \theta_2) \right)^k \\ & + p \sum_{k=0}^{\infty} [F_k(t) - F_{k+1}(t)] \left(1 - \left(\left(g^*(\theta_1) \right)^k + \left(g^*(\theta_2) \right)^k - \left(g^*(\theta_1 + \theta_2) \right)^k \right) \right) \left(g^*(\alpha_1) \right)^k + \left(g^*(\alpha_2) \right)^k - \left(g^*(\alpha_1 + \alpha_2) \right)^k \end{aligned} \quad (5)$$

Since $L(t) = 1 - P(T > t)$ from (5)

$$\begin{aligned} L(t) = {} & \left(1 - g^*(\theta_1)\right) \sum_{k=1}^{\infty} F_k(t) \left(g^*(\theta_1) \right)^{k-1} + \left(1 - g^*(\theta_2)\right) \sum_{k=1}^{\infty} F_k(t) \left(g^*(\theta_2) \right)^{k-1} \\ & - \left(1 - g^*(\theta_1 + \theta_2)\right) \sum_{k=1}^{\infty} F_k(t) \left(g^*(\theta_1 + \theta_2) \right)^{k-1} + p \left(\left(1 - g^*(\alpha_1)\right) \sum_{k=1}^{\infty} F_k(t) \left(g^*(\alpha_1) \right)^{k-1} \right. \\ & - \left(1 - g^*(\theta_1) g^*(\alpha_1)\right) \sum_{k=1}^{\infty} F_k(t) \left(g^*(\theta_1) g^*(\alpha_1) \right)^{k-1} - \left(1 - g^*(\theta_2) g^*(\alpha_1)\right) \sum_{k=1}^{\infty} F_k(t) \left(g^*(\theta_2) g^*(\alpha_1) \right)^{k-1} \\ & + \left(1 - g^*(\theta_1 + \theta_2) g^*(\alpha_1)\right) \sum_{k=1}^{\infty} F_k(t) \left(g^*(\theta_1 + \theta_2) g^*(\alpha_1) \right)^{k-1} + \left(1 - g^*(\alpha_2)\right) \sum_{k=1}^{\infty} F_k(t) \left(g^*(\alpha_2) \right)^{k-1} \\ & - \left(1 - g^*(\theta_1) g^*(\alpha_2)\right) \sum_{k=1}^{\infty} F_k(t) \left(g^*(\theta_1) g^*(\alpha_2) \right)^{k-1} - \left(1 - g^*(\theta_2) g^*(\alpha_2)\right) \sum_{k=1}^{\infty} F_k(t) \left(g^*(\theta_2) g^*(\alpha_2) \right)^{k-1} + \\ & + \left(1 - g^*(\theta_1 + \theta_2) g^*(\alpha_2)\right) \sum_{k=1}^{\infty} F_k(t) \left(g^*(\theta_1 + \theta_2) g^*(\alpha_2) \right)^{k-1} - \left(1 - g^*(\alpha_1 + \alpha_2)\right) \sum_{k=1}^{\infty} F_k(t) \left(g^*(\alpha_1 + \alpha_2) \right)^{k-1} \\ & + \left(1 - g^*(\alpha_1 + \alpha_2) g^*(\theta_1)\right) \sum_{k=1}^{\infty} F_k(t) \left(g^*(\alpha_1 + \alpha_2) g^*(\theta_1) \right)^{k-1} + \left(1 - g^*(\alpha_1 + \alpha_2) g^*(\theta_2)\right) \sum_{k=1}^{\infty} F_k(t) \left(g^*(\alpha_1 + \alpha_2) g^*(\theta_2) \right)^{k-1} \\ & \left. - \left(1 - g^*(\alpha_1 + \alpha_2) g^*(\theta_1 + \theta_2)\right) \sum_{k=1}^{\infty} F_k(t) \left(g^*(\alpha_1 + \alpha_2) g^*(\theta_1 + \theta_2) \right)^{k-1} \right) \end{aligned} \quad (6)$$

By assumption $\{U_i\}$ is a sequence of exchangeable and constantly correlated random variable each following the exponential distribution .As in [4] , we get the cumulative distribution function of $\sum_{i=1}^{k} U_i$ as

$$F_k(t) = \frac{1-\rho}{1-\rho+k\rho}\sum_{i=0}^{\infty}\left(\frac{k\rho}{1-\rho+k\rho}\right)^i\left[1-\sum_{j=0}^{k+j-1}\frac{e^{-y/b}(y/b)^{k+i-j-1}}{(k+i-j-1)!}\right] \tag{7}$$

Taking Laplace-Stieltjes transform on both sides, we have

$$F_k^*(s) = \frac{(1-\rho)(1+bs)^{1-k}}{(1-\rho)(1+bs)+k\rho bs} \tag{8}$$

$$\left[\frac{d}{ds}(F_k^*(s)\right]_{s=0} = -uk \text{ and}$$

$$\left[\frac{d^2}{ds^2}F_k^*(s)\right]_{s=0} = u^2\{(1+\rho^2)k^2+(1-\rho^2)k\} \text{ , where } u = \frac{b}{1-\rho} \tag{9}$$

It is known that

$$E(T) = -\left.\frac{d(l^*(s))}{ds}\right|_{s=0}, E(T^2) = \left.\frac{d^2(l^*(s)}{ds^2}\right|_{s=0} \text{ and } V(T) = E(T^2)-(E(T))^2 \tag{10}$$

Using (6) and (9) in (10) we get the first two moments

$$E(T) = u\left(\frac{1}{1-g^*(\theta_1)}+\frac{1}{1-g^*(\theta_2)}-\frac{1}{1-g^*(\theta_1+\theta_2)}+p\left(\frac{1}{1-g^*(\alpha_1)}+\frac{1}{1-g^*(\alpha_2)}-\frac{1}{1-g^*(\alpha_1+\alpha_2)}-\right.\right.$$
$$\frac{1}{1-g^*(\theta_1)g^*(\alpha_1)}-\frac{1}{1-g^*(\theta_2)g^*(\alpha_1)}+\frac{1}{1-g^*(\theta_1+\theta_2)g^*(\alpha_1)}-\frac{1}{1-g^*(\theta_1)g^*(\alpha_2)}-\frac{1}{1-g^*(\theta_2)g^*(\alpha_2)}$$
$$\left.\left.+\frac{1}{1-g^*(\theta_1+\theta_2)g^*(\alpha_1)}+\frac{1}{1-g^*(\theta_1)g^*(\alpha_1+\alpha_2)}+\frac{1}{1-g^*(\theta_2)g^*(\alpha_1+\alpha_2)}-\frac{1}{1-g^*(\theta_1+\theta_2)g^*(\alpha_1+\alpha_2)}\right)\right) \tag{11}$$

$$E(T^2) = 2u^2\left(\frac{1+\rho^2g^*(\theta_1)}{(1-g^*(\theta_1))^2}+\frac{1+\rho^2g^*(\theta_2)}{(1-g^*(\theta_2))^2}-\frac{1+\rho^2g^*(\theta_1+\theta_2)}{(1-g^*(\theta_1+\theta_2))^2}+p\left(\frac{1+\rho^2g^*(\alpha_1)}{(1-g^*(\alpha_1))^2}+\frac{1+\rho^2g^*(\alpha_2)}{(1-g^*(\alpha_2))^2}-\frac{1+\rho^2g^*(\alpha_1+\alpha_2)}{(1-g^*(\alpha_1+\alpha_2))^2}\right.\right.$$
$$-\frac{1+\rho^2g^*(\theta_1)g^*(\alpha_1)}{(1-g^*(\theta_1)g^*(\alpha_1))^2}-\frac{1+\rho^2g^*(\theta_2)g^*(\alpha_1)}{(1-g^*(\theta_2)g^*(\alpha_1))^2}+\frac{1+\rho^2g^*(\theta_1+\theta_2)g^*(\alpha_1)}{(1-g^*(\theta_1+\theta_2)g^*(\alpha_1))^2}-\frac{1+\rho^2g^*(\theta_1)g^*(\alpha_2)}{(1-g^*(\theta_1)g^*(\alpha_2))^2}-\frac{1+\rho^2g^*(\theta_2)g^*(\alpha_2)}{(1-g^*(\theta_2)g^*(\alpha_2))^2}$$
$$\left.\left.+\frac{1+\rho^2g^*(\theta_1+\theta_2)g^*(\alpha_1)}{(1-g^*(\theta_1+\theta_2)g^*(\alpha_1))^2}+\frac{1+\rho^2g^*(\theta_1)g^*(\alpha_1+\alpha_2)}{(1-g^*(\theta_1)g^*(\alpha_1+\alpha_2))^2}+\frac{1+\rho^2g^*(\theta_2)g^*(\alpha_1+\alpha_2)}{(1-g^*(\theta_2)g^*(\alpha_1+\alpha_2))^2}-\frac{1+\rho^2g^*(\theta_1+\theta_2)g^*(\alpha_1+\alpha_2)}{(1-g^*(\theta_1+\theta_2)g^*(\alpha_1+\alpha_2))^2}\right)\right) \tag{12}$$

where $g^{*}(\tau)=\frac{c}{c+\tau}$ for $\tau=\theta_1,\theta_2,\theta_1+\theta_2,\alpha_1,\alpha_2,\alpha_1+\alpha_2$.

(11) gives the expected time to recruitment, (11)and (12) together with (10) gives the variance of time to recruitment.

Case (ii):

Let X_i be the loss of man-hours due to the i^{th} decision epoch , i=1,2,3…k Let $X_{(1)},X_{(2)},X_{(3)},....X_{(n)}$ be the order statistics selected from the sample $X_1,X_2,....X_n$ with respective density functions $g_{X(1)}(.),g_{X(2)}(.),....g_{X(n)}(.)$

If U_i be exchangeable and constantly correlated exponential random variables denoting inter-decision times between (i-1) and i th decision epoch ,i=1,2,3….

Suppose $g(t)=g_{x(1)}(t)$.

The first two moments are given by (11) and (12) where

$$g^{*}_{x(1)}(\tau)=\frac{kc}{kc+\tau}. \qquad (13)$$

Suppose $g(t)=g_{x(k)}(t)$. The first two moments are given by (11) and (12) where

$$g^{*}_{x(k)}(\tau)=\frac{k!c^{k}}{(\tau+c)(\tau+2c)...(\tau+kc)} \qquad (14)$$

(14)

If U_i form a geometric process with parameter ‘a’ , a>0 then we find that

$$f_k{}^{*}(s)=\prod_{r=1}^{k} f^{*}\left(\frac{s}{a^{r-1}}\right), k=1,2,3.... \qquad (15)$$

Suppose $g(t)=g_{x(1)}(t)$. Since $l^{*}(s)=\frac{d}{ds}(l(t))$ and using (6),(15) in (10) we get the first two moments of time to recruitment

$$E(T) = aE(U_1)\left[C_1 + C_2 - C_3 + p\left(C_4 + C_5 - C_6 - H_{1,4} - H_{1,5} + H_{1,6} - H_{2,4} - H_{2,5} + H_{2,6} + H_{3,4} + H_{3,5} - H_{3,6}\right)\right] \quad (16)$$

$$\begin{aligned}
E(T^2) = {} & \frac{\sigma_{U1}^2 a^2}{(a^2-1)}\left[1 - \frac{(1-g^*(\theta_1))}{a^2 - g^*(\theta_1)} - \frac{(1-g^*(\theta_2))}{a^2 - g^*(\theta_2)} + \frac{(1-g^*(\theta_1+\theta_2))}{a^2 - g^*(\theta_1+\theta_2)}\right] + \frac{E(U_1)a^2}{(a-1)^2}\left[1 - \frac{2(1-g^*(\theta_1))}{a - g^*(\theta_1)} + \frac{1-g^*(\theta_1)}{a^2 - g^*(\theta_1)} - \frac{2(1-g^*(\theta_2))}{a - g^*(\theta_2)}\right. \\
& \left. + \frac{1-g^*(\theta_2)}{a^2 - g^*(\theta_2)} + \frac{2(1-g^*(\theta_1+\theta_2))}{a - g^*(\theta_1+\theta_2)} - \frac{1-g^*(\theta_1+\theta_2)}{a^2 - g^*(\theta_1+\theta_2)}\right] + p\frac{\sigma_{U1}^2 a^2}{(a^2-1)}\left[-\frac{(1-g^*(\alpha_1))}{a^2 - g^*(\alpha_1)} - \frac{(1-g^*(\alpha_2))}{a^2 - g^*(\alpha_2)} + \frac{(1-g^*(\alpha_1+\alpha_2))}{a^2 - g^*(\alpha_1+\alpha_2)}\right. \\
& + \frac{(1-g^*(\theta_1)g^*(\alpha_1))}{a^2 - g^*(\theta_1)g^*(\alpha_1)} + \frac{(1-g^*(\theta_2)g^*(\alpha_1))}{a^2 - g^*(\theta_2)g^*(\alpha_1)} - \frac{(1-g^*(\theta_1+\theta_2)g^*(\alpha_1))}{a^2 - g^*(\theta_1+\theta_2)g^*(\alpha_1)} + \frac{(1-g^*(\theta_1)g^*(\alpha_2))}{a^2 - g^*(\theta_1)g^*(\alpha_2)} + \frac{(1-g^*(\theta_2)g^*(\alpha_2))}{a^2 - g^*(\theta_2)g^*(\alpha_2)} \\
& \left. - \frac{(1-g^*(\theta_1+\theta_2)g^*(\alpha_2))}{a^2 - g^*(\theta_1+\theta_2)g^*(\alpha_2)} - \frac{(1-g^*(\theta_1)g^*(\alpha_1+\alpha_2))}{a^2 - g^*(\theta_1)g^*(\alpha_1+\alpha_2)} - \frac{(1-g^*(\theta_2)g^*(\alpha_1+\alpha_2))}{a^2 - g^*(\theta_2)g^*(\alpha_1+\alpha_2)} + \frac{(1-g^*(\theta_1+\theta_2)g^*(\alpha_1+\alpha_2))}{a^2 - g^*(\theta_1+\theta_2)g^*(\alpha_1+\alpha_2)}\right] \\
& + \frac{pE(U_1)a^2}{(a-1)^2}\left[-\frac{2(1-g^*(\alpha_1))}{a - g^*(\alpha_1)} + \frac{1-g^*(\alpha_1)}{a^2 - g^*(\alpha_1)} - \frac{2(1-g^*(\alpha_2))}{a - g^*(\alpha_2)} + \frac{1-g^*(\alpha_2)}{a^2 - g^*(\alpha_2)} + \frac{2(1-g^*(\alpha_1+\alpha_2))}{a - g^*(\alpha_1+\alpha_2)} - \frac{1-g^*(\alpha_1+\alpha_2)}{a^2 - g^*(\alpha_1+\alpha_2)}\right. \\
& + \frac{2(1-g^*(\theta_1)g^*(\alpha_1))}{a - g^*(\theta_1)g^*(\alpha_1)} - \frac{(1-g^*(\theta_1)g^*(\alpha_1))}{a^2 - g^*(\theta_1)g^*(\alpha_1)} + \frac{2(1-g^*(\theta_2)g^*(\alpha_1))}{a - g^*(\theta_2)g^*(\alpha_1)} - \frac{(1-g^*(\theta_2)g^*(\alpha_1))}{a^2 - g^*(\theta_2)g^*(\alpha_1)} - \frac{2(1-g^*(\theta_1+\theta_2)g^*(\alpha_1))}{a - g^*(\theta_1+\theta_2)g^*(\alpha_1)} \\
& + \frac{(1-g^*(\theta_1+\theta_2)g^*(\alpha_1))}{a^2 - g^*(\theta_1+\theta_2)g^*(\alpha_1)} + \frac{2(1-g^*(\theta_2)g^*(\alpha_2))}{a - g^*(\theta_2)g^*(\alpha_2)} - \frac{(1-g^*(\theta_2)g^*(\alpha_2))}{a^2 - g^*(\theta_2)g^*(\alpha_2)} - \frac{2(1-g^*(\theta_1+\theta_2)g^*(\alpha_2))}{a - g^*(\theta_1+\theta_2)g^*(\alpha_2)} \\
& + \frac{(1-g^*(\theta_1+\theta_2)g^*(\alpha_2))}{a^2 - g^*(\theta_1+\theta_2)g^*(\alpha_2)} - \frac{2(1-g^*(\theta_1)g^*(\alpha_1+\alpha_2))}{a - g^*(\theta_1)g^*(\alpha_1+\alpha_2)} + \frac{(1-g^*(\theta_1)g^*(\alpha_1+\alpha_2))}{a^2 - g^*(\theta_1)g^*(\alpha_1+\alpha_2)} - \frac{2(1-g^*(\theta_2)g^*(\alpha_1+\alpha_2))}{a - g^*(\theta_2)g^*(\alpha_1+\alpha_2)} \\
& \left. + \frac{(1-g^*(\theta_2)g^*(\alpha_1+\alpha_2))}{a^2 - g^*(\theta_2)g^*(\alpha_1+\alpha_2)} + \frac{2(1-g^*(\theta_1+\theta_2)g^*(\alpha_1+\alpha_2))}{a - g^*(\theta_1+\theta_2)g^*(\alpha_1+\alpha_2)} - \frac{(1-g^*(\theta_1+\theta_2)g^*(\alpha_1+\alpha_2))}{a^2 - g^*(\theta_1+\theta_2)g^*(\alpha_1+\alpha_2)}\right]
\end{aligned} \quad (17)$$

In (16) and (17) $E(U_1) = -f^{*'}(0), \sigma_{U1}^2 = f^{*''}(0) - (f^{*'}(0))^2$,

$$C_c = \frac{1}{a - D_c} \text{ and } H_{b,d} = \frac{1}{a - D_a} \text{ , for c=1,2,3…6 , b=1,2,3 and d=4,5,6.} \quad (18)$$

$D_1 = g^*(\theta_1), D_2 = g^*(\theta_2), D_3 = g^*(\theta_1+\theta_1), D_4 = g^*(\alpha_1), D_5 = g^*(\alpha_2), D_6 = g^*(\alpha_1+\alpha_2)$ .are given by (13)

(16) gives the expected time to recruitment, (16) and (17) together with (10) gives the variance of time to recruitment.

Suppose $g(t) = g_{x(k)}(t)$. The first two moments are given by (16), (17) and (14).

Case (iii):

Let X_i be a exponential random variable denoting the loss of man-hours due to i^{th} decision epoch, i=1,2,3….with cumulative distribution function G (.) and probability density function g(.)

If U_i are exchangeable and constantly correlated exponential random variables

Considering the first term of (1) and conditioning upon y we get

$$P\left(\sum_{i=1}^{k} X_i \le Y\right) = \int_0^\infty P\left(\sum_{i=1}^{k} X_i \le Y\right) h(y)\,dy = \int_0^\infty G_k(y)\,h(y)\,dy$$

Since X_i's are assumed to be identical constantly correlated and exchangeable exponential random variables with parameter α , c.d.f of the partial sum $S_k = X_1 + X_2 + ... + X_k$ is given by Gurland(1955) as

$$G_k(y) = (1-\rho)\sum_{i=0}^{\infty} \frac{(k\rho)^i \ \phi\left(k+i, \frac{y}{b}\right)}{(1-\rho+k\rho)^{i+1}(k+i-1)!} \qquad (19)$$

where ρ is the constant correlation between X_i and X_j , i≠j.

$$\phi\left(k+i, \frac{y}{b}\right) = \int_0^{\frac{y}{b}} e^{-z} z^{k+i-1} dz \ \text{ and } \ b = \alpha(1-\rho)$$

Since the thresholds follow exponential distribution

$$h(y) = \theta_1 e^{-\theta_1 y} + \theta_2 e^{-\theta_2 y} - (\theta_1+\theta_2) e^{-(\theta_1+\theta_2)y} \qquad (20)$$

Using (19),(20) and on further simplification we get

$$\sum_{k=0}^{\infty}\left[F_k(t) - F_{k+1}(t)\right] P\left(\sum_{i=1}^{k} X_i \le Y\right) = (1-\rho)\sum_{k=0}^{\infty}\left[F_k(t) - F_{k+1}(t)\right]\left[W_{1k} + W_{2k} - W_{3k}\right] \qquad (21)$$

Similarly,

$$\sum_{k=0}^{\infty}\left[F_k(t) - F_{k+1}(t)\right] P\left(\sum_{i=1}^{k} X_i > Y\right) = \sum_{k=0}^{\infty}\left[F_k(t) - F_{k+1}(t)\right]\left[1-(1-\rho)\left[W_{1k} + W_{2k} - W_{3k}\right]\right] \qquad (22)$$

$$P\left(\sum_{i=1}^{k} X_i < Z\right) = (1-\rho)\left[W_{4k} + W_{5k} - W_{6k}\right] \qquad (23)$$

(23)

$$W_{1k} = \frac{1}{(b\theta_1+1)^{k-1}\left[(1-\rho+k\rho)(b\theta_1+1)-k\rho\right]}, \quad W_{2k} = \frac{1}{(b\theta_2+1)^{k-1}\left[(1-\rho+k\rho)(b\theta_2+1)-k\rho\right]}$$

$$W_{3k} = \frac{1}{(b(\theta_1+\theta_2)+1)^{k-1}\left[(1-\rho+k\rho)(b(\theta_1+\theta_2)+1)-k\rho\right]}, \quad W_{4k} = \frac{1}{(b\alpha_1+1)^{k-1}\left[(1-\rho+k\rho)(b\alpha_1+1)-k\rho\right]}$$

$$W_{5k} = \frac{1}{(b\alpha_2+1)^{k-1}\left[(1-\rho+k\rho)(b\alpha_2+1)-k\rho\right]}, \quad W_{6k} = \frac{1}{(b(\alpha_1+\alpha_2)+1)^{k-1}\left[(1-\rho+k\rho)(b(\alpha_1+\alpha_2)+1)-k\rho\right]}$$

(24)

Using (21) ,(22) and (23) in (1) we get

$$P(T>t) = (1-\rho)\left[\sum_{k=0}^{\infty}\left[F_k(t) - F_{k+1}(t)\right]\left[W_{1k} + W_{2k} - W_{3k}\right] + p\sum_{k=0}^{\infty}\left[F_k(t) - F_{k+1}(t)\right]\left[W_{4k} + W_{5k} - W_{6k}\right] - (1-\rho)\sum_{k=0}^{\infty}\left[F_k(t) - F_{k+1}(t)\right]\left[W_{1k} + W_{2k} - W_{3k}\right]\left[W_{4k} + W_{5k} - W_{6k}\right]\right] \qquad (25)$$

Since $L(t) = 1 - P(T>t)$ from (25).

$$L(t)=1-(1-\rho)\left[\sum_{k=0}^{\infty}\left[F_k(t)-F_{k+1}(t)\right]\left[W_{1k}+W_{2k}-W_{3k}\right]-p\sum_{k=0}^{\infty}\left[F_k(t)-F_{k+1}(t)\right]\right.$$
$$\left.\left[W_{4k}+W_{5k}-W_{6k}\right]+p(1-\rho)\sum_{k=0}^{\infty}\left[F_k(t)-F_{k+1}(t)\right]\left[W_{1k}+W_{2k}-W_{3k}\right]\left[W_{4k}+W_{5k}-W_{6k}\right]\right] \quad (26)$$

Proceeding in the same way we get the first two moments

$$E(T)=(1-\rho)u\sum_{k=0}^{\infty}(W_{1k}+W_{2k}-W_{3k})+p(W_{4k}+W_{5k}-W_{6k})$$
$$-p(1-\rho)\,(W_{1k}+W_{2k}-W_{3k})(W_{4k}+W_{5k}-W_{6k}) \quad (27)$$

$$E(T^2)=\frac{2b^2}{1-\rho}\sum_{k=0}^{\infty}\left(k(1+\rho^2)+1\right)\Big((W_{1k}+W_{2k}-W_{3k})+p(W_{4k}+W_{5k}-W_{6k})$$
$$-p(1-\rho)(W_{1k}+W_{2k}-W_{3k})(W_{4k}+W_{5k}-W_{6k})\Big) \quad (28)$$

(27) gives the expected time to recruitment,(27) and (28) together with (10) gives the variance of time to recruitment.

If U_i form a geometric process with parameter 'a', then the first two moments are given by

$$E(T)=E(U_1)(1-\rho)\sum_{k=0}^{\infty}\left(\frac{1}{a^k}\right)\left[(W_{1k}+W_{2k}-W_{3k})+p(W_{4k}+W_{5k}-W_{6k})\right.$$
$$\left.-p(1-\rho)\,(W_{1k}+W_{2k}-W_{3k})(W_{4k}+W_{5k}-W_{6k})\right] \quad (29)$$

$$E(T^2)=(1-\rho)\sum_{k=0}^{\infty}\left(V(U_1)\left(\frac{1}{a^{2k}}\right)+(E(U_1))^2\left(\sum_{j=1}^{k}\left(\frac{1}{a^{i-1}}\right)^2-\left(\sum_{j=1}^{k}\frac{1}{a^{j-1}}\right)^2\right)\right)\Big((W_{1k}+W_{2k}-W_{3k})$$
$$+p(W_{4k}+W_{5k}-W_{6k})-p(1-\rho)(W_{1k}+W_{2k}-W_{3k})(W_{4k}+W_{5k}-W_{6k})\Big) \quad (30)$$

(29) gives the expected time to recruitment, (29) and (30) together with (10) gives the variance of time to recruitment.

IV. MODEL DESCRIPTION AND ANALYSIS FOR MODEL-II

For this model, the optional and mandatory thresholds for the loss of man-hours in the organization are taken as $Y=\min(Y_A,Y_B)$ and $Z=\min(Z_A,Z_B)$. All the other assumptions and notations are as in model-I.

Case (i): Let X_i be the loss of man hours due to the i^{th} decision epoch , i=1,2,3… forming a sequence of independent and identically distributed exponential random variables with mean $\frac{1}{c}$ (c>0), probability density function g(.),U_i are exchangeable and constantly correlated exponential random variables denoting inter-decision time between $(i-1)^{th}$ and i^{th} decision, i=1,2, 3….k with cumulative distribution function F(.), probability density function f(.) and mean u .

Proceeding as in previous model we get the first two moments

$$E(T) = u\left(\frac{1}{1-g^{*}(\theta_1+\theta_2)} + p\left(\frac{1}{1-g^{*}(\alpha_1+\alpha_2)} - \frac{1}{1-g^{*}(\theta_1+\theta_2)g^{*}(\alpha_1+\alpha_2)}\right)\right) \tag{31}$$

$$E(T^2) = 2u^2\left(\frac{1+\rho^2 g^{*}(\theta_1+\theta_2)}{(1-g^{*}(\theta_1+\theta_2))^2} + p\left(\frac{1+\rho^2 g^{*}(\alpha_1+\alpha_2)}{(1-g^{*}(\alpha_1+\alpha_2))^2} - \frac{1+\rho^2 g^{*}(\theta_1+\theta_2)g^{*}(\alpha_1+\alpha_2)}{(1-g^{*}(\theta_1+\theta_2)g^{*}(\alpha_1+\alpha_2))^2}\right)\right) \tag{32}$$

(31) gives the expected time to recruitment, (31) and (32) together with (10) gives the variance of time to recruitment.

Case (ii):

Let X_i be the loss of man-hours due to the i^{th} decision epoch , i=1,2,3…k Let $X_{(1)}, X_{(2)}, X_{(3)}, \ldots X_{(n)}$ be the order statistics selected from the sample $X_1, X_2, \ldots X_n$ with respective density functions $g_{x(1)}(.), g_{x(2)}(.), \ldots g_{x(n)}(.)$,

If U_i are exchangeable and constantly correlated exponential random variables.

Suppose $g(t) = g_{x(1)}(t)$

The first two moments are given by (31),(32) and (13).

Suppose $g(t) = g_{x(k)}(t)$

The first two moments are given by (31) ,(32) and (14)

If U_i form a geometric process with parameter 'a'

Suppose $g(t) = g_{x(1)}(t)$

$$E(T) = aE(U_1)\left[C_3 + p(C_6 - H_{3,6})\right] \tag{33}$$

$$\begin{aligned} E(T^2) = {} & \frac{\sigma_{U1}^2 a^2}{(a^2-1)}\left[1 - \frac{(1-g^{*}(\theta_1+\theta_2))}{a^2 - g^{*}(\theta_1+\theta_2)}\right] + \frac{E(U_1)a^2}{(a-1)^2}\left[\left[1 - \frac{2(1-g^{*}(\theta_1+\theta_2))}{a-g^{*}(\theta_1+\theta_2)} + \frac{1-g^{*}(\theta_1+\theta_2)}{a^2-g^{*}(\theta_1+\theta_2)}\right]\right. \\ & + p\frac{\sigma_{U1}^2 a^2}{(a^2-1)}\left[\frac{-(1-g^{*}(\alpha_1+\alpha_2))}{a^2-g^{*}(\alpha_1+\alpha_2)} + \frac{(1-g^{*}(\theta_1+\theta_2)g^{*}(\alpha_1+\alpha_2))}{a^2-g^{*}(\theta_1+\theta_2)g^{*}(\alpha_1+\alpha_2)}\right] \\ & \left. + \frac{E(U_1)a^2}{(a-1)^2}\left[-\frac{2(1-g^{*}(\alpha_1+\alpha_2))}{a-g^{*}(\alpha_1+\alpha_2)} + \frac{1-g^{*}(\alpha_1+\alpha_2)}{a^2-g^{*}(\alpha_1+\alpha_2)} + \frac{2(1-g^{*}(\theta_1+\theta_2)g^{*}(\alpha_1+\alpha_2))}{a-g^{*}(\theta_1+\theta_2)g^{*}(\alpha_1+\alpha_2)} - \frac{(1-g^{*}(\theta_1+\theta_2)g^{*}(\alpha_1+\alpha_2))}{a^2-g^{*}(\theta_1+\theta_2)g^{*}(\alpha_1+\alpha_2)}\right]\right] \end{aligned} \tag{34}$$

Where $g^{*}_{x(1)}(\tau)$ $\tau = \theta_1+\theta_2, \alpha_1+\alpha_2$ is given by (13)

(33) gives the expected time to recruitment, (33) and (34) together with (10) gives the variance of time to recruitment.

Suppose $g(t) = g_{x(k)}(t)$

The first two moments are given by (33),(34) and (14).

Case (iii):

Let X_i be a exponential random variable denoting the loss of man-hours due to i^{th} decision epoch, i=1,2,3….with cumulative distribution function G (.) and probability density function g(.)

If U_i are exchangeable and constantly correlated exponential random variables.

The first two moments are given by

$$E(T) = (1-\rho)u\sum_{k=0}^{\infty}\left(W_{3k} + pW_{6k} - p(1-\rho)W_{3k}W_{6k}\right) \tag{35}$$

$$E(T^2) = \frac{2b^2}{1-\rho}\sum_{k=0}^{\infty}\left(k(1+\rho^2)+1\right)\left(W_{3k} + pW_{6k} - p(1-\rho)W_{3k}W_{6k}\right) \tag{36}$$

where W_{ak} ,(a=3,6) are given by (24).

If U_i forms geometric process then the first two moments are given by

$$E(T) = E(U_1)(1-\rho)\sum_{k=0}^{\infty}\left(\frac{1}{a^k}\right)\left(W_{3k} + pW_{6k} - p(1-\rho)W_{3k}W_{6k}\right) \tag{37}$$

$$E(T^2) = (1-\rho)\sum_{k=0}^{\infty}\left(V(U_1)\left(\frac{1}{a^{2k}}\right) + (E(U)_1)^2\left(\sum_{j=1}^{k}\left(\frac{1}{a^{i-1}}\right)^2 - \left(\sum_{j=1}^{k}\frac{1}{a^{j-1}}\right)^2\right)\right)\left(W_{3k} + pW_{6k} - p(1-\rho)W_{3k}W_{6k}\right) \tag{38}$$

where W_{ak} ,(a=3,6) are given by (24).

V. MODEL DESCRIPTION AND ANALYSIS OF MODEL-III

For this model, the optional and mandatory thresholds for the loss of man-hours in the organization are taken as $Y = Y_1 + Y_2$ and $Z = Z_1 + Z_2$ .All the other assumptions and notations are as in model-I.

$$P\left(\sum_{i=1}^{k} X_i < Y\right) = \int_0^{\infty}\left(\frac{\theta_1 e^{-\theta_2 x}}{\theta_1 - \theta_2} - \frac{\theta_2 e^{-\theta_1 x}}{\theta_1 - \theta_2}\right) g_k(x)\,dx$$

$$\text{(i.e) } P\left(\sum_{i=1}^{k} X_i < Y\right) = \frac{\theta_1}{\theta_1 - \theta_2} g^*(\theta_2)^k - \frac{\theta_2}{\theta_1 - \theta_2} g^*(\theta_1)^k$$

Case (i): Let X_i be the loss of man hours due to the i^{th} decision epoch , i=1,2,3… forming a sequence of independent and identically distributed exponential random variables with mean $\frac{1}{c}$ (c>0), probability density function g(.),U_i are exchangeable and constantly correlated exponential random variables denoting inter-decision time between (i-1)th and i^{th} decision, i=1,2, 3….k with cumulative distribution function F(.), probability density function f(.) and mean u .

Proceeding as in model –I we get the first two moments

$$E(T) = u\left(\frac{A_2}{1-g^*(\theta_2)} - \frac{A_1}{1-g^*(\theta_1)} + p\left(\frac{A_5}{1-g^*(\alpha_2)} - \frac{A_4}{1-g^*(\alpha_1)} - \frac{A_1A_4}{1-g^*(\theta_1)g^*(\alpha_1)} + \frac{A_2A_4}{1-g^*(\theta_2)g^*(\alpha_1)} + \frac{A_1A_5}{1-g^*(\theta_1)g^*(\alpha_2)} - \frac{A_2A_5}{1-g^*(\theta_2)g^*(\alpha_2)}\right)\right) \quad (39)$$

$$E(T^2) = 2u^2\left(A_2\frac{1+\rho^2 g^*(\theta_2)}{(1-g^*(\theta_2))^2} - A_1\frac{1+\rho^2 g^*(\theta_1)}{(1-g^*(\theta_1))^2} + p\left(A_5\frac{1+\rho^2 g^*(\alpha_2)}{(1-g^*(\alpha_2))^2} - A_4\frac{1+\rho^2 g^*(\alpha_1)}{(1-g^*(\alpha_1))^2} - A_1A_4\frac{1+\rho^2 g^*(\theta_1)g^*(\alpha_1)}{(1-g^*(\theta_1)g^*(\alpha_1))^2} + A_2A_4\frac{1+\rho^2 g^*(\theta_2)g^*(\alpha_1)}{(1-g^*(\theta_2)g^*(\alpha_1))^2} + A_1A_5\frac{1+\rho^2 g^*(\theta_1)g^*(\alpha_2)}{(1-g^*(\theta_1)g^*(\alpha_2))^2} - A_2A_5\frac{1+\rho^2 g^*(\theta_2)g^*(\alpha_2)}{(1-g^*(\theta_2)g^*(\alpha_2))^2}\right)\right) \quad (40)$$

In (39) and (40) $A_1 = \frac{\theta_2}{\theta_1-\theta_2}, A_2 = \frac{\theta_1}{\theta_1-\theta_2}, A_4 = \frac{\alpha_2}{\alpha_1-\alpha_2}, A_5 = \frac{\alpha_1}{\alpha_1-\alpha_2}$

(39) gives the mean time to recruitment, (39) and (40) together with (10) gives the variance of the time to recruitment .

Case (ii):

Let x_i be the loss of man-hours due to the i^{th} decision epoch , i=1,2,3…k Let $X_{(1)}, X_{(2)}, X_{(3)}, \ldots X_{(n)}$ be the order statistics selected from the sample $X_1, X_2, \ldots X_n$ with respective density functions $g_{x(1)}(.), g_{x(2)}(.), \ldots g_{x(n)}(.)$,

If U_i are exchangeable and constantly correlated exponential random variables.

$$\text{If } g(t) = g_{x(1)}(t)$$

The first two moments are given by (39),(40) and (13) .

$$\text{If } g(t) = g_{x(k)}(t)$$

The first two moments are given by (39) ,(40)and (14)

If U_i form a geometric process with parameter 'a', then the first two moments are given by

Suppose $g(t) = g_{x(1)}(t)$

$$E(T) = aE(U_1)\left[A_2C_2 - A_1C_1 + p\left(A_5C_5 - A_4C_4 - A_1A_4H_{1,4} + A_2A_4H_{2,4} + A_1A_5H_{1,5} - A_2A_5H_{2,5}\right)\right] \quad (41)$$

$$E(T^2)=\frac{\sigma_{U1}^2 a^2}{(a^2-1)}\left[A_2\left(1-\frac{(1-g^*(\theta_2))}{a^2-g^*(\theta_2)}\right)-A_1\left(1-\frac{(1-g^*(\theta_1))}{a^2-g^*(\theta_1)}\right)\right]+\frac{E(U_1)a^2}{(a-1)^2}\left[A_2\left[1-\frac{2(1-g^*(\theta_2))}{a-g^*(\theta_2)}+\frac{1-g^*(\theta_2)}{a^2-g^*(\theta_2)}\right]\right.$$
$$-A_1\left[1-\frac{2(1-g^*(\theta_1))}{a-g^*(\theta_1)}+\frac{1-g^*(\theta_1)}{a^2-g^*(\theta_1)}\right]+p\frac{\sigma_{U1}^2 a^2}{(a^2-1)}\left[A_5\left(1-\frac{(1-g^*(\alpha_2))}{a^2-g^*(\alpha_2)}\right)-A_4\left(1-\frac{(1-g^*(\alpha_1))}{a^2-g^*(\alpha_1)}\right)-A_1A_4\left(\frac{(1-g^*(\theta_1)g^*(\alpha_1))}{a^2-g^*(\theta_1)g^*(\alpha_1)}\right)\right.$$
$$\left.+A_2A_4\left(\frac{(1-g^*(\theta_2)g^*(\alpha_1))}{a^2-g^*(\theta_2)g^*(\alpha_1)}\right)+A_1A_5\left(\frac{(1-g^*(\theta_1)g^*(\alpha_2))}{a^2-g^*(\theta_1)g^*(\alpha_2)}\right)-A_2A_5\left(\frac{(1-g^*(\theta_2)g^*(\alpha_2))}{a^2-g^*(\theta_2)g^*(\alpha_2)}\right)\right]$$
$$+\frac{pE(U_1)a^2}{(a-1)^2}\left[\left[A_5\left(1-\frac{2(1-g^*(\alpha_2))}{a-g^*(\alpha_2)}+\frac{1-g^*(\alpha_2)}{a^2-g^*(\alpha_2)}\right)-A_4\left(1-\frac{2(1-g^*(\alpha_1))}{a-g^*(\alpha_1)}+\frac{1-g^*(\alpha_1)}{a^2-g^*(\alpha_1)}\right)\right.\right.$$
$$-A_1A_4\left(1-\frac{2(1-g^*(\theta_1)g^*(\alpha_1))}{a-g^*(\theta_1)g^*(\alpha_1)}+\frac{1-g^*(\theta_1)g^*(\alpha_1)}{a^2-g^*(\theta_1)g^*(\alpha_1)}\right)+A_2A_4\left(1-\frac{2(1-g^*(\theta_2)g^*(\alpha_1))}{a-g^*(\theta_2)g^*(\alpha_1)}+\frac{1-g^*(\theta_2)g^*(\alpha_1)}{a^2-g^*(\theta_2)g^*(\alpha_1)}\right)$$
$$\left.\left.+A_1A_5\left(1-\frac{2(1-g^*(\theta_1)g^*(\alpha_2))}{a-g^*(\theta_1)g^*(\alpha_2)}+\frac{1-g^*(\theta_1)g^*(\alpha_2)}{a^2-g^*(\theta_1)g^*(\alpha_2)}\right)-A_2A_5\left(1-\frac{2(1-g^*(\theta_2)g^*(\alpha_2))}{a-g^*(\theta_2)g^*(\alpha_2)}+\frac{1-g^*(\theta_2)g^*(\alpha_2)}{a^2-g^*(\theta_2)g^*(\alpha_2)}\right)\right]\right.$$

(42)

(41) gives the mean time to recruitment , (41) and (42) together with (10) gives the variance of the time to recruitment .

where $g^*_{x(1)}(\tau)$, $\tau=\theta_1,\theta_2\alpha_1,\alpha_2$ is given by (13).

Suppose $g(t)=g_{x(k)}(t)$.

The first two moments are given by (41),(42) and (14)

Case (iii):

Let X_i be a exponential random variable denoting the loss of man-hours due to i^{th} decision epoch, i=1,2,3….with cumulative distribution function G (.) and probability density function g(.)

If U_i form a geometric process with parameter 'a'.

The first two moments of time to recruitment is given by

$$E(T)=(1-\rho)u\sum_{k=0}^{\infty}\left(\frac{1}{k}\right)\left[(W_{33k}-W_{34k})+p(W_{35k}-W_{36k})\right.$$
$$\left.-p(1-\rho)(W_{33k}-W_{34k})(W_{35k}-W_{36k})\right] \qquad (43)$$

$$E(T^2)=\frac{2b^2}{1-\rho}\sum_{k=0}^{\infty}\left(k(1+\rho^2)+1\right)\left[(W_{33k}-W_{34k})+p(W_{35k}-W_{36k})\right.$$
$$\left.-p(1-\rho)(W_{33k}-W_{34k})(W_{35k}-W_{36k})\right]$$

(44)

$$W_{33k}=\frac{\theta_1}{(\theta_1-\theta_2)(b\theta_2+1)^{k-1}[(1-\rho+k\rho)(b\theta_2+1)-k\rho]}$$

$$W_{34k} = \frac{\theta_2}{(\theta_1 - \theta_2)(b\theta_1 + 1)^{k-1}[(1-\rho+k\rho)(b\theta_1 + 1) - k\rho]}$$

$$W_{35k} = \frac{\alpha_1}{(\alpha_1 - \alpha_2)(b\alpha_2 + 1)^{k-1}[(1-\rho+k\rho)(b\alpha_2 + 1) - k\rho]} \quad (45)$$

$$W_{36k} = \frac{\alpha_2}{(\alpha_1 - \alpha_2)(b\alpha_1 + 1)^{k-1}[(1-\rho+k\rho)(b\alpha_1 + 1) - k\rho]}$$

(43) gives the expected time to recruitment, (43) and (44) together with (10) gives the variance of time to recruitment.

If U_i form a geometric process with parameter 'a'

Then the first two moments are given by

$$E(T) = (1-\rho)E(U_1)\sum_{k=0}^{\infty}\left(\frac{1}{a^k}\right)\left[(W_{33k} - W_{34k}) + p(W_{35k} - W_{36k}) - p(1-\rho)(W_{33k} - W_{34k})(W_{35k} - W_{36k})\right] \quad (46)$$

$$E(T^2) = (1-\rho)\sum_{k=0}^{\infty}\left(V(U_1)\left(\frac{1}{a^{2k}}\right) + (E(U_1))^2\left(\sum_{j=1}^{k}\left(\frac{1}{a^{i-1}}\right)^2 - \left(\sum_{j=1}^{k}\frac{1}{a^{j-1}}\right)^2\right)\right)\left[(W_{33k} - W_{34k}) + p(W_{35k} - W_{36k}) - p(1-\rho)(W_{33k} - W_{34k})(W_{35k} - W_{36k})\right] \quad (47)$$

Where W_{ak} ,a=33,34,35,36 are given by (45) .

(46) gives the expected time to recruitment, (46) and (47) together with (10) gives the variance of time to recruitment.

VI. NUMERICAL ILLUSTRATIONS

The mean and variance of the time to recruitment for all the models are given in the following tables for the cases (i) and (ii),

Case (i):Table – I(a) (Effect of ρ on performance measures)

$$\theta_1 = 0.4, \theta_2 = 0.6, \alpha_1 = 0.5, \alpha_2 = 0.8, p = 0.8, c = 2.5$$

ρ	MODEL I		MODEL II		MODEL III	
	E(T)	V(T)	E(T)	V(T)	E(T)	V(T)
0.6	26.9969	699.2067	10.8231	139.4303	34.1896	1.3954e+003
0.7	35.9959	1.4628e+003	14.4308	282.2801	45.5861	2.8775e+003
0.8	53.9938	3.8617e+003	21.6462	724.4484	68.3791	7.5047e+003

Case (ii):

Table – II (a) (Effect of ρ and k on performance measures)

$$\theta_1 = 0.4, \theta_2 = 0.6, \alpha_1 = 0.5, \alpha_2 = 0.8, p = 0.8, c = 1.5$$

$g(t) = g_{x(1)}(t)$							
ρ	k	MODEL I		MODEL II		MODEL III	
		E(T)	V(T)	E(T)	V(T)	E(T)	V(T)
0.6	2	31.7785	964.2689	12.4203	184.3391	40.4002	1.9427e+003
0.7	2	42.3713	2.0227e+003	16.5604	374.701	53.8669	4.015e+003
0.8	2	63.5569	5.352e+003	24.8405	965.0629	80.8003	1.0491e+004
0.6	1	17.4197	296.0506	7.6103	68.1898	21.7516	570.7102
0.6	2	31.7785	964.2689	12.4203	184.3391	40.4002	1.9427e+003
0.6	3	46.1127	2.1034e+003	17.1967	356.3135	59.0232	4.1246e+003

Table – II (b) (Effect of ρ and k on performance measures)

$$\theta_1 = 0.4, \theta_2 = 0.6, \alpha_1 = 0.5, \alpha_2 = 0.8, p = 0.8, c = 1.5$$

$g(t) = g_{x(k)}(t)$							
ρ	K	MODEL I		MODEL II		MODEL III	
		E(T)	V(T)	E(T)	V(T)	E(T)	V(T)
0.6	2	11.824	136.893	5.3347	33.1588	14.7110	260.1546
0.7	2	15.7667	280.3428	7.1129	64.8872	19.6147	527.0417
0.8	2	23.65	726.7705	10.6694	161.4127	29.4220	1.3534e+003
0.6	1	17.4197	296.0506	7.6103	68.1898	21.7516	570.7102
0.6	2	11.825	136.893	5.3347	33.1588	14.7110	260.1546
0.6	3	9.8102	94.6229	4.5346	23.7928	12.1695	177.7643

VI. FINDINGS

From the tables we observe the following which agree with reality

case (i) :

- As ρ increases , the mean and variance of time to recruitment increase for all the models .

case (ii)

- As ρ increases , the mean and variance of time to recruitment increase for all models when the probability density function of loss of manpower is the probability density function of first order statistics and k-th order statistics.
- As k increases , the mean and variance of time to recruitment increase for all models when the probability density function of loss of manpower is the probability density function first order statistics and decrease when the probability density function of loss of manpower is the probability density function of k-th order statistics.

Some Properties of Intuitionistic L-Fuzzy Subnearrings of a Nearring

B. Thenmozhi*
Department of Mathematics,
Syed ammal Engineering College
Ramanathapuram
Tamil Nadu, India.

S. Karthikeyan
Department of Mathematics
Velammal College of Engineering and Technology,
Madurai, Tamil Nadu, India.

S. Naganathan
Department of Mathematics,
Government Arts College Pollachi,
Udumalapet, Tamil Nadu, India.

***Abstract*—In this paper, we study some of the properties of intuitionistic L-fuzzy subnearring of a nearring and prove some results on these. With the expectations that these results may be applied in different fields.**

Keywords—L-fuzzy subset, intuitionistic L-fuzzy subset, intuitionistic L-fuzzy subnearring, intuitionistic L-fuzzy relation, Product of intuitionistic L-fuzzy subsets.

I. INTRODUCTION

After the introduction of fuzzy sets by L.A.Zadeh[15], several researchers explored on the generalization of the notion of fuzzy set. The concept of intuitionistic L-fuzzy subset was introduced by K.T.Atanassov[4,5], as a generalization of the notion of fuzzy set. Azriel Rosenfeld[6] defined a fuzzy groups. Asok Kumer Ray[3] defined a product of fuzzy subgroups. We introduce the concept of intuitionistic L-fuzzy subnearring of a nearring and established some results.

II. PRELIMINARIES

Definition 2.1. *Let X be a non-empty set and L = (L, ≤) be a lattice with least element 0 and greatest element 1. A L-fuzzy subset A of X is a function* $A : X \to L$.

Definition 2.2. *Let (L, ≤) be a complete lattice with an involutive order reversing operation* $N : L \to L$.
An intuitionistic L-fuzzy subset (ILFS) A in X is defined as an object of the form $A=\{< x, \mu_A(x), \nu_A(x) > / x \text{ in } X\}$, *where* $\mu_A : X \to L$ *and* $\nu_A : X \to L$ *define the degree of membership and the degree of non-membership of the element* $x \in X$ *respectively and for every* $x \in X$ *satisfying* $\mu_A(x) \le N(\nu_A(x))$.

Definition 2.3. *Let (R, +, •) be a nearring. A intuitionistic L-fuzzy subset A of R is said to be an intuitionistic L-fuzzy subnearring (ILFSNR) of R if it satisfies the following axioms:*

(i) $\mu_A(x - y) \ge \mu_A(x) \wedge \mu_A(y)$

(ii) $\mu_A(xy) \ge \mu_A(x) \wedge \mu_A(y)$

(iii) $\nu_A(x - y) \le \nu_A(x) \vee \nu_A(y)$

(iv) $\nu_A(xy) \le \nu_A(x) \vee \nu_A(y)$, *for all x and y in R.*

Definition 2.4. *Let A and B be any two intuitionistic L-fuzzy subnearrings of nearrings* R_1 *and* R_2 *respectively. The product of A and B denoted by AxB is defined as* $AxB=\{\langle (x, y), \mu_{AxB}(x, y), \nu_{AxB}(x, y)\rangle / \text{for all } x \text{ in } R_1 , y \text{ in } R_2\}$, *where* $\mu_{AxB}(x,y) = \mu_A(x) \wedge \mu_B(y)$ *and* $\nu_{AxB}(x, y) = \nu_A(x) \vee \nu_B(y)$.

Definition 2.5. *Let A be an intuitionistic L-fuzzy subset in a set S, the strongest intuitionistic L-fuzzy relation on S, that is an intuitionistic L-fuzzy relation on A is V given by* $\mu_V(x, y) = \mu_A(x) \wedge \mu_A(y)$ *and* $\nu_V(x, y) = \nu_A(x) \vee \nu_A(y)$, *for all x and y in S.*

Definition 2.6. *Let X and X′ be any two sets. Let* $f : X \to X'$ *be any function and A be a intuitionistic L-fuzzy subset in X, V be an intuitionistic L-fuzzy subset in f(X) = X′, defined by*

$$\mu_V(y) = \sup_{x \in f^{-1}(y)} \mu_A(x) \text{ and } \nu_V(y) = \inf_{x \in f^{-1}(y)} \nu_A(x), \text{ for all}$$

x in X and y in X′. A is called a pre image of V under f and is denoted by $f^{-1}(V)$.

III. SOME PROPERTIES OF INTUITIONISTIC L- FUZZY SUBNEARRINGS OF A NEARRING

Theorem 3.1. *Intersection of any two intuitionistic L-fuzzy subnearrings of a nearring R is a intuitionistic L-fuzzy subnearring of R.*

Proof. Let A and B be any two intuitionistic L-fuzzy subnearrings of a nearring R and x and y in R. Let $A = \{(x,\mu_A(x),\nu_A(x))/x \in R\}$ and $B = \{ (x, \mu_B(x), \nu_B(x)) /$

$x \in R\}$ and also let $C = A \cap B = \{ (x, \mu_C(x), \nu_C(x)) / x \in R\}$, where $\mu_A(x) \wedge \mu_B(x) = \mu_C(x)$ and $\nu_A(x) \vee \nu_B(x) = \nu_C(x)$. Now, $\mu_C(x-y) \geq [\mu_A(x) \wedge \mu_A(y)] \wedge [\mu_B(x) \wedge \mu_B(y)] = [\mu_A(x) \wedge \mu_B(x)] \wedge [\mu_A(y) \wedge \mu_B(y)] = \mu_C(x) \wedge \mu_C(y)$. Therefore, $\mu_C(x - y) \geq \mu_C(x) \wedge \mu_C(y)$, for all x and y in R.
And, $\mu_C(xy) \geq [\mu_A(x) \wedge \mu_A(y)] \wedge [\mu_B(x) \wedge \mu_B(y)] = [\mu_A(x) \wedge \mu_B(x)] \wedge [\mu_A(y) \wedge \mu_B(y)] = \mu_C(x) \wedge \mu_C(y)$. Therefore, $\mu_C(xy) \geq \mu_C(x) \wedge \mu_C(y)$, for all x and y in R. Also, $\nu_C(x - y) \leq [\nu_A(x) \vee \nu_A(y)] \vee [\nu_B(x) \vee \nu_B(y)] = [\nu_A(x) \vee \nu_B(x)] \vee [\nu_A(y) \vee \nu_B(y)] = \nu_C(x) \vee \nu_C(y)$. Therefore, $\nu_C(x-y) \leq \nu_C(x) \vee \nu_C(y)$, for all x and y in R. And, $\nu_C(xy) \leq [\nu_A(x) \vee \nu_A(y)] \vee [\nu_B(x) \vee \nu_B(y)] = [\nu_A(x) \vee \nu_B(x)] \vee [\nu_A(y) \vee \nu_B(y)] = \nu_C(x) \vee \nu_C(y)$. Therefore, $\nu_C(xy) \leq \nu_C(x) \vee \nu_C(y)$, for all x and y in R. Therefore, C is an intuitionistic L-fuzzy subnearring of a nearring R.

Thorem 3.2. *Let (R, +, •) is a nearring. The intersection of a family of intuitionistic L-fuzzy subnearrings of R is an intuitionistic L-fuzzy subnearring of R.*

Proof. It is trivial.

Theorem 3.3. *If A and B are any two intuitionistic L-fuzzy subnearrings of the nearrings R_1 and R_2 respectively, then AxB is an intuitionistic L-fuzzy subnearring of R_1xR_2.*

Proof. Let A and B be two intuitionistic L-fuzzy subnearrings of the nearrings R_1 and R_2 respectively. Let x_1 and x_2 be in R_1 and y_1, y_2 be in R_2. Then (x_1, y_1) and (x_2, y_2) in R_1xR_2. Now, $\mu_{AxB}[(x_1, y_1) - (x_2, y_2)] = \mu_A(x_1 - x_2) \wedge \mu_B(y_1 - y_2) \geq [\mu_A(x_1) \wedge \mu_A(x_2)] \wedge [\mu_B(y_1) \wedge \mu_B(y_2)] = [\mu_A(x_1) \wedge \mu_B(y_1)] \wedge [\mu_A(x_2) \wedge \mu_B(y_2)] = \mu_{AxB}(x_1, y_1) \wedge \mu_{AxB}(x_2, y_2)$. Therefore,

$\mu_{AxB}[(x_1, y_1) - (x_2, y_2)] \geq \mu_{AxB}(x_1, y_1) \wedge \mu_{AxB}(x_2, y_2)$, for all

(x_1, y_1) and (x_2, y_2) in R_1xR_2. Also, $\mu_{AxB}[(x_1, y_1)(x_2, y_2)] = \mu_A(x_1x_2) \wedge \mu_B(y_1y_2) \geq [\mu_A(x_1) \wedge \mu_A(x_2)] \wedge [\mu_B(y_1) \wedge \mu_B(y_2)] = [\mu_A(x_1) \wedge \mu_B(y_1)] \wedge [\mu_A(x_2) \wedge \mu_B(y_2)] = \mu_{AxB}(x_1, y_1) \wedge \mu_{AxB}(x_2, y_2)$. Therefore, $\mu_{AxB}[(x_1, y_1)(x_2, y_2)] \geq \mu_{AxB}(x_1, y_1) \wedge \mu_{AxB}(x_2, y_2)$, for all (x_1, y_1), (x_2, y_2) in R_1xR_2. And, $\nu_{AxB}[(x_1, y_1) - (x_2, y_2)] =$

$\nu_A(x_1 - x_2) \vee \nu_B(y_1 - y_2) \leq [\nu_A(x_1) \vee \nu_A(x_2)] \vee [\nu_B(y_1) \vee \nu_B(y_2)] = [\nu_A(x_1) \vee \nu_B(y_1)] \vee [\nu_A(x_2) \vee \nu_B(y_2)] = \nu_{AxB} (x_1, y_1) \vee \nu_{AxB} (x_2, y_2)$. Therefore, $\nu_{AxB}[(x_1, y_1) - (x_2, y_2)] \leq \nu_{AxB}(x_1, y_1) \vee \nu_{AxB} (x_2, y_2)$, for all (x_1, y_1), (x_2, y_2) in R_1xR_2. Also, $\nu_{AxB} [(x_1, y_1)(x_2, y_2)] = \nu_A(x_1x_2) \vee \nu_B(y_1y_2) \leq [\nu_A(x_1) \vee \nu_A(x_2)] \vee [\nu_B(y_1) \vee \nu_B(y_2)] = [\nu_A(x_1) \vee \nu_B(y_1)] \vee [\nu_A(x_2) \vee \nu_B(y_2)] = \nu_{AxB}(x_1, y_1) \vee \nu_{AxB} (x_2, y_2)$. Therefore, $\nu_{AxB} [(x_1, y_1)(x_2, y_2)] \leq \nu_{AxB} (x_1, y_1) \vee \nu_{AxB}(x_2, y_2)$, for all (x_1, y_1), (x_2, y_2) in R_1xR_2. Hence AxB is an intuitionistic L-fuzzy subnearring of R_1xR_2.

Theorem 3.4. *Let A and B be intuitionistic L-fuzzy subnearrings of the nearrings R_1 and R_2 respectively. Suppose that e and e^l are the identity element of R_1 and R_2 respectively. If AxB is an intuitionistic L-fuzzy subnearring of R_1xR_2, then at least one of the following two statements must hold.*

(i) $\mu_B(e^l) \geq \mu_A(x)$ *and* $\nu_B(e^l) \leq \nu_A(x)$, *for all x in* R_1,

(ii) $\mu_A(e) \geq \mu_B(y)$ *and* $\nu_A(e) \leq \nu_B(y)$, *for all y in* R_2.

Proof. Let AxB be an intuitionistic L-fuzzy subnearring of R_1xR_2. By contraposition, suppose that none of the statements (i) and (ii) holds. Then we can find a in R_1 and b in R_2 such that $\mu_A(a) > \mu_B(e^l)$, $\nu_A(a) < \nu_B(e^l)$ and $\mu_B(b) > \mu_A(e)$, $\nu_B(b) < \nu_A(e)$. We have, $\mu_{AxB}(a, b) > \mu_B(e^l) \wedge \mu_A(e) = \mu_A(e) \wedge \mu_B(e^l) = \mu_{AxB}(e, e^l)$. And, $\nu_{AxB} (a, b) < \nu_B(e^l) \vee \nu_A(e) = \nu_A(e) \vee \nu_B(e^l) = \nu_{AxB} (e, e^l)$. Thus AxB is not an intuitionistic L-fuzzy subnearring of R_1xR_2. Hence either $\mu_B(e^l) \geq \mu_A(x)$ and $\nu_B(e^l) \leq \nu_A(x)$, for all x in R_1 or $\mu_A(e) \geq \mu_B(y)$ and $\nu_A(e) \leq \nu_B(y)$, for all y in R_2.

Theorem 3.5. Let A and B be two intuitionistic L-fuzzy subsets of the nearrings R_1 and R_2 respectively and AxB is an intuitionistic L-fuzzy subnearring of R_1xR_2. Then the following are true:

if $\mu_A(x) \leq \mu_B(e^l)$ and $\nu_A(x) \geq \nu_B(e^l)$, then A is an intuitionistic L-fuzzy subnearring of R_1.

(i) if $\mu_A(x) \leq \mu_B(e^l)$ and $\nu_A(x) \geq \nu_B(e^l)$, then A is an intuitionistic L-fuzzy subnearring of R_1.

(ii) if $\mu_B(x) \leq \mu_A(e)$ and $\nu_B(x) \geq \nu_A(e)$, then B is an intuitionistic L-fuzzy subnearring of R_2.

(iii) either A is an intuitionistic L-fuzzy subnearring of R_1 or B is an intuitionistic L-fuzzy subnearring of R_2.

Proof. Let AxB be an intuitionistic L-fuzzy subnearring of R_1xR_2, x, y in $R_1$and e^l in R_2. Then (x, e^l) and (y, e^l) are in R_1xR_2. Now, using the property that $\mu_A(x) \leq \mu_B(e^l)$ and $\nu_A(x) \geq \nu_B(e^l)$, for all x in R_1, we get, $\mu_A(x-y) = \mu_{AxB} [(x-y), (e^l+e^l)] \geq \mu_{AxB} (x, e^l) \wedge \mu_{AxB} (-y, e^l) = [\mu_A(x) \wedge \mu_B (e^l)] \wedge$

$[\mu_A(-y) \wedge \mu_B(e^l)] = \mu_A(x) \wedge \mu_A(-y) \geq \mu_A(x) \wedge \mu_A(y)$. Therefore, $\mu_A(x- y) \geq \mu_A(x) \wedge \mu_A(y)$, for all x and y in R_1. Also, $\mu_A(xy) = \mu_{AxB} [(xy), (e^le^l)] \geq \mu_{AxB}(x, e^l) \wedge \mu_{AxB}(y, e^l) = [\mu_A(x) \wedge \mu_B(e^l] \wedge [\mu_A(y) \wedge \mu_B(e^l)] = \mu_A(x) \wedge \mu_A(y)$. Therefore, $\mu_A(xy) \geq$

$\mu_A(x) \wedge \mu_A(y)$, for all x and y in R_1. And, $\nu_A(x-y) = \nu_{AxB} [(x-y), (e^l+e^l)] \leq \nu_{AxB}(x, e^l) \vee \nu_{AxB}(-y, e^l) = [\nu_A(x) \vee \nu_B(e^l)] \vee [\nu_A(-y) \vee \nu_B(e^l)] = \nu_A(x) \vee \nu_A(-y) \leq \nu_A(x) \vee \nu_A(y)$. Therefore, $\nu_A(x-y) \leq \nu_A(x) \vee \nu_A(y)$, for all x and y in R_1. Also, $\nu_A(xy) = \nu_{AxB}[(xy), (e^le^l)] \leq \nu_{AxB}(x, e^l) \vee \nu_{AxB}(y, e^l) = [\nu_A(x) \vee \nu_B(e^l)] \vee [\nu_A(y) \vee \nu_B(e^l)] = \nu_A(x) \vee \nu_A(y)$. Therefore, $\nu_A(xy) \leq \nu_A(x) \vee \nu_A(y)$, for all x and y in R_1. Hence A is an intuitionistic L-fuzzy subnearring of R_1. Thus (i) is proved. Now, using the property that $\mu_B(x) \leq \mu_A(e)$ and $\nu_B(x) \geq \nu_A(e)$, for all x in R_2. Let x and y in R_2 and e in R_1. Then (e, x) and (e, y) are in R_1xR_2. We get, $\mu_B(x-y) = \mu_{AxB}[(e+e), (x-y)] \geq \mu_{AxB}(e, x) \wedge \mu_{AxB}(e, -y) = [\mu_A(e) \wedge \mu_B(x)] \wedge [\mu_A(e) \wedge \mu_B(-y)] = \mu_B(x) \wedge \mu_B(-y) \geq \mu_B(x) \wedge \mu_B(y)$. Therefore, $\mu_B(x-y) \geq \mu_B(x) \wedge \mu_B(y)$, for all x and y in R_2. Also, $\mu_B(xy) = \mu_{AxB}[(ee), (xy)] \geq \mu_{AxB}(e, x) \wedge \mu_{AxB}(e, y) = [\mu_A(e) \wedge \mu_B(x)] \wedge [\mu_A(e) \wedge \mu_B(y)] = \mu_B(x) \wedge \mu_B(y)$. Therefore, $\mu_B(xy) \geq \mu_B(x) \wedge \mu_B(y)$, for all

x and y in R_2. And, $\nu_B(x-y) = \nu_{AxB}[(e+e), (x-y)] \leq \nu_{AxB}(e, x) \vee \nu_{AxB}(e, -y) = [\nu_A(e) \vee \nu_B(x)] \vee [\nu_A(e) \vee \nu_B(-y)] = \nu_B(x) \vee \nu_B(-y) \leq \nu_B(x) \vee \nu_B(y)$. Therefore, $\nu_B(x-y) \leq \nu_B(x) \vee \nu_B(y)$, for all x and y in R_2. Also, $\nu_B(xy) = \nu_{AxB}[(ee), (xy)] \leq \nu_{AxB}(e, x) \vee \nu_{AxB}(e, y) = [\nu_A(e) \vee \nu_B(x)] \vee [\nu_A(e) \vee \nu_B(y)] = \nu_B(x) \vee \nu_B(y)$. Therefore, $\nu_B(xy) \leq \nu_B(x) \vee \nu_B(y)$, for all x and y in R_2. Hence B is an intuitionistic L-fuzzy subnearring of a nearring R_2. Thus (ii) is proved. (iii) is clear.

Theorem 3.6. *Let A be an intuitionistic L-fuzzy subset of a nearring R and V be the strongest intuitionistic L-fuzzy relation of R. Then A is an intuitionistic L-fuzzy subnearring of R if and only if V is an intuitionistic L-fuzzy subnearring of of RxR.*

Proof. Suppose that A is an intuitionistic L-fuzzy subnearring of a nearring R. Then for any $x = (x_1, x_2)$ and $y = (y_1, y_2)$ are in RxR. We have, $\mu_V(x-y) = \mu_V[(x_1-y_1, x_2-y_2)] \geq [\mu_A(x_1) \wedge \mu_A(y_1)] \wedge [\mu_A(x_2) \wedge \mu_A(y_2)] = [\mu_A(x_1) \wedge \mu_A(x_2)] \wedge [\mu_A(y_1) \wedge \mu_A(y_2)] = \mu_V(x_1, x_2) \wedge \mu_V(y_1, y_2) = \mu_V(x) \wedge \mu_V(y)$. Therefore, $\mu_V(x-y) \geq \mu_V(x) \wedge \mu_V(y)$, for all x and y in RxR. And, $\mu_V(xy) = \mu_V[(x_1y_1, x_2y_2)] \geq [\mu_A(x_1) \wedge \mu_A(y_1)] \wedge [\mu_A(x_2) \wedge \mu_A(y_2)] = [\mu_A(x_1) \wedge \mu_A(x_2)] \wedge [\mu_A(y_1) \wedge \mu_A(y_2)] = \mu_V(x_1, x_2) \wedge \mu_V(y_1, y_2) = \mu_V(x) \wedge \mu_V(y)$. Therefore, $\mu_V(xy) \geq \mu_V(x) \wedge \mu_V(y)$, for all x and y in RxR. Also we have, $\nu_V(x-y) = \nu_V[(x_1-y_1, x_2-y_2)] \leq [\nu_A(x_1) \vee \nu_A(y_1)] \vee [\nu_A(x_2) \vee \nu_A(y_2)] = [\nu_A(x_1) \vee \nu_A(x_2)] \vee [\nu_A(y_1) \vee \nu_A(y_2)] = \nu_V(x_1, x_2) \vee \nu_V(y_1, y_2) = \nu_V(x) \vee \nu_V(y)$. Therefore, $\nu_V(x-y) \leq \nu_V(x) \vee \nu_V(y)$, for all x and y in RxR. And, $\nu_V(xy) = \nu_V(x_1y_1, x_2y_2) \leq [\nu_A(x_1) \vee \nu_A(y_1)] \vee [\nu_A(x_2) \vee \nu_A(y_2)] = [\nu_A(x_1) \vee \nu_A(x_2)] \vee [\nu_A(y_1) \vee \nu_A(y_2)] = \nu_V(x_1, x_2) \vee \nu_V(y_1, y_2) = \nu_V(x) \vee \nu_V(y)$. Therefore, $\nu_V(xy) \leq \nu_V(x) \vee \nu_V(y)$, for all x and y in RxR. This proves that V is an intuitionistic L-fuzzy subnearring of RxR. Conversely assume that V is an intuitionistic L-fuzzy subnearring of RxR, then for any $x=(x_1, x_2)$ and $y=(y_1, y_2)$ are in RxR, we have $\mu_A(x_1-y_1) \wedge \mu_A(x_2-y_2) = \mu_V[(x_1, x_2) - (y_1, y_2)] = \mu_V(x-y) \geq \mu_V(x) \wedge \mu_V(y) = \mu_V(x_1, x_2) \wedge \mu_V(y_1, y_2) = [\mu_A(x_1) \wedge \mu_A(x_2)] \wedge [\mu_A(y_1) \wedge \mu_A(y_2)]$. If we put $x_2 = y_2 = 0$, we get, $\mu_A(x_1 - y_1) \geq \mu_A(x_1) \wedge \mu_A(y_1)$, for all x_1 and y_1 in R. And, $\mu_A(x_1y_1) \wedge \mu_A(x_2y_2) = \mu_V[(x_1, x_2)(y_1, y_2)] = \mu_V(xy) \geq \mu_V(x) \wedge \mu_V(y) = \mu_V(x_1, x_2) \wedge \mu_V(y_1, y_2) = [\mu_A(x_1) \wedge \mu_A(x_2)] \wedge [\mu_A(y_1) \wedge \mu_A(y_2)]$. If we put $x_2 = y_2 = 0$, we get, $\mu_A(x_1y_1) \geq \mu_A(x_1) \wedge \mu_A(y_1)$, for all x_1, y_1 in R. Also we have,
$\nu_A(x_1-y_1) \vee \nu_A(x_2-y_2) = \nu_V[(x_1, x_2) - (y_1, y_2)] = \nu_V(x-y) \leq \nu_V(x) \vee \nu_V(y) = \nu_V(x_1, x_2) \vee \nu_V(y_1, y_2) = [\nu_A(x_1) \vee \nu_A(x_2)] \vee [\nu_A(y_1) \vee \nu_A(y_2)]$. If we put $x_2 = y_2 = 0$, we get, $\nu_A(x_1-y_1) \leq \nu_A(x_1) \vee \nu_A(y_1)$, for all x_1 and y_1 in R. And, $\nu_A(x_1y_1) \vee \nu_A(x_2y_2) = \nu_V[(x_1, x_2) \quad (y_1, y_2)] = \nu_V(x\ y) \leq \nu_V(x) \vee \nu_V(y) = \nu_V(x_1, x_2) \vee \nu_V \quad (y_1, \quad y_2) = [\nu_A(x_1) \vee \nu_A(x_2)] \vee [\nu_A(y_1) \vee \nu_A(y_2)]$. If we put $x_2 = y_2 = 0$, we get, $\nu_A(x_1y_1) \leq \nu_A(x_1) \vee \nu_A(y_1)$, for all x_1 and y_1 in R. Hence A is a A is an intuitionistic L-fuzzy subnearring of a nearring R.

IV. CONCLUSION

We tried to prove some results to use in the field of Intuitionistic L fuzzy subnearring of a nearing

REFERENCES

[1] Ajmal.N and Thomas.K.V., Fuzzy lattices, Information sciences 79 (1994), 271-291.

[2] Akram.M and Dar.K.H, On fuzzy d-algebras, Punjab university journal of mathematics, 37(2005), 61-76.

[3] Asok Kumer Ray, On product of fuzzy subgroups, fuzzy sets and systems, 105, 181-183 (1999).

[4] Atanassov.K., Intuitionistic fuzzy sets, fuzzy sets and systems, 20(1), 87-96 (1986).

[5] Atanassov.K., Stoeva.S., Intuitionistic L-fuzzy sets, Cybernetics and systems research 2 (Elsevier Sci. Publ., Amsterdam, 1984), 539-540.

[6] Azriel Rosenfeld, Fuzzy Groups, Journal of mathematical analysis and applications 35, 512-517 (1971).

[7] Chakrabarty, K., Biswas, R., Nanda, A note on union and intersection of intuitionistic fuzzy sets , Notes on intuitionistic fuzzy sets , 3(4), (1997).

[8] Davvaz.B and Wieslaw.A.Dudek, Fuzzy n-ary groups as a generalization of rosenfeld fuzzy groups, ARXIV-0710.3884VI(MATH.RA)20 OCT 2007,1-16.

[9] Goran Trajkovski, An approach towards defining L-fuzzy lattices, IEEE, 7(1998), 221-225.

[10] Mohammad M. Atallah, On the L-fuzzy prime ideal theorem of distributive lattices, The journal of fuzzy mathematics, Vol.9, No.4, 2001.

[11] Palaniappan.N and Arjunan.K, The homomorphism, anti-homomorphism of a fuzzy and anti fuzzy ideals, Varahmihir journal of mathematical sciences, Vol.6 No.1 (2006), 181-188.

[12] Palaniappan. N & K. Arjunan, Operation on fuzzy and anti fuzzy ideals , Antartica J. Math ., 4(1); 59-64, 2007.

[13] Palaniappan. N & K.Arjunan, Some properties of intuitionistic fuzzy subgroups, Acta Ciencia Indica, Vol.XXXIII (2); 321-328, 2007.

[14] B.Thenmozhi,S.Naganathan,Some properties of Anti L Fuzzy Subnearring of a nearing, International Journal of Applied Research,38-39.

[15] B.Thenmozhi,S.Naganathan,Propertie on Anti L fuzzy Subnearring of a nearing in Homomorphism,National Conference in Fuzzy Algebra, Paramakudi.

[16] Rajesh Kumar, Fuzzy Algebra, Volume 1, University of Delhi Publication Division, July -1993.

[17] Zadeh.L.A., Fuzzy sets , Information and control ,Vol.8, 338-353 (1965).

Analysis of ECG and EEG Signals to Detect Epileptic Seizures

A. Asuvaran
Department of ECE
University College of Engineering Pattukkottai,
Thanjavur, Tamil Nadu, India.

G. Elatharasan*
Department of Mechanical engineering
University College of Engineering Pattukkottai,
Thanjavur, Tamil Nadu, India.

***Abstract*----Epilepsy is one of the most common neurological disorders, with peak prevalence rates in early childhood and in old age people. It is important to distinguish epilepsy from isolated seizures and cerebral diseases. This epileptic seizure is normally identified from the EEG signal but ECG signal can also be used to detect these seizures. This project intends to develop an algorithm that predicts if a seizure is likely to occur using Electroencephalogram and Electrocardiogram. Features like mean and standard deviation of peak to peak interval, QRS amplitude, QRS time PR interval and QT interval for ECG and spectral power for EEG frequency bands were derived. The power distributions particularly in delta and theta bands were computed to detect the seizures in EEG. Here, both the bio signals are processed simultaneously to predict the extract occurrence of seizure.**

Keywords---- EEG; ECG; Pwave-atrial depolarization; QRS wave-ventricular depolarization; T wave ventricular repolarisation ;Welch power spectrum; seizures

I. INTRODUCTION

Epilepsy is a general term used for a group of disorders that cause disturbances in the electrical signal of the brain. The brain is a highly complex electrical system, powered by roughly many pulses of energy per second. These pulses move back and forth between nerve cells to produce thoughts, feelings, and memories. An epileptic seizure occurs when these energy pulses come much more rapidly for a short time due to an electrical abnormality in the brain This brief electrical surge can happen in just a small area of the brain, or it can affect the whole brain. Diagnosis of epilepsy may be achieved by different examinations, such as positron emission tomography (PET), magnetic resonance imaging (MRI), computed tomography (CT), and Electroencephalogram(EEG). There into, EEG is the most used one with high temporal resolution. In the epileptic EEG, the presence of epileptic activities, such as spikes, sharps and high frequency oscillations confirms epilepsy. An Electrocardiogram (ECG) is another way to diagnose the epilepsy. ECG abnormalities appear to occur more often during seizures and within seizures of longer duration.

II.EXPERIMENTAL PROCEDURE

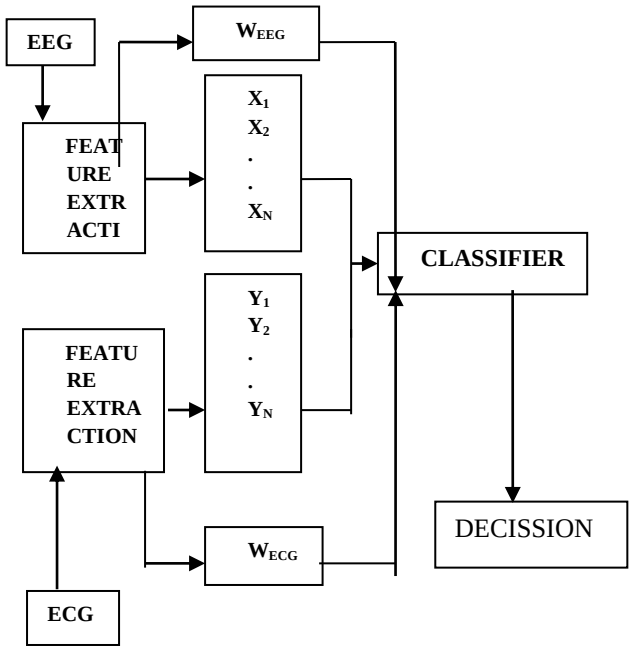

Figure.1. Block Diagram of Epilepsy Detection

The combination of both ECG and EEG is used for seizure detection. Both these signals are capable of identifying seizure from any patient with a minimal false detection rate. The algorithms considered in this study are epoch-based, so each seizure event was rounded to the nearest epoch length. The block diagram of the simulation used in this work is shown in figure.1

A. *EEG and ECG dataset*

The database used in this project was collected at the Children's Hospital Boston, which consists of both EEG and ECG recordings from paediatric subjects and also from young subjects(up to 25 years) with seizures. In this database, recordings were collected from 22 subjects (5 males, ages 322; and 17 females, ages 1.5-19). These signals were sampled at a rate of 256 samples per second with 16-bit resolution. The International 10-20 system for EEG acquisition and one channel ECG was used for these recordings.

III. IMPLEMENTATION

This work mainly consists of two processes namely,

- ECG Analysis
- EEG Analysis

A. ECG Analysis

The algorithm reported in this work utilizes the ECG feature, calculated on a 20 sec (5120 samples) non-overlapping epoch basis. The Mean and S.D of Heart Rate, QRS amplitude, QRS Interval, PR Interval, QT Interval are used in this study.

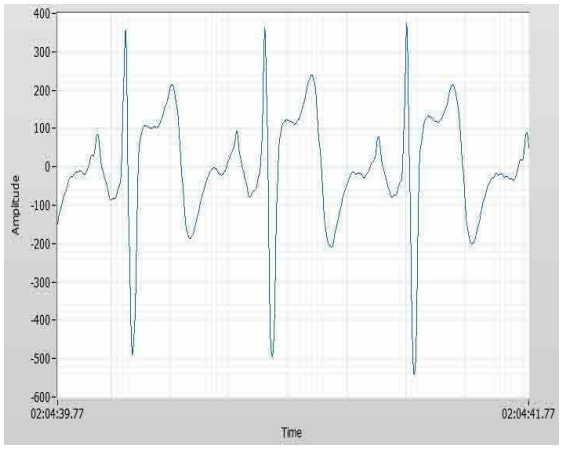

Figure 2 ECG Signal

ECG signal shown in figure 2 was filtered using a band-pass filter (corner frequencies 10 and 25 Hz) to remove baseline wander, power-line noise. The accessibility and the computational simplicity make time domain features the most popular tool for generating outputs.

Mean

The average value, or mean, of a signal x is calculated using the below equation

$$\mu = \frac{1}{N}\sum_{n=0}^{N-1} \mathrm{Xn}$$

It is computed over a time duration of N samples.

Standard Deviation

Standard deviation is equal to the square root of the variance. It is equal to the RMS value for

$$\sigma = \sqrt{\frac{1}{N}\sum_{n=0}^{N-1} |Xn - \mu|^2}$$

signals with a zero mean value.

B.EEG Analysis

In this algorithm in order to reduce the complexity signals from four channels namely right frontal FP2-F8 (RF), right temporal T8-P8 (RT), left frontal FP1-F7 (LF) and left temporal T7-P7 (LT) scalp locations are chosen for seizure detection and analysis.

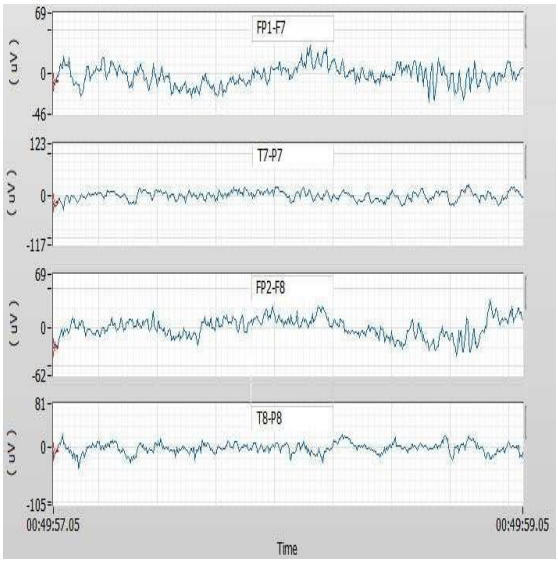

Figure 3 EEG Signal

The EEG signal shown in figure 3 was processed using Daubechies Mother wavelet of order 5 to allow the signal only between 0-32 Hz and also to remove the power-line noise. The frequency domain method is used for EEG analysis. Generally, the rhythmic activity associated with the onset of a seizure is composed of strong frequency components at 2, 5, and 11 Hz. To compute this, the Welch power spectrum estimator was used.

c.Welch Power Spectrum

The Welch method reduces the variance of the periodogram method by averaging. This method first divides a time series into overlapping sub sequences by applying a window to each subsequence and then averaging the periodogram of each subsequence.

$$I_N(e^{jw}) = \frac{1}{N}\left|\sum_{n=0}^{N-1} Xr[m]e^{-jwm}\right|^2$$

d.Neural Network Classifier

In this work, BPN network is employed. Back propagation networks are good classifiers because of their features like robustness, adaptive learning. Here, 26 input nodes, 10 hidden nodes and two output node were used. The MSE Error Goal is set to 0.01, which is sufficient for accurate classification

IV. RESULTS AND DISCUSSION

The features obtained from ECG and EEG were tabulated in the Tables 1, 2 and 3. In all these three tables, the values obtained from the patients under epileptic condition and also under normal conditions were tabulated. In Table1, the mean value of ECG signals from the patients under normal condition and

$$I'_N\left(e^{jw}\right) = \frac{1}{N}\left|\sum_{n=0}^{N-1} X_T[m]e^{-jmn}\right|^2$$

during epilepsy just before the onset of seizure and at the time of seizures were calculated.

In Table2, the standard deviation value of ECG signals from the patients under normal condition and during epilepsy just before the onset of seizure and at the time of seizures were calculated

FEATURE ARTICLE	NORMAL	ABNORMAL	
		PRE SEIZURE	SEIZURE
Heart Rate	81.486	84.042	100.179
QRS Amplitude	1466.497	827.391	951.991
QRS Interval	0.111	0.1	0.097
PR Interval	0.195	0.2	0.148
QT Interval	0.496	0.516	0.409

TABLE I Mean value of ECG

FEATURE ARTICLE	Normal	Abnormal	
		Pre seizure	seizure
Heart rate	3.032	11.05	7.942
QRS Amplitude	97.873	69.09	102.249
QRS Interval	0.011	0.005	0.006
PR Interval	0.012	0.022	0.003
QT Interval	0.012	0.037	0.003

TABLE II Standard Deviation of ECG

In Table3, the Spectral Power calculated from four channels of EEG from the patients under normal condition and during epilepsy just before the onset of seizure and at the time of seizures were calculated.

The calculated features are feed as input to the BPN network from which the occurrence of seizure has been predicted most accurately which is given in figure 4. In this figure, the test data are the features calculated and in the output plot 1 indicates the absence of epilepsy and 2 indicates the presence of epilepsy. Thus in this figure, the occurrence of epilepsy is efficiently predicted.

CHANNEL	BANDS	NORMAL		
			PREICTAL	SEIZURE
T7 - P7	Delta (δ)	232.4	594.01	4599.17
	Theta(Θ)	24.35	39.59	1548.52
	Alpha(α)	11.72	18.18	1439.06
	Beta (β)	4.32	4.94	837.84
FP 1- F7	Delta (δ)	352.49	843.73	5253.54
	Theta(Θ)	31.88	54.12	2109.38
	Alpha(α)	15.13	18.52	1977.46
	Beta (β)	4.26	4.8	1128.86
T8 - P8	Delta (δ)	232.4	594.01	4599.17
	Theta(Θ)	24.35	39.59	1548.52
	Alpha(α)	11.72	18.18	1439.06
	Beta (β)	4.32	4.94	837.84
FP 2- F8	Delta (δ)	257.91	765.91	3936.9
	Theta(Θ)	23.46	51.45	1304.59
	Alpha(α)	10.7	11.66	959.25
	Beta (β)	3.75	2.85	676.98

TABLE III Spectral Power Calculation- four channels

The training performance using the BPN network with mean squared error of 0.01 is shown in figure 5. The features namely mean and standard deviation for ECG signal and power spectrum of the EEG signals were obtained. Finally a BPN classifier is used to classify the feature vectors. The algorithm is evaluated using a large data-set containing ECG and multi-channel EEG. This method provides better performance rates for seizure prediction when compared to methods that uses only the EEG signals.

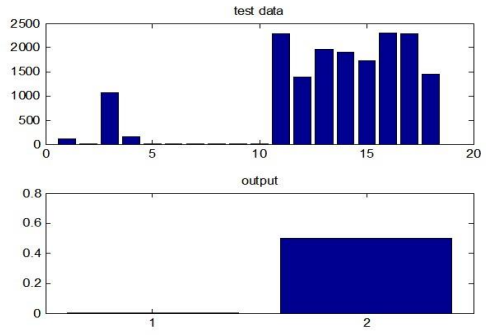

Figure 4 Test data classification using BPN

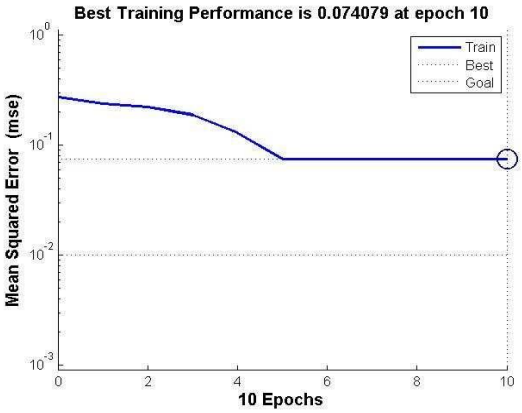

Figure 5 Performance Plot of BPN

V. CONCLUSION

Thereby using this method, as the accuracy rate is higher the false positive rate can be greatly reduced compared to the presently existing methods of which most of them use only the EEG signals for analysing the occurrence of epilepsy This algorithm can be effectively enforced for real time online data processing. Advanced classification methods can be implemented to further increase the performance speed and efficiency of this algorithm.

REFERENCES

[1] AliShoeb, JohnGuttag, "Application of Machine Learning To Epileptic Seizure Detection", 27th International Conference on Machine Learning, Haifa, Israel, 2010.

[2] MaeikeZijlmans, Danny Flanagan, Jean Gotman, "Heart Rate Changes and ECG Abnormalities During Epileptic Seizures: Prevalence and Definition of an Objective Clinical Sign" Epilepsia, 43(8):847–854, 2002.

[3] Thomas Bermudez, David Lowe, Anne-MarieArlaud-Lamborelle, "Schemes for Fusion of EEG and ECG Towards Temporal Lobe EpilepsyDiagnostics", Proceedings of the 29thzAnnualInternational Conference of the IEEE EMBS, Lyon, France August 23-26.

[4] Fabien Massé, JulienPenders, AlineSerteyn,Martien van Bussel, Johan Arends, "Miniaturized Wireless ECG-Monitor for Real-Time Detection of Epileptic Seizures", Wireless Health'10, October 5-7, 2010, San Diego, USA

[5] Zhou, H.-Y. Hou, K.-M. , Sch. of Comput. Sci. & Technol., Harbinnst. of Technol., Harbin "Embedded real-time QRS detection algorithm for pervasive cardiac care system", ICSP 2011.

Multilayer Microstrip Equivalent Antenna Analysis using Finite Difference Time Domain Method

P. Elamaran*
Department of ECE,
University college of Engineering Pattukkottai,
Thanjavur, Tamil Nadu, India.

G. Srivatsun
Department of ECE,
P.S.G College of technology,
Coimbatore, Tamil Nadu, India.

***Abstract:-*Microstrip equivalent antenna used in radio communication is presented. Finite difference time domain (FDTD) method is used for analyzing microstrip antenna which is based on multilayer multipermittivity dielectric substrate. FDTD method is used for modifying equivalent iterative formula in the condition of cylindrical coordinate system. The mixed substrate which consists two kinds of media (one of them is air) takes the place of original single substrate. The results ofmicrostrip equivalent antenna simulation show that the resonant frequency of equivalent antenna is similar to that of the prototype original antenna. The validity of analysis can be validated by means of antenna resonant frequency formula. The radiation pattern of two antennas show that same radiation pattern and gain. This method can be used to reduce the weight and increase the efficiency of compact antenna, which is significant to the design of missile-borne antenna in military applications.**

Keywords-Microstrip antenna; FDTD; multilayer; military applications.

I. INTRODUCTION

In recent years, antenna has been important module for military antennas [1,7]. Particularly for missile-borne antenna which required to be small in size and light in weight. The microstripantenna [2] has many advantages, such as, small size ,light weight and planar structure. Many work has been doneon its miniaturization [3,4].But few research concentrated on decreasing the weight of antenna and leaving its basic parameters unchanged under the conditions of same size and thickness.

In this work, another model design is proposed. The aims of this work are: a) to conserve the shape of antenna; b) to conservethe of antenna electromagnetic parameters; and c) to decrease the weight of antenna. For this, a substrate with low permittivity and high dielectric permittivity media is taken the place of the original substrate, in which air is used as a lower dielectric permittivity media (high dielectric permittivity media can be any mediaas its dielectric permittivity is higher than original media). The introduction of the air media can effectively decrease the weight of antenna in proposed model. The analysis of equivalent antenna is based on FDTD.

II. EQUIVALENT ANTEENA STRUCTURE AND FDTD ANALYSIS

In1966, K.S. Yee introduced the theory of FDTD [5].FDTD is a novel method which can be used to intuitively and succinctly explain the Maxwell's equations. In this method, the electric field and magnetic field are included in a three-dimensionalModel (Yee cell). This model is used for solving all the problem of electromagnetic field. A circular antenna is easily integrated into a warhead of bomb compared to rectangle antenna. So the formulae in References [6,7]should be amended in the cylindrical coordinatesystem (see Fig. 1).

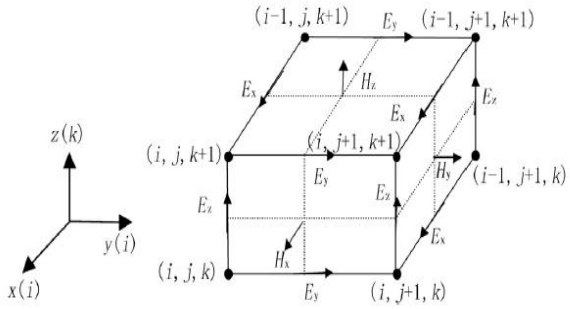

Fig. 1. Yee cell.

$$E_r^{n+1}\left(i+\frac{1}{2},j,k\right)=\frac{2\varepsilon-\sigma\Delta t}{2\varepsilon+\sigma\Delta t}E_r^{n}\left(i+\frac{1}{2},j,k\right)$$

$$+\frac{2\Delta t}{2\varepsilon+\sigma\Delta t}\times\left[\frac{H_z^{n+\frac{1}{2}}\left(i+\frac{1}{2},j+\frac{1}{2},k\right)-H_z^{n+\frac{1}{2}}\left(i+\frac{1}{2},j-\frac{1}{2},k\right)}{\left(i+\frac{1}{2}\right)\Delta r\Delta\varphi}-\frac{H_\varphi^{n+\frac{1}{2}}\left(i+\frac{1}{2},j,k+\frac{1}{2}\right)-H_\varphi^{n+\frac{1}{2}}\left(i+\frac{1}{2},j,k-\frac{1}{2}\right)}{\Delta z}\right]\ldots.(1)$$

$$H_r^{n+\frac{1}{2}}\left(i,j+\frac{1}{2},k+\frac{1}{2}\right)=\frac{2\mu-\sigma\Delta t}{2\mu+\sigma\Delta t}H_r^{n-\frac{1}{2}}\left(i,j+\frac{1}{2},k+\frac{1}{2}\right)-\frac{2\Delta t}{2\mu+\sigma\Delta t}\left[\frac{E_z^n\left(i,j+1,k+\frac{1}{2}\right)-E_z^n\left(i+\frac{1}{2},j,k+\frac{1}{2}\right)}{\Delta r\Delta\varphi}-\frac{E_\varphi^n\left(i,j+\frac{1}{2},k+1\right)-E_\varphi^n\left(i,j+\frac{1}{2},k\right)}{\Delta z}\right]\ldots(2)$$

Equations(1) and (2) are electric and magnetic fields equation for Yee cell.

Two medium exist in Yee grid (the permittivity's are ε_{r1}; ε_{r2}).From Ampere circuital theorem, we have,

$$\oint H^*\,dl=\iint\varepsilon\frac{\partial E}{\partial t}ds+Eds\ldots(3)$$

Assuming that the magnetic conductivities of two dielectric media are the same. It can be known from the boundary condition of electromagnetic field that the normal component of magnetic field on the Interface between the two media is continuous, in cylindrical coordinate system [8]; Equation (3) could be rewritten as

$$\begin{aligned}\oint \mathrm{H^*dl}=\ &\mathrm{H_r^{n+0.5}(i,j+0.5,k)r\Delta}\\&-\mathrm{H_\varphi^{n+0.5}(i,j+0.5,k)\Delta r}\\&-\mathrm{H_r^{n+0.5}(i,j-0.5,k)r\Delta\theta}\\&+\mathrm{H_\varphi^{n+0.5}(i,j+0.5,k)\Delta}\ldots(4)\end{aligned}$$

In FDTD iteration,

$$E_r^{n+\frac{1}{2}}(i,j,k)=\frac{1}{2}[E_r^{n+1}(i,j,k)+E_r^n(i,j,k)]\ldots(5)$$

The right hand side equation (5) can be extended to

$$\iint\varepsilon\frac{\partial E}{\partial t}ds=\sum_{i=1}^m\sum_{j=1}^n\iint_{ij}\varepsilon_{ij}\frac{\partial E}{\partial t}ds\quad_{ij}=\frac{E_r^{n+1}(i,j,k)-E_{r(i,j,k)}^n}{\Delta t}\times[\varepsilon_{11}r_1\Delta_{r1}\Delta_{\theta1}+\varepsilon_{12}r_1\Delta_{r1}\Delta_{\theta2}\ldots\ldots+\varepsilon_{mn}r_m\Delta_{rm}\Delta_{\theta n}]\ldots(6)$$

$$\iint\sigma Eds=\sum_{i=1}^m\sum_{j=1}^n\iint_{ij}\sigma_{ij}Eds_{ij}=\frac{E_r^{n+1}(i,j,k)-E_{r(i,j,k)}^n}{2}\times\sigma_{11}r_{11}\Delta_{r1}\Delta_{\theta1}+[\sigma_{12}r_1\Delta_{r1}\Delta_{\theta2}\ldots+\sigma_{mn}r_m\Delta_{rm}\Delta_{rn}\Delta_{\theta n}]\ldots(7)$$

Substituting equations (4), (6) and (7) into Eq. (3), we have,

$$E_r^{n+1}\left(i+\frac{1}{2},j,k\right)=\frac{2\varepsilon_{eff}-\sigma_{eff}\Delta t}{2\varepsilon_{eff}+\sigma_{eff}\Delta t}E_r^n\left(i+\frac{1}{2},j,k\right)+\frac{2\Delta t}{2\varepsilon_{eff}+\sigma_{eff}\Delta t}\left[\frac{H_z^{n+\frac{1}{2}}\left(i+\frac{1}{2},j+\frac{1}{2},k\right)-H_z^{n+\frac{1}{2}}\left(i+\frac{1}{2},j-\frac{1}{2},k\right)}{\left(i+\frac{1}{2}\right)\Delta r\Delta\varphi}-\frac{H_\varphi^{n+\frac{1}{2}}\left(i+\frac{1}{2},j,k+\frac{1}{2}\right)-H_\varphi^{n+\frac{1}{2}}\left(i+\frac{1}{2},j,k-\frac{1}{2}\right)}{\Delta z}\right)\ldots(8)$$

After the simplification, the equivalent permittivity can be obtained

$$\varepsilon_{eff}=\frac{\varepsilon_{11}r_1\Delta_{r1}\Delta_{\varphi1}+\varepsilon_{12}r_1\Delta_{r1}\Delta_{\varphi2}\ldots+\varepsilon_{mn}r_m\Delta_{rm}\Delta_{\varphi n}}{rdrd\varphi}\ldots(9)$$

Through the analysis mentioned above, the structure of antenna substrate can be designed, as shown in Fig. 2.

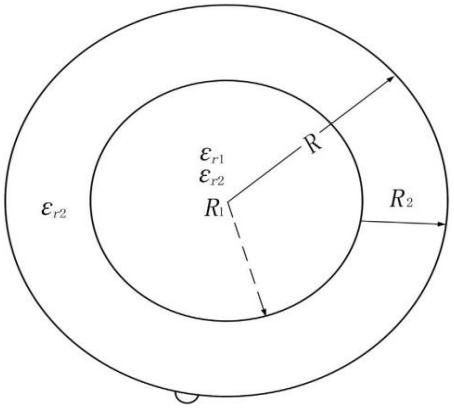

Fig. 2. Structure of substrate.

III. DISCUSSION OF SIMULATION

Through the above analysis, FR4 substrate is chosen for original substrate. The basic parameters of antenna are ε_r= 4:4, R =14 mm, h =2 mm, r= 12 mm. Equation (10) shows the relationship between two medium.Fig.3 shows the prototype antenna design. Table 1 lists the parameters of equivalent antennas.

$$\varepsilon_{r1}R_1^2+\varepsilon_{r2}R_2^2=\varepsilon_rR^2$$

$$R_{1+}R_{2=}\mathrm{R}\qquad\ldots(10)$$

	ε_{r1}	ε_{r2}	R_1	R_2
A	12.8	1	8.56	6.42
B	9.7	1	9.8	5.0

TABLE 1: PARAMETERS OF EQUIVALENT ANTENNAS

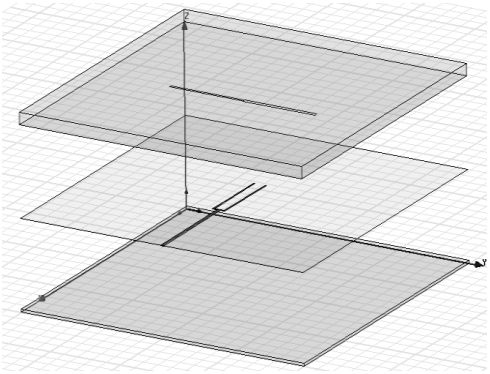

Fig .3.Prototype antenna design

Fig. 4 shows that the resonant frequency of original antenna is 3.2 GHz, and the resonant frequencies of the equivalent antennas A and B are also remain unchanged. It can be concluded from the resonant frequency formula that the permittivity is the only factor which has effect on resonant frequency when the radius of radiation patch and the working mode remain the same. So two media can be treated as a singlemedium which has a same permittivity as that of original medium. The results prove the accuracy of FDTD analysis. Because the position of feed point was not changed in simulation, the S11 parameters of the equivalent antenna deteriorated compared to the original antenna. So the equivalent antenna is not exactly equal to the original antenna.

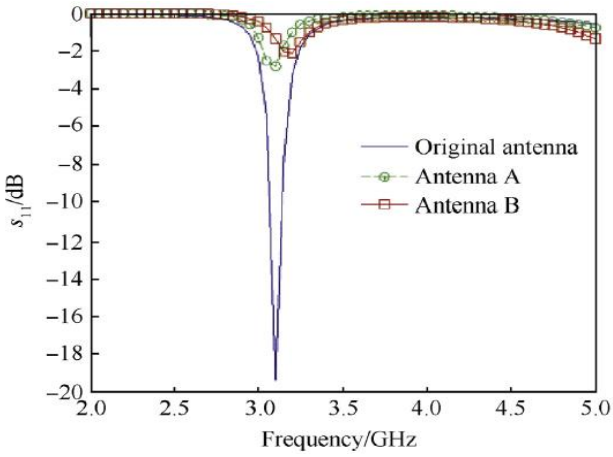

Fig. 4.Resonant frequencies of three antennas.

The parameters can be improved by changing the position of feed point. Fig. 5 shows the S11 parameters after changing the position of feed point.

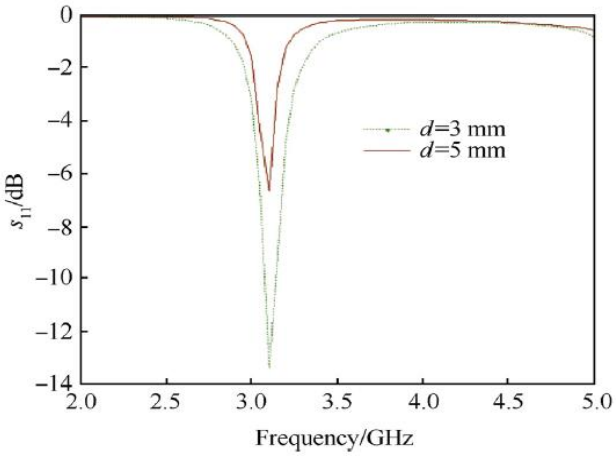

Fig. 5.S11 with different feed feint.

Fig. 6 and 7 show the radiation patterns of equivalent antenna and original antenna. It can be seen from Fig. 6 and 7 that the direction and co polarization of equivalent antenna are similar to those of the original one. This shows that the equivalent antenna can replace the original antenna.

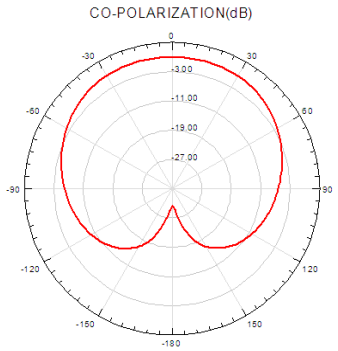

Fig. 6. Original radiation pattern.

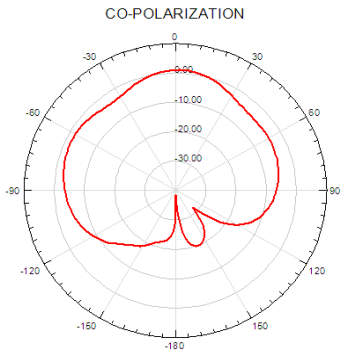

Fig. 7.Equivalent radiation pattern.

IV. CONCLUSION

A method for decreasing the weight of antenna was proposed in the paper. By means of analysis based on FDTD, air medium and a higher permittivity medium are introduced to take the place of original substrate. The simulation results show that resonant frequency, radiation pattern and gain of equivalent antenna did not change. The air media can be used to reduce the weight of antenna.

REFERENCES

[1] Chen N, Ammann MJ, Qing X, Wu XH, See TSP, Cai A. Planar. IEEE Microw Mag 2006;7(6):63e7.

[2] Krstic M, KanellAkopoulos I, Kokotovic P. Nonlinear and adaptive control design. New York: Wiley; 1995.

[3]] Wong KL. Compact and broadband microstrip antennas. John Wiley & Sons Inc; 2002.

[4] Yee KS. Numerical solution of initial boundary value problems involving Maxwell equations in isotropic media. IEEE Trans Antennas Propagate 1966; 14(3):302e7

[5] Taflove A, Hagness SC. Computational electrodynamics: the finite difference time domain method. 2nd ed. Norwood, MA: ArtechHoose; 2000.

[6] Greengard L, Rokhlin V. A fast algorithm for particle simulation. J Comp Phys 1987;73:325e48.

[7] Wu X, Tan YL, Xu J, Fang A. Research on the model of multilayedmulticonductor system with equivalent permittivity, 32 (2). Journal of Zhejiang University of Technology; 2006. p.179e82.

[8] Y. Yorozu, M. Hirano, K. Oka, and Y. Tagawa, "Electron spectroscopy studies on magneto-optical media and plastic substrate interface," IEEE Transl. J. Magn. Japan, vol. 2, pp. 740-741, August 1987 [Digests 9th Annual Conf. Magnetics Japan, p. 301, 1982].

[9] yun-xing yang, hui-changzhao*, cui di. analysis of equivalent antenna based on FDTD method, elsevier b.v.,2014

New Dynamic Programming based Unit Commitment Technique by Reducing Paths

S. Vairamuthu*
Department of EEE,
University college of Engineering Pattukkottai,
Thanjavur, Tamil Nadu, India.

G. Manivannan
Department of EEE,
University college of Engineering Pattukkottai,
Thanjavur, Tamil Nadu, India.

***Abstract*— This project presents a new dynamic programming solution to the unit commitment problem. The unit commitment is the complex decision making process because of multiple constraints the Unit commitment which may not be violated while finding the optimal or suboptimal commitment schedule. Dynamic programming takes a lot of simulation time, so it is not optimal to use in a real power system for performing the unit commitment. Therefore, we need a new dynamic programming method to satisfy both the simulated and the real power system to get the optimal solution. A five generator system will be considered and the unit's commitment schedule will be found considering the demand for 24 hours. The goal of the objective function is in cost minimization, so we use the economic dispatch using the lambda iteration method when we calculate the production costs. Finally, we compare the UC solution by using both methods.**

Keywords- Start up cost, production cost,economic dispatch, feasible state, new dynamic programming constraints.

I. INTRODUCTION

A unit commitment (UC) process decides when to start and shutdown units according to the load status. The UC problem is well known in the power industry and it is important to save millions of dollars per year. Therefore the method of UC has been gradually studied. When we use the priority list method for the unit commitment, we can save simulation time and memory, and it can also be applied in a real power system. The priority list method has drawbacks that result in suboptimal solutions because it does not consider all the possible combinations of generation. Therefore, we have to find a method for always getting an optimal solution. Dynamic programming is the one of these methods. By using dynamic programming for unit commitment, we can get optimal solutions. However, it is well known that there is a problem in the number of combinations of units. When we decide for the optimal start and shutdown of the units, it will take considerable time and use a lot of memory to save all the paths. Because of these problems, dynamic programming can

II. UNIT COMMITMENT

Constraints

We considered three constraints the loading constraint, the unit limit constraint and the minimum-up/down time constraint.

A. Load Constraint

$$PD - \sum_{i=1}^{i=n} PG = 0$$

B. Unit Limit Constraint

$$P_{min} \leq PG \leq P_{max}$$

C. Minimum Up/Down Constraint

C(1) Minimum Up Time

Once starts the generator, it will take some time to shut down.

C(2) Minimum Down Time

Once shut down the generator, it will take some time to recommit.

III. PRODUCTION COST

After considering the constraints we need to calculate the Production cost for each generating unit. Before getting the Production cost, it is necessary to decide the generation of each unit by using the economic dispatch which is realized by

the lambda iteration method. At first, we assumed lambda of any value. By applying this value, we could get the generation of each unit. We then could calculate the error that is difference between the demand and total generation. If the error is not satisfied, the value is smaller than the tolerance; the lambda would have to be updated by applying the projection method. Lastly, after getting the generation of each unit, we could then calculate the production cost by multiplying the fuel cost.

IV. AU POWER CALCULATION

Limits on unit generation

PGmin	PGmax
150.000	455.000
20.000	130.000
20.0000	130.000
20.0000	80.0000
10.0000	55.0000
TOTAL DEMAND:820.0000	

V. RESULTS

INCREMENTAL FUEL COST

dC1/dPG1	16.6268
dC2/dPG2	17.1200
dC3/dPG3	17.0486
dC4/dPG4	23.3992
dC5/dPG5	26.1265

VI. PRODUCTION COST

$$Pcost(k,I) = \sum_{i=1} Pi\lambda i + \text{No load operating cost}$$

Pi - Generating power.

λi - Incremental fuel cost.

(i=1,2,…..,n)

VII. START UP COST

Another cost of UC is the start-up cost. Assume that, there is no cost associated with the shutting down of units is this paper. A simple practice is to assume a constant cost irrespective of the unit shut down time. However, if we are to get more accurate results in the unit commitment, a time dependent start-up cost is needed. Therefore, the start-up cost we considered in this paper is dividend of the cold start-up cost and the hot start-up cost.

A. Flow Chart

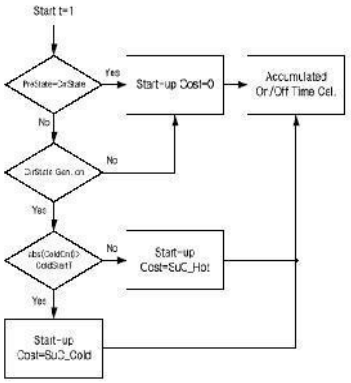

Pre State : Previous Generator State

Crr State : Current Generator State

Cold Cnt : Accumulated Generator State

Cold StartT : Generator Cooling Time

SuC_Hot : Hot Start-up Cost

SuC_Cold : Cold Start-up Cost

Each unit has an individual basis of cooling time. So by comparing between the accumulated status and the cooling time, we could decide the time dependent start-up cost.

VIII. OBJECTIVE FUNCTION

FCOST(K,I) = min [PCOST(K,I)+SCOST(K-1,L:K,I)+FCOST(K-1,L)

where

$State(K,I)$: Combination I of Units at Time K

$F_{cost}(K,I)$: Least Total Cost to Arrive at State (K,I)

$P_{cost}(K,I)$: Production Cost for State (K,I)

$S_{cost}(K-1,L:K,I)$: Transition Cost from State (K-1,L) to State (K,I)

IX. NEW DYNAMIC PROGRAMMING

New dynamic programming, we mention the characteristics of dynamic programming. Dynamic programming is a methodical procedure which systematically evaluates a large number of possible decisions in a multi-step problem .When we utilize the existing dynamic programming method, although its solution is correct and has the optimal value; it takes a lot of memory and spends much time in getting an optimal solution. For example, assume that there are 4 units which can supply the 24 hour load. So, the total maximum path to satisfy the 24 hour load curve is calculated by:

$$Total\ \ Paths = (2^4 - 1)^{24}$$

Because of this disadvantage, a better method of determining the optimum combination of units in service for any given system and load condition is desirable. Fortunately, there is such a method: modified dynamic programming. We already showed the standard dynamic programming method
and we recognize the disadvantage a lot of paths. We

Total Paths = $(2^5\text{-}1)^{24}$

introduce the characteristics of modified dynamic programming. As shown in Figures, modified dynamic programming does not save all the paths in order to get the optimal solution. At K periods, we consider all the feasible states X which could be satisfied by demanding from N paths at the K-1 period. Continuously, we find the lowest new N paths and thereby save memory and time. Similarly, we iterate until the last period.

A.Flow Chart

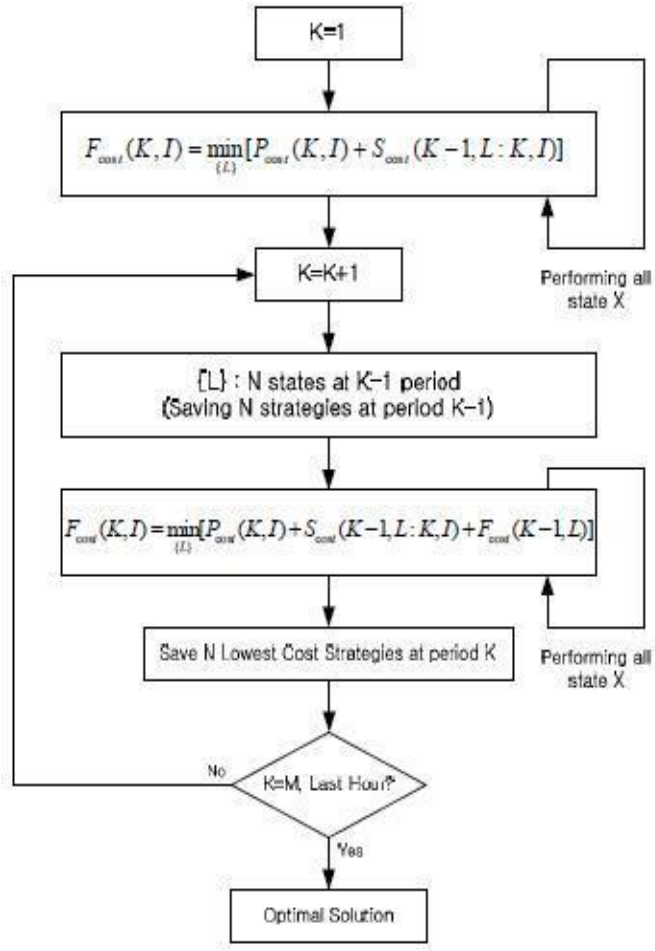

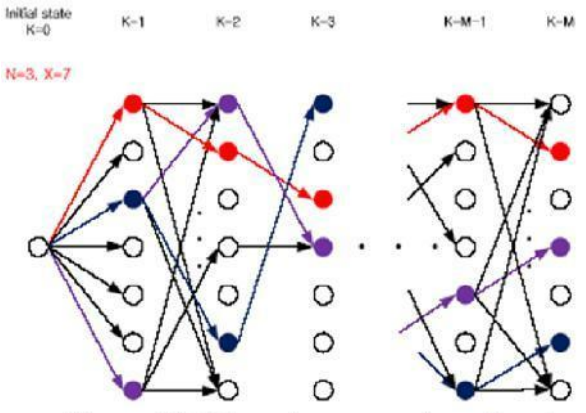

The modified dynamic programming path saving.

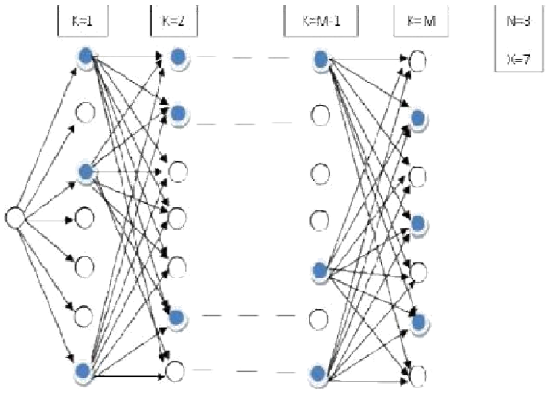

UNIT CHARACTERISTICS

Parameter		Unit 1	Unit 2	Unit 3	Unit 4	Unit 5
MinOutput [MW]		150	20	20	20	10
MaxOutput [MW]		455	130	130	80	55
SuC_Cold [$]		9000	1100	1120	340	60
SuC_Hot [$]		4500	550	560	170	30
ColdStartT [h]		5	4	4	2	0
MinUpTime [h]		8	6	6	4	1
MinDownTime [h]		8	6	6	4	1
Heat rate curves	a	0.00048	0.002	0.00211	0.00712	0.00413
	b	16.19	16.6	16.5	22.26	25.92
	c	1000	700	680	370	660

24 HOURS LOAD DATA

Time (h)	Load (MW)	Time (h)	Load (MW)
1	330	13	810
2	450	14	820
3	480	15	750
4	360	16	800
5	520	17	650
6	590	18	670
7	730	19	790
8	780	20	750
9	620	21	770
10	650	22	610
11	680	23	520
12	630	24	360

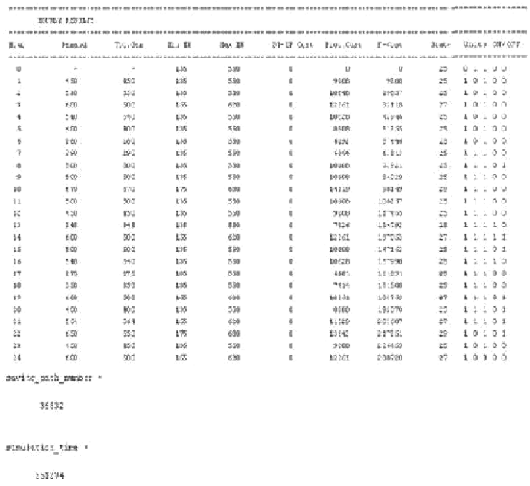

DYNAMIC PROGRAMMING METHOD:

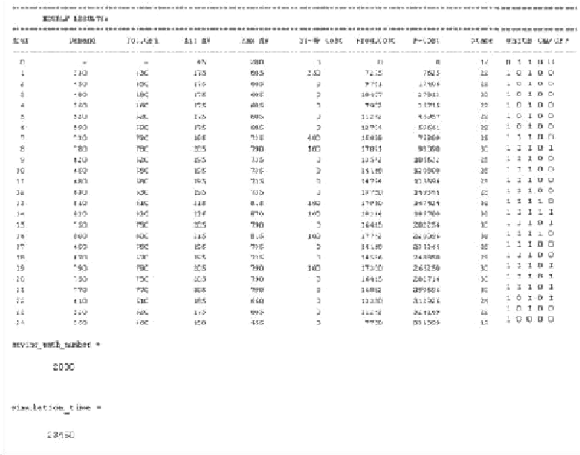

VII.COMPARISON O F DYNAMIC AND NEW DYNAMIC PROGRAMMING

Method	Savin g Path Num ber	Simulation Time
DYNAMIC PROGRAMMING	368 32	551274
NEW DYNAMIC PROGRAMMING	2000	23450

VIII. CONCLUSION

There is lot of method for solving the unit commitment problem and there are both advantage and disadvantages. One of the main problem of the do not get the optimal solution for performing the unit commitment. Dynamic programming was chosen to get an optimal solution despite being impossible to utilize in a real power system. Therefore, we needed to develop a dynamic programming system with that could be applied to a real power system. So introduced the new dynamic programming described in the paper and compare both applied to a real power system. So introduced the new dynamic programming described in the paper and compare both method.

REFERENCES

[1] "Modified Dynamic Programming Based Unit Commitment Technique" Joon-Hyung Park, Sun- Kyo Kim, Geun-Pyo Park, Yong-Tae Yoon, *Member*, and Sang- Seung Lee, *Member.IEEE 2010.*

[2] C. K. Pang and H. C. Chen, "Optimal Short-Term Thermal Unit Commitment," IEEE Transactions on
Power Apparatus and Systems, vol. PAS-95, no. 4, pp. 1336-1346, July/August.1976

[3] John. Muksadt and Richard C. Wilson, "An Application of Mixed-Integer Programming Duality to Scheduling
Thermal Generating Systems," *IEEE Transactions on Power Apparatus and Systems, vol. PAS-87, no. 12, pp. 1968-1978*,December. 1968.

[4] KOREC Walter L. Snyder, H. David Powell, and John C.Rayburn "Dynamic Programming Approach to Unit Commitment" *IEEE Transactions on Power Systems, vol.*PWRS-2, no.2, pp. 339-348, May. 1987.

Second Minimum Weight Spanning Tree of A Network with Triangular Intuitionistic Fuzzy Number As Edge Weight

B. Rajesh*
Department of Mathematics
University College of Engineering
Pattukkottai, Tamil Nadu, India.

S. Ismail Mohideen
PG and Research Department of Mathematics,
Jamal Mohamed College,
Tiruchirappalli, Tamil Nadu, India.

S. Senthilkumar
Department of Computer Science and Engineering,
University College of Engineering
Pattukkottai, Tamil Nadu, India.

***Abstract*— Determination of minimum weight spanning tree of a network is very significant in the field of operations research. The next option for minimum weight spanning tree is second minimum weight spanning tree. In this paper a new algorithm to find the second minimum weight spanning tree of a network has been suggested where edge weights are considered as triangular intuitionistic fuzzy number.**

***Keywords*— Network, Spanning tree, Minimum Weight Spanning Tree, Triangular intuitionistic fuzzy number.**

I. INTRODUCTION

Computing minimum weight spanning tree of a network is one of the most fundamental algorithmic problems in graph theory. In 1957, Prim [10] proposed the method for determining the minimal spanning tree of a network. The determination of the optimal path tree was efficiently determined by Bellman [2], Ford [5] and Moore [9]. Hassan [6] presents a new algorithm based on the distance matrix to solve the least-cost minimum spanning tree problem in 2012. In real world applications, it is not always possible to use the Minimum weight spanning tree. In such situations, second MWST is of equal importance to MWST. In crisp environment, it is assumed that the decision maker is certain about the parameters like distance, cost, time etc. But in real situations there always exists uncertainty about the parameters. In such cases, parameters can be represented by triangular intuitionistic fuzzy numbers. Second Minimum weight spanning tree of a network with crisp values as edge weight was discussed by Ismail Mohideen and Rajesh [7]. Applications of Minimum Weight Spanning Tree (MWST) were found in Foulds [4]. The concept of intuitionistic fuzzy sets was proposed by Atanassov [1] in 1986. In 2004, Mitchell [8], proposed a method to solve intuitionistic fuzzy numbers. In 2010, Deng Feng Li et al. [3] proposed a ranking method for triangular intuitionistic fuzzy number.

II. PRELIMINARIES

2.1 Fuzzy numbers

A fuzzy subset of the real line R with membership function is called a fuzzy number if

i. $\widetilde{A}$ is normal, (i.e.) there exists an element x_0 such that $\mu_{\widetilde{A}}(x_0) = 1$
ii. $\widetilde{A}$ is fuzzy convex, (i.e.) $\mu_{\widetilde{A}}[\lambda x_1 + (1-\lambda)x_2] \geq \mu_{\widetilde{A}}(x_1) \wedge \mu_{\widetilde{A}}(x_2), x_1, x_2 \in R, \lambda \in [0,1]$
iii. $\mu_{\widetilde{A}}$ is upper continuous and
iv. Supp$\widetilde{A}$ is bounded, where Supp $\widetilde{A} = \{x \in R : \mu_{\widetilde{A}}(x) > 0\}$.

2.2 *Fuzzy tree*

Fuzzy tree is a tree in which the weight of the edges constituting the tree is considered as fuzzy number.

2.3 *Weight of a fuzzy tree*

Weight of a fuzzy tree is a fuzzy number with each of its component representing the sum of the corresponding components of the fuzzy number of the edges constituting the tree.

2.4 *Intuitionistic fuzzy number*

Let $\widetilde{A} = \{(x, \mu_{\widetilde{A}}(x), \gamma_{\widetilde{A}}(x)), x \in X\}$ be an intuitionistic fuzzy set, then the pair $(\mu_{\widetilde{A}}(x), \gamma_{\widetilde{A}}(x)$ is refered here as an intuitionistic fuzzy number.

2.3. Triangular intuitionistic fuzzy number

A triangular intuitionistic fuzzy number $\widetilde{A}$ in R, written as $(a_1, b_1, c_1; a_1', b_1, c_1')$ where $a_1' \leq a_1 \leq b_1 \leq c_1 \leq c_1'$ has the membership function

$$\mu_{\widetilde{A}}(x) = \begin{cases} \dfrac{x - a_1}{b_1 - a_1} & a_1 \leq x \leq b_1 \\ \dfrac{x - c_1}{b_1 - c_1} & b_1 \leq x \leq c_1 \\ 0 & \text{othererwise} \end{cases}$$

and non-membership function of $\widetilde{A}$ is given by

$$\gamma_{\tilde{A}}(x) = \begin{cases} \dfrac{b_1 - x}{b_1 - a_1'} & a_1' \le x \le b_1 \\ \dfrac{x - b_1}{c_1' - b_1} & b_1 \le x \le c_1' \\ 1 & \text{othererwise.} \end{cases}$$

III. ALGORITHM

Following is the algorithm to find second minimum weight spanning tree of a network, where triangular intuitionistic fuzzy number is considered as weight of the edges.

Step 1: Initialization
Let k = 0. Let E_k be the set of all edges and n be the number of nodes of a network N_k where $n \geq 3$.
Let E_{ij} be the weight of the edge (i,j). Let T_k be the MWST of a network N_k.
For all $(i,j) \in E$, where $i \neq j$,
let $E_{ij} = (d_{ij}^{1}, d_{ij}^{2}, d_{ij}^{3}; d'^{1}_{ij}, d_{ij}^{2}, d'^{3}_{ij})$

Step 2: Value of the membership function of the triangular intuitionistic fuzzy number
If $E_{ij} = (d_{ij}^{1}, d_{ij}^{2}, d_{ij}^{3}; d'^{1}_{ij}, d_{ij}^{2}, d'^{3}_{ij})$ and
$E_{pq} = (d_{pq}^{1}, d_{pq}^{2}, d_{pq}^{3}; d'^{1}_{pq}, d_{pq}^{2}, d'^{3}_{pq})$ be two edge weight of fuzzy network with triangular intuitionistic fuzzy number, then the value of the membership function of the triangular intuitionistic fuzzy number can be calculated as follows
If $v_\mu(E_{ij}) > v_\mu(E_{pq})$ then $E_{ij} > E_{pq}$
If $v_\mu(E_{ij}) < v_\mu(E_{pq})$ then $E_{ij} < E_{pq}$
If $v_\mu(E_{ij}) = v_\mu(E_{pq})$ then $E_{ij} = E_{pq}$
Where $v_\mu(E_{ij}) = v_\mu(d_{ij}^{1}, d_{ij}^{2}, d_{ij}^{3}; d'^{1}_{ij}, d_{ij}^{2}, d'^{3}_{ij})$
$= 1/6\,(d_{ij}^{1} + 4\,d_{ij}^{2} + d_{ij}^{3})$

Step 3:
Using step 2, select an edge (i,j) from E_k such that $v_\mu(E_{ij})$ is minimum. Tie can be broken arbitrarily. Remove this edge (i,j) from E_k and include it as a part of T_k unless it creates a cycle with the edges already in T_k.

Step 4:
If T_k has $n-1$ edges, then store its weight in $W(T_k)$ and go to step 5.
Else go to step 3.

Step 5:
If $k = n-1$ then go to step 7. Else go to step 6

Step 6:
Let $k = k + 1$
Arbitrarily select an edge (p,q) from T_o.
$T_o = T_o - (p,q)$ and $N_k = N_0 - (p,q)$. Go to step 3.

Step 7:
Minimum of $v_\mu(W(T_k))$, $k = 1\ to\ n-1$, is found and its corresponding T_k is the second MWST.

Step 8:

Path = $< N^{k-j} > \oplus$ Path
Let $x = N^{k-j}$
Go to step 7.

Step 9:

Let $j = j + 1$

If $k - j = 0$, then

{Path = < s > $\oplus$ Path

If $TLN \neq \phi$, go to step 6

Else Terminate}

Else go to step 7.

IV. COMPUTATIONAL COMPLEXITY

In 2012, Zhan Ning and Wu Longshu [11] discussed the computational complexity of finding a spanning tree in a network with minimum total expenses. In the proposed algorithm of section III, from step1 to step3, the computational complexity for determining the MWST of a given network is $O(n^2 logn)$. According to step 4 and step 5, MWST is found for (n-1) networks. Therefore the computational complexity involved from step1 to step 6 is $O(n^3 logn)$. Therefore the computational complexity of the proposed algorithm in Section III is $O(n^3 logn)$.

V. NUMERICAL ILLUSTRATION

Consider a simple undirected network given in figure 5.1 with six vertices and nine edges. Here triangular intuitionistic fuzzy numbers are considered as weight of the edges and is given in table 5.1.

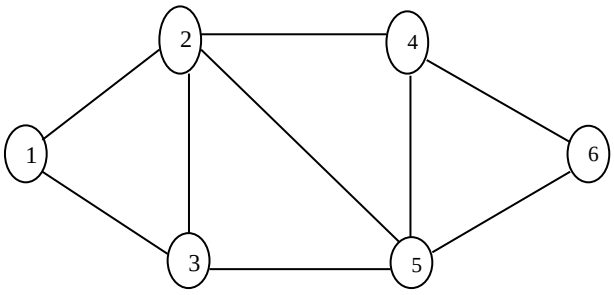

Fig 5.1 Network N_0

Edge	Weight of the edge
$(1,2)$	$(40,45,50;\ 35,45,55)$
$(1,3)$	$(50,52,56;\ 48,52,58)$
$(2,3)$	$(5,10,15;\ 4,10,17)$
$(2,4)$	$(15,20,24;\ 13,20,30)$
$(2,5)$	$(60,64,70;\ 58,64,75)$
$(3,5)$	$(12,18,20;\ 10,18,25)$
$(4,5)$	$(10,14,16;\ 8,14,20)$
$(4,6)$	$(30,34,40;\ 25,34,45)$
$(5,6)$	$(22,28,30;\ 20,28,34)$

Table 5.1 Edge weights of the Network N_0 corresponding to fig 5.1

Weight of MWST of the given network is $(89,115,131;\ 77,115,151)$ and its edges are $(2,3),(4,5),(3,5),(5,6)\ and\ (1,2)$

For constructing network N_1, the edge $(1,2)$ is removed from the network N_0.

Edges of MWST T_1 corresponding to Network N_1 are $(2,3),(4,5),(3,5),(5,6) and (1,3)$. Weight of T_1 is $W(T_1) = (99,122,137;\ 90,122,154)$

For constructing network N_2, the edge $(2,3)$ is removed from the network N_0.

Edges of MWST T_2 corresponding to Network N_2 are $(4,5),(3,5),(2,4),(5,6) and (1,2)$. Weight of T_2 is $W(T_2) = (99,125,140;\ 86,125,164)$

For constructing network N_3, the edge $(3,5)$ is removed from the network N_0.

Edges of MWST T_3 corresponding to network N_3 are are $(2,3),(4,5),(2,4),(5,6) and (1,2)$. Weight of T_3 is $W(T_3) = (92,117,135;\ 80,117,156)$

For constructing network N_4, the edge $(4,5)$ is removed from the network N_0.

Edges of MWST T_4 corresponding to Network N_4 are $(2,3),(3,5),(2,4),(5,6) and (1,2)$. Weight of T_4 is $W(T_4) = (94,121,139;\ 82,121,161)$

For constructing network N_5, the edge $(5,6)$ is removed from the network N_0.

Edges of MWST T_5 corresponding to Network N_5 are $(2,3),(4,5),(3,5),(4,6) and (1,2)$.

Weight of T_5 is $W(T_5) = (97,121,141;\ 80,121,162)$

Hence the second MWST is determined from $T_1, T_2, T_3, T_4\ and\ T_5$.

Min of

$\{v_\mu(w(T_1)), v_\mu(w(T_2)), v_\mu(w(T_3), v_\mu(w(T_4)), v_\mu(w(T_5))\}$

$= v_\mu(w(T_3))$.

Therefore T_3 is the second MWST of the given network.

Weight of second MWST of the given network is $(92,117,135;\ 80,117,156)$ and its edges are $(2,3),(4,5),(2,4),(5,6)\ and\ (1,2)$.

VI. CONCLUSION

In this paper a new algorithm is proposed to find the second minimum weight spanning tree of a given network with triangular intuitionistic fuzzy numbers as edge weights. Computational complexity of the proposed algorithm in section III is $O(n^3 logn)$. An example to illustrate the method is provided.

REFERENCES

[1] Atanassov, K.T., Intuitionistic fuzzy sets, Fuzzy sets and system, Vol. 20, no.1, 1986, 87-96.

[2] Bellman, R.E., On a routing problem, Quarterly Journal of Applied Mathematics, Vol.16, 1958, 87-90.

[3] Deng Feng Li., Jiang Xia Nan. and Mao Jun Zhang., A Ranking Method of Triangular Intuitionistic Fuzzy Numbers and Applications to Decision Making, International Journal of Computational Intelligence Systems, Vol.3, No.5, Oct 2010, 522-530.

[4] Foulds, 1992, "Graph Theory Applications", Springer- Verlag New York, Inc, 234-236.

[5] Ford, L.R., Network flow theory, The Rand corporation report, Santa monica, California, 1956, p-923.

[6] Hassan, M.R., An efficient method to solve least cost minimum spanning tree (LC-MST) problem, Journal of King Saud University-Computer and Information Sciences, Vol. 24, Issue 2, July 2012, 101-105.

[7] Ismail Mohideen S and Rajesh B, Second minimum weight spanning tree in a network, Elixir Appl. Math., ISSN: 2229-712X, 40 (2011) 5103-5104.

[8] Mitchell, H.B., Ranking intuitionistic fuzzy numbers, International Journal of Uncertainty, Fuzziness and Knowledge Based Systems 12, 2004, 377- 386.

[9] Moore. Z.E., The shortest path through a maze, Proceedings of International symposium on theory of switching, Part II, 1957, 258-292.

[10] Prim, R., Shortest connection networks and some generalization, Bell syst, Tech Journal, 36, 1957, 1389-1401.

[11] Zhan Ning., Wu Longshu., The Complexity and Algorithm for Minimum Expense Spanning Trees, Procedia Engineering, Vol. 29, 2012, 118-122.

Simulation Modeling of Land use and Transportation Interaction with Other Infrastructures

K. Devi Priyadarisini*
Department of Civil Engineering
College of Engineering Guindy,
Anna University, Chennai,
Tamil Nadu, India.

G. Umadevi
Department of Civil Engineering,
College of Engineering Guindy,
Anna University, Chennai,
Tamil Nadu, India.

***Abstract*— Peri urban areas refer to the settlements beyond, about or around cities. The population growth rate of peri urban areas of Chennai is around 3.5 compared to the city growth rate of around 1.25. The current population of Chennai Metropolitan Area is about 8.7 million and is estimated to reach about 12.5 million by 2026. Majority of this increase is expected to settle in suburban and peri urban areas as the city is already reaching saturation. Fundamental root cause for traffic congestion is improper neighbourhood planning which does not account the holding capacity of the basic infrastructures and its impact on transportation infrastructure. So neighbourhood planning should be done in such a way that population holding capacity should be estimated based on all basic infrastructures. The main objective is to develop a system dynamics simulation model for peri urban areas in Chennai. The developed model will be used for assessing its possible and preferable growth directions through various scenario analysis based on economic considerations and suggest the best scenario so as to ensure a growth towards sustainable development in the long run. The model is developed with simple mathematical equation for simulation. The outcome of the study is optimum density norms by considering basic infrastructures such as transportation, water supply, sanitation, electricity and telecommunication.**

Keywords*— *System dynamics simulation; Holding capacity; Optimum density norms; Basic infrastructures.

I. INTRODUCTION

Chennai urban agglomeration had a population of about 6.56 million in 2001 and it has increased by 2.13 million to reach 8.69 million in 2011.Real estate development mushroomed in South Chennai after it was catalogued as the growth corridor of the city. The focus of the state government over the last decade in promoting Old Mahabalipuram Road (OMR) as an IT/ ITeS destination, has created immense employment opportunities in South Chennai. South Chennai leads the Chennai residential market in terms of the number of units launched and absorbed. South Chennai continues to account for the lion's share (69%) in the Chennai residential market.

II. OBJECTIVES

- To study the transportation network and other basic infrastructures of peri urban areasto build appropriate simulation model
- To test and validate the model for various scenario and policy options for ensuring sustainable development.
- To recommend the best scenario for achieving sustainable transportation and infrastructure development to enhance quality of life in the study area.

III. STUDY AREA

Peri Urban settlements along OMR are selected as study area. It includes Perungudi, okkiyamThoraipakkam, karapakam and sholinganallur. Perungudi and Sholinganallur are Town Panchayats and OkkiyamThoraipakkam and karapakkam comes under Village Panchayats of St.Thomas Mount Panchayat union as of old Chennai City limit concerned as depicted in Fig.1. The reason behind the selection of study area is that the southern group consisting of developments from Perungudi to Sholinganallur exhibits a very high growth rate.

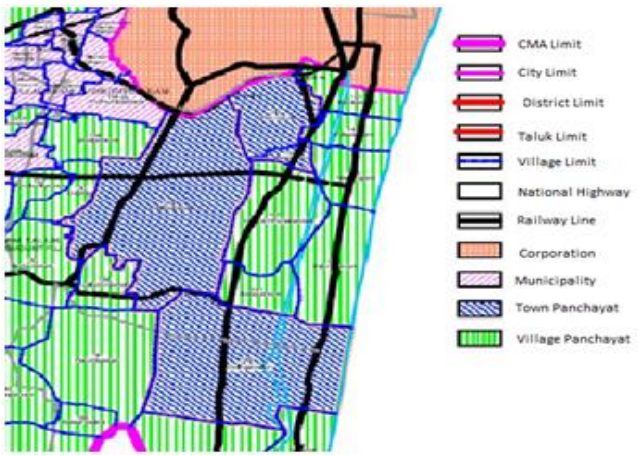

Fig. 1. Study Area **(**Source : CMDA)

III. METHODOLOGY

The methodology of this work is depicted in the figure 2. Essentially the steps involved are data collection, analysis, model building and to suggest appropriate mitigation measures.

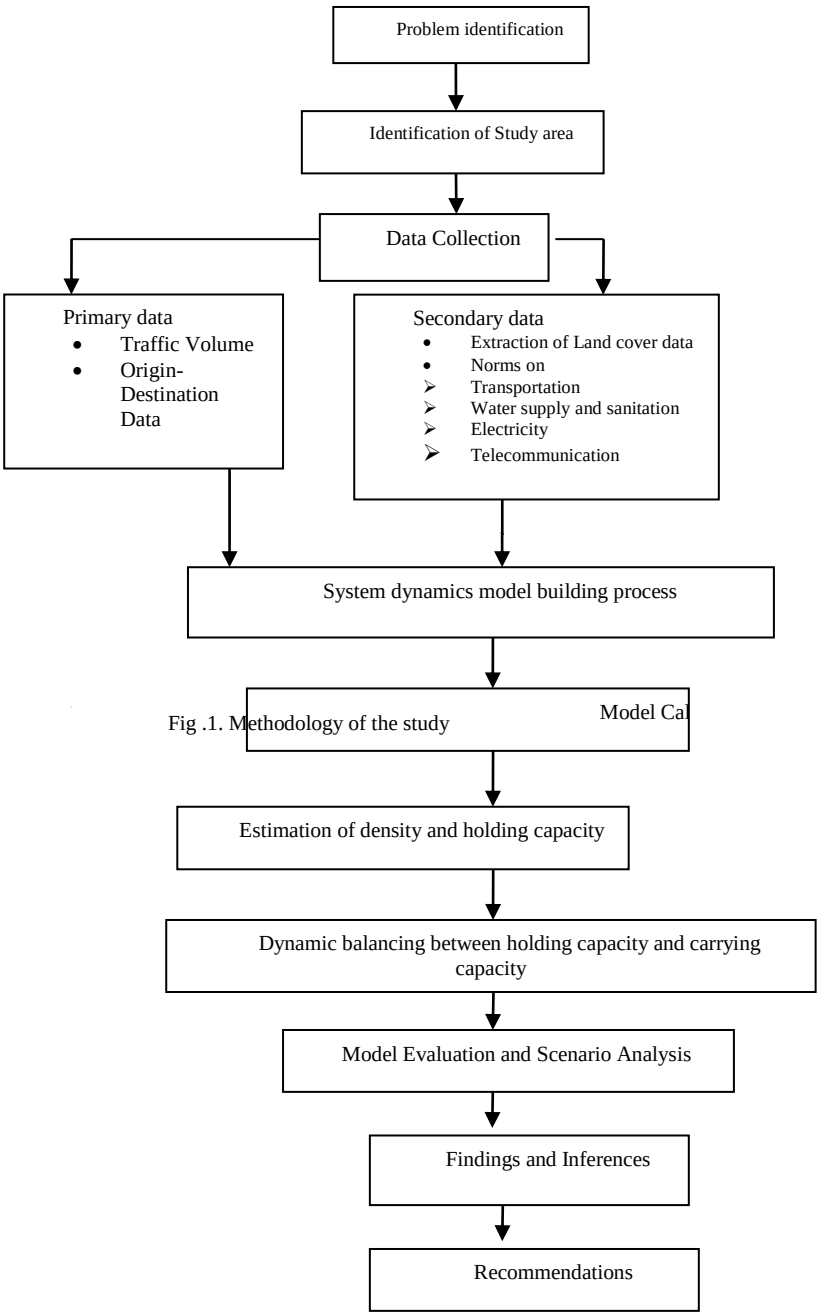

Fig .1. Methodology of the study

Fig. 2. Study Methodology

IV. DATA COLLECTION AND ANALYSIS

A. General

Holding capacity can be determined by considering Traffic volume as primary data and demography, land use and norms on basic infrastructures as secondary data. The collected data are briefly discussed.

B. Primary data collection

Primary data collection involves Local trips bounded in the study area. It is achieved through traffic volume surveys at 3 different locations of Old Mahabalipuram Road between 3.30 p.m and 8.30 p.m. The locations include Perungudi, Thoraipakkam, Sholinganallur.

Fig 3 shows the peak traffic volume observed at 3 survey locations and it depicts that the peak traffic volume is the highest at Perungudi location.

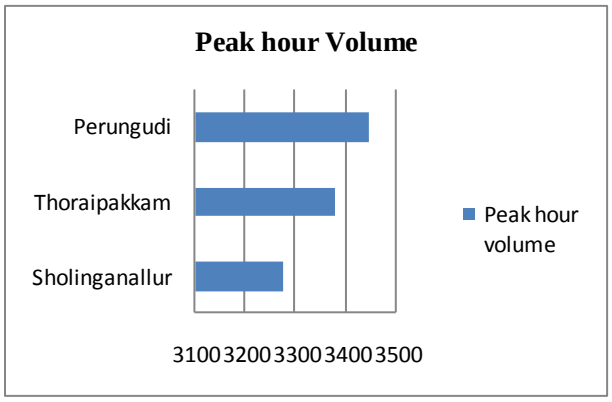

Fig. 3. Peak hour volume

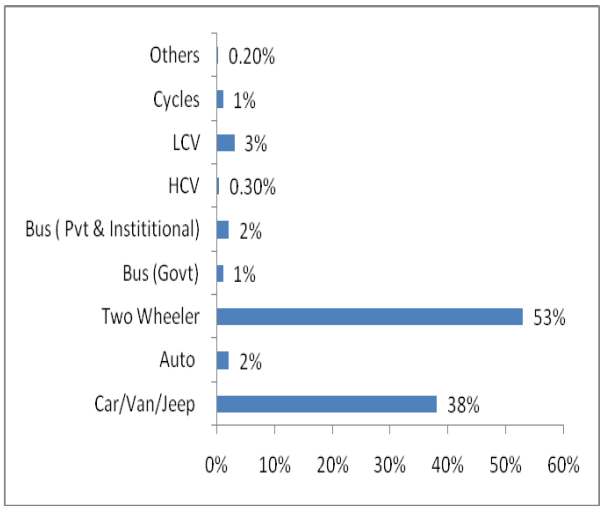

Fig. 4. Vehicle Composition

Figure 4 illustrates the vehicle composition of Chennai IT corridor. Two wheeler and car proportion in the total volumes are observed around 53 and 35 percent and Buses (governments and private & institutional) is around 4 percent only. This seems to be an unhealthy proportion with regard to environment consideration and Level of Service (LOS).

C. Secondary data collection

Collection of secondary data includes Demographic data, Land use data and norms on basic infrastructures such as Water supply and sanitation, Telecommunication and Electricity.

D. Demographic data

Figure 5 shows the demographic profile of study area. From the figure it is observed that Thoraipakkam census town has highest population of 56642 with 14524 households.

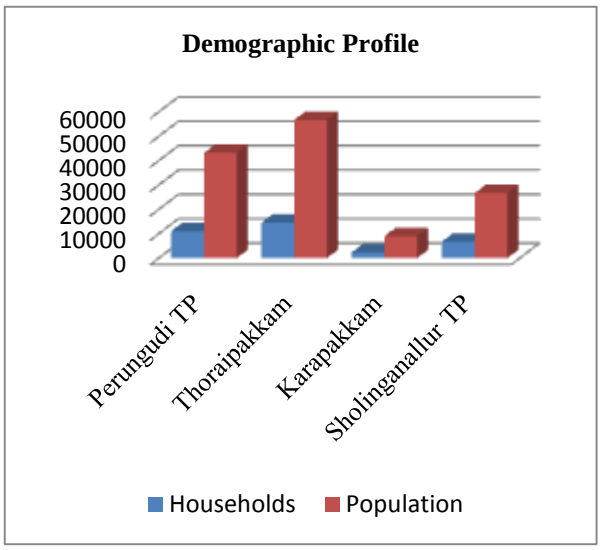

Fig. 5. Demographic profile
(Source: Compiled from census 2011)

E. Telecommunication data

Telecommunication profile was collected from Bharat Sanchar Nigam Limited (BSNL) exchanges and it is given in Fig 4.Karapakkam has highest number of telecommunication network with 3205 broad band connections followed by Perungudi with 1723 broad band connections

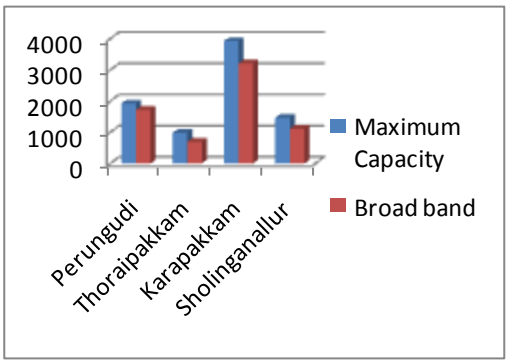

Fig. 6. Telecommunication network
(Source: Compiled from BSNL)

F. Land use data

Land Use	*Perungudi*		*Thoraipakkam*		*Karapakkam*		*Sholinganallur*	
	Ha	%	Ha	%	Ha	%	Ha	%
Primary Residential	152.6	39	289	48	22.4	9	611.4	40
Mixed Residential	51.8	13	79.7	13	34	14	116.4	8
Institutional	84.2	21	17.5	3	18.1	7	32.36	2
Industrial	49.2	12	135.9	23	93.5	39	423.9	28
Water body	17.7	5	48.6	8	9	4	140.29	9
Agricultural	8.6	2	-	-	-	-	-	-
Commercial	-	-	-	-	21	8.7	33.24	2
Non Urban	-	-	-	-	3	1.3	14.11	1
CRZ	-	-	-	-	-	-	140.74	9
Road Network	30.9	8	30.9	5	8.5	3	23.36	1
Total	395	100	601.6	100	242	100	1535.8	100

Table 1.Extent of Land use
(Source: Compiled from CMDA Land use map)

V. MODEL DEVELOPMENT

A. General

Simulation model has been developed for population sector and infrastructures sector using the STELLA simulation software With the System dynamics (SD) model, relationship between the population growth and its level of population and its supply of all basic infrastructures are established and density norm for all basic infrastructures are determined. Optimum density norm is said to be the minimum among all. Holding capacity is calculated based on the optimum density norm.

The existing land use data is used to know the existing area for allocating the projected population and the future land use proportion can be formulated for corresponding population growth. Intuitive scenarios can be analysed for the developed model. The different patterns of possible present and future growth are generated and holding capacity is determined towards achieving sustainable development for the study area.

B. Model Development – Population Sector

Population model has been built to estimate the projected population as given in Fig 7 by accounting birth rate, death rate, immigration and out migration rate.

Equation used:

Population (t) = Population (t-dt) + (Birth_Rate + Inmigration_Rate – Death_Rate – Out_Migration_Rate) * dt

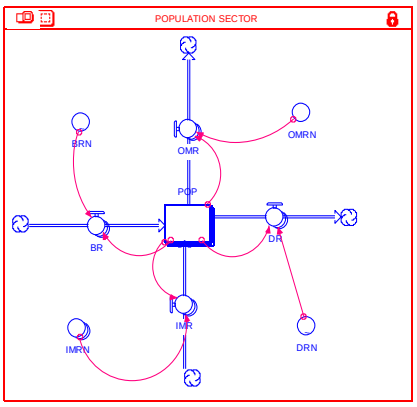

Fig .7.SD Model for Population Sector

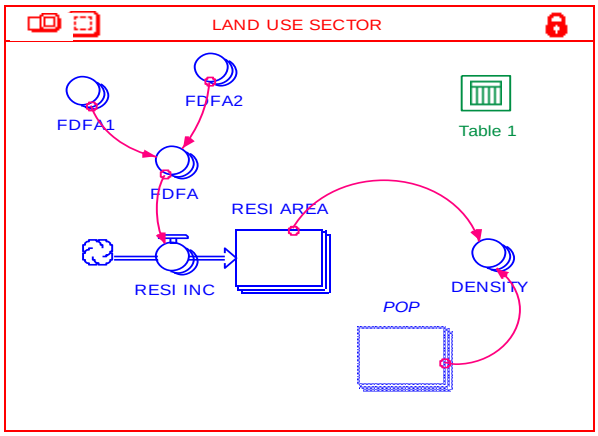

Fig. 8. SD Model for Land Use Sector

C. Model Development – Land use sector

Stella model for land use sector is built by considering existing residential land area and future developable floor area. By accounting residential growth rate extent of land area in projected year is calculated.

Existing residential floor area for every year can be developed with respect to the growth rate of residential

intensity and available residential area of each zone. Residential intensity is inflow into level because of positive polarization.

Equation used :

FDFA1= Existing residential area (Remaining % from already developed) * Plot coverage for constructing house* Undeveloped remaining FSI

FDFA2= Existing residential area (% yet to be developed) * Plot coverage for constructing house* Undeveloped FSI

FDFA = FDFA1 + FDFA2

Residential area= Existing residential area (% from already developed) * Plot coverage for constructing house* Developed FSI.

D. Model Development – Transport sector

Model for transportation sector is built by accounting present vehicular volume and growth rate of vehicles in order to determine the volume/ Capacity ratio and given in Fig 9.

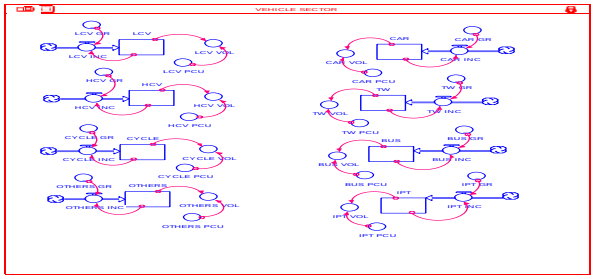

Fig. 9. SD Model for Transport Sector

VI. RESULTS

A. Do Minimum Scenario

In do minimum condition, the existing trend of growth rates has been allowed to continue till the year 2026. It is observed that the v/c ratio varies from 1.26 in the base year 2015 to 2.53 in the horizon year 2026. For basic infrastructures sector, only under construction projects are accounted in do minimum scenario.For water supply sector, the demand supply ratio varies from 1.5 to 1.32 and for Electricity sector a constant D/S ratio of 1.25 continues upto horizon year since there is no power plants under construction.

For sanitation infrastructure, the D/S ratio varies from 0.56 to 1.26 if under construction STPs are alone considered. For Telecom sector, D/S varies from 0.9 to 1.28 by accounting current broadband growth rate. For Land use sector the density varies from 262 persons/hectare to 318 persons/hectare for current trend of Land use intensification.

B. Desirable Scenario

In this scenario, simulation has been carried out such that restricting the growth rate of personalized modes and increasing the capacity of the corridor in terms of providing elevated corridor along the study stretch. A V/C ratio of 0.96 is achieved in desirable scenario. For basic infrastructures sector, all new proposals are introduced in order to make the D/S ratio less than 1.

For telecom sector a D/S ratio of 0.98 is achieved in horizon year by augmenting the rate of increase of exchange capacity. In land use sector a density of 259 persons/hectare is achieved by accelerating the land use intensification trend on par with the population increase.

VII. RECOMMENDATIONS

- Here the mathematical equation is developed and used to develop the model and simulate.
- For Transportation sector, the growth trend of personalised mode has to be decreased by augmenting the public transportation facilities such as BRT.
- For basic infrastructures sector, new proposals like Desalination plant, STP, Power plants and substation has to be implemented to improve the Quality of Life.
- Economy has to be compromised a while for implementing such proposals since these proposals will have lot of intangible benefits like congestion reduction, fuel savings, etc.

REFERENCES

[1] Banuchander T R(2011),"Growth pattern and Travel characteristics of Peri urban areas of Chennai", M.Tech thesis, Anna university, Chennai.

[2] Citizens alliance for sustainable living (sustain), Chennai, India service provision governance in the peri-urban interface of metropolitan areas research project report on" an overview of the water supply and sanitation system at metropolitan and peri-urban level: the case of Chennai".

[3] Haroldo Torres, HumbertoAlves and Maria Aparecida De Oliveira (2007)," Sao Paulo peri urban dynamics: Some social causes and environmentalconsequences", Environment and Urbanization, Vol. 19, No.1 , pp 207-223.

[4] John O. Browder, James R. Bohland and Joseph L. Scarpaci (Sep 1995),Patterns of development on the metropolitan fringe: Urban fringe expansionin Bangkok, Santiago and Jakarta", Journal of American Planning Association, Vol. 61, Issue 3, pp 310-327

[5] Karthik.N and et al. (2011),"Infrastructure Development of Medavakkam", B.E thesis, Division of Transportation Engineering, Anna university, Chennai.

[6] Second Master Plan for Chennai Metropolitan Area 2026, Vol.1 pp 68-80, and Vol.3 pp 157-181, Chennai Metropolitan Development Authority.

[7] Sekar S P and kanchanamala S (2011), "Analysis of growth dynamics of Chennai metropolitan Area", ITPI journal December 2011.

Full Chip Thermal Analysis using Generalized Integral Transforms

C. M. Arun Kumar*
Department of ECE,
University College of Engineering
Pattukkottai,
Thanjavur, Tamil Nadu, India.

P. C. Mukeshkumar
Department of Mechanical
Engineering,
University College of Engineering
Dindigal, Dindigul, Tamil Nadu,
India.

C. Kavitha
Department of Mathematics,
Sathyabama University,
Chennai, Tamil Nadu,
India.

***Abstract*—The estimating the temperature variation is critically important for timing analysis, leakage reduction, power consumption, hotspot avoidance and reliability concerns during modern IC design. In this paper, highly efficient full chip thermal simulator analysis is used in advance stage temperature aware chip design. Here the generalized integral transforms (GIT), used to estimate the temperature distribution of full-chip with a truncated set of spatial bases which only needs very small truncation points. Then, we develop a fast Fourier transform like evaluating algorithm to efficiently evaluate the derived formulation. The proposed GIT-based analyzer can achieve an order of magnitude speedup compared with a highly efficient Green's function-based thermal simulator.**

Keywords— Circuit simulation, generalized integral transforms (GITs), physical design, simulation, thermal analysis,3-DIC.

I. INTRODUCTION

Now a days the CMOS technology scales down in using electronics components so that the power density of VLSI circuits increases monotonically as an increase of components. The power dissipated produced in the circuit's converts into heat and as a result, it raises the temperature of dies and induces hot spots. These thermal related phenomena significantly reduce the performance and reliability of circuits [1]–[16]. For example, the resistance of copper interconnect increases 39% as the temperature rises from 20 C to 120 C, and the mean-time-to-failure of the interconnect exponentially decreases as the temperature increases [1]. Thermal analyser is used to precisely predict the thermal impacts on design performance, an efficiently and accurately .The thermal simulators can be classified into two classes, numerical and analytical methods. The numerical methods use the finite difference method or the finite-element method (FEM) to transfer heat equations to resistance–capacitance(RC) network equations. Based on the RC network equations, several methods have been proposed to save the runtime. Wang et al. [2] utilized the alternating-direction-implicit method to split the equivalent RC system into different alternating directions, andalternately performed the line smooth scheme in each direction. In [3], the model order reduction technique was employed to improve the efficiency of transient analysis. Li et al. [4] applied the multi-grid method to speed up the convergence rate of iterative methods, and developed an order reduction scheme to save the runtime of dynamic thermal simulation. Because of the flexibility for dealing with the complicated structure, the numerical framework is the main stream in back-end design stages such as the post layout thermal verification. As pointed out in [1], [5], and [6], temperature-aware designshould be brought to early design stages such as thermal-aware floor-planning and placement. To give a reasonably accurate temperature prediction with little computational effort, [1] proposed a compact thermal model which modeled the package and interconnect layers as effective heat transfer coefficients for the boundary conditions of die. With the modeled heat transfer coefficients for the heat sink, prelayout interconnect and package, recently, an efficiently numerical thermal simulator developedby Yong et al. [7] is very suitable for early temperature-aware design stages. Because their simulator applies an adaptive discretization algorithm for spatial and temporal domains to analyse the temperature profile without degrading the accuracy, the number of temperature variables and simulating time steps can be significantly reduced. The other category of thermal simulators being suitable for early design stages is the analytical method. The primary advantage of analytical approaches is that they avoid the volume meshing procedure of entire substrate, and have closed-form representations for the temperature distribution of the entire die. Hence, they are flexible to obtain the temperature distribution of certain user-specified regions without performing the thermalsimulation for the entire die. Furthermore, based on the closedform representations, the fast temperature evaluation of the die can be achieved for early design stages.One analytical thermal solver is the Green's function-based method [6]. First, the steady-state Green's function of chip with a unity impulse power source is calculated. After that, its steadystate temperature distribution with arbitrary power source map is got by taking the convolution of Green's function and its power density distribution with a table lookup method. To enhancethe efficiency for lots of power sources, they used a seriesof cosine waveforms to approximate the power density map, andthe temperature map of all grid cells were cast into the form ofdiscrete cosine transform (DCT). Although their computationalcost is, where and are numbers of divisionsin the power density map along - and -directions, respectively,they can only provide the steady state thermal simulation. Moreover, as indicated in [6], a large number of truncation points for the Green's function is usually required

to achieve an accurate solution. To overcome these shortcomings, our major contributions are as follows.

• Compared with a highly efficient Green's function-based method [6], improve the bound of the error decaying rate of analytical solution for the steady state temperature distribution and provide a transient temperature simulation by utilizing the generalized integral transforms (GITs) [17]–[19] to construct a set of spatial bases and calculate their time-varying coefficients.

• Develop a fast Fourier transform (FFT) like evaluating algorithm to efficiently evaluate the temperature map of all grid cells, and its computational cost is in the order of O(MN $\log_2 N_x N_y$), where N_x,N_y are truncationpoints of bases in the - and -directions, respectively.

• Build an efficient 3-D IC thermal simulator by combining the GIT and numerical schemes, and its efficiency and accuracy are demonstrated by experimental work.

II. THERMAL MODELING FOR EARLY DESIGN STAGES

A compact thermal structure of the chip, as illustrated in Fig. 1, can be used for early design stages. This model consists of three portions [1]: the primary heat flow path, the secondary heat flow path, and the heat transfer characteristic of each macro/block on the silicon die. The primary heat flow path is composed of thermal interface material, heat spreader and heat sink. The secondary heat flow path contains interconnect layers, input/output (I/O) pads and the print circuit board (PCB). The functional blocks are modelled as many power generating sources attached to a thin layer close to the top surface of die with the thickness being equal to the junction depth. The major concerns of early-stage temperature-aware optimization procedure are to reduce the temperature or the thermal gradient of die. Here, the main focus on estimating the temperature distribution.

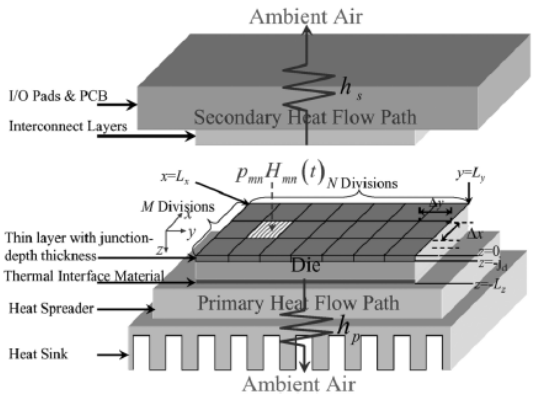

Fig. 1. Compact thermal model for early design stages

According to energy conservation law, the changing rate ofenergy in a unit volume of substrate equals to the conductionheat through the unit volume [17]. Based on this heat conduction mechanism,the temperature $T_d(r,t)$ of die can be governed by thefollowing heat transfer equations [2], [4], [5], [7]:

$$\sigma(T_d)\frac{\partial T_d(\mathbf{r},t)}{\partial t} = \nabla\cdot(\kappa(T_d)\nabla T_d(\mathbf{r},t)) + p(\mathbf{r},t); \quad \mathbf{r}\in D$$

$$\kappa(T_d)\frac{\partial T_d(\mathbf{r},t)}{\partial n_{b_s}} + h_{b_s}T_d(\mathbf{r},t) = f_{b_s}(\mathbf{r}).$$

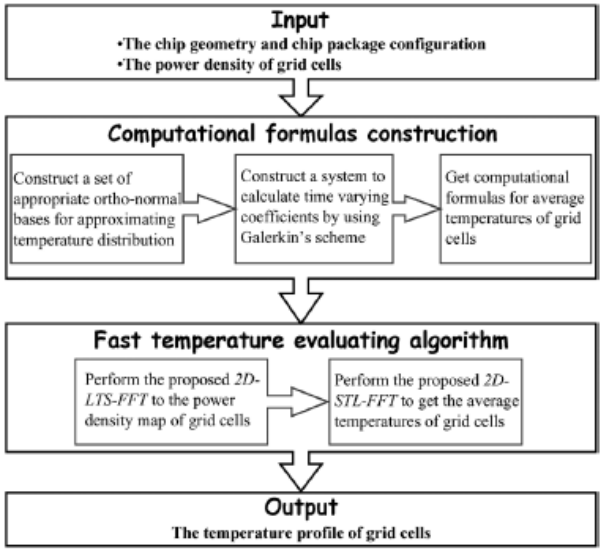

Fig.2. Executing flow of the proposed GIT-based thermal simulator

III. FULL CHIP THERMAL SIMULATION

The executing flow of our GIT-based thermal simulator is summarized in Fig.2.The GIT-based computational formulas for the full-chiptemperature distribution was used. The two efficient FFT like evaluating algorithms,2D-LTS-FFT and 2D-STL-FFT to getthe transformed coefficients for the power density map of gridcells and the desired temperature distribution, respectively.In reality, the leakage power of chip is temperature dependent.

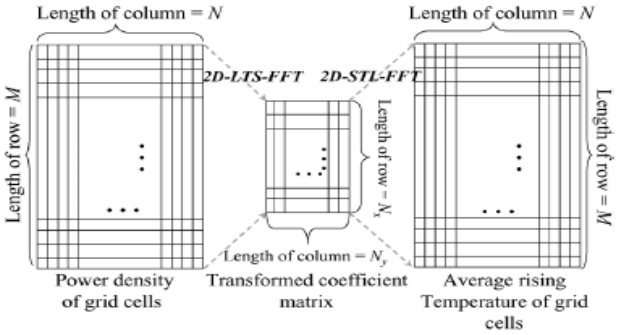

Fig .3.Overview of using 2D-SLT-FFT and 2D-LTS_FFT to evaluate the average rising temperature of grid cells.

IV. EXPERIMENTAL RESULTS

Here GIT-based thermal simulator and the Algorithm of a highly efficient Green's function based method [6] in C++ language. The results are compared with a commercial computational fluid dynamic software ANSYS.

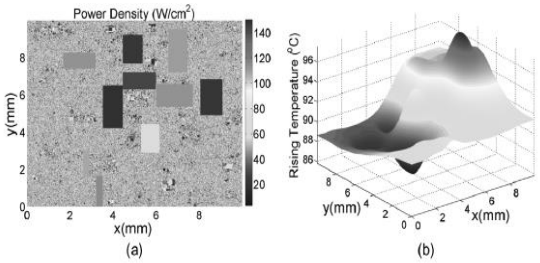

Fig 4.Powerdensity and temperature distribution

CONCLUSION

An accurate and efficient GIT-based thermal simulator has been explained. The proposed algorithm only takes0.13 s for a chip with one million functional blocks and overone million grid cells, and 0.48 s for a 3-D IC with 3.146million grid cells in the post-calculating stage to achieve accuratelysteady state temperature distribution. Therefore, theproposed GIT-based thermal simulator is very suitable for thethermal-aware design flow.

REFERENCES

[1] W. Huang, S. Ghosh, S. Velusamy, K. Sankaranarayanan, K. Skadron,and M. R. Stan, "HotSpot: A compact thermal modeling methodology for early-stage VLSI design," *IEEE Trans. Very Large Scale Integr.(VLSI) Syst.*, vol. 14, no. 5, pp. 501–513, May 2006.

[2] T.-Y. Wang and C. C.-P. Chen, "Thermal-ADI: A linear-time chiplevelthermal simulation algorithm based on alternating-direction implicit(ADI) method," *IEEE Trans. Very Large Scale Integr. (VLSI)Syst.*, vol. 11, no. 4, pp. 691–700, Aug. 2003.

[3] T.-Y.Wang and C. C.-P. Chen, "SPICE-compatible thermal simulationwith lumped circuit modeling for thermal reliability analysis based onmodel reduction," in *Proc. Int. Symp. Quality Electron. Des.*, 2004, pp.357–362.

[4] P. Li, L. T. Pileggi, M. Asheghi, and R. Chandra, "IC thermal simulationand modeling via efficient multigrid-based approaches," *IEEETrans. Comput.-Aided Des. Integr. Circuits Syst.*, vol. 25, no. 9, pp.319–326, Sep. 2006.

[5] J.-L. Tsai, C. C.-P. Chen, G. Chen, B. Goplen, H. Qian, Y. Zhan,S.-M. Kang, M. D. F. Wong, and S. S. Sapatnekar, "Temperature-aware placement for SOCs," *Proc. IEEE*, vol. 94, no. 8, pp.1502–1518, Aug. 2006.

[6] Y. Zhan and S. S. Sapatnekar, "High efficiency Green function-basedthermal simulation algorithms," *IEEE Trans. Comput.-Aided Des. IntegrCircuits Syst.*, vol. 26, no. 9, pp. 1661–1675, Sep. 2007.

[7] Y. Yang, Z. Gu, C. Zhu, R. P. Dick, and L. Shang, "ISAC: Integratedspace-and-time-adaptive chip-package thermal analysis," *IEEE Trans.omput.-Aided Des. Integr. Circuits Syst.*, vol. 26, no. 1, pp. 86–99,Jan. 2007.

[8] K. Banerjee, S. J. Souri, P. Kapur, and K. C. Saraswat, "3-D ICs: Anovel chip design for improving deep-submicrometer interconnect performanceand systems-on-chip integration," *Proc. IEEE*, vol. 89, no. 5,pp. 602–633, May 2001.

[9] G. L. Loi, B. T. Agrawal, N. Srivastava, S.-C. Lin, T. Sherwood, andK. Banerjee, "A thermally-aware performance analysis of verticallyintegrated (3-D) processor-memory hierarchy," in *Proc. Des. Autom.Conf.*, 2006, pp. 991–996.

[10] H. Hua, C. Mineo, K. Schoenfliess, A. Sule, S. Melamed, R. Jenkal, andW. R. Davis, "Exploring compromises among timing, power and temperaturein three-dimensional integrated circuits," in *Proc. Des. Autom.Conf.*, 2006, pp. 997–1002.

[11] J. Cong, G. Luo, J. Wei, and Y. Zhang, "Thermal-aware 3D IC placementvia transformation," in *Proc. Asia South Pacific Des. Autom.*,2006, pp. 780–785.

[12] J. Cong, J. Wei, and Y. Zhang, "A thermal-driven floorplanning algorithmfor 3D ICs," in *Proc. Int. Conf. Comput.-Aided Des.*, 2004, pp.306–313.

[13] B. Goplen and S. Sapatnekar, "Efficient thermal placement of standardcells in 3D ICs using a force directed approach," in *Proc. Int. ConfComput.-Aided Des.*, 2003, pp. 86–89.

[14] K. Balakrishnan, V. Nanda, S. Easwarm, and S. K. Lim, "Wire congestionand thermal aware 3D global placement," in *Proc. Asia SouthPacific Des. Autom.*, 2005, pp. 1131–1134.

[15] Y.-K. Cheng, P. Raha, C.-C. Teng, E. Rosenbaum, and S.-M. Kang,"ILLIADS-T: An electrothermal timing simulator for temperature-sensitive reliability diagnosis of CMOS VLSI chips," *IEEE Trans.Comput.-Aided Des. Integr. Circuits Syst.*, vol. 17, no. 8, pp. 668–681,Aug. 1998.

[16] K. Skadron, M. R. Stan, K. Sankaranarayanan, W. Huang, S.Velusamy, and D. Tarjan, "Temperature-aware microarchitecture:Modeling and implementation," *ACM Trans. Arch. Code Opt.*, vol. 1,no. 1, pp. 94–125, Mar. 2004.

[17] M. D. Mikhailov and M. N. Ozisik, *Unified Analysis and Solutions ofHeat and Mass Diffusion*. New York: Wiley, 1983.

[18] N. Y. Olcer, "On the theory of conductive heat transfer in finite region,"*Int. J. Heat Mass Transfer*, vol. 7, pp. 307–314, 1964.

[19] M. D. Mikhailov, "General solutions of the heat equation in finite regions,"*Int. J. Eng. Sci.*, vol. 10, pp. 577–591, 1972.

Implementation of Lean Manufacturing Technique with Matlab Simulation Software in An Automobile Industry–A Case Study

S. Mahendran*
Department of Mechanical Engineering,
University College of Engineering Pattukkottai,
Thanjavur, Tamil Nadu, India.

A. Senthil Kumar
Department of Mechanical Engineering,
University College of Engineering Panruti,
Panruti, Tamil Nadu, India.

***Abstract*—Today's automobile industries are high competitive, volatile and fluctuation in demand in market. So these industries are planned how to improve their performance. A common technique lean is followed to reduce the wastage, cost and increase the productivity of the industry. The main aim of this project is using the lean principle to reduce the overall cost and increase the percentage of value addition. The objective of this article is to draw the current state value stream map and identify the waste area of the project. The batch processing is converted into lean manufacturing method. The various lean tools JIT, kanban card, value stream mapping methods are used to reduce the non value added time, lead time and increase the percentage value addition. The future state value stream mapping indicates the improved status of the lean manufacturing method. The matlab simulation software method is used to check the values within the range. The overall efficiency of the manufacturing industry is gradually increased.**

Keywords—Value stream mapping, 5s, jit, matlab simulation, value addition.

I. INTRODUCTION

The lean manufacturing concept was first used in toyota production system, japan. In traditional manufacturing, inventory is made in manufacturing, but lean manufacturing there is no inventory. Now the markets are more competitive, so lean manufacturing is important principle to satisfy the customer, worker and improve the productivity and efficiency of the industry. Lean is defined in 5 ways, define customer value, define value stream, make it flow, establish pull, strive for excellence [1]. The various industries are surveyed and improvement programmes are followed in process and equipment, human resources, product design, supplier relationships and customer relationships [2]. The lean sigma concept (DMAIC) and kaizen is used to reduce wastage and increase the industries productivity. The various automobile tool industries are identified and surveys are made. The tool was validated and faced, content and reliability test and involvement in reliability is calculated. Only 31% of the industries are implementing lean concepts. Remaining industries are not aware the lean concept and make awareness of lean concept in workers, supervisors and all levels [3]. The rotary switch manufacturing organaisation is implemented lean six sigma methodology, cause and effect diagram is drawn to invent the faulty switches. The various process parameters with design of experiment were conducted to improve in defects are made. The overall equipment effectiveness (OEE) is calculated and overall defects are reduced [4]. The value stream mapping method is used to identify the current status of the industry. The welding and grinding operations are made separately and man machine chart is prepared for indicating the current position. The combined working of welding and grinding operations are made then future state man machine chart is drawn. Overall performance of industry is improved [5]. The manufacturing industry is identified and value stream mapping is drawn. The wasted area are identified and 5 why method is implemented to know the reason for wastage. The cause and effect diagram is drawn to calculate the root causes of the wastage. The various lean techniques are followed to reduce the lead time and wastage [6]. The process industry is identified and value stream mapping is drawn. The lean tools 5s, jit, kaizen, kanban are used to reduce the wastage[7].The impact of lean methods and tools are studied through various manufacturing industries. Structural modelling equation is used to validate the various lean tools. Jit and automation is highly responsive and kaizen, TPM, vsm are lesser effective [8]. The kaizen improvement technique is used to reduce the wastage and improve the overall efficiency of the industry. The new financial metric is used to reduce the wastage [9]. The lean manufacturing have seven levels: system, object, operation, activity, resource, characteristic, application. Poka yoke- fault proof device used in industry [10]. A case study is made in leading forging industry, value stream map is drawn. Various lean tools are used to reduce the wastage and cost. s/n ratios and anova methods are used to reduce the wastage . The lead time and non value added activities are reduced [11]. The 5s methodology is followed in an industry and to reduce the wastage. There are various actions are used, management teamwork training, test laboratory selection, guide designation, implementation team establishment, implementation planning, launch meeting, 5s establishment, implementation development, other laboratories development and continuous improvement to reduce the cost [12]. To get a better result in lean manufacturing, few activities are additionally used, special trolley or cart for product transportation, heat exchanger installation for cooling

purpose in the industry [14]. Cellular manufacturing is a group technology, certain group of products produced in unique method. Takt time is calculated and lean techniques are applied to improve the productivity [15]. The lean manufacturing implementation in an industry is barriered for two reasons –the redundancy programme, lack of employees education about lean knowledge. These two problems are overcome in that paper [16]. The lean manufacturing method means not only reduce the defect, but also reduce the cost of production. The structural equation modeling (SEM) equation is used to build the measurement and structural models [17]. The IT industries and lean manufacturing are interdependent, using structural model various lean tools are used to reduce the effects and improve the industries performance [18]. The lean manufacturing material is handling manually in conventional method. By adoption of lean anchorage, the handling method and work material travelled are controlled by lean principles [19]. The lean tools are used in industries, jit, tqm and HRM are implemented, results show that Just In Time and Total Quality Management have a direct and good effect on operational performance while HRM has a normal effect on it [20] .The JIT is a main tool used in lean manufacturing. The relationship between lean manufacturing and just in time linkages are studied and analyzed [21]. Lean manufacturing have a number of operational performances such as efficiency and productivity [22], quick time [23] and quick delivery [24]. The lean manufacturing company is more productivity if the wastage is reduced. The kaizen is a advanced technique, design changes are made to improve the companys performance [25]. Lean manufacturing techniques promote improved flexibility, enhanced reliability and substantial cost reductions [26]. The kanban system works effectively in multinational organizations, the study suggest that top management, commitment, inventory management and quality improvement [27]. The kanban system is applied in small manufacturing company in malaysia, reduce the leadtime, minimize inventory on floor and optimize storage area [28]. The various 5s methodologies stage action is management team action, test laboratory selection, guide designation, implementation of team establishment, implement the planning, launch meeting, 5s board establishment, implementation development and continuous improvement are implemented. The 5s methodology applicable in university organizations and it becomes like industries. A clean workplace, well organized and visual indication of risks are a safe workplace [29]. The kanban based jit environment for single stage single product kanban controlled production line is developed. The queuing synchronizing mechanisms have simulated the interaction of the different system parameters [30]. The lean implementation in one third of the industry is failure due to lack of management and less awareness. The lean practice bundle is prepared and executed. the framework is developed for sustainable lean implementation using interpretive lean manufacturing[31]. The lean manufacturing with operational performance is explained, the survey made at 266 plants in 9 countries. The results say that JIT and TQM have direct and positive effect and HRM has mediating effect [32]. The various factors influencing the lean implementation, 4 case studies made in a manufacturing company and seven factors affect the implementation of lean practices. The seven factors are the reason for adopting LP, the experience of the company with LP, the need for involvement of supporting areas in LP practices, the interdependence of some practices, the variety of models produced by cell, the synergy between LP and MC, the size of equipment. The results says that presence and impact factors on it [33]. The MRP and JIT systems are combined to reduce the wastage and increase the profit of the industry. The material requirement planning is a push method and jit is a pull method, combination of these tools used to reduce the wastage [34]. The jit is an important tool which affect the financial status of the industry. If the inventory is more the storage cost is high and vice versa [35].

Research gap

From literature survey, more number of researchers follows the lean manufacturing method with value stream mapping (current and future state). But few of them used value stream mapping with simulation software method. The matlab simulation software is used to check the values within the range or not. The overall lean anchorage is used to overcome the defects of Indian automobile industries.

II. CASE STUDY OF THE COMPANY

A case study is made in leading automobile valve manufacturing company (XY) located in trichirappalli, tamilnadu, India. Currently, the plant has 8 manufacturing lines that produce valves for various original equipment manufacturers. The lean manufacturing concept is applied in manufacturing line 2 and the valves are produced by batch production method. Since the productivity is decreased, the arrival of new customers whose requirement is noted in table 1. The line2 is modified by adapting the techniques of lean production system. Average customer's demand has been calculated as 2,15,000 valves per month. Manufacturing of engine valve happens in two phases. The first phase is called as pre-machining, where the valves are forged, heat-treated. The second phase is called as machining for which each model of valves are produced in a dedicated line. In the pre machining process, the long bar is cut in to the required length. In the machining shop the valve undergoes series of process to become a complete valve as per the customer's demand. The process, right from start to end is mapped using current state value stream mapping. In table 1, the various automobile industry customers (A1, A2, B1, B2, C1, C2) for both inlet and exhaust valves with part numbers and requirement per month are noted.

A. Process sequence in forge shop

The raw material (cutbar) is deburred and it is inspected for upsetting and forging process. A heat treatment process is made on this material. Three separate processes such as hardening, washing and tempering are made. After that the material is allowed for straightening then admitted for stress relieving. It is processed in wet end grinding, shot blasting and it is converted in to forging approval process, then sent to kanban area. There are various machines used for this process rough centerless grinding, turning, groove grinding, undercut, stress relieving, finish centerless grinding, nitriding, seat grinding, induction hardening and auto cleaning.

Table 1

Customer	*Part Number*	*Requirement per Month (In Numbers)*
Automobile Industry-A1	A1 – Inlet valve-50152	75000
Automobile Industry-A2	A2 – Exhaust valve - 50157	75000
Automobile Industry-B1	B1 – Inlet valve - 50491	7500
Automobile Industry-B2	B2 – Exhaust valve - 50496	7500
Automobile Industry-C1	C1 – Inlet valve - 50460	25000
Automobile Industry-C2	C2 – Exhaust valve-50465	25000

B. Simulation used with VSM

In this manufacturing industry, it is very difficult to predict the exact values of raw material requirement, inventory management and number of employees, production planning and control. The current state of value stream mapping indicates the actual position of the industry. The matlab simulation software is used to calculate the simulated completion time, distance travelled, non value added time and lead time. Matlab is used to check the values within the range or not. In table 2, takt time is calculated. Automobile industry A,B,C and the customer's various part number are noted. The total demand per month and demand per day are noted. There are 3 shifts, total break time and total available time per day is calculated. Finally the takt time is calculated as 8.62 sec.

Customer	*Automobile industry A,B,C*
Part Number	46152/46157/46491/46496/40460/ 40465
Demand/month	215000 (Constant Demand)
Demand/day	8600 (Constant Demand)
No of Shifts	3
Shift Hours	8 hrs
Lunch Break	30 min
Autonomous Maintenance	10 min
Tea Break	10 min
Allowances	10 min
Part changeover time/month	10 hrs/month
Part changeover time/shift	8 min/shift
Available time / Shift	412 min/shift
Total Available Time / Day =	1236 min
	74160 sec
Takt Time =	Total Available Time / Demand
	8.62 sec

Table 2. Takt time calculation for line 2

III. RESULTS AND DISCUSSION

A. Matlab program output

In table 3, the various automobile valves part number and actual requirement per month are noted. The approximate completion period (30 days) and actual completion time are also noted in this table. Using matlab simulation software, simulated completion time is noted. The simulated values are within the range of actual completion of time. The difference of actual and simulated values are noted.

Part Number	*Requirement per month*	*Period (approximate days)*	*Actual Completion time (days)*	*Simulated Completion Time in Days*	*Time/ Job*	*Difference in Time*	*% of Difference*
46152	75000	30	49	47.12	54.28	1.88	**-3.84**
46157	75000	30	62	59.01	67.98	2.99	**-4.82**
46491	7500	30	8	6.57	75.68	1.43	**-17.87**
46496	7500	30	9	5.94	68.48	3.06	**-34**
40460	25000	30	27	22.56	77.98	4.44	**-16.44**
40465	25000	30	23	19.81	68.48	3.19	**-13.87**

Table. 3

Process Sequence	*Distance Travelled*	*Non Value Added time (sec)*
RC to Lathe	4.7 m to 1.91 m	79.17 m to 13m
Lathe to Groove Grinding	4m to 0.5 m	25 m to 13.5 m
Groove Grinding to undercut	10.1 m to 2.37 m	47.68m to 13 m
Undercut to stress relieving	15m to 0.2 m	120 m to 14 m
Stress relieving to finish centreless grinding	16.5 m to 2.91 m	0 m to 14.5 m
Finish centreless grinding to induction hardening	10 m to 3 m	105 m to 14m
Induction hardening to seat grinding	3m to 4.5 m	33 m to 13.5 m
Seat grinding to Finish end	1m to 0.5 m	48 m to 13 m
Finish end to auto cleaning	8m to 0.5 m	30 m to 14 m
TOTAL TIME WITHOUT CONSIDERING DISTANCE BY ORDER	DISTANCE REDUCED	72.3 m is reduced to 15.87m
TOTAL TIME CONSIDERING DISTANCE BY ORDER	NON V/A TIME REDUCED	8.130833 is reduced to 2

Table 4. Sequencing order 1

As per sequencing order given in table 4, matlab software is used to calculate the distance and non value added time. They are rough centreless grinding to lathe, lathe to groove grinding, groove grinding to undercut, undercut to stress relieving, stress relieving to finish centreless grinding, finish centreless grinding to induction hardening, induction hardening to seat grinding, seat grinding to finish end, finish end to autocleaning. The distance travelled for each process is noted in metre. The non value added time is noted in sec. Finally the distance is reduced from 72.3 m to 15.87 m. The non value added time is reduced from 8.13 sec to 2 sec.

Process Sequence	*Distance Travelled*	*Non Value Added time (sec)*
RC to Lathe	4.7 m to 13 m	15 m to 13m
Lathe to Groove Grinding	4m to 1.1 m	14 m to 13.5 m
Groove Grinding to undercut	10.1 m to 2 m	12m to 13 m
Undercut to stress relieving	15m to 2.4 m	15 m to 14 m
Stress relieving to finish centreless grinding	16.5 m to 2.2 m	18 m to 14.5 m
Finish centreless grinding to induction hardening	10 m to 1 m	17 m to 14m
Induction hardening to seat grinding	3m to 3 m	12 m to 13.5 m
Seat grinding to Finish end	1m to 0.2 m	1 m to 13 m
Finish end to auto cleaning	8m to 1.7 m	28 m to 14 m
TOTAL TIME WITHOUT CONSIDERING DISTANCE BY ORDER	DISTANCE REDUCED	14.9m
TOTAL TIME CONSIDERING DISTANCE BY ORDER	NON V/A TIME REDUCED	2.2

Table. 5

In table 5, the same process sequence is followed. Rough centreless grinding to lathe, etc. The distance travelled is noted in metre and non value added time is also noted in sec. The distance reduced to 14.9 m and non value added time reduced to 2.2 sec.

In table 6 and 7, the various machines coverage areas are noted. Rough centreless grinding, Turn head dia+ radius back of head, groove grinding +tappet end radius grinding, turn undercut, stress relieving ,finish centreless grinding, tappet end hardening, seat grinding, finish end, auto cleaning. The Lead time before LPS and after LPS are noted. Finally , without considering space, lead time is reduced from 31106.26 sec to 31029.26 sec. With considering space, lead time is reduced from 6729.26 sec to 6585.26 sec.

Machines	*Machine coverage area in metres*	*Lead time (sec) Before LPS*	*Lead time (sec) after LPS*
Rough Centreless Grinding	3.6*3.6m =12.96 m	6.26	6.26
Turn head dia +Radius back of head	2.3*1.1m = 2.53 m	4750	19
Groove Grinding +Tappet end radius grinding	3.4*2.3 m =7.82m	1500	21
Turn Undercut	2.3*1.1m=2.53m	2860	23
Stress relieving	2.5*1.7m=4.25m	7123	3456
Finish centreless grinding	3.6*3.6m=12.96m	1800	1800
Tappet End Hardening	3.7*3m =11.1 m	6300	16
Seat grinding	4.5*4m =18m	2010	21
Finish end	2.8*3.2m= 8.96m	2880	23
Auto Cleaning	1.1*2.8m=30.8m	1800	1200
TOTAL TIME WITHOUT CONSIDERING SPACE	31029.26 seconds	8.619238 hour	
TOTAL TIME CONSIDERING SPACE	6585.26 seconds	1.829238 hour	

Table. 6

Machines	*Machine coverage area in metres*	*Lead time (sec) Before LPS*	*Lead time (sec) after LPS*
Rough Centreless Grinding	3.6*3.6m =12.96 m	6.26	6.26
Turn head dia +Radius back of head	2.3*1.1m = 2.53 m	4750	19
Groove Grinding +Tappet end radius grinding	3.4*2.3 m =7.82m	1500	21
Turn Undercut	2.3*1.1m=2.53m	2860	23
Stress relieving	2.5*1.7m=4.25m	7200	3600
Finish centreless grinding	3.6*3.6m=12.96m	1800	1800
Tappet End Hardening	3.7*3m =11.1 m	6300	16
Seat grinding	4.5*4m =18m	2010	21
Finish end	2.8*3.2m= 8.96m	2880	23
Auto Cleaning	1.1*2.8m=30.8m	1800	1200
TOTAL TIME WITHOUT CONSIDERING SPACE	31106.26 seconds	8.6406 hour	
TOTAL TIME CONSIDERING SPACE	6729.26 seconds	1.86923 hour	

Table 7- Total time considering space

In table 8, lead time for each process before and after implementation of LPS is noted. The process machines are rough centreless grinding, turn head dia+ radius back of head, groove grinding +tappet end radius grinding, turn undercut, stress relieving ,finish centreless grinding, tappet end hardening, seat grinding, finish end and auto cleaning. The lead time is reduced from 8.64 hour to 1.86 hour.

Process	*Before LPS(sec)*	*After LPS(sec)*
Rough Centerless grinding	6.26	6.26
Turn head dia +Radius Back of head	4750	19
Groove Grinding + Tappet end radius grinding	1500	21
Turn under cut	2860	23
Stress relieving	7200	3600
Finish centreless grinding	1800	1800
Tappet end hardening	6300	16
Seat grinding	2010	21
Finish end	2880	23
Auto Cleaning	1800	1200
Total (sec)	31106	6729
Total (Hr)	8.64	1.86

Table 8. Lead time for each process before and after LPS

IV. CONCLUSION

By using various lean tools like 5s, JIT, set up time reduction and total quality management, the machines are aligned and used in compact space, the floor space is reduced from 351 metres to 174 meters (50.4 % improved). JIT tool is mainly used to reduce inventory and it is improved from 3309 to 568 (82% of improvement). Set up time reduction is the main tool used to reduce the Lead time from 8.64 hour to 1.86 hour (61% improvement). The man machine ratio is improved from 1. 2 to 2 (60% improvement) . The manpower utilization is improved from 48% to 80% (66% improvement). The distance travelled is reduced from 72.2 m to 15.87 m. Finally the number of machines are reduced from 12 to 10. The number of operators per shift is reduced from 9 to 5. The man machine ratio is increased from 1.3 to 2. The takt time is increased from 8.4 to 8.62 sec. Manpower utilization is increased from 48% to 85%. The floor space is reduced from 351 sq. m to 174 sq.m. Thus the implementation of lean principle, the non value added time is reduced from 61 min .The man power ratio is improved by 60%, inventory control by 93%, floor space by 49.5%, lead time by 8.5 times, distance travelled 4.56 times, man power utilization by 1.75 times. After implementing the line2, 259 m^2 free space is recieved as compared to the previous line before implementing.

REFERENCES

[1] Womack, J., Jones, T. and Roos.D, 1990, The Machine that Changed the World,Harper Business: New York.

[2] Roberto Panizzolo, Patrizia Garengo, Milind Kumar Sharma and Amol Gore, 2012, Lean manufacturing in developing countries: evidence from Indian SMEs, production planning and control, Vol. 23, Nos. 10–11, 769–788.

[3] M. Eswaramoorthi, G. R. Kathiresan , P. S. S. Prasad , P. V. Mohanram , 2011, A survey on lean practices in Indian machine tool industries, , International Journal of Advanced Manufacturing Technology 52: 1091–1101.

[4] S. Vinodh , S. Vasanth Kumar and K.E.K Vimal, 2014, Implementing lean sigma in an Indian rotary switches manufacturing organization , Production Planning and Control, Vol. 25, No. 4, 288–302.

[5] K. L. Jeyaraj , C. Muralidharan , R. Mahalingam ,S. G. Deshmukh, 2013. Applying Value Stream Mapping Technique for Production Improvement in a Manufacturing Company- A Case Study, Journal of Institute of Engineering and Indian Service –C 94(1):43–52.

[6] Anisur Rahman, Azharul Karim, 2013, Application of lean production to reducing operational waste in a tile manufacturing process, International Journal of Management Science and Engineering Management. Vol. 8, No. 2, 126–134.

[7] Fawaz A. Abdulmalek, Jayant Rajgopal ,2007 , A Classification Scheme for the Process Industry to guide the implementation of Lean, Kim La Scola Needy, PE, University of Pittsburgh, Engineering Management Journal, vol 49, no . 10, 2, 866-878.

[8] B. Modarress; A. Ansari; D. L. Lockwood,2005, Kaizen costing for lean manufacturing: a case study, International Journal of Production Research, Vol. 43, No. 9, 1 , 1751–1760.

[9] Modarress. b., a. ansari and d. l. lockwood,2005, Kaizen costing for lean manufacturing: a case study , International Journal of Production Research, Vol. 43, No. 9, 1, 1751–1760.

[10] Pavnaskar.s.j, j. k. gershenson and a. b. jambekar, 2003, classification scheme for lean manufacturing tools , international journal of production research, vol. 41, no. 13, 3075–3090.

[11] Ajit Kumar Sahoo,N. K. Singh, Ravi Shankar, M. K. Tiwari , 2008, Lean philosophy: implementation in a forging company, International journal of advanced manufacturing Technology, 36:451–462.

[12] Mariano Jiménez , Luis Romero , Manuel Domínguez , María del Mar Espinosa, 2015, 5S methodology implementation in the laboratories of an industrial engineering, university school Safety Science 78 ,163–172.

[13] Ahmad Wasim & Essam Shehab & Hassan Abdalla & Ahmed Al-Ashaab & Robert Sulowski & Rahman Alam, 2013, An innovative cost modelling system to support lean product and process development,International Journal of advanced manufacturing technology 65:165–181.

[14] Abdullah Ismail, Jaharah A. Ghani, Mohd Nizam Ab Rahman, Baba Md Deros, Che Hassan CheHaron. 2014, Application of Lean Six Sigma Tools for Cycle Time Reduction in Manufacturing: Case Study in Biopharmaceutical Industry,Arabian journal of science and engineering, 39:1449–1463.

[15] L. N. Pattanaik , B. P. Sharma, 2009, Implementing lean manufacturing with cellular layout- a case study. International journal of advanced manufacturing technology, 42:772–779.

[16] Bamber.L, Dale. B.G. 2000, Lean production: a study of application in a traditional manufacturing environment, production planning and control, vol. 11, NO. 3, 291-298.

[17] Vinodh.S and Dino Joy, 2012, Structural Equation Modelling of lean manufacturing practices, , International Journal of Production Research, Vol. 50, No. 6, 15, 1598–1607.

[18] Morteza Ghobakhloo and Tang Sai Hong, 2014, IT investments and business performance improvement: the mediating role of lean manufacturing implementation, International Journal of Production Research, Vol. 52, No. 18, 5367–5384.

[19] James C. Green, Jim Lee and Theodore A. Kozman, 2010 , Managing lean manufacturing in material handling operations, International Journal of Production Research, Vol. 48, No. 10, 2975–2993.

[20] Giorgia Dal Pont, Andrea Furlan, Andrea Vinelli, 2008, Interrelationships among lean bundles and their effects on operational performance,journal of operational management resource 1:150–158.

[21] Pietro Romano1, Pamela Danese2, and Thomas Bortolotti , 2010, The Moderating role of JIT Links with suppliers on the relationship between lean manufacturing andoperational Performances, International federation for information processing, 338, pp. 89–96.

[22] Wafa, M.A, Yasin, M.M, Swinehart.K 1996, The impact of supplier proximity on JIT success: an informational perspective. International Journal of Physical Distribution and Logistics Management 26(4), 23–34.

[23] Tan, K.C. 2001, A framework of supply chain management literature. European Journal of Purchasing & Supply Management 7, 39–48.

[24] Zhu, Z., Meredith, P.H, 1995. Defining critical elements in JIT implementation: a survey. Industrial Management and Data Systems 95(8), 21–28.

[25] Modarress, a. ansari and d. l. lockwood, Kaizen costing for lean manufacturing: a case study, International Journal of Production Research, Vol. 43, No. 9, 1 May 2005, 1751–1760.

[26] D.rajendhirakumar, r.sridhar, a.dominic savio, s.jerine chrispal prakash, n.srinath, Lean manufacturing –a study of application in a customery atmosphere, , international journal of lean thinking ssue 1(2012).

[27] Azian Abdul Rahman, Sariwati Mohd Sharif, Mashitah Mohamed Esa, Lean manufacturing case study with kanban syatem implementation. international conference on economics and business research, 2013, procedia economics and finance 7, 2013, 174-180.

[28] Ahmad naufal, ahmed jaffar, noriah yusoff, nurul hayati, Development of kanban system at local manufacturing company in malaysia- case study, international symposium on robotics and intelligent sensors 2012, procedia engineering, 41 (2012) 1721-1726.

[29] Mariano Jimenez, luis romero, manuel dominguez, maria del mar espinosa,5s methodology implementation in the laboratories of an industrial engineering university school, journal of safety science 78 (2015), 163-172.

[30] Mohammad d al tahat, adnan m.mukattash, Design and analysis of production control scheme for kanban based jit environment, journal of the franklin institute, 343 (2006), 521-531.

[31] Jagdish rajaram jadhav, ss mantha, santosh b rane, Development of framework for sustainable lean implementation- an ISM approach, Journal of industrial engineering institute , 10-72, 2014.

[32] Giorgia Dal Pont & Andrea Furlan & Andrea Vinelli Interrelationships among lean bundles and their effects on operational performance, Operational management resource ,2008, 1:150–158.

[33] Giuliano Almeida Marodin & Tarcísio Abreu Saurin & Guilherme Luz Tortorella & Juliano Denicol,How context factors influence lean roductionpractices in manufacturing cells, International journal of advanced manufacturing technology (2015) 79:1389–1399.

[34] Hojung shin, Manufacturing planning and control, the evolution of mrp and jit integration, European journal of operational research, 110, 1998, 411- 440.

[35] A Rosemary R. Fullerton , Cheryl S. McWatters , Chris Fawson, n examination of the relationships between JIT and financial performance, Journal of Operations Management 21 ,2003, 383–404.

Design of Compressors for Multiplication

S. V. Thilagan
Department of ECE,
University College of Engineering Pattukkottai,
Thanjavur-614701, Tamil Nadu, India.

***Abstract*— Current mode signaling scheme with dynamic overdriving is one of the most promising scheme for high speed low power communication over long on-chip interconnects. They are sensitive to parameter variations due to reduced voltage swing on the line. The proposed current mode signaling scheme and a competing Current mode signaling Bias scheme are fabricated in 180nm CMOS technology. Measurement results show that the power will be reduced in the proposed scheme when compared with the current mode signaling bias scheme. In proposed scheme we use D-latch as a Delay element. By using D-latch as a delay element throughput will be increased that depends on the latency. In our proposed scheme we can also reduce the area by combining the Vbn, Vbp bias circuits.**

Keywords—CMOS technology; CMS scheme, weak driver; strong driver.

I. INTRODUCTION

On-chip communication is getting more attention, as global interconnects are rapidly becoming a speed, power and reliability bottleneck for digital CMOS systems. While gate speed increases under scaling, smaller cross-sectional wire dimensions will decrease the interconnect bandwidth for a given length. In the deep-submicron era, interconnect wires (and the associated driver and receiver circuits) are responsible for an ever increasing fraction of the energy consumption of an integrated circuit. Most of this increase is due to global wires, such as busses, clock, and timing signals. For gate array and cell-library- based designs, found that the power consumption of wires and clock signals can be up to 40% and 50% of the total on-chip power consumption, respectively. The impact of interconnect is even more significant for reconfigurable circuits. Measured over a wide range of applications, more than 90% of the power dissipation of traditional FPGA devices have been reported to be due to the interconnects.

Speed and power consumption of on-chip interconnect network have become important in advanced CMOS technologies. It is difficult to meet desired power and performance specifications of modern system-on-chips (SoCs) and multicore processors. Many alternate repeater circuits and signaling schemes have been suggested in recent past to achieve high-speed low-power communication over long on-chip interconnects. In modern CMOS technologies, process variations cause significant variations in device parameters which can lead to performance degradation of these signaling techniques. Hence, a signaling scheme for on-chip interconnects is also required to be robust against parameter variations. Current-mode signaling (CMS) scheme has the potential to improve both speed and dynamic power consumption. It consumes much less power compared to the improved repeater circuits.

The huge reduction in energy consumption offered by the low-swing signaling schemes and the CMS schemes is mainly due to the reduced voltage-swing on the line. However, low voltage swing on the line reduces the noise margin of the data communication system. Hence, CMS schemes are more susceptible to parameter variations than the voltage-mode repeater insertion scheme. In highly scaled technologies, process variations cause significant variations in device parameters. The variations in the transistor parameters can be categorized as either inter-die variations or intra-die parameters. In the case of inter-die variations similar devices on a chip have identical electrical parameters but the device parameters vary from die to die, wafer to wafer and batch to batch. In modern technologies, variations in the parameters of devices on the same chip are also significant. This class of variations is referred to as intra-die variations. The variations can cause the voltage swing on the line to change which can lead to significant changes in the performance of a scheme.

Existing system

This scheme uses feedback at both the transmitter and the receiver ends to adjust the operating points of these circuits. The transmitter used by this scheme is shown below: The feedback inverter converts low swing logic levels on the line to full rail to rail CMOS. levels. The NAND/NOR gates ensure that the strong driver is turned on only during data transitions and is turned off as soon as the line crosses the switching point of the feedback inverter to make the logic level on the line equal to the input. The weak driver supplies I_{static} and the line voltage swing at the receiver end is VCM Rx ± I_{static} RL. The receiver also uses feedback to adjust its common-mode voltage. Take the case where V_{CMTx} at the transmitter end.

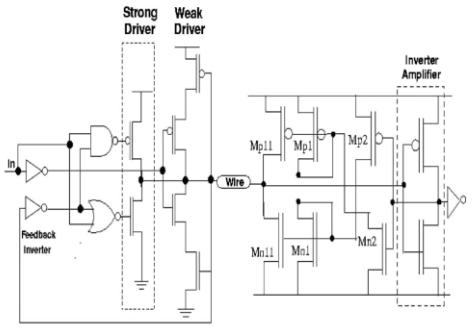

Fig 1. Existing system

Limitations

- Increased delay due to the feedback in the CMS- FB.
- The delay of CMS-Fb becomes 2.5 times its nominal value in the presence of intra-die variations.

- Robust against only inter-die variations due to the feedback in the transmitter and receiver circuits.

Proposed system

The proposed transmitter employs two drivers (a strong driver and a weak driver) with NAND and NOR gates like the transmitter of CMS- Fb scheme.

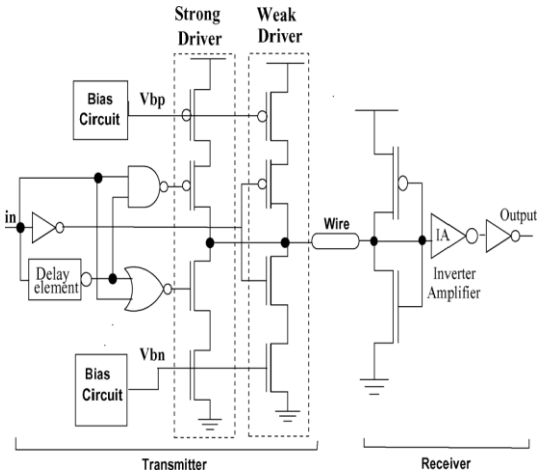

Fig 2. Proposed system

In the proposed transmitter, duration for which the strong driver is turned on is controlled by a delay element and not by the feedback. The strong and weak drivers employ single transistor current sources. The bias voltages (and) of these current sources are generated from a specially designed bias circuit such that current through strong and weak driver remain constant across all process corners. Operation of the bias circuit is discussed in the next section. The proposed receiver uses a diode connected pMOS and nMOS (terminating inverter) followed by an inverter chain. The terminator inverter holds the line voltage near its switching. threshold. Inverter amplifier (IA) and subsequent inverters amplify the small line voltage swing to digital logic levels

II. BIAS GENERATION CIRCUIT

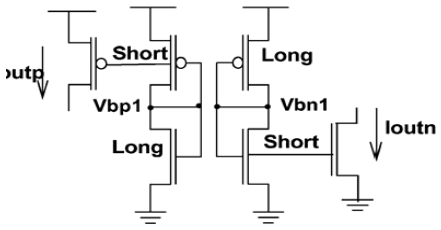

Fig 3. diode-connected transistor based

Bias circuit is used to set an operating point, which provides a steady state operating condition of an active device. The receiver uses a diode connected pMOS and nMOS (terminating inverter) followed by an inverter chain. The bias circuit in the transmitter and the inverter amplifier in the receiver is used for static power consumption.

Weak driver

The weak driver provides the minimal drive required to keep the line (terminated by low impedance) at the desired voltage level. When the input is 1, the p channel driver gate is low. (Weak) Driver (enabled). These charges up the output. As the line voltage reaches VDD − V_{Tp}, the upper p channel transistor turns off, restricting line voltage swing in the up direction. Similarly when the input is 0 the n channel driver transistor is enabled by a high level at its gate.

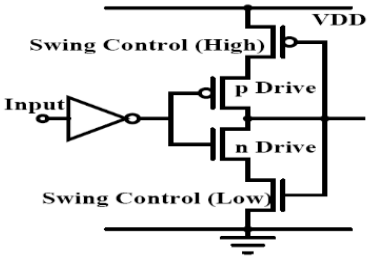

Fig. 3. Steady State (Weak) Driver

The transistor discharges the line. However, when the line voltage approaches V_{Tn} during discharge, the lower transistor turns off, stopping the discharging process. Thus the line can only swing between VDD – V_{Tp} and $V_{Tn.}$

Strong Driver

The strong driver should be enabled only when the input and the level on the output line do not represent the same logic. The feedback inverter acts as an inverting amplifier converting low swing logic levels on the wire to full swing (inverted) CMOS logic level on its output. The P channel gate is low (enabled) only when both inputs to the NAND are 1. This will happen only when the input is high AND the line is at 0. This is indeed the condition when we we want the strong driver to charge the line. The N channel gate is high (enabled) only when both inputs to the NOR gate are 0. This will happen only when the input is low AND the line is at 1.Notice that the input to the feedback inverter is a low swing level around VDD/2. There-fore it consumes static power. The action of the strong driver is self-limiting. This is because both NAND and NOR receive the input and the inverted logic level of the line. If the input and the logic level of the line are the same, NAND and NOR are fed with input and input. Thus one of the inputs to NAND/NOR is 1, while the other is 0. This ensures that the output of NAND is 1, while that of NOR is 0, so that both the p and n channel transistors are OFF. Therefore the strong driver does not need a series transistor as was the case for the weak driver. When the Input = 1 and Wire voltage < Vm, the inverter output = 1, NAND output = 0 and NOR output = 0.The P channel driver is ON and dumps current to charge the line. When the Input = 0 and Wire voltage > Vm, the inverter output = 0, NAND output = 1 and NOR output = 1.the N channel driver is ON and sinks current to discharge the line. As soon as low swing logic level on the line becomes equal to the logic level at the input Inverter output = input, and so NAND output = 1, NOR output = 0; which disables both drive transistors automatically

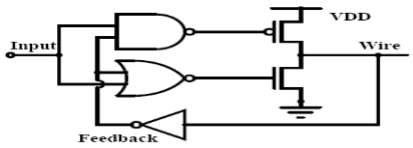

Fig. 4. Dynamic (Strong) Driver

III. ON CHIP TEST CIRCUITS

Two delay measurement schemes were implemented on the chip: one with a 2* 1 multiplexer-de multiplexer (2 *1ux-demux) and the other with a 4 *1 multi plexer-de multiplexer (4* 1 Mux-De mux). A 2* 1 Mux-De mux scheme includes CMS-Fb scheme and CMS-Bias scheme. Hence, it gives only the difference in delay of the two CMS schemes. A 4*1 Mux-De mux scheme includes the two CMS schemes as well as an RO with direct connection. Hence, 4 *1 Mux-De mux scheme also gives the absolute delay of the CMS schemes. Separate pins are assigned to of the digital circuits, output buffers and CMS schemes.

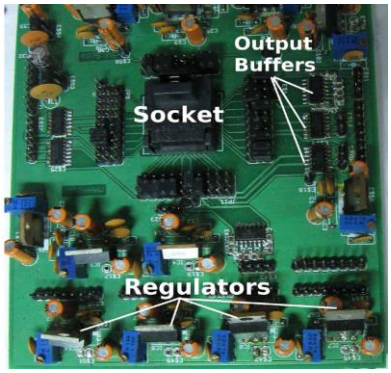

Fig. 5. PC board used for testing

The currents through weak drivers in both the signaling schemes are made externally programmable by using additional current mirrors on the chip . The frequency of the ring oscillator was divided by 16 using a 4-bit on-chip counter before taking it to I/O pads. The counter outputs are buffered by on-board buffers and the frequency is measured using a 6-digit frequency counter. The chip was placed in a socket mounted on a PC board for testing The PC board also includes electronics for generation of variable supply and substrate bias.

Software specification

Tools Used:

Tanner EDA

- S-EDIT
- TSPICE
- W-EDIT

IV. SIMULATION RESULTS

Performance in nominal conditions

Performance in nominal conditions summarizes measured results of the CMS schemes under nominal operating condition (no additional currents and 1.8 V). Frequency measurements of 2 1 Mux-De muxbased scheme show that delay of CMS-bias scheme is less than that of CMS-Fb scheme by 143 ps. Measurement results from 4 1 Mux-De mux-based scheme show that CMS-bias scheme offers 9% improvement in delay over CMS-Fb. This difference is primarily because the inverter amplifier in the receiver of CMS-Fb scheme has to drive transistors and unlike

CMS-Bias scheme The additional capacitive load offered by and is significant as their channel lengths are chosen to be more than 180 nm in order to reduce static power consumed in the receiver.

oscillator signal divided down by 16 as observed on a digital storage oscilloscope (DSO). Since CMS-Fb scheme has more delay than CMS-Bias scheme, the ring oscillator oscillates at lower frequency when CMS-Fb is selected. For fair comparison of energy/bit, of digital circuits (multiplexers, de multiplexers and inverters) was adjusted so that the ring oscillates at the same frequency in both the cases. Hence, for the digital circuit was kept 2.5 V when CMS-Fb was selected and 2.0V when CMS-Bias was selected for energy measurements. The proposed CMS scheme offers 34% gain in energy/bit and 42% improvement in EDP at data rates of 0.64 Gbps over CMS-Fb scheme. Measurements on 2 1 Mux-Demux-based scheme show that the proposed scheme consumes 0.622 pJ/bit at data rate of 0.78 Gbps.

Effect of Inter-Die variations

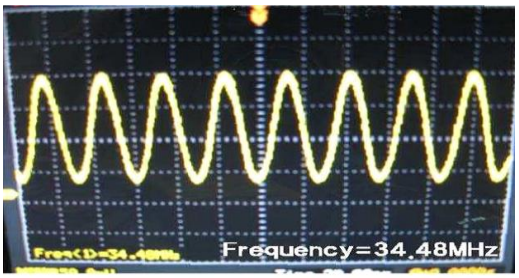

To assess the effects of inter-die variations, we vary N Well bias in the transmitter and the receiver from 1.8 to 2.3 V identically. Table III shows the delay and energy/bit of both the schemes for different N Well bias voltages. The last two

columns in the table shows the data rate at which the energy/bit was measured. It is apparent from the table that delay of both the signaling schemes do not change much with inter-die variations. Also, they do not consume much additional energy to keep the delay constant with inter-die variations.

These experiments do not capture the effect of variations in parameters of nMOS transistors. energy/ bit and throughput of the two schemes in all process corners. It shows that delay and throughput of both the schemes remain practically the same in the four digital process corners and the nominal case without consuming much additional energy. The local feedback in the transmitter and receiver of CMS-Fb scheme that makes it susceptible to intra-die variations makes it robust against inter-die variations. As long as these of the inverters in the transmitter and in the receiver are matched, CMS-Fb scheme is robust against inter-die variation.

REFERENCES

[1] J. Dwens, W. J. Dally, R. Ho, D. N. Jayasimha, S. W. Keckler, and L.-S. Peh, "Research challenges for on-chip interconnection networks," *IEEE Micro*, vol. 27, no. 5, pp. 96–108, Sep./Oct. 2007

[2] H. Zhang, V.George, and J. M. Rabaey, "Low-swing on-chip signaling techniques: Effectiveness and robustness," *IEEE Trans*. Very Large Scale Integr. *(VLSI) Syst.*, vol. 8, no. 6, pp. 264–272, Jun. 2000.

[3] A. Nalamalpu, S. Srinivasan, and W. Burleson, "Boosters for driving on-chip interconnects: Design issues, interconnect synthesis and comparison with re-peaters," *IEEE Trans. Comput.-Aided Design Integr.Circuits Syst.*, vol. 50, no. 4, pp. 50–62, Jan. 2002.

[4] R. Ho, K. Mai, and M. Horowitz, "Efficient on-chip global interconnects,"in *VLSI Symp., Dig. Tech. Lett.*, 2003, pp. 271–273.

[5] H. Kaul and D. Sylvester, "Low-power on-chip communication based on: Transition-aware global signaling (TAGS)," *IEEE Trans. Very Large Scale Integr. (VLSI) Syst.*, vol. 12, no. 5, pp. 464–476, May 2004.

[6] J. sun. Seo, P. Singh,D. Sylvester, and D. Blaauw, "Self-timed regenerators for high-speed and low-power interconnect," in *Proc. ACM/IEEE Int. Symp. Quality Electron. Design (ISQED)*, 2007, pp. 621–626.

[7] R. T. Chang, N. Talwalkar, C. P. Yue, and S. S.Wong, "Near speed-oflight signaling over on-chip electrical interconnects," *IEEE J. Solid-State Circuits*, vol. 38, no. 5, pp. 834–838, Apr. 2003.

[8] N. Tzartzanis and W. W. Walker, "Differential current-mode sensing for efficient on-chip global signaling," *IEEE J. Solid-State Circuits*, vol. 40, no. 11, pp. 2141–2147, Nov. 2005.

[9] A. Narasimhan, "A low-power asymmetric source driver level converter based current-mode signaling scheme for global interconnects," in *Proc. IEEE Int. Conf. VLSI Design*, 2006, pp. 491–494.

[10] V. Venkatraman and W. Burleson, "An energy-efficient multi-bit quaternary current mode signaling for on-chip interconnects," in *Proc. Custom Integr. Circuits Conf. (CICC)*, 2007, pp. 301–304.

[11] A. Katoch, H Veendrick, and E. Seevinck, "High speed current-mode signaling circuits for on-chip wires," in *Proc. IEEE Int. Symp. Circuits Syst.*, 2005, pp. 4138–4141.

[12] D. Shinkel, E. Mensink, E. A. M. Klumperink, E. van Tuijl, and B. Nauta, "A 3-Gb/s/ch transceiver for 10-mm uninterrupted RC-limited global on-chip interconnects," *IEEE J. Solid-State Circuits*, vol. 41, no.1, pp. 297–306, Jan. 2006.

[13] L. Zhang, J.Wilson, R. Bashirullah, L. Luo, J. Xu, and P. Franzon, "A 32 Gb/s on-chip bus with driver pre-emphasis technique for on-chip buses," in *Proc. Custom Integr. Circuits Conf. (CICC)*, 2006, pp. 265–268.

[14] M. M. Tabrizi, N. Masoumi, and M. M. Deilami, "High speed currentmode signalling for interconnects considering transmission line and crosstalk effects," in *Proc. MWCAS*, 2007, pp. 17–20.

[15] R. Ho, T. Ono, R. D. Hopkins, A. Chow, J. Schauer, F. Y. Liu, and R. Drost, "High speed and low energy capacitively driven on-chip wires," *IEEE J. Solid-State Circuits*, vol. 43, no. 1, pp. 52–60, Jan. 2008.

[16] J. Sun Seo, R.Ho, J. Lexau, M. Dayringer, D. Sylvester, andD. Blaauw, "High-bandwidth and low-energy on-chip signaling with adaptive preemphasis in 90 nm CMOS," in *IEEE ISSCC Dig. Tech. Papers*, 2010, pp. 182–183.

[17] E. Mensink, D. Shinkel, E. A. M. Klumperink, E. van Tuijl, and B. Nauta, "Power efficient gigabit communication capacitively driven RC-limited on-chip interconnects," *IEEE J. Solid-State Circuits*, vol. 45, no. 2, pp. 447–457, Feb. 2010.

Combined Clustering Approach for Privacy Preserving Data Mining using Fuzzy Logic

J. Paranthaman
Department of Computer Science and Engineering,
University College of Engineering Panruti,
Cuddalore, Tamil Nadu, India.

***Abstract*— Data mining technology is more significant in identifying patterns and trends from large collections of data. It provides Business intelligent supports, solutions and decisions. Data mining provides large benefits to the individual, commercial and government security sectors, but the aggregation and storage of huge amounts of data leads to an erosion of privacy. we present Combined Clustering approach for a number of non trivial tasks related to privacy preserving advanced data mining. The advantages of all clustering techniques are combined with the K-Means Clustering and Expectation Maximization clustering (EM-clustering) for privacy preserving advanced data mining.**

Keywords—Combined Clustering Approach; Privacy Preserving Data Mining; Fuzzy Logic.

I. INTRODUCTION

Privacy preserving data mining has become an important problem because of the large amount of personal data which is tracked by many business applications. In many cases, users are unwilling to provide personal details unless the privacy of sensitive information is guaranteed. Privacy-preserving data mining has been an active area of research since it was introduced by Agrawal and Srikant [7] and Lindell and Pinkas [3].

A. Data mining

Data mining is a recently emerging field, connecting the three worlds of Databases, Artificial Intelligence and Statistics. The information age has enabled many organizations to gather large volumes of data. However, the usefulness of this data is negligible if "meaningful information" or "knowledge" cannot be extracted from it. Data mining, otherwise known as knowledge discovery, attempts to answer this need. In contrast to standard statistical methods, data mining techniques search for interesting information without demanding a priori hypotheses. As a field, it has introduced new concepts and algorithms such as association rule learning. It has also applied known machine-learning algorithms such as inductive-rule learning (e.g., by decision trees) to the setting where very large databases are involved. Data mining techniques are used in business and research and are becoming more and more popular with time [1-3] [18].

B. Confidentiality issues in data mining

A key problem that arises in any e-mass collection of data is that of confidentiality. The need for privacy is sometimes due to law (e.g., for medical databases) or can be motivated by business interests. However, there are situations where the sharing of data can lead to mutual gain. A key utility of large databases today is research, whether it be scientific, or economic and market oriented [4] [18].

C. Very large databases and efficient secure computation

We have described a model which is exactly that of multi-party computation. Therefore, there exists a secure protocol for any probabilistic polynomial time functionality [10]. However these generic solutions are very inefficient, especially when large inputs and complex algorithms are involved. Thus, in the case of private data mining, more efficient solutions are required. It is clear that any reasonable solution must have the individual parties do the majority of the computation independently. Our solution is based on this guiding principle and in fact, the number of bits communicated is dependent on the number of transactions by a logarithmic factor only. We remark that a necessary condition for obtaining such a private protocol is the existence of a (non-private) distributed protocol with low communication complexity [5-7] [18].

Privacy also takes many different forms. Some of the more relevant ones to event correlation include:

1. Source anonymity refers, in particular, to the producer of an event. A source that is anonymous cannot be traced by recipients of the event. there is no explicit identifier linking the event to a known producer and the data in the event cannot reliably be linked to the producer.

2. Data privacy is related to, but not equivalent to, source anonymity: it specifically refers to the semantics of the data in the event and whether they contain information that may be deemed sensitive by the producer of the event.

3. Physical privacy refers to the access of sensitive information or resources via direct access to the repositories or interference with servers of data. This includes intruders, malicious insiders, and resource starvation (e.g., denial of service) mechanisms.

4. Time privacy corresponds to the fact that this thesis considers an event as being time stamped. The distribution of event arrival times could yield some aggregate

information; more interestingly, the correlation of curious or insidious activities with event arrival times could potentially violate the source anonymity stated above [5].

This thesis focuses on the first two forms of privacy. It is possible to maintain data privacy without maintaining source anonymity (e.g., an event came from source X but it is free of what X deems sensitive), as well as vice-versa (e.g., it is unknown exactly who the event came from, but it contains classified information privy to only a small number of organizations). Of course, both can exist in tandem. With both, I argue that recipients cannot trace the source or information for relevant applications [8-10].

As for the latter two forms, physical privacy poses a unique set of challenges on its own most systems secure from remote access have physical backdoors and is considered outside the scope of this thesis. Meanwhile, the definition of events and event correlation assume an ordering amongst events. Some of the data privacy approaches in the proposal do indirectly provide time privacy, but full time privacy poses its own unique correlation challenges; a complete discussion is outside the scope of this work. Finally, a privacy policy is both a promise by an organization to originators of data contained within the organization, as well as a compliance statement to consumers of data produced by the organization. It may contain one or both of the first two privacy requirements, as well as other additional requirements.

II. DATA MINING TECHNIQUES

Data mining techniques include the following:

- Decision Trees/Rules
- Clustering
- Statistics
- Neural networks
- Logistic regression
- Visualization
- Association rules
- Nearest neighbor
- Text mining
- Web mining
- Bayesian nets / Naive Bayes
- Sequence analysis
- SVM (Support Vector Machine)
- Hybrid methods
- Genetic algorithms

In the following, we will discuss some of these techniques briefly. The above Data mining techniques are divided into the following three categories data mining techniques. They are classification, prediction and estimation which are observed from the references [11-14].

A. Rule induction

A data mine system has to infer a model from the database; that is, it may define classes such that the database contains one or more attributes that denote the class of a tuple. The class can then be defined by the condition of the attributes. When the classes are defined, the system should be able to infer the rules that govern classification. In other words, the system should find the description of each class. Production rules have been widely used to represent knowledge in expert systems and they have the advantage of being easily interpreted by human experts because of their modularity, i.e. a single rule can be understood in isolation and does not need reference to other rules [18].

B. Association rules

Association rule mining finds interesting associations and/or correlation relationships among large sets of data items. Association rules show attributes value conditions that occur frequently together in a given dataset. A typical and widely-used example of association rule mining is Market Basket Analysis. For example, the data are collected using bar-code scanners in supermarkets. Such market basket databases consist of a large number of transaction records. Each record lists all items bought by a customer on a single transaction. Managers would be interested to know if certain groups of items are consistently purchased together. They could use this data for adjusting store layouts (placing items optimally with respect to each other), for cross-selling, for promotions, for catalog design and to identify customer segments based on buying patterns. Association rules provide information of this type in the form of "if-then" statements. These rules are computed from the data and, unlike the if-then rules of logic, association rules are probabilistic in nature [18].

C. Clustering

In an unsupervised learning environment, the system has to discover its own classes and one way in which it does this is to cluster the data in the database. The first step is to find subsets of related objects and then find descriptions which identify each of these subsets. Clustering and segmentation essentially partition the database so that each partition or group is similar according to some criteria or metric. Clustering according to similarity is a concept which appears in many disciplines. If a measure of similarity is available, there are a number of techniques for forming clusters. Membership of groups can be based on the degree of similarity between members and from this the rules of membership can be defined. Another approach is to construct a set of functions that measure some property of partitions; that is, groups or subsets as functions of some parameter of the partition. This latter approach achieves what is known as optimal partitioning. Many data mining applications make use of clustering according to similarity for example to segment a client/customer base. Clustering according to optimization of set functions is used in data analysis, e.g. when setting insurance tariffs, the customers can be divided according to a number of parameters and the optimal tariff segmentation achieved [13-17].

D. Decision trees

Decision trees are an easy knowledge representation technique and they divide examples to a limited number of classes. The nodes are labeled with dimension names, the edges are labeled with potential values for this dimension and the leaves labeled with distinct classes. Objects are classified by following a route down the tree, by taking the edges, proportionate to the values of the attributes in a target [18].

E. Neural networks

Neural networks are an access to computing that involves developing numerical structures with the ability to learn. The methods are the result of academic investigations to model nervous system learning. Neural networks have the extraordinary power to infer significance from complicated or inexact information and can be used to distill patterns and discover trends that are overly complicated to be noticed by either humans or new computer techniques. A skilled neural network can be thought of as an "expert" in the class of data it has been given to analyze. This expert can so be used to offer projections, given original situations of stake and respond to "what if" questions. Neural networks have broad applicability to real world business problems and have already been successfully applied in many industries. Since neural networks are best at identifying patterns or trends in data, they are well suited for prediction or forecasting needs, among them

- Sales forecasting
- Industrial process control
- Customer research
- Data validation
- Risk management
- Target marketing etc.

Neural networks take a lot of processing elements similar to neurons in the mind. These processing elements are interconnected in a web that can so describe patterns in information once it is exposed to the information. This distinguishes neural networks from conventional computation programs that merely follow instructions in a fixed sequential decree.

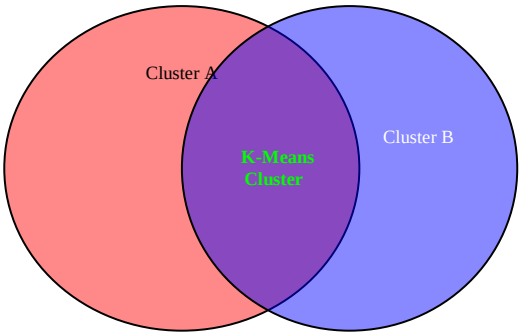

Fig. 1. K-means clustering

Cluster Analysis is the problem of decomposing or partitioning a (usually Multivariate) data set into groups so that the points in one group are similar to each other and are as different as possible from the points in other groups. There are many situations where clustering can lead to the discovery of important knowledge but privacy/security reasons restrict the sharing of data.

Imagine the following scenario. A law enforcement agency wants to cluster individuals based on their financial transactions, and study the differences between the clusters and known money laundering operations. Knowing the differences and similarities between normal individuals and known money launderers would enable better direction of investigations. Currently, an individual's financial transactions may be divided between banks, credit card companies, tax collection agencies, etc. Each of these (presumably) has effective controls governing release of the information. These controls are not perfect, but violating them (either technologically or through insider misuse) reveals only a subset of an individual's financial records. The law enforcement agency could promise to provide effective controls, but now overcoming those gives access to an individual's entire financial history. This raises justifiable concerns among privacy advocates. What is required is a privacy preserving way of doing clustering [13-17].

III. MODIFIED K-CLUSTERING

We focus on k-means clustering which is a simple technique to group items into k clusters. k-means clustering is an iterative algorithm, which starts off with random cluster centers. A single iteration assigns all objects to the closest clusters based on their distances from the cluster means and then re-computes the cluster means. Iterations are repeated until the algorithm converges to a set of stable clusters. The basic k-means clustering algorithm is given below:

Initialize the k means $\mu_1, \mu_{2...} \mu_k$ to 0.
Arbitrarily select k starting points $\mu'_1, \mu'_{2...} \mu'_k$

Repeat
  Assign $\mu'_1, \mu'_{2...} \mu'_k$ to $\mu_1, \mu_{2...} \mu_k$ respectively
    for all points i do
      Assign point i to cluster j if distance d(i, μ_j) is
      the minimum over all j.
    end for
  Calculate new means $\mu'_1, \mu'_{2...} \mu'_k$
until the difference between $\mu_1, \mu_{2,...,} \mu_k$ and $\mu'_1, \mu'_{2,...,} \mu'_k$ is acceptably low.

Algorithm 2. K-means clustering

The results come in two forms: Assignment of entities to clusters, and the cluster centers themselves. We assume that the cluster centers μ_i are semiprivate information, i.e., each site can learn only the components of μ that correspond to the attributes it holds. Thus, all information about a site's attributes (not just individual values) is kept private; if sharing the μ is desired, an evaluation of privacy/secrecy concerns can be performed after the values are known.

At first glance, this might appear simple - each site can simply run the k-means algorithm on its own data. This would preserve complete privacy. Figure 2 shows why this will not work. Assume we want to perform 2-means clustering on the data in the figure. From y's point of view (looking solely at the vertical axis), it appears that there are two clusters centered at about 2 and 5.5. However in two dimensions it is clear that the difference in the horizontal axis dominates. The clusters are actually "left" and "right", with both having a mean in the y dimension of about 3. The problem is exacerbated by higher dimensionality.

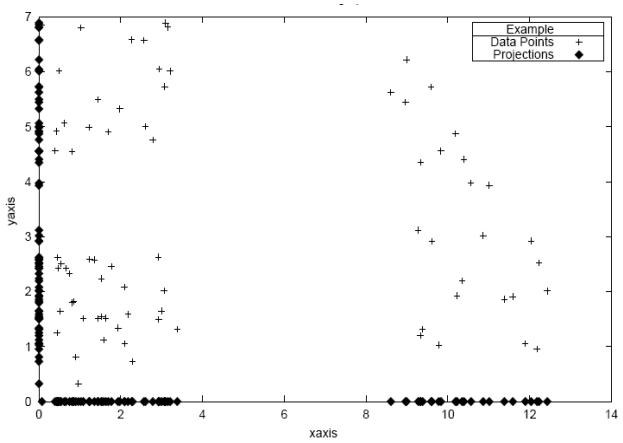

Fig. 2. Two dimensional problems

Basic approach

Given a mapping of points to clusters, each site can independently compute the components of μ_i corresponding to its attributes. Assigning points to clusters, Specifically computing which cluster gives the minimum d(i, μ_j), requires cooperation between the sites. We show how to privately compute this in Section 3.3.2. Briefly, the idea is that site A generates a (different) vector (of length k) for every site (including itself) such that the vector sum of all the site vectors is $\vec{0}$. Each site adds its local differences |point - μ_i | to its vector. At the same time, the vector is permuted in an order known only to A. Each site (except a single holdout) sends their permuted vector to site B. Site B sums the received vectors, then the holdout site and B perform a series of secure additions and comparisons to find the minimum i without learning distances. B now asks A the real index corresponding to i, giving the proper cluster for the point.
Securely Finding the Closest Cluster

This algorithm is used as a subroutine in the k-means clustering algorithm to privately find the cluster which is closest to the given point, i.e., which cluster should a point be assigned to. Thus, the algorithm is invoked for every single data point in each iteration. Each party has as its input the component of the distance corresponding to each of the k clusters. This is equivalent to having a matrix of distances of dimension k x r. For common distance metrics; such as Euclidean, Manhattan, or any other Minkowski; this translates to finding the cluster where the sum of the local distances is the minimum among all the clusters. It Require: r parties, k clusters, n points.

1: for all sites $j = 1 \ldots r$ do
2: for all clusters $i = 1 \ldots k$ do
3: initialize μ'_{ij} arbitrarily
4: end for
5: end for
6: repeat
7: for all $j = 1 \ldots r$ do
8: for $i = 1 \ldots k$ do
9: $\mu_{ij} \leftarrow \mu'_{ij}$
10: $Cluster[i] = \emptyset$
11: end for
12: end for
13: for $g = 1 \ldots n$ do
14: for all $j = 1 \ldots r$ do
15: {Compute the distance vector $\vec{X}_j$ for point g.}
16: for $i = 1 \ldots k$ do
17: $x_{ij} = |data_{gj} -_D \mu_{ij}|$
18: end for
19: end for
20: Each site puts g into $Cluster[closest\_cluster]$
21: end for
22: for all $j = 1 \ldots r$ do
23: for $i = 1 \ldots k$ do
24: $\mu'_{ij} \leftarrow$ mean of j's attributes for points in $Cluster[i]$
25: end for
26: end for
27: until $checkThreshold$

Algorithm 2. Privacy preserving k-means clustering

IV. MODIFIED EXPECTATION MAXIMIZATION (E. M.) CLUSTERING

We present a privacy preserving EM algorithm for secure clustering. Only the one dimensional case is shown; extension to multiple dimensions is straight forward. The convention for notations is given below:

k	Total number of mixture components (clusters).
s	Total number of distributed sites.
n	Total number of data points.
nl	Total number of data points for site L.
yj	Observed data points.
μi	Mean for cluster i.
σ^2i	Variance for cluster i.
πi	Estimate of proportion of items in cluster i.
zij	Cluster membership. If yj = 1 for cluster i, zij ≈ 1, else zij ≈ 0.

i, j, l are the indexes for the mixture component, data points and distributed sites respectively. t denotes the iteration step. From conventional EM mixture models for clustering, we assume that data yj are partitioned across s sites ($1 \leq l \leq s$). Each site has nl data items, where summation over all the sites gives n. To obtain a global estimation for $\mu_i^{(t+1)}$, $\sigma_i^{2(t+1)}$, and $\pi_i^{(t+1)}$ the step requires only the global values n and

$$\begin{aligned} \sum_{j=1}^{n} z_{ij}^{(t)} y_j &= \sum_{l=1}^{s}\sum_{j=1}^{n_l} z_{ijl}^{(t)} y_j \\ \sum_{j=1}^{n} z_{ij}^{(t)} &= \sum_{l=1}^{s}\sum_{j=1}^{n_l} z_{ijl}^{(t)} \\ \sum_{j=1}^{n} z_{ij}^{(t)} (y_j - \mu_i^{(t+1)})^2 &= \sum_{l=1}^{s}\sum_{j=1}^{n_l} z_{ijl}^{(t)} (y_j - \mu_i^{(t+1)})^2 \end{aligned}$$

Observe that the second summation in each of the above equations is local. Using secure sum, we can compute the global values securely, without revealing yj. The estimation step giving z can be partitioned and computed locally given global μi, σ^2i , and πi:

$$z_{ijl}^{(t+1)} = \frac{\pi_i^{(t)} f_i(y_j; \mu_i^{(t)}, \sigma_i^{2(t)})}{\sum_i \pi_i^{(t)} f_i(y_j; \mu_i^{(t)}, \sigma_i^{2(t)})}$$

where yj is a data point at site l. The E-step and M-step iterate until

$$|L^{(t+1)} - L^{(t)}| \leq \epsilon, \text{ where}$$

$$L^{(t)}(\theta^{(t)}, \mathbf{z}^{(t)}|y) = \sum_{j=1}^{n}\sum_{i=1}^{k} \{z_{ij}^{(t)} [\log \pi_i f_i(y_j^{(t)}|\theta^{(t)})]\}$$

Again, this can be computed using a secure sum of locally computed partitions of z.

A. Quantifying Privacy

One focus of this project will be to understand and define privacy and security in ways that make sense for data mining. The secure multiparty computation approach has two limitations:

1. It is too restrictive; truly secure solutions may be inefficient. (E.g., for set intersection to be completely secure, each site must send enough data to represent all possible values, even if much is just "dummy" data).
2. It doesn't guarantee privacy. It only guarantees that nothing is disclosed beyond the result, but what if the result itself violates privacy?

We need ways to define and measure privacy to ensure that privacy preserving data mining results do meet actual privacy constraints. Sketches of several approaches are given below.

B. Knowledge query

Bounded Knowledge Approaches that alter the data generally use a bounded knowledge definition of privacy, perhaps the best method to date is the entropy based metric of [1]. While secure multiparty computation appears to achieve "perfect" privacy, in that nothing is shared but the results, even the results can provide bounded knowledge on the data sources.

Need to know is well established in controlling access to data. In the U.S., access to classified data requires both a security clearance and a justification of why the data should be accessed.

For Protected from disclosure, we want to protect specific items: individual data items, or specific rules. The problem becomes more difficult when we want to protect against disclosure of classes of information – in the limit this prevents data mining altogether [12]. We will develop privacy measures to address this issue; a likely starting point is ability to learn a classifier for a protected attribute from the results.

V. PRIVACY-PRESERVING COLLABORATI APPROACH USING FUZZY LOGIC

The works referenced here are most similar in nature to the proposed work. In particular, they make privacy preservation one of the key requirements, and support it to varying degrees.

Anonymity is an established measure of privacy, including concepts such as k-anonymity. We have proposed a p-in distinguish ability metric that extends this concept to data mining, allowing results that reveal information about an individual as long as the results reveal equivalent information for all individuals.The proposed project will formalize these measures and use them to analyze the developed privacy preserving data mining constructs. We will also investigate the applicability of these measures, and identify and formalize new measures as appropriate [15] [18].

Lincoln et al. describe a privacy-preserving mechanism for sharing security alerts, and addresses several techniques to sanitize alert data, including scrubbing and hashing. They propose the use of multiple hash functions, some keyed, to build solutions that avoid dictionary attacks. They also employ multiple repositories that randomly forward alerts to each other to obfuscate event sources. There appears to be no implementation of the above model; however, they conducted some small performance tests of hashing and correlation overhead. As opposed to Lincoln, et al., this thesis is application agnostic. the infrastructure behind Worminator can be applied to other forms of intrusion detection or software fault correlation. It suggests approaches to support privacy preserving collaborative payload anomaly detection. Additionally, this thesis introduces the notion of a framework to enable scalable, heterogeneous privacy preserving mechanisms, while focuses on a fixed basket of techniques. Finally,

Worminator has several significant differences to enable practical deployment, including the use of Bloom filters, fast Bloom filter correlation techniques, and publish-subscribe infrastructures. To the best of my knowledge, the

work proposed in remains unimplemented, and in fact postdates much of the Worminator work [13].

Kissner just completed a thesis proposal titled "Privacy-Preserving Distributed Information Sharing" [14], and some of the results are published in [15]. In the thesis proposal, she outlines two different privacy-preserving mechanisms: a polynomial set representation that supports not only privacy-preserving intersection, but also union and element reduction and a pair of hot item algorithms, one defining an identification mechanism and the other defining a publication mechanism.

Huang et al. describe Privacy-Preserving Friends Troubleshooting Network [16], which extends Wang et al.'s Peer Pressure research a collaborative model for software configuration diagnosis with a privacy preserving architecture utilizing a "friend"-based neighbor approach to collaboration. The key relevant aspects of the paper include a variation of secure multi party computation problem to "vote" on the popularity of a configuration to determine the configuration outlier, and the use of hash functions to enable secure multiparty computation (SMC) to support an unknown set of values; the relation of this proposal to SMC is discussed further in the next section. Finally, as with the previous work, they do not address temporal constraints in their correlation mechanisms [17].

In data mining, the user looks for new knowledge from database, such as relations between variables rules for instance. Data mining in databases or data warehouses in fuzzy domain is not that much easy. The purpose is to find related homogeneous categories, prototypical behaviors, general associations, important features for the recognition of a class of data. In this case, using fuzzy sets brings flexibility in interpretability, knowledge representation in the obtained results.. Looking for strict a relation between variables may be impossible because of the variety of descriptions in the database, while looking for an imprecise relation between variables or to a crisp relation between approximate values of variables may lead to a solution. For Example educated people who saves nation can solved by fuzzy relation. The expressiveness of fuzzy rules and relations or fuzzy values of attributes in a simplified natural language is a major quality for the interaction with the final user in providing the needed information in secured manner.

VI. CONCLUSION

A set of algorithms and techniques were proposed to solve privacy preserving data mining problems. The algorithms were implemented in java code. The experiments showed that the algorithms perform well on large databases. We introduced the notion of privacy preserving data mining with the primary goal of enabling collaboration of two clustering algorithms using fuzzy logic. It is very much useful in privacy preserving real world applications. This Combinatorial modified approach for secured date privacy is better than other approaches.

REFERENCES

[1]. Qian Wang, Cong Wang, Kui Ren, Wenjing Lou, and Jin Li, "Enabling Public Auditability and Data Dynamics for Storage Security in Cloud Computing,"IEEE Transactions on Parallel and Distributed Systems (TPDS), Vol. 22, No. 5, pp. 847-859, May, 2011

[2]. Anna Squicciarini, Barbara Carminati, Sushama Karumanchi., "Privacy-preserving Service Selection in Business Oriented Web Service Composition", IEEE International Conference on Web Services (ICWS), July 2011.

[3]. Kun Liu, Hillol Kargupta, and Jessica Ryan, "Random Projection-based Multiplicative Perturbation for Privacy Preserving Distributed Data Mining". IEEE Transactions on Knowledge and Data Engineering (TKDE), VOL. 18, NO. 1, pages 92--106, Piscataway, NJ, January 2006.

[4]. A. C. Squicciarini, E. Bertino, and E. Ferrari. "Achieving Privacy with an Ontology-Based approach in Trust Negotiations". IEEE Transaction on Dependable and Secure Computing (TDSC), Vol. 3 N. 1, pp. 13-30, January-March 2006.

[5]. N. Yvas, A. Squicciarini, Chih-Cheng Chang, D. Yao. "Towards Automatic Privacy Management in Web 2.0 with Semantic Analysis on Annotations". Collaborate Com Conference, IEEE. November 2009.

[6]. A. De Santis, G. Di Crescenzo, R. Ostrovsky, G. Persiano, and A. Sahai. "Robust Noninteractive Zero Knowledge", Advances in Cryptology - CRYPTO 2001, volume 2139 of Lecture Notes in Computer Science, pages 566-598, 2001.

[7]. R. Agrawal and R. Srikant. "Privacy-preserving data mining". In SIGMOD '00, pages 439-450. ACM Press, 2000.

[8]. Y. Lindell and B. Pinkas. "Privacy preserving data mining". Journal of cryptology, 15(3):177-206, 2002.

[9]. Gagan Aggarwal, Tom_as Feder, Krishnaram Kenthapadi, Rajeev Motwani, Rina Panigrahy, Dilys Thomas, and An Zhu. "Approximation algorithms for k-Anonymity". Journal of Privacy Technology (JOPT), 2005.

[10]. Y. Lindell and B. Pinkas, "Privacy Preserving Data Mining, Advances in Cryptology" - CRYPTO 2000. Lecture Notes in Computer Science, Vol. 1880, pp. 36–53Springer-Verlag, 2000.

[11]. Maurizio Atzori, Francesco Bonchi, Fosca Giannotti, and Dino Pedreschi. "k-anonymous patterns". In PKDD '05: Proceedings of the 9th European Conference on Principles and Practice of Knowledge Discovery in Databases, pages 10-21, 2005.

[12]. Maurizio Atzori, Francesco Bonchi, Fosca Giannotti, and Dino Pedreschi. "Blocking anonymity threats raised by frequent itemset mining". In ICDM, pages 561 -564, 2005.

[13]. Patrick Lincoln, Phillip Porras, and Vitaly Shmatikov. "Privacy-Preserving Sharing and Correlation of Security Alerts". In USENIX Security, 2004.

[14]. Lea Kissner. Thesis Proposal: "Privacy Preserving Distributed Information Sharing. PhD thesis", CMU, 2005.

[15]. Lea Kissner and Dawn Song. Privacy-Preserving Set Operations. In CRYPTO, 2005.

[16]. Qiang Huang, Helen J. Wang, and Nikita Borisov. "Privacy-Preserving Friends Troubleshooting Network". In NDSS, San Diego, CA, 2005.

[17]. Helen J.Wang, John C. Platt, Yu Chen, Ruyun Zhang, and Yi-MinWang. „Automatic Misconfiguration Troubleshooting with PeerPressure". In OSDI, San Francisco, 2004.

[18]. Charu C. Aggarwal and Philip S. Yu. "Privacy-Preserving Data Mining: Models and Algorithms". Springer Publishing Company, Incorporated, July 2008.

A Survey on Trust Management for Mobile Ad Hoc Networks

J. Sathiya Jothi
Department of Information Technology,
Anjalai Ammal Mahalingam Engineering College,
Thiruvarur-614403, Tamil Nadu, India.

S. Senthilkumar*
Department of Computer Science and Engineering,
University College of Engineering Pattukkottai,
Thanjavur-614701, Tamil Nadu, India.

B. Rajesh
Department of Mathematics,
University College of Engineering Pattukkottai,
Thanjavur-614701, Tamil Nadu, India.

***Abstract*— Mobile Ad hoc Network (MANET) is featured by the absence of centralized communication system to access the resources and sharing the information in between the wireless mobile nodes. In MANET, every node is dependent on the neighbor nodes for relaying the data towards the destination. So every mobile node is responsible for forwarding the data to neighbor node because of non-routing device in the system. In some situations, due to resource limitations, some nodes are neglecting the data to forward to another node. In this circumstance, the vital role is to detect the misbehavior nodes and induce them to involve in the communication system. We give a survey of trust management plans created for MANETs and talk about normally accepted classifications, possible attacks, performance metrics, and trust metrics in MANETs. At last, we confer future investigate areas on trust management in MANETs based on the idea of social networks.**

Keywords—Trust management; Mobile ad hoc networks; Trust; Trust Attacks; Secure Routing; Trust Metrics.

I. INTRODUCTION

In an increasingly distributed collaborative network world, could lead to efficient data transmission and information sharing in mobile ad hoc networks. It is composed of a set of independent devices that work as network nodes agreeing to forward packets for each other and have no central coordinator, absence of support infrastructure, dynamic topology and resource constraints and so on. These characteristics (memory size, processing power, battery life and unique wireless characters and others), force a node to be cautious when communicating with other nodes and its behavior .Nodes must act as a router, server, client, compelling them to cooperate for the perfect operation of the network.

A node should be capable of self-configuration, self-managing and self-learning by means of collecting local information and exchanging information with its trustworthy neighbors. In MANETS, decision making trust the terms through input, process and output of the information. This trust must often be derived under time critical conditions, Environmental condition, and in a distributed way.

The notion of trust, the degree of subjective belief about the behavior of a particular entity, trust relationship among participating nodes are critical in cooperative and collaborative environments to enhance system goals in terms of scalability,reconfigurability,reliability,availability,maintainability,confidentiality,integrity and safety.(i.e. survivability). For each node, a trust relationship to all neighbors .The trust is based on previous individual experience of the node and the recommendations of its neighbors. The formation and prolonged existence of MANET services are mainly based on an individual node's cooperating in packet forwarding. Therefore identifying and qualifying behavior of nodes in the form of trust essential for ensuring proper co-operation of MANETS.

First introduced the term "Trust Management" and identified it as a separate component of service in networks and clarified that "trust management provides a unified approach for specifying and interpreting security policies, credential and relationships"

Trust management in MANETS is needed when participating nodes, forwarding data to others nodes, there is no introduction about other nodes, desire to establish a network with an acceptable level of trust relationship among them.

II. RELATED WORK

Mobile Ad Hoc Network (MANETs) is a collection of mobile nodes connected with wireless links. MANET has no fixed topology as the nodes are moving constantly from one place to another place. In ad hoc networks, nodes can perform several actions, like sending packets, forwarding packets, responding to routing messages, sending recommendations, among others. The set of performed actions define the node's behavior. Therefore, the learning plan monitors the neighbor's actions trying to evaluate their behavior. All the nodes must co-operate with each other in order to route the packets. Cooperating nodes must trust each other.

Trust is characterized as the degree to which one gathering is willing to participate in a given activity with a given accomplice, considering the dangers and motivators included. Reputation is characterized as a discernment a gathering makes through past activities about its expectations and standards. In the greater part of the writing, reputation management is viewed as a component of trust management. Further, the terms trust management and trust foundation are

likewise reciprocally utilized. Aivaloglou et al., (2006) trust establishment is a procedure to manage the representation, assessment, upkeep, and dispersion of trust among nodes. Trust management manages issues, for example, the definition of assessment guidelines and strategies, representation of trust confirmation, and assessment and management of trust connections among nodes. Agreeing George et al.,(2006) The detail of permissible sorts of proof, the era, conveyance, disclosure, and assessment of trust confirmation are all in all called Trust Establishment.

III. TRUST MANAGEMENT FOR MANETS

This section discusses classifications, attacks and trust based solutions for trust management. Before reviewing the literature, we would like to clarify (some terminologies that have been used interchangeably but sometimes confusingly in the context of trust management.) trust related terms.

Trust Classifications:

Adams et al.,(2005) propose three sorts of reputation frameworks: positive reputation, negative reputation, and a mix of the two. Positive reputation frameworks just consider perceptions or input of the positive practices of a node. Negative reputation frameworks just record objections or perceptions of the negative practices of a node. Companions are thought to be trusted thus input on practices is utilized to adversely mirror a node's reputation.

Aivaloglou et al.,(2006) groups two sorts of trust establishment frameworks for MANETs: certificate-based framework versus behavior-based framework. In the previous, components are characterized for pre-sending learning of trust connections inside of the network, utilizing certificates which are conveyed, kept up and oversaw, either freely or agreeably by the nodes. Trust choices can be made taking into account a legitimate testament that demonstrates reliability of the objective node by a certificate authority or by different nodes that the backer trusts. In behavior-based framework, every node consistently screens practices of its neighboring nodes with a specific end goal to assess trust. The behavior-based framework is a responsive methodology, working under the supposition that the personalities of nodes in the system are guaranteed by preloaded confirmation mechanisms. For instance, if a node utilizes system assets as a part of an unapproved way, it will be viewed as a selfish or malicious node, and will at long last be disconnected from different nodes.

Aivaloglou et al.,(2006) likewise order trust establishment plans as far as the sort of architectures utilized: hierarchical framework versus distributed framework. In the previous, a hierarchy exists among the nodes taking into account their abilities or levels of trust. In this framework, unified declaration powers or trusted third parties are normally accommodated on-line or disconnected from the net proof. Such a centralized infrastructure does not exist in a distributed system; subsequently, every node has a few, potentially measure up to, obligation regarding obtaining, keeping up, and appropriating trust evidence.

George et al.,(2006) recommends two diverse ways to deal with register trust (i)Proactive trust calculation utilizes more transmission capacity for keeping up the trust connections precise. Thus, the trust choice can be come to immediately. (ii) Reactive systems compute trust values just when explicitly required. The decision depends generally on the particular circumstances of the application and the network. For instance, if nearby trust values change a great deal more frequently than a trust choice should be made, then a proactive calculation is not favored: The transmission capacity used to stay up with the latest will be squandered, subsequent to the greater part of the processed data will be out of date before it is utilized.

Li et al.,(2007) and Li et al.,(2008) classify trust management as reputation-based framework and trust establishment framework. A reputation-based framework utilizes direct observations and second-hand information disseminated among nodes in a network to evaluate a node. A trust establishment framework assesses neighboring nodes based on direct observations while trust relations between two nodes without earlier direct interactions are built through a mix of suppositions from intermediate nodes.

Yonfang (2007) suggests two diverse approaches to assess trust: policy-based trust management and reputation-based trust management. Policy-based trust management is based on well-built and objective security schemes such as logical rules and verifiable properties programmed in signed recommendation for access control of users to resources. In addition, the access decision is typically on the basis of mechanisms having a well defined trust management language that has well-built verification and evidence support. Such a policy-based trust management approach usually makes a binary decision according to which the requester is trusted or not, and accordingly the access demand is allowed or not. Due to the binary nature of trust evaluation, policy-based trust management has less suppleness. Moreover, the accessibility of (or access to) trusted certificate authorities (CA) cannot always be assured, mostly for disseminated systems such as MANETs. On the other hand, reputation-based trust management utilizes mathematical and computational mechanisms to evaluate trust. Typically, in such a system, trust is planned by collecting, aggregating, and disseminating reputation among the entities.

According to Li and Singhal, (2007) trust management can be classified as evidence-based trust management and monitoring-based trust management. Evidence-based trust management considers something that proves trust relationships between nodes these could incorporate public key, address, identity, or any confirmation that any node can create for itself or different nodes through a test and reaction process. Monitoring based trust management rates the trust level of each taking part node taking into account direct information (e.g., watching the considerate or malicious practices of neighboring nodes, for example, packet dropping, and packet flooding prompting intemperate asset utilization in the network, or denial of service attacks) as well as indirect information (e.g., notoriety evaluations, for example, suggestions sent from different nodes).Despite the fact that reputation management is a piece of trust management, numerous scientists further order reputation management plans.

Govindan et al.(2012) Trust computations can be widely requested into the going with categories:1.Distributed trust computations: Every node enlists its own specific estimation of trust on its neighbor's 2.Centralized trust computations: a Central master administers/helps the node in trust calculations. Disseminated trust counts can be appointed: Neighbor sensing speak to a trustor depends all alone experience around a trustee. Recommendations based trust speak to a trustor depends on different nodes experience of managing a trustee and Hybrid technique. There are three method in distributed trust computations.(i)Neighbor sensing through the way of watching the neighbors conduct over the time, routing based direct trust computations, past activities and present conduct are joined in Bayesian evaluation to decide trust. (ii)Recommendation based trust (Indirect trust) taking into account nearby voting, trust assessment in light of controlled flooding suggestions. (iii)Hybrid method based on input suggestion and own assessments in P2P system, taking into account proposal accumulation furthermore neighbor detecting, estimation taking into account packet sending conduct, and works in light of both direct associations furthermore proves gathered. In centralized trust computation can be grouping based trust calculations ,Nodes inquiry the specialists for the beginning trust and after that compute the last trust esteem taking into account averaging, Cluster head totals the trust reports got from individual nodes and decides the last trust, Centralized Trust Block which gathers votes and ascertains the trust.

Govindan et al.,(2012) Trust dynamics can be characterized by trust propagation, prediction and aggregation (i) Trust propagation using mechanism learning along with web of trust, tiny world net, public neighbors, dispersed hash table, individual meetings are used for trust information Exchange, rendezvous based trust propagation It can serve as a first level data to set up a node to have cooperation with any unusual node. It can help nodes to create a new group and together battle the getting into mischief exercises. (ii)Trust aggregation using trust properties like subjectivity, iterated belief trust values, Weighted Ordered Weighted Averaging (WOWA) operator trust values, sequence and parallel operator trust values. It enhances exactness on the trust estimation.(iii) Trust prediction Uses Kalman filter theory to predict the future trust values, Kalman filter model based on aggregation and prediction, past actions are used to predict the future trust value using mathematical inductions. In that some interior parameters of the objective node are used in trust prediction. It helps the node to be careful to avoid any possible hazard whereas communicating with abnormal nodes and also increase more accuracy.

Zhexiong Wei et al.,(2014) recommends trust management plot, the trust model has two parts: trust from direct observation and trust from indirect observation. With direct observation from a viewer node, the trust quality is inferred utilizing Bayesian inference, which is a form of vague calculation when the complete probability form can be mentioned. On the supplementary give, through indirect observation, which is called as secondhand information with the function of is obtained from neighbor nodes of the observer node, the trust value is calculated using the Dempster–Shafer theory (DST), which is a different type of uncertain reasoning when the proposition of attention can be formed by an indirect method.

Antesar and Keshav,(2015) to sort out the disobedient nodes as searching for a packet release route. Here trust was calculated by removing dishonest recommendations between certain time, number of connections, compatibility of information and closeness between the nodes. The recommending node is picked in light of three components to check its genuineness: Recommendations are gathered over a time frame to guarantee the consistency of proposals gave by a prescribing node with respect to the assessed node. Bunching strategy is embraced to progressively sift through proposals between certain time allotments in light of: (i) Identification of confidence value using number of interactions (ii) Compatibility of data with the assessed node through deviation test (iii) Closeness between the nodes. Distinctive nodes are picked in the trust evaluation system to test the execution of the filtering against different movable topologies and neighbor nodes.

The utilization recommendation based trust method can be profitable to nodes in finding making trouble nodes before collaboration, in this way maintaining a strategic distance from a potential awful ordeal. Recommendation can be classified into four categories. (i)Dishonest recommendation used CONFIDENT model. It applies the deviation test on the got suggestions and rejects the ones veering off over the limit esteem.(ii)Positive recommendation used CORE model, which just acknowledges positive proposal by other nodes.(iii).Negative recommendation is the main data traded between nodes.(iv). False recommendation used a trust-based motivating force model for self-policing versatile spontaneous systems to diminish the effect of false proposal on the precision of trust worth.

IV. TRUST MANAGEMENT ATTACKS

In this section, we discuss different type of attacks and explain various features from the viewpoint of trust management.

Active Attacks

An active attack occurs when an illegal person modifies a message, change data stream within the system, or introduce invalid data into a system; destroy data already stored in the he system or file. It is characterized by the attacker attempting to smash into the system. Comparison of different types of active attacks in MANETs is provided in Table 1.

Passive Attacks

A passive attack is a network attack in which a framework is observed and infrequently examined for open ports and vulnerabilities. The design is exclusively to pick up data about the objective and no information is changed on the objective. It is characterized by the attacker listening in on communication. Here the hacker does not try to break into the method or else modify data. Comparison of different types of passive attacks in MANETs is provided in Table 2.

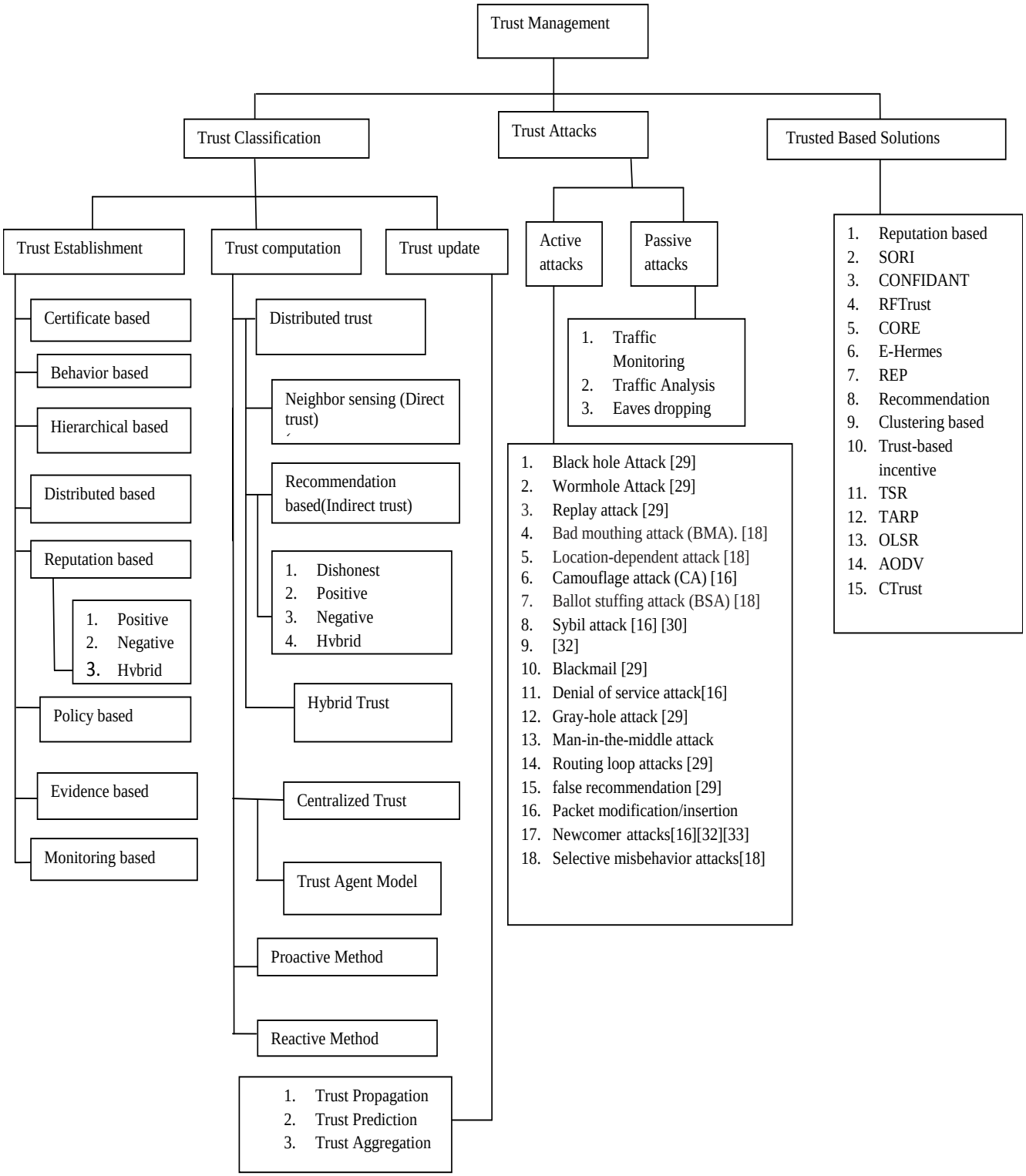
Trust Management
Trust Classification
Trust Attacks
Trusted Based Solutions
Trust Establishment
Trust computation
Trust update
Active attacks
Passive attacks
Certificate based
Behavior based
Hierarchical based
Distributed based
Reputation based
1. Positive
2. Negative
3. Hybrid
Policy based
Evidence based
Monitoring based
Distributed trust
Neighbor sensing (Direct trust)
Recommendation based(Indirect trust)
1. Dishonest
2. Positive
3. Negative
4. Hybrid
Hybrid Trust
Centralized Trust
Trust Agent Model
Proactive Method
Reactive Method
1. Trust Propagation
2. Trust Prediction
3. Trust Aggregation
1. Traffic Monitoring
2. Traffic Analysis
3. Eaves dropping
1. Black hole Attack [29]
2. Wormhole Attack [29]
3. Replay attack [29]
4. Bad mouthing attack (BMA). [18]
5. Location-dependent attack [18]
6. Camouflage attack (CA) [16]
7. Ballot stuffing attack (BSA) [18]
8. Sybil attack [16] [30]
9. [32]
10. Blackmail [29]
11. Denial of service attack[16]
12. Gray-hole attack [29]
13. Man-in-the-middle attack
14. Routing loop attacks [29]
15. false recommendation [29]
16. Packet modification/insertion
17. Newcomer attacks[16][32][33]
18. Selective misbehavior attacks[18]
1. Reputation based
2. SORI
3. CONFIDANT
4. RFTrust
5. CORE
6. E-Hermes
7. REP
8. Recommendation
9. Clustering based
10. Trust-based incentive
11. TSR
12. TARP
13. OLSR
14. AODV
15. CTrust

Table 1: Types of Active Attacks

ACITVE ATTACKS	DESCRIPTION
Newcomer attacks**(2009)(2012)**	The attacker fools, by joining and leaving the system alternatively to gain a new hope and hide its prior bad records.
Conflicting behavior attacks**(2009)(2012)**	The reference for a good node can be spoiled by a wicked node by carrying out information in a different way to different peers.
On-off attacks**(2009) (2012)(2015)**	In order to get unobserved while making trouble to services, a malicious node may alternatively appear as outstanding and awful node.
Blackmail **(2011)**	A particular node is threatened by malicious node that it will propagate bad intuition about it .
Gray-hole attack**(2011)**	It is a unique case of black hole attack in which a frightful node may fussily drop packets.
Black hole Attack **(2011)**	A malicious node respond positive information for all kind of route requests
Wormhole Attack **(2011)**	It makes up connection with low-latency, disturbs routing information.
Replay attack **(2011)**	A replay attack (also known as playback attack) in which a legitimate data transmission is unspitefully repeated or delayed.
Routing loop attacks **(2011)**	The routing packets are amended by the malicious node. As a result it cannot reach the intended recipient.
False information or false recommendation**(2011)**	A malicious node plan to isolate good nodes by offering false Inference/ Information, at the same time keeping dreadful nodes connected.
Incomplete information**(2011)**	Possibly, a malicious node may not lend a hand in providing appropriate or comprehensive information.
Denial of service attack**(2012)**	The normal utilization or process of communication services may be obstructed by a malevolent node , for example-extreme resource utilization
Camouflage attack (CA) **(2012)**	Here, the fraudulent users tries to make trust by constantly informing what they observed .After gaining trust they behave fraudulently for particular instance.
Sybil attack **(2012) (2013)**	It can damage the entire topology through multiple references such as location based routing.
Bad mouthing attack (BMA) **(2015)**	A malicious node may unlawfully broadcast bad ratings for good nodes in order to smudge their character.
Location-dependent attack **(2015)**	From the individual property of trust i.e.(deeds at one location cannot affect assessing fidelity of nodes at another location) this attack has been derived
Ballot stuffing attack (BSA) **(2015)**	In this attack, a malicious node tries to provide fair rating for scantily performing node in order to deceive trust mechanism.
Selective misbehaving attacks**(2015)**	This attack proliferate fake ranking for some faithful nodes. Whereas, behave normal to other nodes.
Man-in-the-middle attack	An Intruder tries to access information passed between sender and receiver without their knowledge. Sometimes intruder tries to pretend itself as either sender or receiver.
Packet modification/insertion	Depraved packets such as packets with erroneous routing information may be inserted by malicious node on other hand it may also alter packets.

Table 2: Types of Passive Attacks

PASSIVE ATTACKS	DESCRIPTION
Traffic Monitoring	It could provide information to launch further attacks.
Traffic analysis	Analyzing patterns of data transmission.
Eavesdropping	Attacker observe transmissions of message content, and may also include fake message in the network

V. TRUST BASED SOLUTIONS

In this section, we review various trust based solutions for secure routing.

Secure Routing:

Marti et al.,(2000) proposed a reputation based trust management plot that contains watch dog strategy utilizing which the practices of the nodes are observed notwithstanding that pathrater plan accumulates notoriety and give an answer about independent bamboozling node so as to discover find terrible assaults. It includes direct observation in light of expanded DSR.

Buchegger et al.,(2002) Initiated another outline called CONFIDANT (Cooperation of Nodes-Fairness in Dynamic Ad-hoc Networks) a notoriety based trust establishment plan which tosses fiendish node through DSR by giving deceptive proposal. It considers any kind of suggestions of trust esteem than the obsession of limit worth negative proposals. At the point when the season of transmission among the nodes the wrong message is infiltrated .Hence this technique is badly designed.

Michiardi and Molva,(2002) proposed CORE (Collaborative REputation) show, that consider idealistic suggestion instead of negative suggestion which prompts wasteful transmission.

He et al.,(2004) planned SORI (Secure and Objective Reputation-based Incentive) a notoriety based trust management plan utilizing an incentive based method. This technique advance transmission of packets and deject self absorbed practices which relies on upon taking into account counted target measures and notoriety multiplication through a restricted hash chain based acceptance. However this might have a constraint in the existence of malicious node.

Nekkanti and Lee,(2004) created AODV (Ad hoc On demand Distance Vector) using trust variable and security level at each node. Their procedure deals unmistakably with each course request considering the node's trust variable and

security level. In a common arrangement, coordinating information for every requesting would be encoded provoking tremendous outlay; they recommend using unmistakable levels of encryption in light of the trust variable of a node, along these lines diminishing overhead. This procedure adjusts the security level in light of the apparent opposing vibe level and therefore can spare resources; regardless, the technique does not treat evaluation of trust itself.

Li et al.,(2004) also enlarged AODV and received a trust model to make arrangements for malignant practices of nodes at the system layer. They address trust as supposition beginning from subjective method of reasoning. The inclination reflects the characteristics of trust in MANETs, particularly dynamicity. The key component is to consider system execution perspectives by dealing with each request in light of its level of trust. Dependent upon the level of trust of nodes incorporated into the request, there is no necessity for a node to request and check verifications always, thusly provoking paramount diminishment of estimation and correspondence overhead. This work advances trust organization by considering a non particular trust organization structure for MANETs.

Pisinou et al.,(2004) considered a safe AODV-based routing convention for multi-hop specially appointed systems for finding a secured end-to-end course free of any exchanged off nodes. Their trust-based guiding tradition discovers trust values develop just in light of direct observations, expecting that trust must have the property of transitivity.

Asad Amir Pirzada et al.,(2006) The primary thought of trust-based routing protocols is to find trusted course as opposed to secure courses. It is broke down by the trustworthiness of the nodes in the connection. Routing circles can be disposed of through utilization of arrangement numbers in AODV. In this method permit the portability operation which depict about the current circumstance of system.

Wang et al.,(2008) prescribe a trust-based incentive model for self-policing versatile system frameworks to decrease the impact of false proposal on the exactness of trust quality. In any case, the execution of the model is not attempted against specific attacks, for instance, ballot-stuffing.

Moe et al.,(2008) proposed a trust-based routing protocol as an increase of DSR considering a persuading power part that actualizes cooperation among nodes and diminishes the points of interest that self important nodes can acknowledge (e.g., saving resources by particularly dropping groups). This work is novel in that they used a covered Markov model (HMM) to quantitatively measure the dependability of nodes. In this work, extremist nodes are agreeable and particularly drop packets.

Abusalah et al.,(2008) proposed a Trust-Aware Routing Protocol (TARP) and added to a trust metric in light of six trust parts including program structure, architecture of equipments, battery power, record as a purchaser, presentation and legitimate hierarchy of leadership. On the other hand, no musing was given to trust decay after some time and space to reflect powerlessness in view of components and divided information in MANET circumstances.

Luo et al., (2009) proposed RFSTrust, which compute the reliability of node through a trust taking into account fuzzy suggestion. They propose relationship among nodes in light of the closeness idea. There is a relentless assessment between nodes when there is more similitude in the middle of assessing and suggesting node. It is not suitable to manage distinctive sorts of assault including immature node assault.

Hermes (2009) is a proposition in light of suggestion trust demonstrates that uses an additional parameter known as a sufficiency edge (in association with the confidence level). The thought of value is used as a part of the computation of recommendation to ensure that adequate view of the behavior of taking an interest center point have been gained. Regardless, the determination of value is a tradeoff between getting more exact dependability regard and the combining time required to procure it.

Recommendation Exchange Protocol was proposed by *Velloso et al.,(2010)* to allow nodes to send and get recommendations from neighboring center points. It displays the thought of relationship advancement considering to what degree nodes have known each other. Recommendations sent by whole deal accomplices are weighed higher than that from transient accomplices. The advancement of relationship is evaluated on the reason of a lone variable by considering only the period of time of relationship.

*Yu et al.,(2011)*propose a clustering method to filter through trustworthy recommendations from deceptive ones. They take after the larger part direct by selecting the group with the greatest number of proposals as tried and true one. They attempted their model against a couple strikes like upbraiding and ticket stuffing. Then again, predominant part regulate could truly be destructive as a couple of nodes can plot to perform a strike, and not give a honest to goodness judgment about various nodes. Clustering strategy to dynamically filter through ambushes related to conniving recommendations between certain time in light of number of correspondences, comparability of information and closeness between the nodes.

Huanyu Zhao(2013) proposed layout a response for cyclic improvement plan nodes in trust administration manets for upgrading precision and profitability. It takes the issue of trust affiliation and collection issues with cTrust Distributed Trust Aggregation Algorithm. It assembles the trust rate in trust route for each one of the nodes in the framework than the neighbors trust associations. Trust rating limits considering distinctive parts in the recorded trades, for instance, noteworthiness, nature of organization, time, and area. In additionally, it compute how to rate an administration and how to make the exact and stable direct trust assessments. The cTrust all out arrangement impacts a stochastic coursed Bellman–Ford calculation to achieve fast and lightweight trust rating mixture. The idea of Ctrust, depends on two categories.1) The improvement plans and trust associations in cMANET as a trust outline and show the most trustable way (MTP)- discovering process as the Markov decision technique (MDP). 2. Trust trade limit,

regard cycle work, and spread trust aggregation estimation to deal with the MTP-finding issue. This figuring uses a stochastic Markov-chain-based methodology, which fundamentally diminishes the message overhead. It requires simply adjacent correspondence between neighbor nodes and gets a brief delineation of the whole framework from each node's point of view.

Zhexiong Wei et al.,(2014) proposed new thought of trust organization plan for uncertain deduction to upgrade more accuracy trust regard in the viewer node. It incorporates two sorts of trust modules.(i) Direct observation viewer node can choose trust estimations of its neighbors by using Bayesian obstruction, which is a general framework to infer the estimation of the dark probability by using examination. (ii) In the indirect observation, which is in like manner called utilized information is gotten from viewer nod and convenient node, the trust worth is induced using the Dempster–Shafer therory(DST)

Antesar and Keshav,(2015) Proposed a suggestion based trust management to deal with the getting out of hand nodes and secure the coordinating tradition amidst source and destination nodes when the season of package transport by using Bayesian quantifiable philosophy, filtering algorithms. The issue of data sparsity can be shed by disengaging recommendations using dynamic grouping methods. It relies on upon number of correspondences, pleasing information with the appraisal center nodes, and closeness between the center nodes.

VI. CONCLUSION

Trust and its management are energizing fields of examination. The rich literature developing around trust gives us a well-built indication that this is an imperative range of research. Trust as an idea has a wide collection of adjustments and applications, which causes dissimilarity in trust management phraseology. The objective of this paper is to give MANETs architects various points of view on the idea of trust, a comprehension of the properties that ought to be considered in developing a trust metric, and bits of knowledge on how trust can be processed. We begun this paper by introducing different meanings of trust also, measurements utilized for assessing trust.

We then exhibited a exhaustive overview of different trust computing approaches, their correlations regarding different attack models and computational requirements.

We discussed different literature on the trust establishment, for example, trust computation, updating and predictions. In this paper, we studied and dissected existing trust management plans in MANETs to give MANET trust system convention fashioners with different points of view on the idea of trust, a comprehension of trust properties that should be seen in creating trust measurements for assessing trust, and bits of knowledge on how a trust metric can be tweaked to meet the necessities and objectives of the focused on framework. A composite trust metric that catches parts of correspondences and interpersonal organizations, and comparing trust estimation, trust conveyance, and trust administration plans are intriguing exploration headings. For dynamic networks, such as military MANETs, these plans ought to have alluring credits, for example, capacity to adjust to ecological progress, adaptability, unwavering quality, and reconfigurability.

We expect that the near potential will bring consolidation around a set of basic principles for building trust and its a range of related issues, and that these will be realized in practical and commercial applications.

REFERENCES

[1] Abusalah.L,Khokhar.A,&Guizani.M.,(2008).A Survey of Secure Mobile Ad Hoc Routing Protocols. *IEEE Commun. Surveys and Tutorials*, vol.19, no. 4, pp.78-93.

[2] Adams.W.J Hadjichristofi G.C.,&Davis. N.J.,(2005).Calculating a Node's Reputation in a Mobile Ad Hoc Network. *Proc. 24th IEEE Int'l Performance Computing and communications Conference*, Phoenix, AX, pp. 303-307.

[3] Aivaloglou.E,Gritxalis.S.,&C.Skianis.,(2006).Trust Establishment in Ad Hoc and Sensor Networks Proc. 1st Int'l Workshop on Critical Information Infrastructure Security, Lecture Notes in Computer Science,vol.4347, pp. 179-192, Samos, Greece, 31, Springer.

[4] Antesar M. Shabut, Keshav P. Dahal, Senior Member, IEEE, Sanat Kumar Bista, & Irfan U. Awan,(2015).Recommendation Based Trust Model with an Effective Defence Scheme for MANETs.*IEEE TRANSACTIONS ON MOBILE COMPUTING*, VOL. 14, NO. 10.

[5] Ben- Jye Chang, Member, IEEE, & Szu-Liang Kuo,(2009).Markov Chain Trust Model for Trust-Value Analysis and Key Management in Distributed Multicast MANETs.*IEEE TRANSACTIONS ON VEHICULAR TECHNOLOGY*, VOL. 58, NO. 4.

[6] Buchegger.S & Le Boudec.J,(2002).Performance Analysis of the CONFIDANT Protocol: Cooperation Of Nodes- Fairness In Dynamic Ad-hoc NeTwork Proc. 3rd IEEE/ACM Symposium on Mobile Ad Hoc Networking and Computing, Lausanne, CH, 9-11,pp.226-236.

[7] George.G ,Theodorakopoulos & Baras.J.S,(2006).On Trust Models and Trust Evaluation Metrics for Ad Hoc Networks. *IEEE J. Sel. Areas Commun.*, vol. 24, no. 2.

[8] Grandison.T & Sloman.M ,(2000).A Survey of Trust in Internet Applications. *IEEE Comm. Surveys and Tutorials*, vol. 3, no. 4, pp. 2-16.

[9] He.Q ,Wu.D,& P. Khosla,(2004)SORI: A Secure and Objective Reputation-based Incentive Scheme for Ad-Hoc Networks, Proc. *IEEE Wireless Communications and Networking Conf*., vol. 2, pp. 825- 830.

[10] Huanyu Zhao, Xin Yang, and Xiaolin Li, Member, IEEE,(2013).cTrust: Trust Management in Cyclic Mobile Ad Hoc networks. *IEEE TRANSACTIONS ON VEHICULAR TECHNOLOGY*, VOL. 62, NO. 6.

[11] Jin-Hee Cho, Member, IEEE, Ananthram Swami, Fellow, IEEE,& Ing-Ray Chen, Member, (2011).A Survey on Trust Management for Mobile Ad Hoc Networks, *IEEE COMMUNICATIONS SURVEYS & TUTORIALS*, VOL. 13, NO. 4.

[12] Kamvar.S, Scholsser.M & H. Garcia-Molina,(2003).The Eigen Trust Algorithm for reputation Management in P2P Networks, *Proc. 12th Int'l Conf*. World Wide Web (WWW).

[13] Kannan Govindan,Member IEEE & Prasant Mohapatra, Fellow IEEE,(2012).Trust Computations and Trust Dynamics in Mobile Adhoc Networks:A Survey *IEEE COMMUNICATIONS SURVEYS & TUTORIALS, VOL. 14, NO. 2*.

[14] Karim Rostamzadeh,Student Member, IEEE, Hasen Nicanfar, Student Member, IEEE, NarjesTorabi, Student Member, IEEE, Sathish Gopalakrishnan, Member, IEEE, & Victor C. M. Leung,Fellow,IEEE,(2015).A Context-Aware Trust-Based Information Dissemination Framework for Vehicular Networks, *IEEE INTERNET OF THINGS JOURNAL*,VOL. 2, NO. 2.

[15] Lee. S, Sherwood.R,& Bhattacharjee.B,(2003).Cooperative Peer Groups in NICE, Proc. *IEEE INFOCOM*, pp. 1272-1282.

[16] Li.R,Li.J, Liu.P, Chen.H.H,(2007).An Objective Trust Management Framework for Mobile Ad Hoc Networks," *Proc. IEEE 65th Vehicular Technology Conf*., 22-25, pp. 56-60.

[17] Li.J,Li.R ,& Kato.J,(2008).Future Trust Management Framework for Mobile Ad Hoc Networks: Security in Mobile Ad Hoc Networks, *IEEE Commun. Mag.*, vol. 46, no. 4, pp. 108-114.

[18] Li.R, Li.J, Liu.P,& Kato.J,(2009).A novel hybrid trust management framework for MANETs in Proc. *29th IEEE Int. Conf. Distrib.Comput. Syst. Workshops* , pp. 251–256.

[19] Li.X, Lyu.M.R &Liu.J,(2004).A Trust Model Based Routing Protocol for Secure Ad Hoc Networks,Proc. *IEEE Aerospace Conf., Bug Sky, Montana*, 6-13, vol. 2, pp. 1286-1295.

[20] Li.H & Singhal.M.,(2007).Trust Management in Distributed Systems Computers, vol. 40, no.2, pp. 45-53.

[21] Michiardi.P &Molva.R.,(2002).Core: A Collaborative Reputation mechanism to enforce node cooperation in Mobile Ad Hoc Networks, in *Proc.Commun. Multimedia Security Conf*.,pp. 107–121.

[22] Moe.M.E.G.,Helvik.B.E., &Knapskog.S.J.,(2008).TSR: Trust-based Secure MANET Routing using HMMs, *Proc. 4th ACM Symposium on QoS and Security for Wireless and Mobile Networks*, Vancouver, British Columbia, Canada, 27-28 , pp. 83-90.

[23] Nekkanti.R.K.,&Lee.C.,(2004).Trust-based Adaptive On Demand Ad Hoc Routing Protocol, *Proc. 42th Annual ACM Southeast Regional Conf*., Huntsville, Alabama, pp. 88-93.

[24] Pirzada &McDonald.C,(2004).Establishing trust in pure adhoc networks, in Proc. *27th Australasian Conf. Comput. Sci*.,vol. 26, pp. 47–54.

[25] Pirzada.A.,McDonald.C.,&Datta.A.,(2006).Performance Comparison of Trust-based Reactive Routing Protocols, *IEEE Trans. Mobile Comput.*, vol. 5, no. 6, pp. 695-710.

[26] Pedro Velloso.B., Rafael Laufer.P.,Daniel de Cunha.O.,Otto Carlos Duarte.M.B.,&Guy Pujolle(2010). Trust Management in Mobile Ad Hoc Networks Using a Scalable Maturity-Based Model, *IEEE TRANSACTIONS ON NETWORK AND SERVICE MANAGEMENT*, VOL. 7, NO. 3.

[27] Pisinou.N.,Ghosh.T., &Makki.K.,(2004). Collaborative Trust-based Routing in Multi-hop Ad Hoc Networks,*Proc. 3rd Int'l IFIP-TC06 Networking Conf*., Lecture Notes in Computer Science, Athens, Greece, 9-14 ,vol. 3042, pp. 1446-1451.

[28] Pissinou.N.,Ghosh.T.,Makki.K., (2004).Collaborative trust-based secure routing in multi hop adhocnetworks,*inProc.Netw.Netw.Technol.,Services,Protocols;Perform.Comput.Commun.Netw.,Mobile Wireless Commun.*, pp. 1446–1451

[29] Sohail Abbas, MadjidMerabti, David Llewellyn-Jones,&KashifKifayat,(2013).Lightweight Sybil Attack Detection in MANETs",*IEEE SYSTEMS JOURNAL*, VOL. 7, NO. 2.

[30] Velloso.P.B.,Laufer.R.P., Cunha.D.,Duarte.O.C.M., & Pujolle.G., (2010). Trust management in mobile ad hoc networks using a scalable maturity-based model,*IEEE Trans.Netw. Service Manage.*, vol. 7, no. 3, pp. 172–185.

[31] Luo.J., Liu.X., & Fan.M.,(2009).A trust model based on fuzzy recommendation for mobile ad-hoc networks,Comput. Netw., vol. 53, no. 14, pp. 2396–2407.

[32] Marti.S,Giuli.T.,Lai.K.,,& Baker.M.,(2000).Mitigating Routing Misbehavior in Mobile Ad Hoc Networks,Proc. *6th Annual ACM/IEEE Mobile Computing and Networking*, Boston, MA, pp.255-265.

[33] Wang.K.,Wu.M.,&Shen.S.,(2008). A trust evaluation method for node cooperation in mobile ad hoc networks,*in Proc. 5th Int. Conf. Inform. Technol*., New Generations, pp. 1000–1005.

[34] Younghun Chae, Lisa Cingiser DiPippo, Member, IEEE Computer Society,&Yan Lindsay Sun,Member,IEEE,(2015).Trust Management for Defending On-Off Attacks.,*IEEE TRANSACTIONS ON PARALLEL AND DISTRIBUTED SYSTEMS*, VOL. 26, NO. 4, 32.

[35] Yu.H.,Liu.S.,Kot.A.C.,Miao.C.,,&Leung.C.,(2011).Dynamic witness selection for trustworthy distributed cooperative sensing in cognitive radio networks, *in Proc. IEEE 13th Int. Conf. Commun. Technol.*,pp. 1–6.

[36] Yu.H.,Shen.Z.,Miao.C.,Leung.C.,&Niyato.D.,(2010).A survey on trust and reputation management systems in wireless communications,*Proc. IEEE*, vol. 98, no. 10, pp. 1755–1772.

[37] Yunfang.F., Adaptive Trust Management in MANETs, (2007). *Int'l Conf. on Computational Intelligence and Security*, Harbin, China, 15-19, pp. 804-808.

[38] Zhexiong Wei, Helen Tang, Member, IEEE, Richard Yu.F., Senior Member, IEEE, Maoyu Wang, & Peter Mason.,(2014). Security Enhancements for Mobile Ad Hoc Networks with Trust Management Using Uncertain Reasoning, *IEEE TRANSACTIONS ON VEHICULAR TECHNOLOGY*, VOL. 63, NO. 9.

[39] Zouridaki.C, Mark.B.L,Hejmo.M, & R. K. Thomas.,(2009). EHermes: A robust cooperative trust establishment scheme for mobile ad hoc networks, Ad Hoc Netw., vol. 7, no. 6, pp. 1156–1168.

Monitoring and Detecting of Air Pollution using Wireless Sensors Network

K. Preethi
Department of Computer Science and Engineering,
University College of Engineering Pattukkottai,
Thanjavur, Tamil Nadu, India.

***Abstract*— In recent technological developments in the wireless communication technology have to the emergence of environmental pollution sensor and air pollution sensor network.it is monitoring system provides real time information about the level of air pollution particular region. Lacks of implementation of environmental regulation are contributing to the bad air quality of most of the Indian cities. Analytical measuring equipment is costly, time and power consuming, and can seldom be used for air quality reporting in real time. Wireless Sensor Networks are a new and very challenging research field for embedded system design automation, as their design must enforce stringent constraints in terms of power and the problem of air pollution is becoming a major concern for the health of pollution and all sector of our life and identify the approach in various application like leakage of gas industry and oil sector. I can also calculate the better power management and real time measuring and monitoring in an urban area to ultimately improve quality of life on earth. Air pollution in the urban environment is a major threat to human health. As the global population is becoming more concentrated in urbanized areas, new ideas and approaches are needed to help maintain clean air that is safe for everyone to breathe. I propose a indoor and outdoor air pollution monitoring system which uses ZigBee and ARIMA prediction model for monitoring air pollution. It predicts the carbon dioxide level in ubiquitous cities and system integrates wireless sensor board and also integrates with the dust, temperature and humidity and reducing power consumption. In this module is the small range, low power, low data rate wireless networking technology for many wireless application.**

Keywords—Zig Bee Model, ARIMA Prediction model, Wireless Sensor Network.

I. INTRODUCTION

The detectable presence of different chemicals in the air, together with their concentration, is a source of valuable information for many applications ranging from pollution monitoring to explosives and drug factories detection. In particular, several gases are considered responsible for respiratory illness in citizens, some of them (e.g. benzene) are known to induce cancers in case of prolonged exposure even at low concentrations [1]. Awkwardly, volatile organic compounds (e.g. formaldehyde) released as off-gas by furniture's adhesives or cleaning agents or by smoking in indoor environments reach concentrations levels that are order of magnitudes higher than in outdoor settings. The estimation of chemicals distribution is hence significantly relevant for citizens safety and consequently for the definition of integrated urban and mobility plans designed to face these problems.

Chemicals monitoring can be of paramount importance for security applications e.g. for the detection of explosives and drug factories in cities [2]. However, chemicals monitoring both in outdoor and indoor environment are affected by the peculiarity of chemicals propagation process. To be concise, diffusion and turbulence make a single point of measure ineffective, calling for distributed approaches to chemicals detection and concentration estimation. In many applications this, in turn, require the monitoring task to be fulfilled by a network of wireless (sometime mobile) modules, with the wireless term being related to either connectivity and/or power supply (Wireless Chemical Sensor Networks, WCSN). Different applications lead to different specific requirements but a number of challenges repeatedly recurs when engineer try to design real world operating WCSN systems. In facts, single module calibration and sensor stability, efficient power usage and cooperative reconstruction seems to be the most common challenges to face both in indoor and outdoor settings. In this paper will review these challenges together with the solution proposed by our group during our commitment in the wireless chemical sensing topic.

II. LITERATURE SURVEY

Due to recent technological advances, the construction are monitored are light, temperature, humidity, pressure, etc. a converter that transforms the sensed signal from an analog to a digital signal; A Processing Unit in the Microcontroller, process the signals sensed form sensor with help of embedded memory , operating system and associated circuitry. A Radio component that can communicate the sink node or zigbee router which collects the sensed pollution gas level from sensor node and forwards to pollution server which is in our campus. Powering these components is typically one or two small batteries. There are also wireless sensors utilized in applications that use a fixed value, wired power source and do not use batteries as a power source. In an external environment where the power source is batteries, wireless sensors are placed in an area of interest that is to be monitored, either in a random or known fashion.

The sensors self-organize themselves in a radio network using a routing algorithm, monitor the area for measure the gas levels in air , and transmit the data to a central node, sometimes called a pollution server or base station (interfaced with coordinator), or sink node(interfaced with router), that collects the data from all of the sensors. This node may be the same as the other detection nodes, or because of its increased requirements, may be a more sophisticated sensor node with

increased power. The most advantage of wireless sensors is that they may be implemented in an environment for extended over a time period, continuously detecting the environment, without the need for human interaction or operation.

III. ZIGBEE STANDARD

The ZigBee standard is the new short range, low power, low data rate wireless networking technology for many real time application. It is best specified the bottom three layers (Physical, Data Link, and Network), as well an Application material for small and low cost sensors became technically and economically feasible. Even though, Industrialization increase the degree of automation and at the same time it increases the air pollution by releasing the unwanted gases in environment especially in industrial areas. Inorder to implement the project, we selected four areas to deploy the application. To detect percentage of pollution ,we used the array of sensor to measure gas quantity in the physical environment in surrounding the sensor and convert them into an electrical signals for processing. Such a signal reveals some properties about interested gas molecule.

A huge number of these sensors nodes can be networked in many applications that require unattended operations creates a wireless sensor network. Wireless sensors are devices that range in size from a piece of glitter to a deck of cards. Integration of various components create the air pollution monitoring system.. They are functionally composed of: A Sensing unit that is designed and programmed to sense gas pollutants in air in Programming Interface (API) based on the 7-layer OSI model for layered communication systems.

Fig. 1. Application Layer of OSI Model

Programming Interface (API) based on the 7-layer OSI model for layered communication systems. Figure-1 shows the layered architecture adopted by the alliance industries. It should be noted that the ZigBee Alliance chose to use an already existing data link and physical layer specifications. These specifications are the published IEEE 802.15.4 standards for low rate personal area networks(PAN) as shown in Figure 1. Communication network is composed of many nodes, each of which can interact by transmit and receive data over communication channesl. The ZigBee network model supports star, tree and mesh topologies as shown in Figure

ZigBeecoordinator(ZC) is responsible for initiating and maintaining the devices on the network, and all other devices, known as end devices(ZE) including routers (ZR), directlycommunicate with the ZigBee coordinator. In mesh and tree topologies, the coordinator(ZC) is responsible for initiating the network with default values and for choosing certain key network parameters but the network may be extended through the use of routers. The configurations of coordinator and router using X-CTU interface shown in Figure 6. In tree networks, routers move data and control messages through the network using a hierarchical routing strategy.

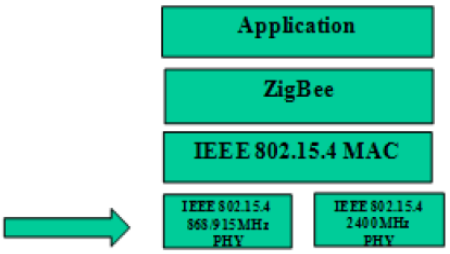

Architecture diagram for Zig Bee and ARIMA prediction model fig 2

Below is a brief description of each component of **ARIMA** prediction model.

Reading Sensor generates a random value whose range is set based on the value of a “seriousness” variable.
Reading Transmitter gets the generated value from the reading sensor and transmits it through the communicator.
Power Controller: Each node will have a method called “turn on” that will start the node and we just call it. As for power-saving modes, this will depend on what the simulator will
provide to us.
Communicator: This is implemented by the simulator. Inter-Process communication is usuallydone using sockets; the simulator to provide us with sockets as well as methods such as “send” and “receive”.
Launcher informs the data collector to start collection based on the delivery mode set by the user.
Data collector gets a list of nodes from which it has to collect readings, then sends messages to inform them and finally receives the required values.
Aggregator implements the RCQ algorithm for data aggregation that we will discuss in the next section.
Data extractor uses SQL queries to extract data from database.
Data displayer: This extracts data as required by the user and displays them in a table aswell as evaluates the AQI for the selected area.
Trend analyser gets previous readings and determines relationship between them to be able to extrapolate future readings.

Nodes Deployment Viewer displays deployment of nodes in the WSN field and their AQI colours.
Connection Initiator: The java DriverManager allows for a method to open a database, providing it the name of the database, user name and password as parameters. So, this component just has to make a call to this method and store the return reference to theconnection.
Connection destructor: Connection object, in java.sql package, usually provides for a close method that closes the latter safely and frees associated memory.

The following table shows the various types of nodes that are present in WAPMS.

Type of Node	Energy Requirements	Location	Role
Source (sensor node)	Constrained	Random	Sensing and multihop routing
Cluster Head (collector)	Not-Constrained	Fixed	Collection and aggregation
Sink /Gateway	Not-Constrained	Fixed	Collection

These nodes will form a hierarchy that is shown in Fig 3.

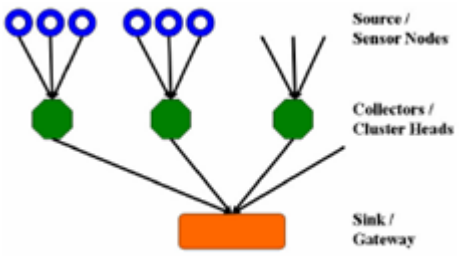

Fig. 3. Hierarchy of nodes

The strategy to deploy the WSN for our system is as follows:

First partition our region of interest into several smaller areas for better management of huge amount of data that will be collected from the system and for better coordination of the various components involved o Deploy one cluster head in each area; these will form cluster with the nodes in their respective areas, collect data from them, perform aggregation and send these back to the sink.Then, randomly deploy the sensor nodes in the different areas. These will sense the data, send them to the cluster head in their respective area through multihop routing o Multiple sinks that will collect aggregated from the cluster heads and transmit them to the gateway. Each sink will be allocated a set of cluster heads. The gateway will collect results from the sinks and relay them to the database and eventually to our application.

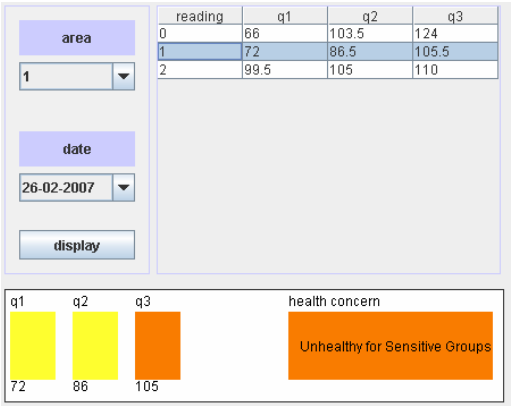

Fig. 4. Reading health concern in particular area

The system is simulated over a small region as a prototype and then it will be extended to the whole island. The town of Port Louis, the capital of the country, is chosen for the prototype implementation as it is an urban area and therefore, more exposed to air pollution than rural areas. The site is partitioned the site into 6 smaller areas as shown in figure 7. With this small number of areas, we will use a single sink and we further simplify the system by allowing the gateway to play the role of the latter. An Air Quality Index (AQI) is used in Zig Bee model. The AQI is an indicator of air quality, based on air pollutants that have adverse effects on human health and the environment. The pollutants are ozone, fine particulate matter, nitrogen dioxide, carbon monoxide, sulphur dioxide and total reduced sulphur compounds. Figure 8 and figure 9 illustrate the AQI range.

IV. CONCLUSION

As discussed in this paper, recent technological developments in the miniaturization of electronics and wireless communication technology have led to the emergence of Environmental Sensor Networks (ESN). These will greatly enhance monitoring of the natural environment and in some cases open up new techniques for taking measurements or allow previously impossible deployments of sensors. WAPMS is an example of such ESN. ZigBee and ARIMA prediction model S will be very beneficial for monitoring different high risk regions of the country. It will provide real-time information about the level of air pollution in these regions, as well as provide alerts in cases of drastic change in quality of air. This information can then be used by the authorities to take prompt actions such as evacuating people or sending emergency response team. WAPMS uses an Air Quality Index to categorise the various levels of air pollution. It also associates meaningful and very intuitive colours to the different categories, thus the state of air pollution can be communicated to the user very easily. The major motivation behind our study and the development of the system is to help the government to devise an indexing system to categorise air pollution in Mauritius. The system also uses the AQI to evaluate the level of health concern for a specific area. ZigBee and ARIMA prediction model uses a novel technique to do data aggregation in order to tackle the challenge of power consumption minimization in WSN. We have named this novel technique as Recursive Converging

Quartiles. It also uses quartiles to summarize a list of readings of any length to just three values. This highly reduces the amount of data to be transmitted to the sink, thus reducing the transmission energy required and at the same time representing the original values accurately. Another strength of ZigBee and ARIMA prediction model is the high quality of results it produces. The collected readings are saved in a database and these can be accessed individually in a table or summarized area wise in a line graph. The table uses the AQI to provide the results using the associated colors' and it also provided the level of health concern for a particular area. The line graph allows the user to view the trend of air pollution for several areas at a time ZigBee and ARIMA prediction model also displays a map of the town of Port Louis, showing the locations of the deployed sensors nodes and the readings collected by each one. Thus, ZigBee and ARIMA prediction model is very flexible, very easy and yet very powerful due to its ability to provide highly summarized results as well as fine-grain results at the level of sensors.

REFERENCES

[1] H. Karl and A. Willig, Protocols and Architectures for Wireless Sensor Networks, John Wiley and Sons Ltd, The Atrium, Southern Gate, Chichester, West Sussex, England, 2005.

[2] D. Culler, D. Estrin, and M. Srivastava, "Overview of Sensor Networks", *IEEE Computer*, August 2004.

[3] K. Martinez, J. K. Hart, and R. Ong, "Environmental sensor networks", *IEEE Computer Journal*, Vol. 37 (8), 50-56, August 2004.

[4] A. Mainwaring, D. Culler, J. Polastre, R. Szewczyk, and J. Anderson, "Wireless sensor networks for habitat monitoring", Proceedings of the 1st ACM International workshop on Wireless sensor networks and applications, Atlanta, Georgia, USA, 88-97, 2002.

[5] I. F. Akyildiz, D. Pompili and T. Melodia, "Underwater acoustic sensor networks: research challenges", *Ad Hoc Networks*, Vol. 3 (3), 257-279, May 2005.

[6] Y. Ma, M. Richards, M. Ghanem, Y. Guo and J. Hassard, "Air Pollution Monitoring and Mining Based on Sensor Grid in London", *Sensors 2008*, Vol. 8(6), 3601-3623.

[7] G. Hassard , M. Ghanem , Y. Guo , J. Hassard , M. Osmond , and M. Richards, "Sensor Grids For Air Pollution Monitoring", in the Proceedings of 3rd UK e-Science All Hands Meeting, 2004.

[8] I. Khemapech, I. Duncan, and A. Miller, "A survey of wireless sensor networks technology," in PGNET, In the Proceedings of the 6th Annual Postgraduate Symposium on the Convergence of Telecommunications, Networking & Broadcasting , Liverpool, UK, EPSRC, June 2005.

[9] B. Warneke and K.S.J. Pister, "MEMS for Distributed Wireless Sensor Networks," 9th International Conference on Electronics, Circuits and Systems, Croatia, September 2002.

[10] B. Son, Y. Her, J. Kim, "A design and implementation of forest-fires surveillance system based on wireless sensor networks for South Korea mountains", *International Journal of Computer Scienceand Network Security (IJCSNS)*, 6, 9, 124–130, 2006.

Comparative Analysis of Mathematical Model and Software Investigation on Emission of Bio-Diesel in Internal Combustion Engine

P. C. Mukesh Kumar*
Department of Mechanical Engineering,
University College of Engineering Dindugul,
Tamil Nadu, India.

M. Vijayakumar
Department of Mechanical Engineering,
Centre for Thermal and Energy Research,
M. Kumarasamy College of Enginerring,
Karur-639113, Tamil Nadu, India.

***Abstract*–Major problem faced by the entire world is depletion of energy source and increasing energy demand. Due to reduction of energy source an alternate way have to be found to accommodate the energy demand. One of the best ways to accommodate this energy gap is Bio-Diesel. There are numerous Bio Diesel has been founded until now, all the Bio Diesel blends have to be run on engine and emission analysis been done using large amount of manpower and time. This work suggested a mathematical model for emission parameters like CO, CO_2, HC, NO_x, and smoke. These mathematical models are checked for fidelity criteria's. Moreover, comparative analysis of mathematical model on emission of bio-diesel in internal combustion engine has been done with Software generated (MINITAB) model and found that the mathematical model is predicting the values correctly at all part loads and software generated model predicts for MCR load by the fidelity criteria Average Percentage Deviation (APD).**

Keywords: Bio-diesel; Minitab; regression; method of least squares; emission.

I. INTRODUCTION

World transport growth fuel consumption rate is increasing every year. At the same time fuel availability decreases due to continuous extraction of oil from well. Biofuel is a one of the solutions for the future fuel demands. Most of the researchers concentrate to extract the bio fuel from vegetables. The major drawback of biofuel research is the volume of oil collection. Whereas inIndian biodiesel research from nonedible oil source like Jatropha and Karanja for internal combustion engine powered by diesel fuel. The non edible biodiesel production in india is more than 20 million tons in an year. [1-3].Vivek and AK Gupta, FangruiMaa and Milford detail mentioned about Karanja oil extraction of oil from seeds and transesterification oil (biodiesel production) is a major process and lengthy process in bidiesel research [4-5].

Chen Zheng analyzed the data by using mathematical model and artificial neural networks. Minitab software analysis mainly analyzeddiesel engine parameters [6]. Win et al. analyzed diesel engine diesel engine working parameters like noise, emission and fuel consumption by using mintab software[7]. Ganapathy et al analyzed various engine design datas like operation and combustion parameters[8]. Anand and Karthikeyan analyzed the engine parameters such as efficiency and combustion [9]. R.Ganapathy and P. Gakkharreported the optimized injection parameters and exhaust gas recirculation method in the diesel engine [10].In this paper mathematical model for investigating on emission of biodiesel in internal combustion engine is proposed. It is also compared with the experimental data and the minitab software data.

II. EXPERIMENTAL ANALYSIS

A. *Experimental Setup*

The engine used in this work is Kirloskar made, four-stroke, single cylinder, direct-injection, water-cooled, constant speed (1500 rpm), and naturally aspirated VCR engine. Engine cylinder a bore of 87 mm and stroke of 110 mm; the compression ratio of 15:1 to 18:1 and the manufacturer's recommended injection timing and injection pressure of 23^{o}crank angle before TDC and 210 bar, respectively. The combustion chamber is direct injection type with a bowl-in piston design. This work has been done with single compression ratio of 17:1. Figure 1 shows the engine setup.

B. *Data Acquisition System*

The cylinder pressure at each crank angle is measured and stored by a digital data acquisition system. It consists of a Kistler water-cooled flush mounted piezoelectric pressure transducer in conjunction with Kistler charge amplifier for converting the electric charge into voltage. It could measure and store up to 200 cycles engine pressure histories. The measured data can be analyzed online or stored for post – processing.The test shown in fig 1.

III. MATHEMATICAL INVESTIGATION

The simulation or optimization of a thermal system is the first step of modeling the characteristics of the equipment or processes. The simulation and optimization operations always use the data in an equation form. The conversion of experimental data into equation form is called mathematical modeling. Engineers may have a variety of reasons for wanting to develop equations, but the crucial one in the design of thermal systems are,

i. To facilitate the process of system simulation

ii. To develop a mathematical statement for optimization.

Fig 1.Experimental setup

A. *Criteria for Fidelity of Representation*

In order to measure the effectiveness of this proposed mathematical model, the mathematical fitting needs the constant, co-efficient and criteria for the closeness of the mathematical model. In this work criteria are,

- Sum of deviations squared (SDS).
- Average Percent Absolute Deviation (APD).
- Goodness of Fit (GOF).[11]

SDS criteria is estimated by the following equation

$$SDS = \sum_{i=1}^{n}(y_i - Y_i)^2 \quad (1.1)$$

APD criteria is estimated by the following equation

$$APD = \frac{n}{100}\sum_{i=1}^{n}\sqrt{\left(\frac{Y_i - y_i}{Y_i}\right)^2} \quad (1.2)$$

The third criterion GOF is estimated by the following equation

$$\text{GOF}, \% = 100\left(1 - \frac{\text{SDS}}{\text{G}}\right)^{0.5} \quad (1.3)$$

Where G= sum of the squares of the deviations of Y_i from the mean value of Y.

$$G = \sum_{i=1}^{n}(y_i - Y_{mean})^2 \quad (1.4)$$

Various Mathematical Models:

There are various types of equations available;

- Polynomials
- Polynomials with negative exponents
- Exponential Equations
- Gompretz Equation
- Combination Forms

Two methods of solving the equations;

- Method Of Least Squares
- Lagrange Interpolation

In this work, the "method of least squares" is used.

B. *Minitab Software*

Minitab is statistical software used by industrial experts for statistical data analysis. Minitab can also be used as a optimization tool in four designs (Factorial, Response surface method, mixture and Taguchi designs). It is one of the effective tools to analyze the trend of data, pattern of data and manipulate the data by creating the mathematical model.

Some of the statistical data analyses have been done by the Minitab software are ANOVA table, Regression analysis like ordinary least square, weighted least square, two stage least square, Non-linear least square, Logistic Regression and many other. In this work mathematical model developed by ordinary least square regression analysis. Minitab 14 is used to develop a mathematical model.

IV. MATHEMATICAL MODEL USING METHOD OF LEAST SQUARES

A. *Mathematical model for diesel engine emission*

The mathematical model equation for hydrocarbon is given below. Mathematical model has been developed by using cubical polynomial equation with two independent variables like load (L) and different concentration of biodiesel (D).

Mathematical Model for hydrocarbon:

$$HC = (41.45833 - 0.8 * L + 0.006354 * L^2) + (-0.055 + 0.0125 * L - 0.00014 * L^2) * D + (0.002267 - 0.0001 * L + 1.33E^{-06} * L^2) D^2 \quad (1.5)$$

Mathematical Model for carbon monoxide:

$$CO = (0.104583 - 0.00233 * L + 0.0000219 * L^2) + (-0.00133 + 0.00006 * L - 0.00000069 * L^2) * D + (0.0000157 - 0.000067 * L + 0.0000000075 * L^2) * D^2 \quad (1.6)$$

Mathematical Model for Oxides of nitrogen:

$$NO_x = (-100.333 + 11.25833 * L - 0.04708 * L^2) + (0.5475 + 0.028 * L + 0.000231 * L^2) * D + (-0.00137 - 0.00065 * L + 0.0000000833 * L^2) * D^2. \quad (1.7)$$

Mathematical Model for smoke intensity:

$$HSU = (38.9125 + 0.459167 * L - 0.00191 * L^2) + (-1.3065 + 0.0354 * L - 0.00024 * L^2) * D + (0.01072 - 0.00039 * L + 0.000003 * L^2) * D^2. \quad (1.8)$$

Mathematical Model for Carbon dioxide:

$$CO_2 = (1.89583 + 0.05583 * L - 3E-05 * L^2) + (-.003 + 0.0006 * L - 7E-06 * L^2) * D + (6.7E-05 - 9E-06 * L + 1E-07 * L^2) * D^2 \quad (1.9)$$

Mathematical Model for Oxygen:

$$O2 = (18.15542 - 0.08908 * L + 0.000191 * L^2) + (-.01108 - 4E-05 * L + 3.19E - 06 * L^2) * D + (1.63E-05 + 6.93E-06 * L - 8.7E-08 * L^2) * D^2. \quad (1.10)$$

V. MATHEMATICAL MODEL USING MINITAB SOFTWARE

Minitab software uses linear Regression method to form a mathematical model. The following are the equations are to analyze the engine emission parameters. All the pollutant equationsare generated by Minitab software.

$$NO_X = 69.48 + 6.54\ L - 1.1776\ D \quad (1.11)$$
$$SMOKE = 28.476 + 0.4912\ L - 0.1752\ D \quad (1.12)$$
$$O_2 = 17.1616 - 0.05994\ L + 0.004896\ D \quad (1.13)$$
$$CO_2 = 2.536 + 0.0444\ L - 0.00552\ D \quad (1.14)$$
$$HC = 20.34 - 0.011\ L + 0.2832\ D \quad (1.15)$$
$$CO = 0.0518 - 9e\text{-}005\ L + 0.000104\ D \quad (1.16)$$

VI. RESULTS AND DISCUSSION

Numerical study on emission is carried out by the above mentioned mathematical models (using method of least squares and regression analysis using Minitab software). The same is compared with the experimental data. The comparison is reduced to five bio diesel blends (B0, B25, B50, B75 AND B100) and five loading conditions (20%, 40%, 60%, 80% and 100%). In this work, fidelity for criteria is considered for comparison of experimental with two mathematical models by Average Percent Absolute Deviation (APD). The data have been plotted in figure 2-7. Experimental result consider as base result for both mathematical model as well as software analysis. Deviation always consider from experimental result. The variation of mathematical model APD and software analysis APD calculated and it is also clearly mentioned in graph. All the graph positive side mentioned mathematical variation and negative side mentioned software investigation values variation. Below cited the entire graphs clearly bring up the level of deviation from experimental results. The graph values which is near to zero (X axis reference line) that values very closer to experimental result.

It is clear from fig.2 that the mathematical results are very closer then the software results in most of the load. It is also seen that DAPD is nearly zero values in many load except 40%, from this result mathematical model analysis of NOx is more suitable than software analysis. It is found that average (APD) deviation between mathematical results and software results is ± 0.00813%.

Fig 3 clear indicated from fig.3 that the mathematical results are very closer then the software results in most of the load. It is found that deviation between mathematical results and software results is ± 0.00124%.It is clear from fig.4 that the mathematical results are very closer then the software results in most of the load. It is found that deviation between mathematical results and software results is ± 0.0024%.

It is clear from fig.5 that the mathematical results are very closer then the software results in most of the load. It is found that deviation between mathematical results and software results is ± 0.00524%. It is clear from fig.6 that the mathematical results are very closer then the software results in most of the load. It is found that deviation between mathematical results and software results is ± 0.01914%.

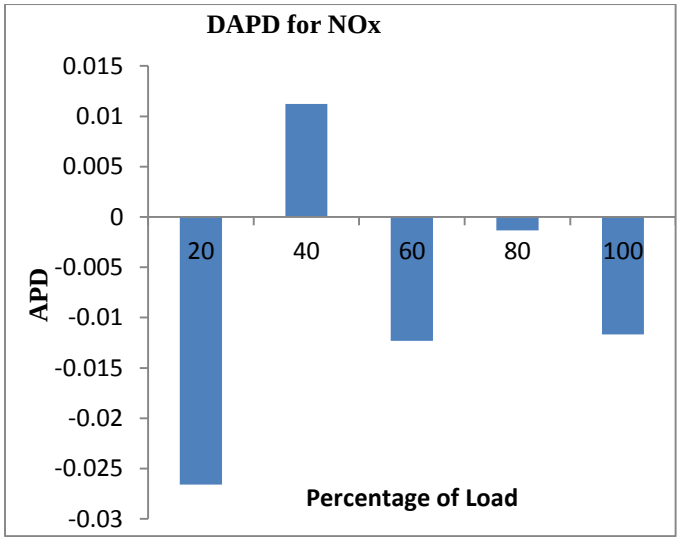

Fig 2. Mathematical and software APD difference for NO_x

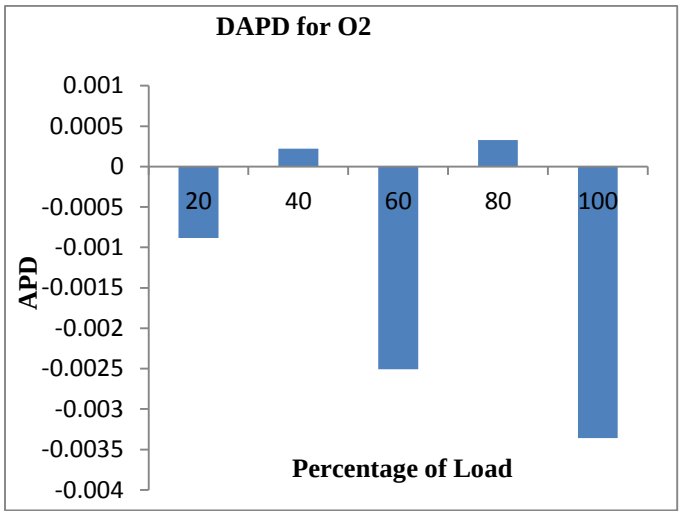

Fig3. Mathematical and software APD difference for O_2

It is clear from fig.7 that the mathematical results are very closer then the software results in most of the load. It is found that deviation between mathematical results and software results is ± 0.00186%.

It is found that the average percentage deviation for manual mathematical model is lesser than the Minitab software generated model. It is because of, the Minitab software consider the equation for mathematical model is of polynomials of Single order equation, but the manual mathematical model considered in this work is polynomials of third order equation. Therefore the error has been squared in manual mathematical model than the software model.

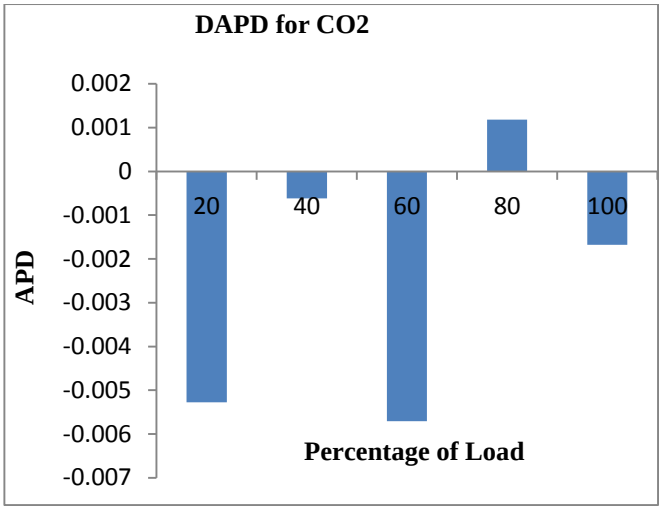

Fig4. Mathematical and software APD difference for CO_2

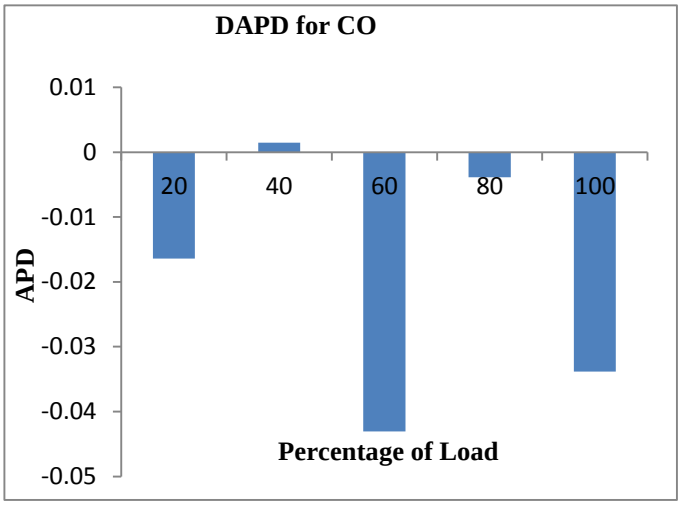

Fig 6. Mathematical and software APD difference for CO

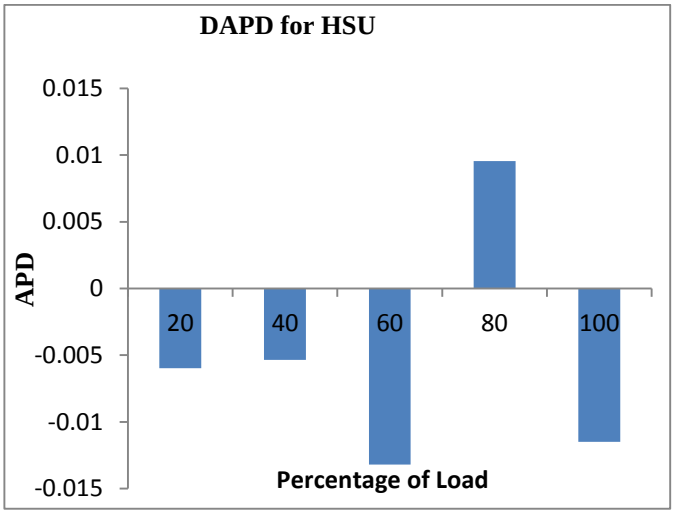

Fig 5. Mathematical and software APD difference for Smoke

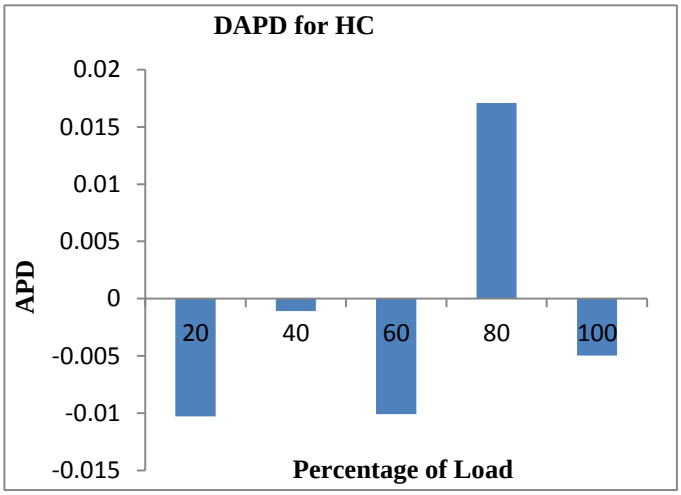

Fig 7. Mathematical and software APD difference for HC

VII. CONCLUSION

In this work, comparative analysis of mathematical model and software investigation on emission of bio-diesel in internal combustion engine is proposed. The following are the conclusion of the proposed work.

1. Mathematical model is found to be more suitable for NOx analysis at 20%, 60%, 80% and 100% loads, and manual mathematical model found to be accurate than the software generated mathematical model.
2. It is studied that the CO analysis 40% load gives very closer to experimental result compare with software result.
3. The MCR (Maximum Continues Rating) i.e., the 80% load for HSU, CO_2, HC produced maximum variation in the mathematical model than software results. Therefore the software generated mathematical model is found to be accurate for HSU, CO_2, HC at 80% load.
4. It is also found that the O_2, two loads (40% and 80%) produced minimum variation in mathematical model. At the same time three loads (20%, 60% and 100%) produced maximum variation in software analysis
5. It is concluded that the Mathematical model seems to be accurate at many load and maximum pollutant analysis in internal combustion engine. Therefore, Mathematical model more suitable for internal combustion engine emission analysis compare with software analysis.

NOMENCLATURE

D	Percentage of diesel
L	Percentage of load
HC	Hydrocarbon
CO	Carbon monoxide
CO_2	Carbon dioxide
O_2	Oxygen
NO_x	Oxides of nitrogen
SDS	Sum of deviations squared
APD	Average Percent Absolute Deviation
DAPD	Difference of mathematical and software APD
GOF	Goodness of Fit
y_i	value of the dependent variable computed from the equation.

Y_i value of the dependent variable computed from simulated.
n Total number of data points.
MR Mathematical Result
ER Experimental Result

REFERENCE

[1] Joshi, H. C. (2003). "Biodiesel from Jatropha—An alternative fuel for the future." Scientific research magazine, National Research Development Corporation, New Delhi, 205–216.
[2] Hiremath, R. B., and Kumar, B. (2012). "Low-cost bioenergy options for rural India." J. Energy Eng., 10.1061/ (ASCE) ME. 1943-5479.0000072, 70–80.
[3] Anand, K., Sharma, R. P., and Mehta, P. S. (2009). "Experimental investigation on combustion of jatrophamethylester in a turbocharged direct-injection diesel engine." J. Automob. Eng., 222(10), 1865–1877.
[4] Vivek and AK Gupta, "Biodiesel production from Karanja oil". Journal of scientific and industrial research, vol.63, jan 2014, pp 39-47s
[5] FangruiMaa and Milford, "Biodiesel production: a review", Bioresource Technology, vol 70, 1999 pp 1-15.
[6] Chen Zheng, He Ping & Chen Yan (1999) "A mathematical model using artificial neural networks to forecast shares tendency" Applied Mathematics and Computation 99 (1999) 71-76
[7] Win, Z., Gakkhar, R. P., Jain, S. C., and Bhattacharya, M. (2005). "Investigation of diesel engine operating and injection system parameters for low noise, emissions and fuel consumption using Taguchi methods." J. Automob. Eng., 219(10), 1237–1251.
[8] .Ganapathy, T., Murugesan, K., and Gakkhar, R. P. (2009). "Performance optimization of Jatropha biodiesel engine model using Taguchi approach." Appl. Energy, 86(11), 2476–2486.
[9] Anand, G., and Karthikeyan, B. (2005). "An investigation and engine parameters optimization of a spark ignition engine with gaseous fuels." Proc., 4th Dessau Gas Engine Conf., WTZ RoBlau, Germany.
[10] Ganapathy, T., Gakkhar, R. P., and Murugesan, K. (2011). "Influence of injection timing on performance, combustion and emission characteristics of Jatropha biodiesel engine." Appl. Energ., 88(12), 4376–4386.
[11] Stoecker W. F., Design of Thermal Systems, McGraw Hill Edition, 1989.

Design and Simulation of Dual Frequency Circularly Polarized Shared Aperture Antenna Array

E. Samuel John Antony*
Department of ECE,
University College of Engineering Pattukkottai,
Thanjavur, Tamil Nadu, India.

A. Thenmozhi
Department of ECE,
Thiagarajar College of Engineering,
Madurai, tamil Nadu, India.

***Abstract*—This paper discusses the 2×2 array of Aperture Coupled Microstrip Antenna (ACMA). That generates orthogonal circularly polarized waves at two different frequencies in a simultaneously. This array of antennas can be used as a communication tool in satellite internet (VSAT) and wireless applications. Sequential rotation technique was applied to create dual frequency. The technique was verified in a 2×2 array of aperture coupled microstrip antennas with frequency of operation at 4GHZ and 6GHZ . Simulation result shows that the return loss is -35 dB. For both the low band and high band mode of operation. The isolation between the two modes is around --30dB.**

Keywords— Aperture Coupled Microstrip Antennas (ACMAs); dual frequency; very small aperture terminal; shared aperture.

I. INTRODUCTION

In modern days of communication, several satellite communication application like TV and internet access (like VSAT) make use of the compact shared aperture dual frequency array with specific polarization features and provides isolation between two modes of operation. Very Small Aperture Terminals(VSAT)[1].It is used for the reliable transmission of data or voice via satellite with maximum speed reaching 2Mbps.

VSAT equipment consists 2 units,

1. Outdoors for a line of sight to the satellite.

2. Indoor to interface with the user's communications device (e.g.dataterminal equipment).

A shared aperture reduces size, weight and cost. It helps to improve the performance in focal-plane arrays since the phase centers for both frequencies are at the same location. Antenna aperture can be reused for transmitting (6GHZ) and receiving (4GHZ) data. Electronic beam scanning over a limited scan range requirement was fulfilled in this array of microstrip antennas. The antenna is required to generate circular polarization with excellent receive (Rx) versus transmit (Tx) isolation. Some recent papers have reported on shared apertures for dual polarization and dual frequency. The antenna for the low band and high band operation are used and are integrated into each other.

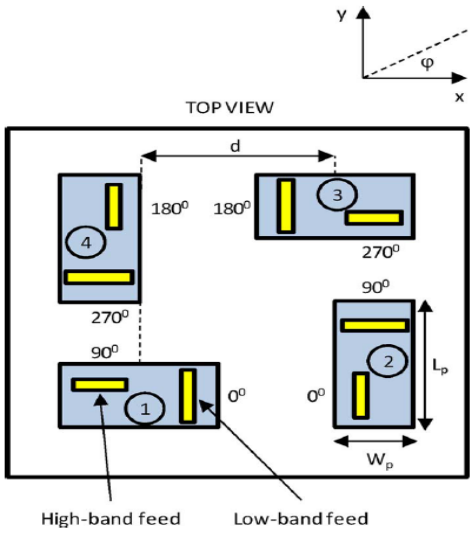

Figure.1 Shared aperture antenna array

In order to avoid grating lobes, the element spacing for the low frequency operation is chosen different from the element spacing for the high frequency band. This concept typically lack ease of manufacturing and have limitations with respect to aperture and cross polarization levels. In this study we explore a concept in which the antennas physically "share" the same aperture for the low band and high band mode of operation. The most elegant way to create circular polarization (CP) with linearly polarized (LP) elements in an array by using the sequential rotation technique as introduced by Huang, An extension of this technique in a 2×2 array for dual frequency operation with circular polarization[2]-[6]. The specifications of the antenna are:

1. Circular polarization of low band and high band with separation in the frequency.

2. Isolation between lower and higher frequency bands. It will eliminate the need of using a filter.

3. Compact aperture-reflector for both frequencies benefit from a compact shared aperture.

II. DUAL BAND SHARED APERTURE ARRAY USING THE SEQUENTIAL ROTATION TECHNIQUE

Circular Polarization (CP) can be achieved by applying proper phase shifts to the sequentially rotated Linearly Polarized (LP) antenna elements. This idea was extended in this 2x2 prototype array which is a part of larger array[8]. The configuration of Figure.1 generates Right Hand Circular (RHC) Polarization at low band operation and Left Hand Circular (LHC) Polarization at high band operation. Each patch is fed by two microstrip lines that are coupled via slot apertures in the ground plane. In sequential rotation technique each patch is placed at different angles to create circular polarization. One of the main drawbacks of sequential rotation with linear polarized elements is that relative high side lobes of cross polarization may appear in the diagonal plane. This effect depends on the element spacing d, So it is also taken into account for design.

III. ARRAY DESIGN AND EVALUATION

The proposed shared aperture antenna uses 4GHz for low band and 6GHz for high band operation. The prototype is designed in order to scale upto higher frequencies of 20/30 GHz in future. In order to introduce the phase shifts, the Wilkinson Power dividers and delay lines were used in the array. The prototype demonstrates the concept only for broadside scan. The beamforming networks contains the phase shifters that generate the required phases for creating RHC polarization for low-band operation and LHC polarization for high-band operation . The radiating element is a rectangular microstrip patch antenna, of which the length L_P is approximately $\lambda/2$ at the lower frequency band and the width W_p is approximately $\lambda/2$ at the higher frequency band, where λ is the effective wavelength of the substrate on which the patch is printed and a single element is shown in Figure.2[9]-[10]. Each patch is fed by two microstrip lines that are coupled to the patch via slot apertures in the ground plane. In this way, each of the elements can operate in two frequency bands. This particular choice increases the isolation between lower and upper band[11]. The element spacing of d=35mm in the array avoids the grating lobes in both frequency bands. The low band and high-band signals are each connected to a feed network consisting of delay lines and three 1:2 Wilkinson power dividers and the array was optimized[12]. The main advantages of the configuration of Figure.1 as compared to conventional solutions are its simplicity, compactness, and the fact that mutual coupling between the elements is reduced.

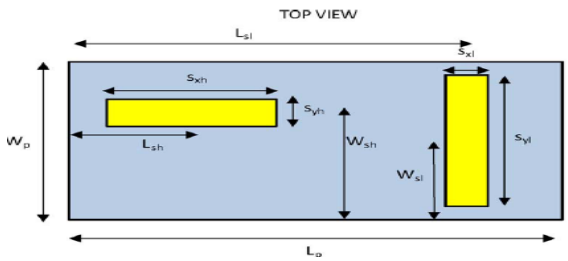

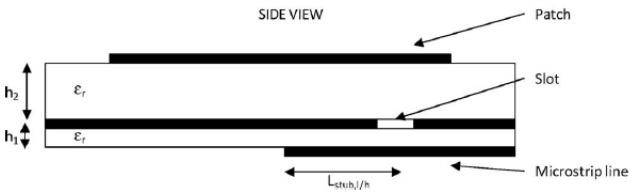

Figure. 2 Single element of an array

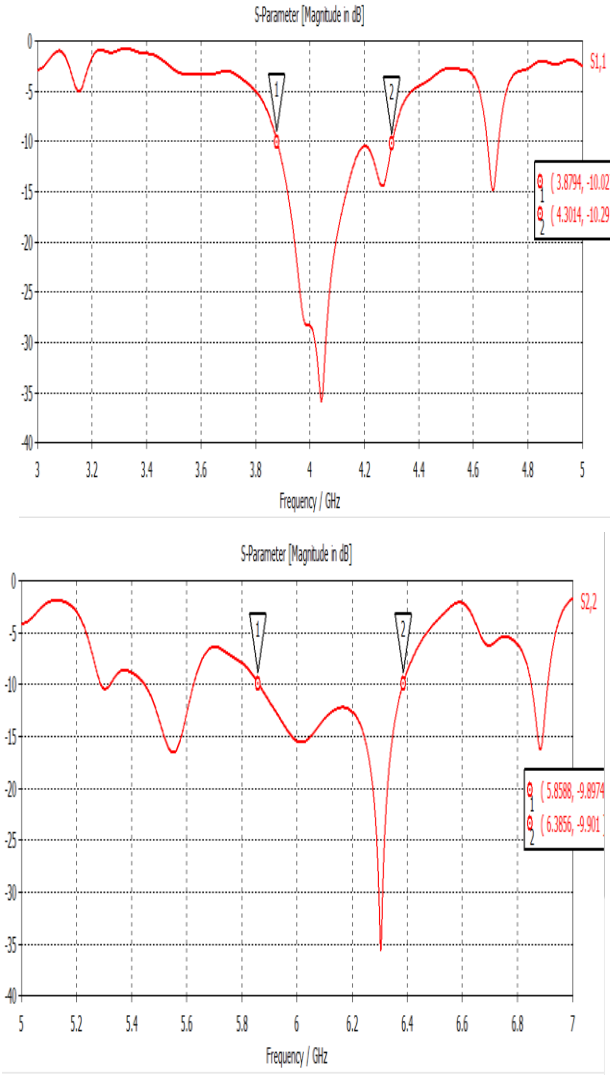

Figure. 3 Return loss of an array

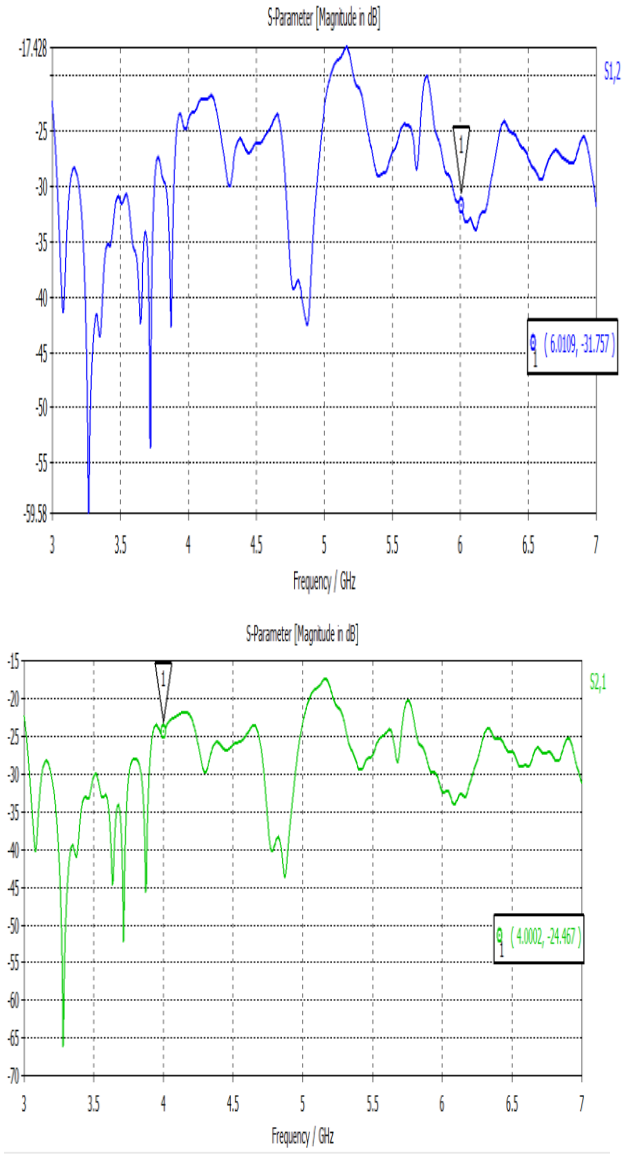

Figure. 4 Isolation of an array

As a first step in the evaluation of the prototype, the return loss of the 2x2 array with 4-GHz and 6-GHz feed network was simulated and the results was measured using the Computer Simulation Technology (CST) software[13]. The simulation results is shown in Figure.3 for the low and high-band mode of operation. The return loss for both high band and low band in the array was found to be-35dB. Secondly, The isolation is measured between the antenna elements for both the high band and low band ports,it is shown in Figure.4 and its found to be around -30dB. The emphasis is not done on the gain,since the array is a prototype and the gain for this array in both bands is 9dBi.

IV. CONCLUSION

In this paper, a shared aperture antenna array was designed that operates at two frequency bands simultaneously and generates orthogonal circular polarization. A novel implementation of the sequential rotation technique provides excellent circular polarization properties of a 2x2 array of dual-frequency ACMAs. The concept was demonstrated with a prototype consisting of a 2x2 sub array of ACMA radiators and the low-band and high-band feed networks. The isolation between both bands is larger than 26 dB, eliminating the need of high-performance duplexers in the overall system ACMA radiators and the low-band and high-band feed Networks. The return loss of both the bands is about- 35dB and it is satisfactory. Further improvement is done by using Electromagnetic Band Gap (EBG) structures or by using electronic phase shifters which can enable in beam scan.

REFERENCES

[1] J. Dell, “The maritime market: VSAT rules,” SatMagazine, vol. 6, no.8, pp. 30–34, Dec. 2008.

[2] D. M. Pozar and S. D. Targonski, “A shared-aperture dual-band dualpolarizedmicrostrip array,” IEEE Trans. Antennas Propag., vol. 49,no. 2, pp. 150–157, Feb. 2001.

[3]] M. Meng, F. Zhang, X.Ding, K. Ding, and L. Li, “Design of a sharedaperture dual-band dual- polarized microstrip antenna,” in IEEE AP Symp. Dig., 2009, pp. 680–683.

[4] S. Chakrabarti, “Development of shared aperture dual polarized microstrip antenna at L-band,” IEEE Trans. Antennas Propag., vol. 59,no. 1, pp. 294–296, Jan. 2011.

[5] J. Granholm and N. Skou, “Dual-frequency, dual-polarization microstrip antenna development for high-resolution, airborne SAR,” in Proc. Asia–Pacific Microw. Conf., 2000, pp. 17–20.

[6] J. Huang, “A technique for an array to generate circular polarization with linearly polarized elements,” IEEE Trans. Antennas Propag., vol. AP-34, no. 9, pp. 1113–1124, Sep. 1986.

[7] P. S.Hall, J. Huang, E. Rammos, and A. Roederer, “Gain of circularly polarized arrays composed of linearly polarized elements,” Electron.Lett., vol. 25, no. 2, pp. 124–125, 1989.

[8] P. S. Hall, “Application of sequential feeding to wide bandwidth, circularly polarized microstrip patch arrays,” Proc. Inst. Elect. Eng., vol. 136, pt. H, pp. 390–398, May 1989.

[9] D. M. Pozar, “Microstrip antenna aperture coupled to a microstrip line,” Electron. Lett., vol. 21, pp. 49–50, Jan. 1985.

[10] F.Corq and A. Papiernik, “Large bandwidth aperture coupled microstrip antennas,” Electron. Lett., vol. 26, pp. 1293–1294, Aug. 1990.

[11] C. H. Tsao, Y. M. Hwang, F. Killburg, and F. Dietrich, “Aperture coupled patch antennas with wide bandwidth and dual polarization capabilities,”in IEEE AP Symp. Dig., Jun. 1988, pp. 936–939.

[12] M.Edimo, A. Sharaiha, and C. Terret, “Optimized feeding of dualpolarized broadband aperture coupled printed antenna,” Electron. Lett., vol. 28, pp. 1785–1787, Sep. 1992.

[13] Computer Simulation Technology (CST) software version 2010.

Detection of Toxic Gases using Arduino and GSM Network

T. Siddharthan*
Department of Control &Instrumentation,
Valliammai Engineering College,
Chennai-603203, Tamil Nadu, India.

S. M. Kasiraj
Department of Control &Instrumentation,
Valliammai Engineering College,
Chennai-603203, Tamil Nadu, India.

***Abstract* -The main objective of this project is to detect the toxic gases while cleaning the drainage. During the cleaning process the toxic gases like nitrogen oxide, carbon monoxide and other gases are emitted. It can be detected by different sensors and indicated to alert the users and also a warning message is send to the base station to make the safety measures to the workers from the effect of toxic gases. Hence the system will help to solve the problem while cleaning the drainage.**

Keywords: CO,CH4,GSM

I. INTRODUCTION

A. CAUSES OF TOXIC GASES:

The increase in the development of technology and the human race, we failed to take care about the surroundings in which we live in. Thus we polluted the environment and thereby reducing the quality of the place we live. Even though there are several aspects of pollution such as soil, air and water pollution, out of these air pollution acts as the serious aspect as the other can detected visually and by taste, but the polluted air cannot be detected as it can be odorless, tasteless and colorless. Hence there is a growing demand for the environmental pollution monitoring and control systems. In the view of the ever-increasing pollution sources with toxic chemicals, these systems should have the facilities to detect and quantify the sources rapidly. Toxic gases are one that causes serious health impacts, but are also used in industries in large quantities. These gases have to be monitored; such that increase in the normal level of them could be known and proper precaution measures can be taken. But the current systems available are not so portable and are costly and difficult to implement. Hazardous gases refer to all kinds of gas that can be potential harmful to humans in certain concentrations. The major harmful gases such as CO2, NO2, SO2, CO that evolve from the drainage not only effect the environment but also the natural habitat. The various impacts are environmental impacts, human health impacts and economic impacts. The environmental impacts include, Overall average annual temperatures are expected to increase and Global warming will decrease snow, sea ice and glacier coverage, resulting in rising sea levels and increased coastal flooding.

B. EFFECTS OF TOXIC GAS:

City municipal sewer is one of the city's critical infrastructure, due to it is relatively closed, environment specific, easy to produce large amounts of toxic, hazardous, flammable and explosive gases. If it is in poor management, when hazardous gas leak, there is likely to cause gas accumulation, at last, fire or explosion occurred. In recent years, Chongqing, Nanjing, Wuhan and other places have occurred such serious explosion of City municipal sewer. Sanitation workers suffered gas poisoning incidents have also occurred; It is harmful to people's personal and property safety seriously. With the development of city size and people to enhance environmental awareness, concerns and input of municipal government and community in on-site of the environment is growing, the establishment of an effective monitoring and warning system of municipal sewer is not only an important part of the urban environment, but also imperative requirement of modernization of municipal facilities. Using GPS wireless communication technology, combined with high-performance infrared gas sensor, to design the program for the signal send back to the remote monitoring centre based on the signal processing system and wireless network sensors, the monitoring centres in different position use GPS technology to monitor the municipal sewer pipe to achieve continuous and automatic monitoring for sewer combustible gas in all-weather and alert the users.

II. BASIC WORKING PRINCIPLE

A. TOXIC GAS DETECTION

The toxic gases like carbon monoxide, methane, hydrogen sulphide which is emitted from the drainage wastes. While cleaning the drainage these gases are emitted. The emitted gases are inhaled by the workers in drainage cleaning and it causes a major health effects. The effects like skin allergies, nervous system blockage, aphysixation etc. These toxic gases which give these effects based on their concentration in drainage wastes. If the gas concentration are more than the threshold value it may cause to death also. Hence these gases are sensed by the different sensors and it should be given to the microcontroller to alert the workers by alarm indication. If the sensor value is greater than the threshold value the microcontroller gives the signal to alarm to indicate the warning to labours. This system will help to keep the workers from the effect of toxic gases.

B. GAS DETECTOR

A gas detector is a device that detects the presence of gases in an area, often as part of a safety system. This type of equipment is used to detect a gas leak and interface with a control system so a process can be automatically shut down. A gas detector can sound an alarm to operators in the area where the leak is occurring, giving them the opportunity to

leave. This type of device is important because there are many gases that can be harmful to organic life, such as humans or animals. Gas detectors can be used to detect combustible, flammable and toxic gases, and oxygen depletion. This type of device is used widely in industry and can be found in locations, such as on oil rigs, to monitor manufacture processes and emerging technologies such as photovoltaic. They may be used in firefighting. Gas leak detection is the process of identifying potentially hazardous gas leaks by sensors. These sensors usually employ an audible alarm to alert people when a dangerous gas has been detected. Common sensors include infrared point sensors, ultrasonic sensors, electrochemical gas sensors, and semiconductor sensors.

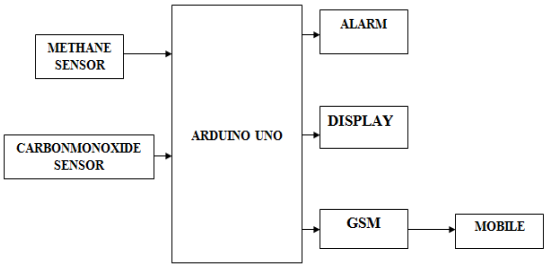

Figure 1. Basic block diagram

III. HARDWARE DESIGN

The toxic gas detection part includes the different hardware setup in it. It consists of arduino setup, methane sensor, carbon monoxide sensor, LCD display, alarm and it can be shown in Figure no.1. The system includes the toxic gas sensors like carbon monoxide and methane. These sensors sense the gases while cleaning the drainage. The sensed values are given to the analog ports of microcontroller which is placed in the arduino board. The microcontroller compares the sensor value to the threshold value of each sensor which is programmed in the microcontroller. If the sensor value exceeds the threshold value the microcontrollers sends the signal to the alarm also sends the message to base station through GPS module and display the value in the LCD display. This will alert the workers to get out from the place.

A. Methane sensor

Methane is commonly generated when organic matter is decomposed by a variety of bacterial processes. It is a colourless, extremely flammable and explosive gas that can cause fire and explosion. The accumulation of methane in a poorly ventilated area will displace normal air and result in an oxygen deficient environment. The methane gas can be sensed by the MQ 4 type sensor. Sensitive material of MQ-4 gas sensor is SnO2, which with lower conductivity in clean air. When the target combustible gas exist, The sensor's conductivity is more higher along with the gas concentration rising. Please use simple electro circuit, convert change of conductivity to correspond output signal of gas concentration.MQ-4 gas sensor has high sensivity to Methane, also to Propane and Butane. The sensor could be used to detect different combustible gas, especially Methane; it is with low cost and suitable for different application. Its characteristics include good sensitivity to Combustible gas in wide range, high sensitivity to natural gas, long life and low cost, simple drive circuit.

B. Carbon Monoxide sensor

The lethal colourless and odourless gas – carbon monoxide, is given off when charcoal is burnt in poorly ventilated areas. Similarly, it is produced when gasoline/diesel generators or other fuel-driven tools are used in inadequately ventilated workplaces. Exposure to carbon monoxide at concentrations over350 ppm can cause confusion, fainting on exertion and collapse. An airborne concentration of carbon monoxide above 1,200 ppm is immediately dangerous to life or health.This sensor which belongs to the type MQ-7 . Sensitive material of MQ-7gas sensor is SnO2, which with lower conductivity in clean air. It make detection by method of cycle high and low temperature, and detect CO at low temperature(heated by 1.5V).The sensor's conductivity gets higher along with the CO gas concentration rising. At high temperature (heated by 5.0V),it cleans the other gases adsorbed at low temperature. Users can convert the change of conductivity to correspond output signal of gas concentration through a simple circuit. It has good sensitivity to carbon monoxide in wide range, and has advantages such as long lifespan, low cost and simple drive circuit &etc. It is widely used in domestic CO gas leakage alarm, industrial CO gas alarm and portable CO gas detector.

C. Arduino Uno

Arduino is an open-source computer hardware and software company, project and user community that designs and manufactures kits for building digital devices and interactive objects that can sense and control the physical world. Arduino boards may be purchased preassembled, or as kits; at the same time, the hardware design information is available for those who would like to assemble an Arduino from scratch. The project is based on a family of microcontroller board designs manufactured primarily by Smart Projects in Italy, and also by several other vendors, using various 8-bit Atmel AVR microcontrollers or 32-bit Atmel ARM processors. These systems provide sets of digital and analog I/O pins that can be interfaced to various extension boards and other circuits. The boards feature serial communications interfaces, including USB on some models, for loading programs from personal computers. For Programming the microcontrollers, the Arduino platform provides an integrated development environment (IDE) based on the Processing project, includes support for C and C++ programming languages. Arduino is a tool for making computers that can sense and control more of the physical world than your desktop computer. It's an open-source physical computing platform based on a simple microcontroller board, and a development environment for writing software for the board. It can be used to develop interactive objects, taking inputs from a variety of switches or sensors, and controlling a variety of lights, motors, and other physical outputs. Arduino projects can be stand-alone, or they can communicate with software running on your computer (e.g. Flash, Processing and MaxMSP). The boards can be assembled by hand or purchased pre-assembled; the open-source IDE can be downloaded for free.

D. Arduino Uno microcontroller

"Uno" means one in Italian and is named to mark the upcoming release of Arduino 1.0. The Uno and version 1.0 will be the reference versions of arduino, moving forward. The Uno is the latest in a series of USB arduino boards, and the reference model for the arduino platform. The arduino Uno microcontroller board based on the ATmega328 (datasheet). It has 14 digital input/output pins (of which 6 can be used as PWM outputs), 6analog inputs, a 16 MHz ceramic resonator, a USB connection, a power jack, an ICSP header, and a reset button. It contains everything needed to support the microcontroller. Simply connect it to a computer with a USB cable or power it with an AC-to-DC adapter or battery to get started. The Uno differs from all preceding boards in that it does not use the FTDI USB-to-serial driver chip

E. GSM

Global system for mobile communication (GSM) is a globally accepted standard for digital cellular communication. GSM is the name of a standardization group established in 1982 to create a common European mobile telephone standard that would formulate specifications for a pan-European mobile cellular radio system operating at 900 MHz It is estimated that many countries outside of Europe will join the GSM partnership. Throughout the evolution of cellular telecommunications, various systems have been developed without the benefit of standardized specifications. This presented many problems directly related to compatibility, especially with the development of digital radio technology. The GSM standard is intended to address these problems. From 1982 to 1985 discussions were held to decide between building an analog or digital system. After multiple field tests, a digital system was adopted for GSM.The next task was to decide between a narrow or broadband solution. In May 1987, the narrowband time division multiple access (TDMA)solution was chosen. GSM provides recommendations, not requirements. The GSM specifications define the functions and interface requirements in detail but do not address the hardware. The reason for this is to limit the designers as little as possible but still to make it possible for the operators to buy equipment from different suppliers. The GSM network is divided into three major systems: the switching system (SS), the base station system (BSS), and the operation and support system (OSS).

F. LCD display

LCD display is an inevitable part in almost all embedded projects and this article is about interfacing 16×2 LCD with microcontroller. Many guys find it hard to interface LCD module with the but the fact is that if you learn it properly, its a very easy job and by knowing it you can easily design embedded projects like digital voltmeter / ammeter, digital clock, home automation displays, status indicator display, digital code locks, digital speedometer/ odometer, display for music players etc etc. Thoroughly going through this article will make you able to display any text (including the extended characters) on any part of the 16×2 display screen. In order to understand the interfacing first you have to know about the 16×2 LCD module. This module is a very common type of LCD module that is used in 8051 based embedded projects. It consists of 16 rows and 2 columns of 5×7 or 5×8 LCD dot matrices. It is available in a 16 pin package with back light ,contrast adjustment function and each dot matrix has 5×8 dot resolution.

G. Threshold value

GAS	CHARACTERSTICS	MAXIMUM RANGE(ppm)	EFFECT
CH4	Colourless, odourless	>1200	DEATH
CO	Colourless, explosive	>1200	DEATH

Figure 2. Maximum Range Value

GAS	THRESHOLD VALUE GIVEN	OUTPUT VOLTAGE(v)
CH4	700	2.5 to 4.5
CO	400	2.8 to 5

Figure 3. Threshold Value

IV. SOFTWARE USED

Arduino integrated development environment (IDE) is a cross-platform application written in java, and derives from the IDE for the processing programming language and the wiring projects. it is designed to introduce programming to artists and other newcomers unfamiliar with software development. it includes a code editor with features such as syntax highlighting, brace matching, and automatic indentation, and is also capable of compiling and uploading programs to the board with a single click. a program or code written for arduino is called a "sketch".Arduino programs are written in c or c++. The arduino IDE comes with a software library called "wiring" from the original wiring project, which makes many common input/output operations much easier. Most arduino boards contain a led and a load resistor connected between the pin 13 and ground, which is a convenient feature for many simple tests.[1] the previous code would not be seen by a standard c++ compiler as a valid program, so when the user clicks the "upload to i/o board" button in the IDE, a copy of the code is written to a temporary file with an extra include header at the top and a very simple main() function at the bottom, to make it a valid c++ program. Arduino is open-source hardware: the arduino hardware reference designs are distributed under a Creative Commons Attribution Share-Alike 2.5 license and are available on the arduino Web site. Layout and production files for some versions of the arduino hardware are also available. The source code for the IDE is available and released under the GNU General Public License, version 2. Although the hardware and software designs are freely available under copy left licenses, the developers have requested that the name "arduino" be exclusive to the official product and not be used for derivative works without permission. The official policy document on the use of the arduino name emphasizes that the project is open to

incorporating work by others into the official product. Several Arduino-compatible products commercially released have avoided the "Arduino" name by using "-duino" name variants.

V. RESULTS AND DISCUSSION

In this project I successfully completed the design of the toxic gas detection .The methane sensor was sensed the gas. The carbon monoxide sensor was successfully sensed the gas .when detecting the gas by the sensor and its value was exceeded from the threshold value the alarm was indicated and it alerted successfully. When the threshold value is reached the warning message was sent successfully to the base station. The value of the sensor was displayed successfully in the LCD display. The arduino board was interfaced with the sensors and LCD display successfully. In the arduino the microcontrollers was successfully programmed for alarm indication, getting input from sensors and print the values. Hence the system was successfully designed and implemented and results were checked.

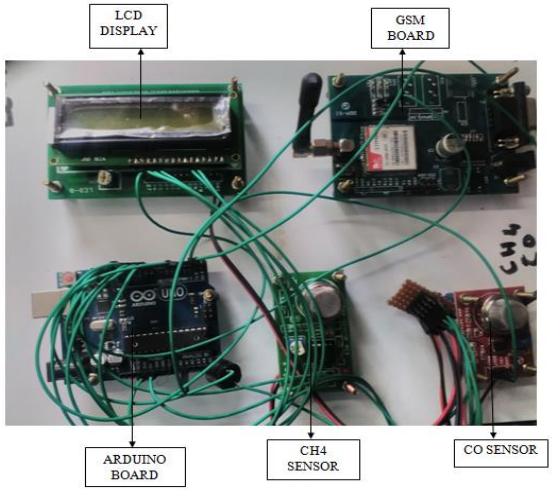

Figure 4. Overall Setup Diagram

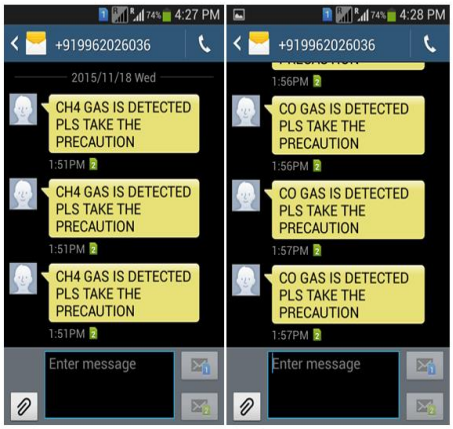

Figure 5. Mobile Output

VI. CONCLUSION

The above system helps the workers in drainage cleaning from the effect of toxic gases. The gases which can be sensed by the sensors. The sensor signal sends to the microcontroller through input ports and it should take the action by warning through the alarm indication and also sends the warning message to the registered mobile number. The signal which alert the users to make sufficient emergency actions and also get out the workers from the drainage. Hence this system will helps the labors in the sufficient manner and it protect from the deaths and reduce the manpower in drainage cleaning.

REFERENCES

[1] Ai-Ali A. R, Zualkernan I, and Aloul F, (2010) "A mobile GPRS-sensors array for air pollution monitoring", IEEE Sensors J., vol. 10, no. 10, pp. 1666–1671.

[2] Francis Tsow, Forzani E, Rai A, Wang R, Tsui R,Mastroianni S, Knobbe C, Gandolfi A. J, and Tao N. J,(2009) "A wearable and wireless sensor system for real-time monitoring of toxic environmental volatile organic compounds", IEEE Sensors J., vol. 9, no. 12, pp.1734–1740.

[3] Hui Yang, Yong Qin, Gefei Feng, and Hui Ci, (2013)"Online Monitoring of Geological CO2 Storage and Leakage Based on ireless Sensor Networks", IEEE Sensors J, Vol.13, no. 2, pp. 556–562.

[4] Gary W. Hunter, Joseph R. Stetter, Peter J. Hesketh,Chung-Chiun Liu, (2010) "Smart Sensor Systems", The Electrochemical Society Interface, pp. 29–34. environmental volatile organic compounds", IEEE Sensors J., vol. 9, no. 12, pp.1734–1740.

[5] Monika Verma, Richard Jack and Carl Fisher, (2010)"The Importance of Anion and Organic Acid Determinations in Fracking Wastewater by Ion Chromatography", Thermo Fisher Scientific, Sunnyvale, A, USA.

[6] Kularatna N and Sudantha B. H, (2008) "An environmental pollution monitoring system based on the IEEE 1451 standard for low cost requirements", IEEE Sensors J., vol. 8, no. 4, pp. 415–422.

Design and Implementation of Dual Band Aperture Coupled Antenna Array

M. Jeyaseelan*
Department of ECE,
PRIST University,
Thanjavur, Tamil Nadu, India.

A. Rijuvana Begum
Department of ECE,
PRIST University,
Thanjavur, Tamil Nadu, India.

***Abstract*—Light-weight antenna arrays require utilizing thesame antenna aperture to provide multiple functions (e.g., communications and radar) in separate frequency bands. In this paper, we present a novel antenna element design for a dual -band array, comprising interleaved printed dipoles spaced to avoid grating lobes in each band. The folded dipoles are designed to be resonant at octave -separated frequency bands (1 and 2 GHz), and inkjet- printed on photographic paper. Each dipole is gap- fed by voltage induced electromagnetically from a microstrip line on the other side of the substrate.**

Keywords— Dual band antenna; dual frequency; inkjetprinting; multifunctional antennas; nested antennas; phased array; printed dipole; shared aperture design.

I. INTRODUCTION

In aerospace communications, the planar antenna array comprising interleaved folded dipoles of two different resonant sizes, but similar shapes, sharing the same physical aperture. The array is inkjet printed on photo-graphic paper using a low-cost process [6]. Several researchers have investigated planar antennas for multiband operation, using a single feed to excite all the bands. A T-shaped planar monopole antenna with two asymmetrical horizontal strips to produce the lower and upper resonant modes is reported in [7] to cover the 2.4/5.2 GHz ISM bands. The authors in [8] present the design of a planar L -shaped monopole antenna fed by a micro strip line, which utilizes parasitic coupling between the driven elements and modes for tri-band operation. The concept of adjusting reactive coupling between parasitic and driven elements to produce dual-band operation has been used extensively inplanar patch antenna geometries, including the use of fl at-plate radiator above a ground plane with a shorted parasitic strip on the same face [9], printing two dissimilar coupled monopoles on either side of a substrate [10], and the use of slots and shorted pins on patches to produce modes with widely separated resonant frequencies [11], [12]. However, none of these design approaches are suitable for multiband array operation, because they are all based on single feed design, and depend on either shaping the radiating elements or adjusting parasitic coupling to produce multiband operation. A few design approaches exist for multi feed dual band antennas using stacked dielectric layers [13]–[15]. A micro strip patch antenna design with dual-band dual circular polarization is discussed in [13], where high-permittivity dielectric bars are inserted under the radiating edge of the patch in order to minia-turize the antenna and generate circularly polarized Ease of Use waves. Two stacked patches, one coax- fed and the other aperture-coupled, are used in [14] to produce closely spaced dual-band operation. As the two bands are tightly coupled, these designs introduce significant mutual coupling when integrated into an array. Mutual coupling between elements needs to be controlled in a shared aperture array to prevent excessive interchannel interference, and it may not be used for simultaneous tuning of the elements.

The concept of multifunctional array antennas with widely separated frequency bands, such as PCS, GSM communications bands, L, C, and X radar bands, sharing the same physical aper-ture, is a challenging problem, and has been largely unexplored [1]. The avoidance of grating lobes places an upper limit on the element spacing for each band, which in turn increases the array size for a wide scanning range. One established design approach is to utilize wideband (i.e., one band encompasses all the individual narrow bands of interest) antenna elements, such slots, with each element connected to a wideband feed [16]. Wideband elements are not convenient for electronic scanning, because a single interelement spacing, typically im-plemented at the highest frequency, will not provide a symmet-rical lobe structure over the entire frequency range of interest. In addition, the associated complexity of receiver design escalates considerably for wideband operation in a phased array system, requiring expensive, heavy and bulky front-ends to channelize signals from the wideband feed into multiple narrow frequency bands typically allocated for communications and radar. Alter-natively, an interleaved element layout can be used to accom-modate widely separated (in frequency) narrow-band channels, utilizing a different interelement spacing for each band to avoid grating lobes. A major problem in such a layout is the electro-magnetic (EM) interference between channels, which can cause undesirable cross-polarization and mutual coupling.

Considerable effort has been devoted to determine an inter-leaved element design with minimal interchannel interference. Interleaved microstrip patches for C-band operation and printed slots for X-band are used in [2] to form a shared aperture, dual-band dual -polarization (DBDP) array. Good isolation between the bands is observed because the feed networks for the two bands are separated by two dielectric layers. The bidirectional radiation pattern of the X-band slots necessitates a reflecting ground plane, increasing the thickness and weight of the an-tenna. The slots also contribute to increased cross-polarization and side-lobe levels at X-band. Instead of interleaving the ele-ments in alternate

substrates as in [2], the design in [3] utilizes a dual-band coplanar element comprising one L-band perforated patch symmetrically enclosing four C-band patches. To increase the bandwidth, stacked patches are used in both bands, with the bottom layer of patches fed by direct-coupled microstrip lines or slots, and the top layer of patches electromagnetically coupled to currents on the bottom layer patches. Considerable attention has been given to maintaining geometrical symmetry and good iso-lation of the feed lines, resulting in low cross-polarization over a scan range of 20 degrees in each principal plane. A variation of this design is implemented in [4] using proximity - coupled per-foratedmicrostrip patch elements at L-band, with X - band aper-ture coupled patches inserted below the openings of the L-band patches. However, the scan range is limited and the cross-polar-ization levels are relatively high. A novel design of DBDP mi-crostrip array, with a frequency ratio of about 1:3, is presented in [5], wherein stacked, proximity-coupled microstrip dipoles and probe- fed square patches are used as the radiating elements at S- and X-bands, respectively. The prototype array depicts mea-sured impedance bandwidth (VSWR $\leq$ 2) of 8.9% and 17%, and cross -polarization levels of 26 dB and 31 dB, for S- and X-bands, respectively.

In this paper, we present a novel antenna design for a shared aperture dual-band array, comprising interleaved printed folded dipoles resonant at octave-separated frequency bands (1 and 2 GHz), with individual feeds for each element. Similar to the design in [3], we enforce geometrical symmetry in the array configuration for low cross-polarization and interchanneliso-lation, and electromagnetically couple the dipoles to feed lines printed on the other side of the substrate. However, unlike the previous design approaches for a shared aperture array [2]–[5],

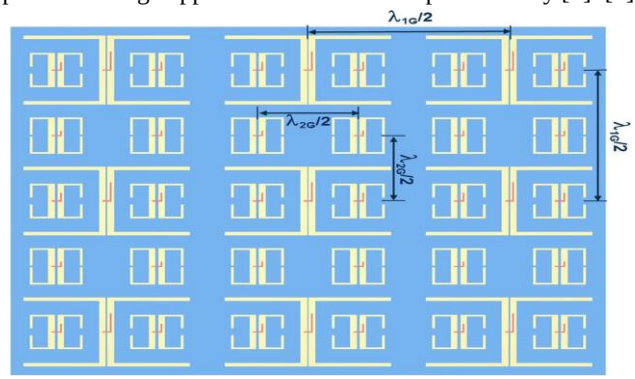

Fig. 1. Nested element dipole array with self-similar elements for dual-band operation. The wavelengths at 1 and 2 GHz are denoted as λ_{1G} and λ_{2G}, re-spectively.

we use self-similar antenna elements for direct scaling to other frequencies. Both the feed lines and antennas are printed on photographic paper (dielectric constant of 3.1) using low -cost ink-jet printing technology [17]–[20]. This nested element con-figuration has been simulated, fabricated and measured, and excellent corroboration observed between simulated and mea-sured data. Measurements on a 39-element dual-band array (9 low- band and 30 high -band) printed on paper reveal broadside gain of 12–17 dBi in both bands, with cross-polarization less than 25 dBi. This is the first practical demonstration of a large array printed on paper.

Section II introduces the layout of the dual-band array and discusses the design of self-similar nested folded dipoles. The fabrication of the antenna on photographic paper using inkjet printing is treated in Section III. Simulated and measured results of the element pattern as well as the fixed-scan broadside array pattern are discussed in Section IV, and the losses incurred by antenna fabrication on paper are addressed. The paper concludes with a brief summary in Section V.

II. ANTENNA DESIGN

The proposed antenna design involves using coplanar nested or interleaved printed dipoles to provide adequate isolation be-tween channels, as depicted in Fig. 1 for a dual-band phased array application. The folded dipoles are assumed to be resonant at 1 GHz and 2 GHz for the design reported herein, but can be scaled easily due to self-similar pattern. It is noted that channel separation at integer multiples of the fundamental frequency is necessary only if self-similarity in element shape is to be pre-served. In order to reduce the backlobe level and also to improve the impedance bandwidth, a ground plane is inserted $0.25\lambda_{2G}$ below the antenna substrate, where λ_{2G} is the wavelength at 2 GHz. In future design iterations Wideband elements are not convenient for electronic scanning, because a single interelement spacing, typically im-plemented at the highest frequency, will not provide a symmet-rical lobe structure over the entire frequency range of interest. In addition, the associated complexity of receiver design escalates considerably for wideband operation in a phased array system, requiring expensive, heavy and bulky front-ends to channelize signals from the wideband feed into multiple narrow frequency bands typically allocated for communications and radar. Alter-natively, an interleaved element layout can be used to accom-modate widely separated (in frequency) narrow-band channels, utilizing a different interelement spacing for each band to avoid grating lobes. A major problem in such a layout is the electro-magnetic (EM) interference between channels, which can cause undesirable cross-polarization and mutual coupling dipole is gap -fed by voltage induced electromagnetically from a microstrip line on the top side of the substrate (see Fig. 2). The feed line for each antenna element also includes a series stub for independently tuning its impedance. Two high-band el-ements are nested inside the low-band folded dipole, one in each leg, with a spacing of half -wavelength (at 2 GHz) to provide grating-lobe-free operation in the array environment. In order to provide identical scan performance in the orthogonal plane, a pair of high-band elements are inserted vertically half-way be-tween two low -band elements. Likewise, the low-band elements are spaced by half wavelength at 1 GHz, both horizontally and vertically. This self-similar dual- band element design and place-ment offers the capability to use the single physical aperture for multiple antenna functions, and can also be integrated with in-dependent elements (such as patches) in stacked layers if more than two bands are desired.

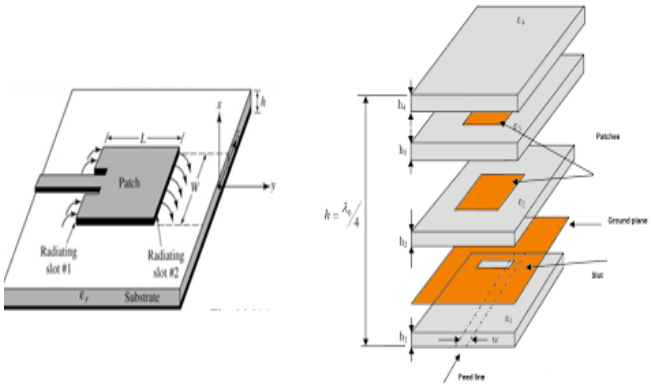

Fig. 2. Feed configuration for the dual -band element (dipole arms exaggerated in width for clarity). The ground plane is supported by a foam layer in the fab-ricated prototype.

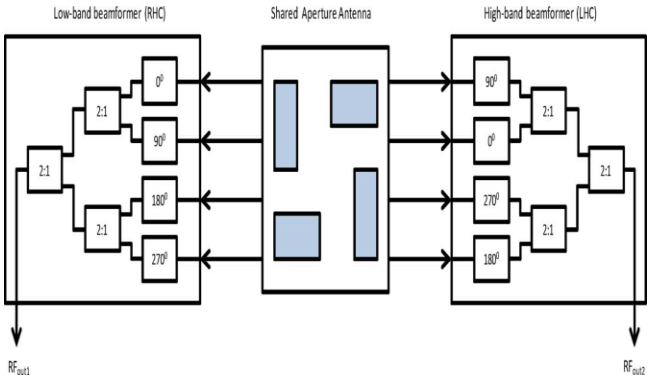

Using EM simulation software (CST Microstripes—www. cst.com), the length of each dipole in the array is optimized in an infinite array environment to tune the low-band dipole to 1 GHz and the high -band one to 2 GHz. The optimized dimensions of each dipole are shown in Fig. 3. After tuning, the mean path length of each arm of the dipole is found to be about *two-third* wavelength at the corresponding resonant frequency. Notice the difference in folding between the dipoles for each band, neces-sitated by nesting two high-band dipoles within one low-band dipole. The latter is folded only once while the former is folded twice to miniaturize within the form factor required to maintain half-wavelength spacing between the elements. The series stub on each feed line is adjustable in length for impedance matching, independently.

The substrate has the dimensions 200mm× 160 mm × 52mm, and a dielectric constant of 3.1. The ground plane reflector is of size 200 mm × 160 mm. As shown in Fig. 2, the center conductor of the coaxial feed cable is connected to the microstrip feed line, which induces by EM coupling a voltage at the gap between the two dipole arms on the other side of the substrate. One end of the cable shield is connected to an antenna arm, and the other end is terminated on the reflector. In order to minimize perturbation of antenna currents at the junction with the shield, we use SSMA connectors, with one feed per antenna. EM coupling to the dipole minimizes the feed line radiation and the associated spurious interaction between antenna elements. Since the substrate is thin, the coax-microstrip transition is pre-dominantly capacitive and can be inductively compensated by adjusting the length of the microstrip stub. The tuning of the an-tenna to its resonant frequency is controlled by symmetrically adjusting the overall length of each folded arm of the dipole.

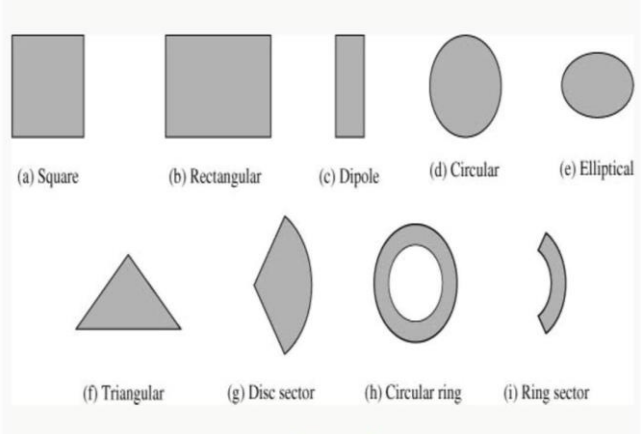

Fig. 3. Optimized dimensions (in mm) of the nested dipole geometry and the feed lines. Note the scalability in design

III. ANTENNA FABRICATION

In this work, we utilized inkjet printing of conductive inks to pattern the antennas on photographic paper sheets.

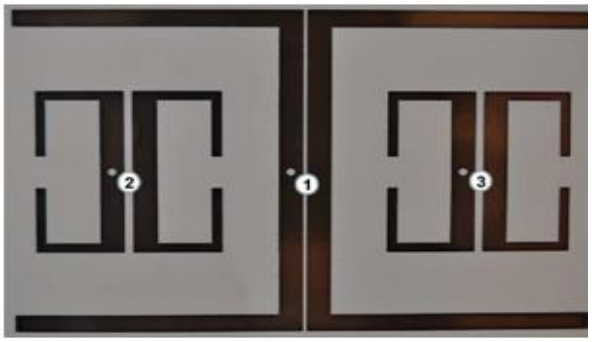

Fig. 4. Fabricated nested antenna element

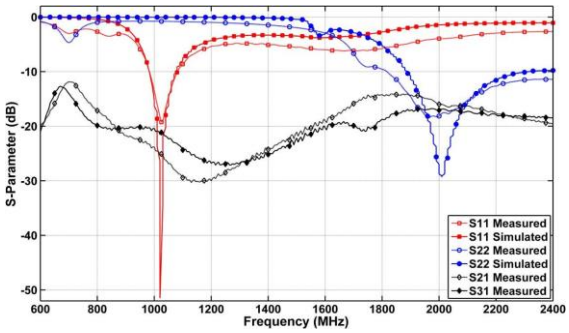

Fig. 5. Comparison between measured and simulated scattering parameters

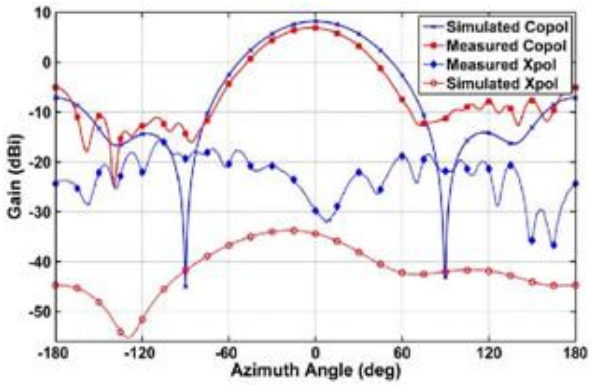

Fig. 6. Comparison of simulated and measured E-plane patterns at 1 GHz

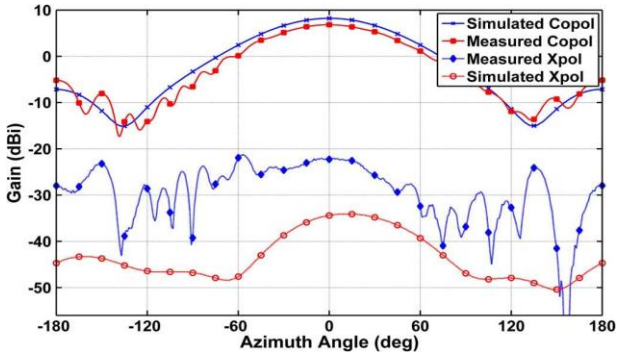

Fig. 7. Comparison of simulated and measured H-plane patterns at 1 GHz

The comparison of simulated and measured scattering param-eters is depicted in Fig. 5. The antenna elements are numbered as indicated in Fig. 4. Excellent agreement is observed between the two sets of data, with the measured return loss of the low-band (1 GHz) at 19 dB and that of the high -band (2 GHz) at 17 dB. Because the ground plane is located at a depth of quarter wave-length (at 2 GHz) below the substrate, the bandwidth of the high-band is larger than that of the low-band. The measured return loss of the two symmetrical high-band elements show similar variation with frequency, and only S22 is plotted. The measured isolation between the low-band element and either of the two high-band elements is observed to be around 17 dB around 2 GHz, and 25 dB at 1 GHz. Therefore, it is antici-pated that the interference between the two bands in an array environment will not be significant. Radiation pattern of the antenna has been measured in an ane-choic chamber at Georgia Tech Research Institute. Fig. 6 com-pares the simulated and measured E-plane patterns at 1 GHz. The measured peak gain is 7 dBi whereas the simulated direc-tivity is 8.2 dBi. Considering the losses in the element and the systematic as well as random measurement errors attributed to chamber and test equipment, which are collectively estimated as 0.5 to 1 dB, it is evident that the simulated and measured gain values are in good agreement. The measured cross-polarization is better than 30 dB relative to the main beam level. In gen-eral, the absolute measured cross-polarization levels are higher than the simulated levels because losses are not considered in the simulation, and the measurement accuracy degrades at the lower gain amplitudes.

Fig. 7 compares the simulated and measured H-plane patterns at 1 GHz. The measured peak gain is 6.9 dBi whereas the simulated directivity is 8.2 dBi. Considering the losses in the antenna and the measurement errors, it is evident that the simulated and measured gain values are in reasonable agreement. The beamwidth is broader for the H -plane pattern than the E-plane pattern. This is typical of printed dipoles because of the uneven influence of ground plane currents in the two principal planes. The measured cross-polarization over the extent of the main beam is higher in the H-plane, but still lower than 25 dB relative to the beam maximum. In summary, the agreement be-tween the simulated and measured patterns in both planes is within the measurement accuracy.

Fig. 8 compares the simulated and measured E-plane patterns of Element 2 at 2 GHz. The pattern is asymmetric for both sets of data because of mutual coupling with the other high-band ele-ment located half wavelength away along the E-plane. A similar result, showing asymmetry in the E-plane pattern, has been ob-served for Element 3. The mutual coupling between the 2 GHz dipoles is higher in the E- plane than in the H - plane, and there-fore, the pattern is much less asymmetric in the H-plane (see Fig. 9). The measured peak gain (see Fig. 8) is 6 dBi whereas the simulated directivity is 7.8 dBi. This discrepancy is larger than that in the low-band pattern in Fig. 6.

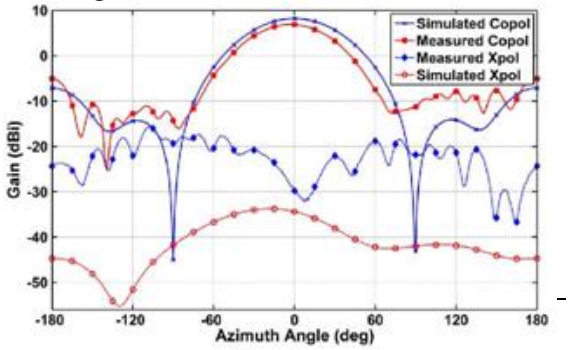

Fig. 8. Comparison of simulated and measured E-plane patterns at 2 GHz for Element 2 (Element 3 terminated)

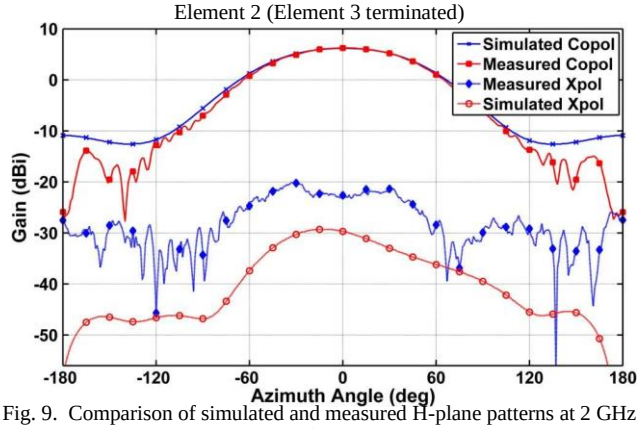

Fig. 9. Comparison of simulated and measured H-plane patterns at 2 GHz for
Element 2 (Element 3 terminated)

Agreement between measured and simulated radiation pattern data is gratifying given that the two high-band elements are sep-arated by only a half wavelength, and are completely interleaved within the low-band element.

Fig. 9 compares the simulated and measured H-plane patterns of Element 2 at 2 GHz. A similar result (not plotted) has been observed for Element 3. The measured cross-polarization ratio is better than 25 dBi and is considerably better than that in the E-plane due to lower mutual coupling. The measured peak gain is 5.3 dBi whereas the simulated directivity is 6.2 dBi. The lower cross-polarization at 2 GHz results in good agreement between the two sets of copol data.

B. Array Radiation Pattern

The array layout shown in Fig. 1 has been fabricated by ink-jet printing the pattern on 3″×4″ sections of paper and joining them using Kapton tape. The fabricated array, shown in Fig. 10, consists of 39 elements (9 1-GHz elements, 30 nested 2-GHz elements) mounted on 39 mm thick foam layer backed by an aluminum ground plane. The wooden support is only for mechanical interface with the antenna positioner. The dipole antenna elements are on the back side of the (white) paper substrate, and the microstrip feed lines, numbered sequentially per the corresponding radiators, are shown on the front side. Coaxial connections are made using room-temperature con-ductive silver epoxy (H20E from Ted Pella, Inc., Catalog No. 16014), with the shield terminated on a dipole arm and the center conductor on the microstrip line (see Fig. 2). In order to eliminate parallel plate modes, one end of the coaxial shield is connected to the ground plane. Silver epoxy has considerable conductive loss at microwave frequencies compared to solder, and thus will affect the radiation efficiency of the array. In addition, epoxy contacts to the antenna elements can be brittle, causing potential disruption in current flow and affecting the radiation pattern.

The gain of the array has been measured in an anechoic chamber, exciting each 1 GHz element separately. The thirty high-band elements are measured in interleaved pairs at 2 GHz using Narda 4372-2 3 dB power dividers. The elements which are not excited are terminated in 50 Ω. All the elements are assumed to be fed with equal amplitude and constant phase. The measured gain patterns of all the elements are coherently added to compute the broadside array pattern.

Fig. 11 compares the measured and simulated H -plane gain patterns for the 1 GHz array. Reasonable agreement is observed for the main lobe amplitude and beamwidth, with peak measured gain of 12 dBi and peak simulated directivity of 15.3 dBi.

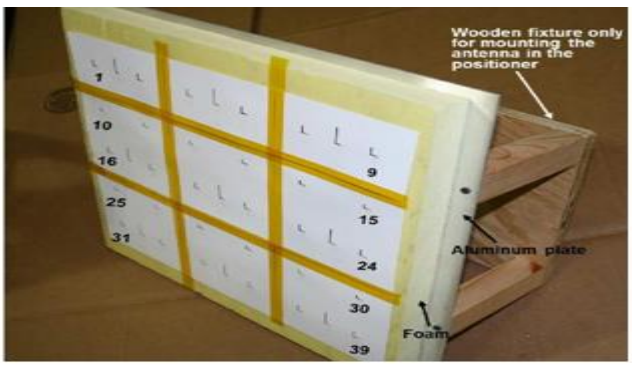

Fig. 10. Fabricated dual-band array

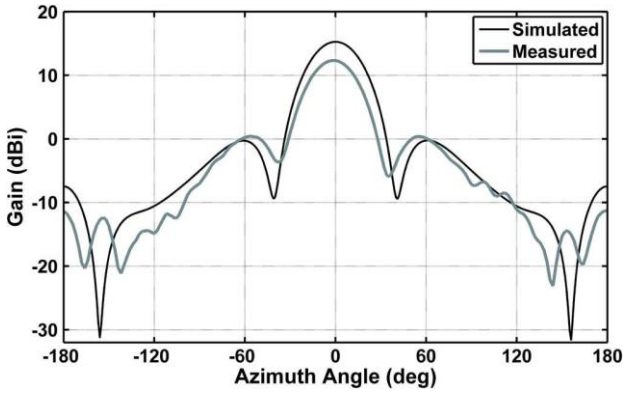

Fig. 11. Comparison of simulated and measured H-plane patterns for the 1 GHz array (9 elements)

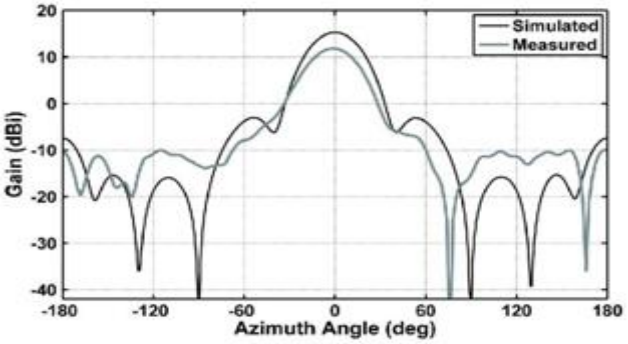

Fig. 12. Comparison of simulated and measured E-plane patterns for the 1 GHz array (9 elements)

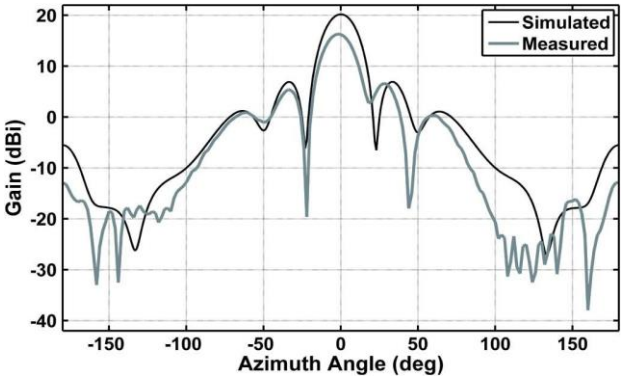

Fig. 13. Comparison of simulated and measured H-plane patterns for the 2 GHz array (30 elements)

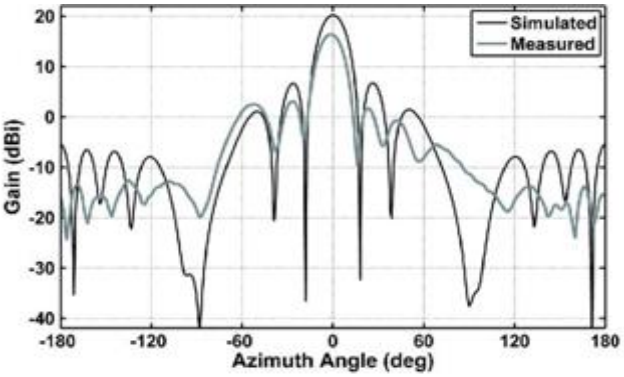

Fig. 14. Comparison of simulated and measured E-plane patterns for the 2 GHz array (30 elements)

The antenna, comprising silver epoxy ohmic loss, substrate loss, and the mismatch loss due to slight detuning of the fabricated array, are not accounted in the simulation. Gain measurement error on the large array has been estimated at ±1 dB. Fig. 12 plots the measured and simulated gain patterns for the 1 GHz array in the E-plane. A similar agreement as in the H-plane pattern is observed, with the simulated results tracking the measurements closely after taking into account the estimated antenna losses. The cross-polarization in each case is measured to be lower than -25 dB.

Before we performed pattern measurements on the 2 GHz array, we measured the frequency -dependent insertion loss of Narda 4372-2 3 dB power divider used in data collection. The frequency-averaged insertion loss over 200 MHz span, mea-sured at the two output ports, is found to be 0.76 dB. This loss is added to the measured element pattern before coherent array summation to compute the broadside fixed scan pattern.

Fig. 13 compares the measured and simulated H-plane gain patterns for the 2 GHz array, comprising 30 dipoles nested within 9 low-band dipoles (see Fig. 1). Reasonable agreement is observed for the main lobe amplitude and beamwidth, with peak measured gain of 16.2 dBi and peak simulated directivity of 20.2 dBi. This discrepancy of 4 dB is attributed to higher conductive and dielectric losses at 2 GHz compared to 1 GHz.

Fig. 14 compares the measured and simulated gain patterns for the 2 GHz array in the E-plane, showing a similar agreement as in the H -plane pattern. The cross-polarization in each case (not shown for clarity) is about 26 dB for the H-plane pattern and 22 dB for the E-plane pattern.

IV. CONCLUSION

We have presented a novel self-similar antenna design for a dual- band phased array configuration, comprising nested printed dipoles with individual feeds to independently control the element amplitude and phase in each band for adaptive beam-forming and MIMO applications. The folded dipoles are resonant at octave-separated frequency bands (1 GHz and 2 GHz), and fabricated on paper using eco -friendly, low-cost ink-jet printing technology. Each dipole is gap-fed in an un-balanced mode by voltage induced electromagnetically from a microstrip line on the other side of the substrate. The feed line includes a stub for improving the impedance match. This nested element configuration has been simulated, fabricated and measured, and excellent corroboration observed between sim-ulated and measured data. The return loss shows well-centered dual bands with 10-dB bandwidth of at least 5% for each, and measured interchannel isolation better than 15 dB. The measured copolarized element gain is about 5.3 to 7 dBi in the two prin-cipal planes, with cross-polarization less than 25 dBi in the H-plane,and slightly higher in theE-plane. It hasbeen shown that shielding provided by the interleaved design reduces coupling between the high-band elements in the H-plane. The light-weight nested antenna elements have been integrated into the first fully functional dual-band array on paper substrate. Without the 39 mm spacer below the substrate to minimize the backlobe, the 39-element antenna array weighs less than 500 grams, and is suitable for conformal installation on unmanned aerial vehicles. The peak gain of the array at broadside has been measured to be approximately 12 dBi and 16 dBi at 1 GHz and 2 GHz, respectively, with cross-polarization better than 25 dB of inkjet printing on paper are offset by several limitations: (a) relatively high conductive and dielectric losses, (b) vias and plated-through-holes cannot be reliably fabricated using inkjet printing, and (c) considerable mechanical warping that we ob-served on a relatively small array precludes paper as an antenna substrate in array applications. Nonetheless, printing antennas on paper makes it easier to develop prototypes compared to wet etching.

REFERENCES

[1] "Multifunction antennas and antenna systems," *IEEE Trans. AntennasPropag.*, vol. 54, no. 1, Jan. 2006.

[2] R. Pokuls, J. Uher, and D. M. Pozar, "Dual-frequency and dual-po-larizationmicrostrip antennas for SAR applications," *IEEE Trans. An-tennasPropag.*, vol. 46, no. 9, pp. 1289–1296, Sep. 1998.

[3] L. L. Shafai, W. A. Chamma, M. Barakat, P. C. Strickland, and G. Séguin, "Dual-band dual-polarized perforated microstrip antennas for SAR applications," *IEEE Trans. Antennas Propag.*, vol. 48, no. 1, pp. 58–66, Jan. 2000.

[4] D. M. Pozar and S. D. Targonski, *A Shared-Aperture Dual-Band Dual-Polarized Microstrip Array*, vol. 49, pp. 150–157, Feb. 2001.

[5] X. Qu, S. S. Zhong, Y. M. Zhang, and W. Wang, "Design of an S/X dual-band dual-polarised microstrip antenna array for SAR applications," *IET Microw. Antennas Propag.*, vol. 1, no. 2, pp. 513–517, Apr. 2007.

[6] A. Rida, L. Yang, R. Vyas, and M. M. Tentzeris, "Conductive inkjet-printed antennas on flexible low-cost paper-based substrates for RFID and WSN applications," *IEEE Antennas Propagat. Mag.*, vol. 51, no. 3, pp. 13–23, Jun. 2009.

[7] Y.-L. Kuo and K.-L. Wong, "Printed double-T monopole antenna for 2.4/5.2 GHz dual-band WLAN operations," *IEEE Trans. AntennasPropag.*, vol. 51, no. 9, pp. 2187–2192, Sep. 2003.

[8] J.-Y. Jan and L.-C. Tseng, "Small planar monopole antenna with a shorted parasitic inverted-L wire for wireless communications in the 2.4, 5.2, and 5.8-GHz bands," *IEEE Trans. Antennas Propag.*, vol. 52, no. 7, pp. 1903–1905, Jul. 2004.

[9] K.-L. Wong, L.-C. Chou, and C.-M. Su, "Dual-band flat-plate antenna with a shorted parasitic element for laptop applications," *IEEE Trans.Antennas Propag.*, vol. 53, no. 1, pp. 539–544, Jan. 2005.

[10] R. L. Li, B. Pan, J. Laskar, and M. M. Tentzeris, "A novel low-profile broadband dual-frequency planar antenna for wireless handsets," *IEEETrans. Antennas Propag.*, vol. 56, no. 4, pp. 1155–1162, Apr. 2008.

[11] B. F. Wang and Y. T. Lo, "Microstrip antennas for dual-frequency op-eration," *IEEE Trans. Antennas Propag.*, vol. 32, no. 9, pp. 938–943, Sep. 1984.

[12] J.-H. Lu, "Broadband dual-frequency operation of circular patch an-tennas and arrays with a pair of L-shaped slots," *IEEE Trans. AntennasPropag.*, vol. 51, no. 5, pp. 1018–1023, May 2003.

[13] B. Lee, F. J. Harackiewicz, K.-H. Kong, J. Byun, and S.-H. Yang, "Dual-band dual-circularly polarized sector antenna for GPS and DAB systems," *Microw. Opt. Tech. Lett.*, vol. 46, no. 1, pp. 43–46, Jul. 2005.

[14] J.-F. Zürcher, A. Skrivervik, O. Staub, and S. Vaccaro, "A compact dual port, dual frequency printed antenna with high decoupling," *Microw.Opt. Tech. Lett.*, vol. 19, no. 2, pp. 131–137, Oct. 1998.

[15] P. Li, K. M. Luk, and K. L. Lau, "A dual-feed dual-band L-probe patch antenna," *IEEE Trans. Antennas Propag.*, vol. 53, no. 7, pp. 2321–2323, Jul. 2005.

[16] T.-Y. Yun, C. Wang, P. Zepeda, C. T. Rodenbeck, M. R. Coutant, M. Li, and K. Chang, "A 1–21 GHz low-cost, multi-frequency and full-duplex phased array antenna system," *IEEE Trans. Antennas Propag.*, vol. 50, no. 5, pp. 641–650, May 2002.

[17] D. C. Thompson, O. Tantot, H. Jallageas, G. E. Ponchak, M. M. Tentzeris, and J. Papapolymerou, "Characterization of liquid crystal polymer material and transmission lines on LCP substrates from 30 to 110 GHz," *IEEE Trans. Microw. Theory Tech.*, vol. 52, no. 4, pp. 1343–1352, Apr. 2004.

[18] L. Yang, A. Rida, R. Vyas, and M. M. Tentzeris, "RFID Tag and RF structures on a paper substrate using inkjet-printing technology," *IEEETrans. Microw. Theory Tech.*, vol. 55, no. 12, pp. 2894–2901, Dec.2007.

[19] M. Berggren, T. Kugler, T. Remonen, D. Nilsson, M. Chen, and P. Nor-berg, "Paper electronics and electronic paper," in *Proc. IEEE PolymersAdhesives Microelectron. Photon. Conf.*, Oct. 2001, pp. 300–303.

[20] B. Farrell and M. St. Lawrence, "The processing of liquid crystalline polymer printed circuits," in *Proc. IEEE Electron. ComponentsTechnol. Conf.*, May 2002, pp. 667–671.

[21] R. Hasse, K. Naishadham, W. H. Hunsicker, M. M. Tentzeris, and T. Wu, "Full wave analysis of a dual-frequency printed slot antenna with a microstrip feed," presented at the IEEE Antennas Propag. Symp., Toronto, ON, Canada, Jul. 2010.

[22] W. Hunsicker, K. Naishadham, and R. Hasse, "Integration of an X-band microstrip patch array and beamformer for a multifunctional antenna array," presented at the IEEE Phased Array Syst. Technol. Symp., Boston, MA, Oct. 2010.

[23] K. Hirose and H. Nakano, "Dual loop slot antenna with simple feed," *Electron. Lett.*, vol. 25, no. 18, pp. 1218–1219, 1989.

Automation of Solid Waste Bin State Management using ZIGBEE

P. Siva
Department of ECE,
PRIST University,
Thanjavur, Tamil Nadu, India.

***Abstract*— In this project proposes automatic and dynamic solid waste bin status information using integrated sensing system. It presents the implementation mainly for difficulties such as manual monitoring of solid wastages in commercial areas like shopping malls, hospitals, commercial complexes and some crowd related entertaining places. Proposed system develops sensor based automatic monitoring and detection of bin disposing the solid wastages in the regular time interval as per the dynamic information given to the management. Here using different types of sensors to analyzing the bin status in three behaviors to sends the in sequence to microcontroller from end to end ADC to relay driver and bin control using zigbee transmitter.**

Keywords—Zigbee;SWM system.

I. INTRODUCTION

An intelligen solid waste bin operates to ensure the efficient measurement of its status while consuming minimum energy. At present, main cities around the world necessitate challenging solutions for solid waste administration (SWM), as a result of increase in suburban areas and the economy. SWM is a costly urban service that consumes around 20% - 50% of municipallity's annual budget in developing countries. Furthermore, 85% of solid waste management funds are spent on waste collection and transportation. It becomes an excessive wastage of resources when bins are collected that are filled up partially.

In dissipate collection and heartrending behavior, the operational cost can be reduced by optimizing the quantity and consumption of group bins and their collection rate. Estimating the status with waste level and weight of waste inside bins help to optimize compilation routes and improve compilation competence. A SWM system having static development and routing to collect waste strain more in service costs, longer transportation distances and increased labor hours compare to a system with active development and direction-finding attitude. And the designed potential cost savings of 10-20% and transport mileage savings of 26% when vibrant scheduling and routing were used.

For a truly active and automatic system, it is important to know the current and actual fill level of a bin slightly than a prediction relays on historical fill level data, which arises questions as 'at what instance will the bin be at an sufficient fill level to stick up for collection?'. So, to realize a SWM system with dynamic homework and direction-finding for waste collection, it is very useful and important to get real time data about the bin status. more than a few researches have been done over the last few decades concerning solid waste monitoring and administration. But a few of them deal with genuine time bin position data with a motive to apply dynamic scheduling and routing approach for an habitual solid waste administration system.

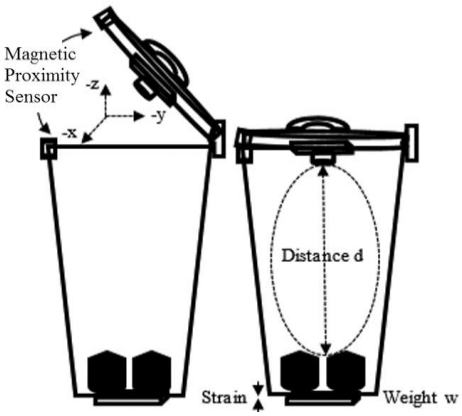

Fig.1 (a) Lid status sensing.

(b) Waste filling level and weight sensing.

II. DESIGN

As give details in the prospect chapter, the considerate of complete possible of the display board and the wireless intermediate in information transfer is the main issue that the following thesis of the following plan deals with.

we see in the more than outline, there are at least three interfacing circuit, MAX-232 with Microcontroller, LCD display with microcontroller, and MAX-232 with ZIGBEE[9] unit. Dedicating a general purpose computer at each and every site of the exhibit boards, although makes the task a lot easier but is too expensive to be a possibility.

Hence we employ PIC 16F877A microcontroller [2][4][6]. The complexity of coding substantially increases, but once programmed the module works at its robust best since it is a enthusiastic set in system and not a general purpose computer. The design procedure involves identifying and assemble all the necessary hardware and ensuring fail safe interfacing between all the components.

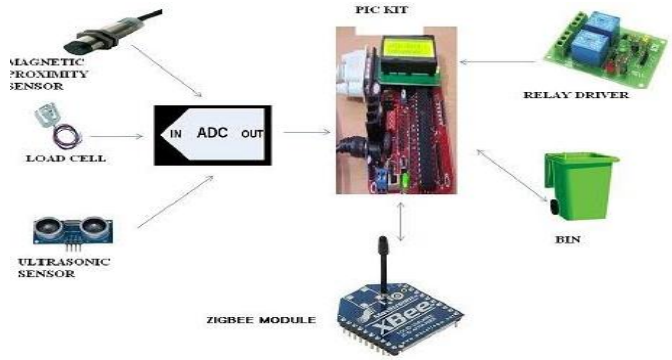

Fig 2. Architecture diagram

Therefore we utilize PIC 16F877A microcontroller. The complexity of coding substantially increases, but once programmed the module moving parts at its robust best since it is a dedicated embedded system and not a general purpose computer. The design process involves identifying and assemble all the required hardware and ensuring fail safe interfacing between all the components.

Then we have the coding procedure which has to take care of the delays between two successive transmission and most outstandingly the justification of the sender's number. The number of valid users can be more than one[7][8][9]. The limiting limitation is the RAM of the microcontroller to a certain extent than the coding complexity.

Initializations

The baud rate of the modem was set to be 4800 bps. The ECHO from the modem was turned off using the command ATE/ATE0 at the overexcited workstation[11]. For sequential broadcast and response to be possible both the DTE and DCE should have same operational baud rates. therefore to set the microcontroller on a baud rate of 4800bps, we set fatal count of regulator 1 at 0FFh (clock frequency = 1.8432). The TCON and SCON register were set consequently.

Serial transfer using TI and RI flags

After setting the baud rates of the two devices together the devices are now ready to transmit and collect data in form of characters. broadcast is done when TI standard is set and similarly data is recognized to be received when the Rx flag is set. The microcontroller then send an AT authority to the modem in form of string of font serially just when the TI standard is set. After reception of a character in the SBUF register of the microcontroller (reaction of MODEM with the understand message in its default format or ERROR communication or OK message), the RI standard is set and the received character is stimulated into the physical memory of the microcontroller.

Validity Check

After in sequence getting the characters the code then checks for start of the sender's number and then compare the number nature by character with the valid numeral pre-stored in the memory. Since we are employ just one suitable number, we are able to do the validation procedure vigorously i.e. without store the new communication in another position in the memory[10][18]. For more than one suitable information we would need more memory location to first store the total (valid/invalid) message in the memory and then do the association process.

Display

After authority check the control flow goes into the LCD plan unit to exhibit the valid communication stored in the memory. In case of multiple suitable numbers all invalid stored messages are deleted by proper branch in the code to the "apparent display" module.

Fig 3. LCD display

Fig.4 MPLAB software

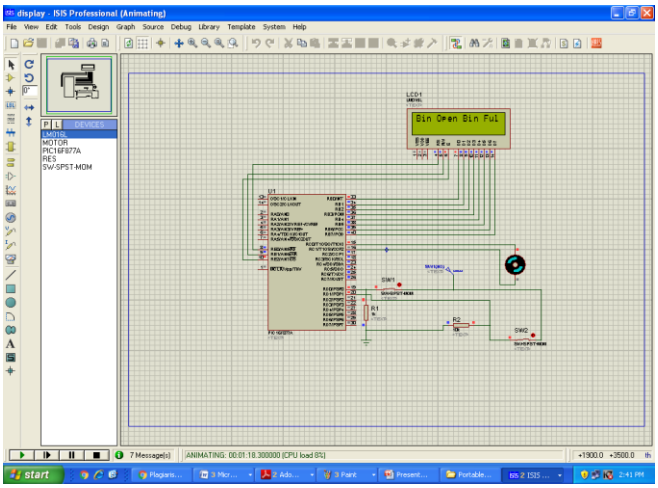

Fig 5. Software Result of the bin management system

Sensed sensor output standards are given to the ADC that converts the analog signals into digital, that digital value is given as a input of Microcontroller 16f877a. **PIC** is a

family of modified Harvard architecture microcontrollers completed by Microchip Technology, resulting from the PIC initially urban by General Instrument's Microelectronics Division. The name PIC originally referred to Peripheral Interface Controller. The primary parts of the family were available in 1976; by 2013 the corporation had ship more than twelve billion entity parts, used in a broad diversity of embedded systems.

Features of Microcontroller

Timer0: 8-bit timer/counter with 8-bit prescaler
Timer1: 16-bit timer/counter with prescaler, can be incremented during Sleep via external crystal/clock
Timer2: 8-bit timer/counter with 8-bit period register, prescaler and postscaler
Two Capture, Compare, PWM modules
Capture is 16-bit, max. resolution is 12.5 ns
Compare is 16-bit, max. resolution is 200 ns
PWM max. resolution is 10-bit
Synchronous Serial Port (SSP) with SPI™ (Master mode) and I2C™ (Master/Slave)
Universal Synchronous Asynchronous Receiver Transmitter (USART/SCI) with 9-bit address detection
Parallel Slave Port (PSP) – 8 bits wide with external RD, WR and CS controls (40/44-pin only)
Brown-out detection circuitry for Brown-out Reset (BOR)

III. SERIAL DATA COMMUNICATION

Computers must be able to communicate with other computers in modern multi-processor distributed systems. One cost-effective way to communicate is to send and receive data bytes serially. The P16F77 micro controller has serial data communication circuits that transmits and receive the data. By configuring the SPEN in RCSTA we can enable the serial communication in P16F877. Similarly by configuring the TXSTA (Transmit Status and Control Register) and RCSTA (Receive Status and Control Register) we can transmit and receive the data serially. The any date in TXREG (Transmit Register) transmit the data and the data which is in RCREG (Receive Register) is the receive data. The following figure shows the TXSTA and RCSTA.

IV. STANDARDS BASED

The foundation of every ZigBee standard and specification is the powerful IEEE 802.15.4 physical radio standard operating in unlicensed bands worldwide at 2.4GHz (global), 915Mhz (Americas) and 868Mhz (Europe). It delivers raw data throughput rates of 250Kbs at 2.4GHz (16 channels), 40Kbs at 915Mhz (10 channels) and 20Kbs at 868Mhz (1 channel). Transmission distances are remarkable for a low-power solution, ranging from 10 to 1,600 meters, depending on power output and environmental conditions, such as other buildings, interior wall types and geographic topology.

V. INTERFACING

A. *V.Interfacing*

DTE and DCE The terms DTE and DCE are very common in the data communications market. DTE is short for Data Terminal Equipment and DCE stands for Data Communications Equipment. But what do they really mean? As the full DTE name indicates this is a piece of device that ends a communication line, whereas the DCE provides a path for communication

VI. PIC MICROCONTROLLER

The term PIC, or Peripheral Interface Controller, is the name given by Microchip Technologies to its single – chip microcontrollers. These devices have been phenomenally successful in the market for many reasons, the most significant ones are mentioned below. PIC micros have grown in steadily in popularity over the last decade, ever since their inception into the market in the early 1990s. PIC micros have grown to become the most widely used microcontrollers in the 8- bit microcontroller segment. The PIC16F877 is 40 pin IC. There are six ports in this microcontroller. Namely PORT A, PORT B, PORT C, PORT D and PORT E. Among these ports PORT B, PORT C and PORT D contains 8-pins, where PORTA contains 6-pins and PORT E contains 3-pins.

VI. SOFTWARE TOOLS

ProteusISIS7 is used to run the MPLAB coding. Result of the bin management system is shown in fig. above. Figure shows the output as a form of LCD Display[6][7]. There are 3 sensors are used that is Weight sensor, Magnetic proximity sensor, Ultrasonic sensor. Weight sensor is used to sense the fill level of dusts and Magnetic proximity sensor is used to sense the lid position whether it is open or close and Ultrasonic sensor is used to sense the distances. An ultrasonic sensor transmit ultrasonic influence from its sensor skull and once more receives the ultrasonic waves reflect from an item.

VII. CONCLUSION

This is a exclusive effort which integrate accelerometer, magnetic proximity, ultrasonic and mass sensing methodologies respectively. The integrated sensing system is calculated by rule-based conclusion procedure to offer a proficient and repeated bin status monitor system. The vital end is the algorithm which synthesize bin operative situation, its lid category, time threshold and weighted down status sensitivity. The operation of the system is assess by a number of check run. The algorithm with the intellect scheme has lead to an clear bin which is very well-organized for solid waste organization automation.

REFERENCES

[1] P. H. Brunner and J. Fellner, "Setting priorities for waste management strategies in developing countries," *Waste Manage. Res.*, vol. 25, no. 3, pp. 234–240, Jun. 2007.
[2] T. Kulcar, "Optimizing solid waste collection in Brussels," *Eur. J. Oper. Res.*, vol. 90, no. 1, pp. 71–77, 1996.

[3] M. Faccio, A. Persona, and G. Zanin, "Waste collection multi objective model with real time traceability data," *Waste Manage.*, vol. 31, no. 12, pp. 2391–2405, 2011.

[4] L. A. Guerrero, G. Maas, and W. Hogland, "Solid waste management challenges for cities in developing countries," *Waste Manage.*, vol. 33, no. 1, pp. 220–232, 2013.

[5] H. Krikke, I. L. Blanc, M. van Krieken, and H. Fleuren, "Low-frequency collection of materials disassembled from end-of-life vehicles: On the
value of on-line monitoring in optimizing route planning," *Int. J. Prod. Econ.*, vol. 111, no. 2, pp. 209–228, 2008.

[6] O. M. Johansson, "The effect of dynamic scheduling and routing in a solid waste management system," *Waste Manage.*, vol. 26, no. 8, pp. 875–885, 2006.

[7] F. McLeod *et al.*, "Dynamic collection scheduling using remote asset monitoring: Case study in the UK charity sector," *Transp. Res. Rec., J. Transp. Res. Board*, vol. 2378, no. 1, pp. 65–72, 2013, doi: 10.3141/2378-07. AL MAMUN *et al.*: INTEGRATED SENSING SYSTEMS AND ALGORITHMS 567.

[8] M. Hannan, M. Arebey, R. A. Begum, and H. Basri, "Radio frequency identification (RFID) and communication technologies for solid waste bin and truck monitoring system," *Waste Manage.*, vol. 31, no. 12,pp. 2406–2413, 2011.

[9] M. Arebey, M. A. Hannan, H. Basri, and H. bdullah, "Solid waste monitoring and management using RFID, GIS and GSM," in *Proc. IEEE*
Student Conf. Res. Develop. (SCOReD), Nov. 2009, pp. 37–40.

[10] A. Rovetta, F. Xiumin, F. Vicentini, Z. Minghua, A. Giusti, and H. Qichang, "Early detection and evaluation of waste through sensorized containers for a collection monitoring application," *Waste Manage.*,vol. 29,no.12,pp.2939–2949,2009.

[11] M. Faccio, A. Persona, and G. Zanin, "Waste collection multi objective model with real time traceability data," *Waste Manage.*, vol. 31, no. 12, pp. 2391–2405, 2011.

[12] S. Longhi *et al.*, "Solid waste management architecture using wireless sensor network technology," in *Proc. 5th IEEE Int. Conf. New Technol.,Mobility Secur. (NTMS)*, May 2012, pp. 1–5.

[13] M.-H. Tsai, Y.-C. Liu, and W. Fang, "A three-axis CMOS-MEMS accelerometer structure with vertically integrated fully differential sensing electrodes," *J. Microelectromech. Syst.*, vol. 21, no. 6, pp. 1329–1337, 2012.

[14] M. J. Caruso, T. Bratland, C. H. Smith, and R. Schneider, "A new perspective on magnetic field sensing," *Sensors-Peterborough*, vol. 15, pp. 34–47, Dec. 1998. [15] A. Carullo and M. Parvis, "An ultrasonic sensor for distance measurement in automotive applications," *IEEE Sensors J.*, vol. 1, no. 2,pp. 1–143, Aug. 2001.

[15] C. Huddleston, "Sensor application-pressure and load sensors," in *Intelligent Sensor Design Using the Microchip DsPIC*. Amsterdam, The Netherlands: Elsevier, 2006, pp. 209–227.

[16] (Mar. 24, 2014). *Waspmote*. [Online]. Available: http://www.libelium. com/products/waspmote/

[17] (Mar. 24, 2014). LIS331DLH, MEMS Digital Output Motion Sensor Ultra Low Power High Performance 3-Axes 'Nano' Accelerometer.

[18] [Online]. Available: http://www.st.com/web/en/resource/technical/document/datasheet/CD0 0213470.pdf

[19] (Mar. 24, 2014). *PLA41201, Magnetic Proximity Sensor*. [Online].Available: http://www.wce-electronics.com/

[20]] (Mar. 24, 2014). *XL-MaxSonar- WR/WRC Series, High Resolution,IP67 Weather Resistant, Ultra Sonic Range Finder*. [Online].Available: http://www.maxbotix.com/documents/XL-MaxSonar-WR _Datasheet.pdf

[21] (Mar. 24, 2014). *AMS Load Sensor*. [Online]. Available: http:// china-hanyu.en.alibaba.com/product/201058465-00005013/AMS_ load _sensor.html.

Design and Implementation of Function Generator Prototype by Additive, Subtractive Manufacturing and Programming

J. Archana*
Department of Control & Instrumentation,
Valliammai Engineering College,
Chennai-603203, Tamil Nadu,
India.

S. Gomathi
Department of Control & Instrumentation,
Valliammai Engineering College,
Chennai-603203, Tamil Nadu,
India.

T. Meenakshi
Department of Control & Instrumentation,
Valliammai Engineering College,
Chennai-603203, Tamil Nadu,
India.

***Abstract*— In new product development, time to market (TTM) is critical for the success and profitability of next generation products. In general, most of the time has been spent in manufacturing phase to develop a prototype. In current method of prototype time taken on waiting for required prototype to be send back to the user. If any bugs occur in the prototype that has to be debugged and the process is repeated until the required quality has been achieved. The aim of this project is to reduce the time taken for developing the prototype by using additive, subtractive manufacturing and Microcontroller programming. The manufacturing techniques of 3D printing, CNC machining, Circuit builder are integrated. CNC machine are inherently more precise and accurate. It is a technology which aims to generate and execute sequential actions that describes the behavior of the end effector. By combining the above processes, we can achieve the required prototype in lesser time.**

Keywords*— *Additive, subtractive manufacturing

I. INTRODUCTION

A new product typically undergoes several transformations before becoming available for sale to the general public. A new device idea is initially prototyped in order to evaluate the fit and finish of the mal part as well as to optimize the fabrication process to identify difficulties in manufacture. These steps can be time-consuming and expensive, creating a significant obstacle for new product introductions especially for starts that may not have the appropriate, usually expensive, machining equipment required for prototyping. Additive Manufacturing (AM) was introduced in the late1980's in order to rapidly prototype structures and allow manufacturers to circumvent the lengthy process of traditional prototyping by providing either a scaled down or full-scale mechanical replica of the designed product.

These devices were typically only conceptual models due to limitations of the AM technologies in which compromises were made in terms of material choices, surface finish and dimensional accuracies.AM technology continues to advance in terms of material properties and minimum features sizes, the technology until recently has remained best suited for manufacturing prototypes for conceptual modelling relegated to only satisfying the need for evaluation of form and of the device casing or structural features.

A CNC router is a CNC router tool that shapes an object. The CNC works on the Cartesian coordinate system (X, Y, Z) for 3D motion control. Parts of a project can be designed in the computer with a CAD/CAM program, and then cut automatically(SM) using a router or other cutters to produce a finished part. In this project, driller machine acts and performs the operation of CNC router. It subtracts the waste materials and shape an object. It moves along its axial direction of X, Y, Z which is directed by programmed Arduino board.

II. BASIC WORKING PRINCIPLE

First, confirm that you have the correct template for your paper size. This template has been tailored for output on the A4 paper size. If you are using US letter-sized paper, please close this file and download the file "MSW_USltr_format".

A. 3D printer, circuit builder

Though typical methodologies like clay models, one-off samples handmade by skilled craftsmen, and more recently AM technologies have largely addressed the need for prototype these types of parts have been exclusively made to test appearance and of the completed part. When the device included sophisticated electronics, these methodologies could not address the need for prototyping a fully functional part.

AM process can fabricate prototypes that will enable at least a comprehensive evaluation of the design, not only for form and appearance, but also for electronics functionality simultaneously. Although this new manufacturing technology allows for more complete evaluations with high fidelity prototypes, substantial challenges remain. The area of electronics design (e.g. schematic capture, simulation, and physical implementation of printed circuit boards _ PCBs) includes mature, commercially available software packages that allow for component placement and routing of wires to create electrical interconnects on a PCB. These programs however, operate under the assumption of the workspace being a two-dimensional surface for the circuit based on traditional PCB manufacturing.

As a result, the component placement and routing for 3D printed designs has been done manually in 3D space using mechanical engineering CAD software like Solid Works without the inherent features for electronics functionality. This lack of software support has relegated.

For circuit builder, conductive ink is used as an input into extruder to draw the path as designed in the EAGLE CAD software.

B. CNC Mechanism

CNC (Computerized Numeric Control) Machining has been widely used in manufacturing industry for many years. Most of the standardized codes (G and M Codes) and CAM (Computer Aided Manufacturing) software have made its application and learning processes easier. Machining of very complex shapes is only possible with CNC machines. Therefore not only in the industry but also in the education sector, CNC is becoming an integral part of manufacturing courses in most of the universities worldwide.

A CNC router is a computer controlled cutting machine related to the hand held used for cutting various hard materials, such as wood, composites, aluminium, steel, plastics, and foams. CNC stands for computer numerical control. CNC routers can perform the tasks of many carpentry shop machines such as the panel saw, the spindle moulder, and the boring machine. A CNC router is very similar in concept to a CNC milling machine. Instead of routing by hand, tool paths are controlled via computer numerical control. The CNC router is one of many kinds of tools that have CNC variants.

A CNC router typically produces consistent and high-quality work and improves factory productivity. Unlike a jig router, the CNC router can produce a one-off as effectively as repeated identical production. Automation and precision are the key benefits of CNC router tables. CAM software makes the CAD drawing/design into a code called g-code. This code the CNC machine can understand. In short, CNC technology is not very complicated. It is a tool controlled by a computer. It only becomes more sophisticated when considering how the computer controls the tool. The illustration shows what a bare bones CNC machine might look like without its controller.

Applications

A CNC router can be used in the production of many different items, such as door carvings, interior and exterior decorations, wood panels, sign boards, wooden frames, moldings, musical instruments, furniture, and so on. In addition, the CNC router helps in the thermoforming of plastics by automating the trimming process. CNC routers can help ensure part repeatability and sufficient factory output.

C. Micro controller

A typical embedded system involves both hardware and software components. The hardware may include sensors and actuators, while the software is used to control these hardware modules. For example, to implement an auto-pilot system, we can apply camera to locate the road markings and motors to drive the robot. The software written should process signals received from the camera and then produce a proper output to control the actuators so that the robot can follow a path.

The initial stages of the operation mechanism are defining the input and output modules included in the current design. The system will provide a list of available I/O components for the user to select and the user only need to input information regarding the port and pin number that the component is connected to; all these are through a graphical user interface (GUI). Once the I/O components have been defined, the next step which is optional, user can also define the initial operation to be performed when powered is on. The next step is most important; it allows the user to relate the action to be performed.

Hardware modules

The hardware components do not require special design consideration provided that they can be interfaced with the I/O ports of the processor. On the other hand, the software of the system is more significant and is presented in the next section.

The software system

The major role of the software component is to assist students to develop a proper C language program for the ADuC832 processor so that control of the input/output devices can be achieved. Based on the design of a similar system [4], which was tailored for assembly language programming, we had identified the following design criteria:

1) User-friendliness;
2) Proper support of hardware modules; and
3) Able to produce the correct C program.

In order to make the system user-friendly, a graphical user interface (GUI) based on the Windows Forms programming is adopted as it is easy to implement and maintain.

D. Function generator prototype

A function generator is usually a piece of electronic test equipment used to generate different types of electrical waves over a wide range of frequencies. This prototype of function generator can generate the waves of sine, triangle and square. It is the prototype of mobile function generator in which 5v battery is placed on the top and it is acts as a power source. The tuner for amplitude and frequency is taken on the both sides of the prototype. By using the probe connection the waves are finally displayed in CRO. PIC16F876 is placed inside the function generator, where it is already programmed and stored in Micro controller programmer kit.

III. MATHEMATICAL MODEL

Transfer function for stepper motor

$$\frac{C(S)}{R(S)} = \frac{\omega_n^2}{+2\varepsilon\omega_s}$$

$\omega_n - undamped\ frequency$

S -- Variable
ε -- damping ratio

Transfer function for CNC router

$$\frac{C(S)}{R(S)} = \frac{1}{TS}$$

T – Time variant
S – Variable

Transfer function heater

$$\frac{C(S)}{R(S)} = \frac{T_2 S}{1 + T_1 T_2 S}$$

$T_1 - Heater$
$T_2 - Thermistor$
$T_1 T_2$ - Time taken to reach 0.632 times the final value
S – Variable

Laplace transform stepper motor for step signal

$$\frac{\omega_n^2}{s^2 + 2\varepsilon\omega_n} = \frac{A}{s} + \frac{B}{s^2} + \frac{C}{s + 2\varepsilon\omega_n}$$

$$A(S)(S + 2\varepsilon\omega_n) + B(S + 2\varepsilon\omega_n) + CS^2 = {\omega_n}^2$$

$$(A + C)S^2 + (2A\varepsilon\omega_n + B)S + 2B\varepsilon\omega_n = \omega_n^2$$

$$2B\varepsilon\omega_n = \omega_n^2$$

$$B = \frac{\omega_n}{2\varepsilon}$$

$$2A\varepsilon\omega_n + \frac{\omega_n}{2\varepsilon} = 0$$

$$A = \frac{-1}{4\varepsilon^2}$$

$$C = \frac{1}{4\varepsilon^2}$$

$$C(s) = \frac{\frac{-1}{4\varepsilon^2}}{s} + \frac{\frac{\omega_n}{2\varepsilon}}{s^2} + \frac{\frac{1}{4\varepsilon^2}}{s + 2\varepsilon\omega_n}$$

Router for step signal

$$\frac{C(S)}{R(S)} = \frac{K_p}{TS} \qquad C(s) = \frac{K_p}{Ts^2}$$

Heater for step signal

$$\frac{C(S)}{R(S)} = \frac{\frac{K_p}{TS}}{1 + \left({}^{K_p}/_{T_1 S}\right)\left({}^{1}/_{T_1 S}\right)}$$

$$= \frac{\frac{K_p}{T_1 S}}{\frac{T_1 T_2 S^2 + K_p}{T_1 T_2 S^2}}$$

$$= \frac{K_p T_2 S}{T_1 T_2 S^2 + K_p}$$

$$C(S) = \frac{1}{S} \frac{K_p T_2 S}{T_1 T_2 S^2 + K_p}$$

$$C(S) = \frac{K_p T_2}{T_1 T_2 S^2 + K_p}$$

Inverse Laplace transform

$$C_1(t) = \frac{-1}{4\varepsilon^2} + \frac{\omega_n}{2\varepsilon}(\sin 0^2) + \frac{1}{4\varepsilon^2} e^{-2\varepsilon\omega_n}$$

$$C_1(t) = \frac{-1}{4\varepsilon^2} + \frac{1}{4\varepsilon^2} e^{-2\varepsilon\omega_n}$$

$$C_2(t) = t\frac{K_p}{T}$$

$$C_3(t) = \frac{{}^{K_p T_2}/_{T_1 T_2}}{s^2 + ({}^{K_p}/_{T_1 T_2})}$$

$$C_3(t) = T_2 \sin(\sqrt{K_p T_1 T_2})t$$

IV. SIMULATION AND RESULTS

Block 1 Data Acquisition

In this data acquisition block, the G code file is acquired from the file. Then the file is split into different entities for future processing. After that, based on type of interpolation the data is split.

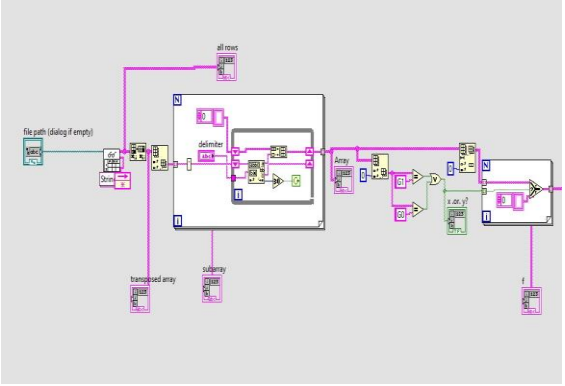

Block 2 Value Allocation

After the completion of data acquisition, the next step is to use this semi processed data to run the stepper motors and other actuators. This is done by segregation of data based on the path actuator connected, interpolation being used and feed rate in G code. The output is in integer array form.

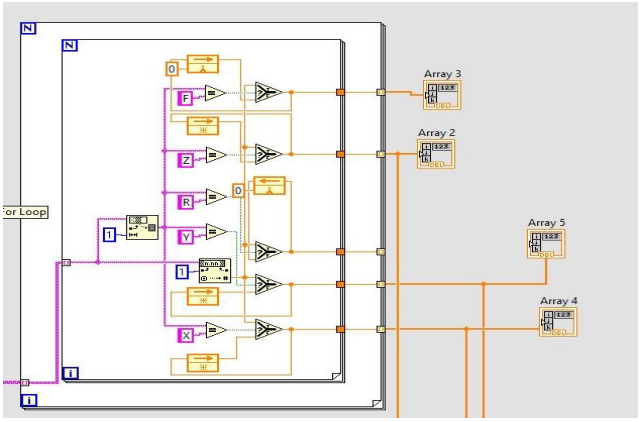

Block 3 Control and simulation loop for output

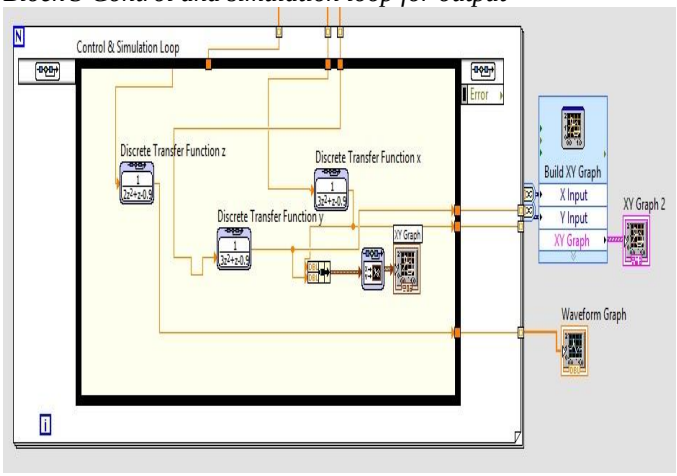

Here the processed data which is in integer form is given as input. This input is given to simulation equivalent of actuator based on their transfer function. The output is plotted on XY graph and waveform graph. The movement in X and Y axes are plotted on XY graph. The movement in Z axis is plotted in waveform graph.

Output 1 Output for the word-HELLO

From the above description, for the word HELLO the axes of XY is plotted in XY graph and Z axes is taken in waveform graph.

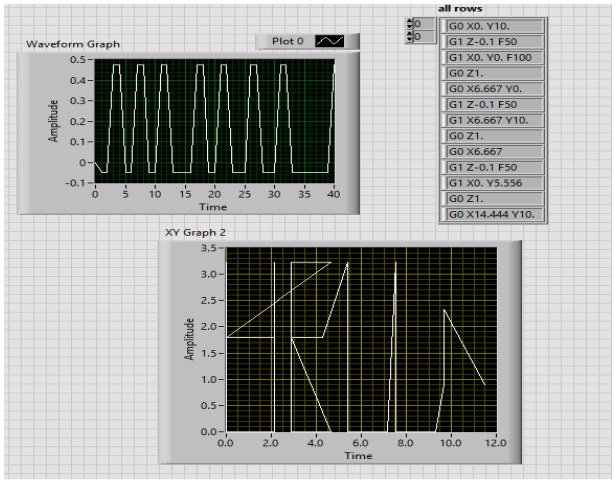

Output 2 Output for the word-archana

From the above description, for the word archana the axes of XY is plotted in XY graph and Z axes is taken in waveform graph.

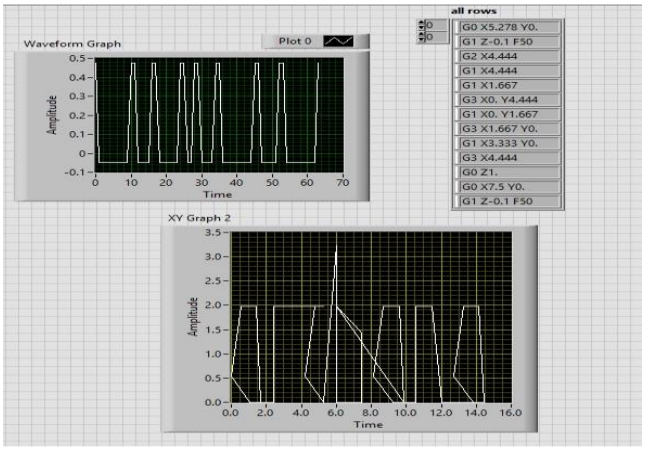

V. RESULTS AND DISCUSSION

The aim of this project is to reduce the time taken to develop a prototype. It makes use of additive manufacturing, subtractive manufacturing and Microcontroller programming. The simulation part is being completed in LABVIEW 2013 software. In this simulation, the simulated mechanical movement of 3D printer, CNC router and circuit builder is being done in all 3 axes. The output of this simulation is plotted in the XY graph and Z axis is in waveform graph. Then the transfer function is taken for all actuators and net transfer function of the control system design is calculated.

REFERENCES

[1] Jovitha Jerome, "Virtual instrumentation LAB VIEW" 2010, 2013.

[2] Eric MacDonald, Rudy Salas, David Espalin, Mireya Efrain,Aguilera, Dan Muse and Ryan B. Wicker,"3D Printing for the Rapid Prototyping of Structural Electronics",vol. 7, pp. 181-194,2014.

[3] D.Espalin, D. W. Muse, F. Medina, E. MacDonald, and R. B. Wicker, "3D Printing multi-functionality: Structures with electronics", vol.3 170-192, Mar. 2014.

[4] D.Periard, E.Malone,"A System to Assist the Learning of Embedded Microprocessor Programming", IEEE 2014.

[5] Hassan Iqbal, Anwar. K. Sheikh, and M. Abdul Samad. "Introducing CAD/CAM and CNC machining by using a feature based methodology in a manufacturing lab course, a conceptual frame work" No.5,pp. 726-732,IEEE 2014.

[6] R. Olivas, R. Salas, D. Muse, E. MacDonald, and R. Wicker, "Structural electronics through additive manufacturing and micro-dispensing, "Proc. IMAPS Nat. Conf., 2010, pp. 940-946.

Simulation of Vehicle Adhoc NET Work (VANET) using Network Simulator (NS-2) Tools

S. Sridharan
Department of Computer Science and Engineering,
University College of Engineering Thirukkuvalai,
Nagappattinam, Tamil Nadu, India.

S. Ramprakash*
Department of Computer Science and Engineering,
University College of Engineering Pattukkottai,
Thanjavur, Tamil Nadu, India.

***Abstract*— In this paper we have discussed about the number of automobiles that has been increased on the road in the past few years. Due to high density of vehicles, roadaccident is increasing. The vehicular safety application should be thoroughly tested before it is deployed in a real time use. Simulator tool has been preferred over Adhoc networks experiment because it simple, easy and cheap. VANET requires that a network simulator(NS-2) should be used together to perform this test. Many tools exist for this purpose but most of them have the problem with the proper interaction. In this paper we present a tool SUMO, MOVE that allows users to easily generate real world mobility models for VANET simulations. MOVE tool is built on top of SUMO which is open source micro-traffic simulator. Output of MOVE is a real world mobility model and can used by NS-2.**

***Keywords*— Road safety; Vanet; Sumop; Move.**

I. INTRODUCTION

Vehicular ad hoc network (VANET) is a vehicle to vehicle (Inter-vehicle communication-IVC) and roadside to vehicle (RVC) communication system.

The network is put forth with the novel objectivesof providing safety and comfort related services to vehicle users.[1] Collision warning,traffic congestion alarm, lane-change warning, road blockade alarm (due to construction works etc.) are among the major safety related services addressed by VANET. Vehicular Ad hoc networks (VANETs) are a special type of mobile ad hoc networks; where vehicles are simulated as mobile nodes. VANET contains two entities: access points and vehicles, the access points are fixed and usually connected to the internet, and they could participate as a distribution point for vehicles [1]. VANET addresses the wireless communication between vehicles (V2V), and between vehicles and infrastructure access point (V2I). Vehicle to vehicle communication (V2V) has two types of communication: one hop communication (direct vehicle to vehicle communication), and multi hop communication (vehicle relies on other vehicles to retransmit). VANET also has special characteristics that distinguish it from other mobile ad hoc networks; the most important characteristics are: high mobility, self-organization, distributed communication, road pattern restrictions, and no restrictions of network size.In the other category of comfortrelated services, vehicle users are equipped with Internet and Multimedia connectivity. VANET, therefore, has brought a lot of promises as a powerful and attractive emerging technology for the future. However, to meet this communication network successful, the data flow needs to be real time and interrupt-free. This has brought several research challenges in the communication field[1]. High mobility of vehicles, uncertainty in prediction of vehicle speed and direction, traffic density are some of the key issues that make VANET different from other ad hoc network and its operation.

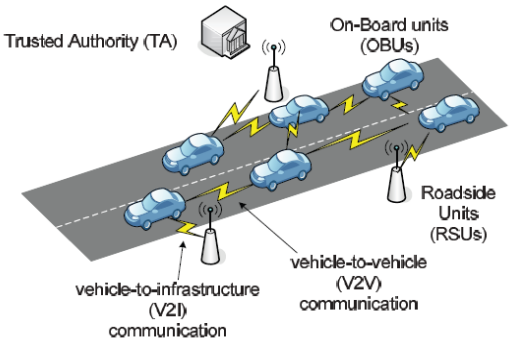

Fig. 1. Overview of vanet

The past few years the research work is going on mobile ad-hoc networks also called MANETS. Mobile ad-hoc network allow a mobile node to communicate in one to one and one to many nodes without any predefined infrastructure.[1] The required protocols to support MANET are more complex as compared to other non-mobile networks because due to mobility there is no predefined infrastructure or topology of MANET. VANET is a unique type of network which comes under the umbrella of MANET. VANET has some predefined basics which includes (1) Predictable mobility of vehicles because movement is in two directions only (2) The transmission mode is often broadcast (3) The power available is sufficient [2]. There are two communication modes which are vehicle to vehicle and vehicle to network infrastructure.

II. RELATED WORK

VEHICULAR Ad-Hoc Network (VANET) communication has recently become an increasingly popular research topic in the area of wireless networking as well as the automotive industries. While it is crucial to test and evaluate protocol implementations in a real world environment, simulations are still commonly used as a first step in the protocol development for VANET research.

Several communication networking simulation tools already existed to provide a platform to test and evaluate network protocols, such as ns-2. However, these tools are designed to provide generic simulation scenarios without being particularly tailored for applications in the transportation environment. On the other hand, in the transportation arena, simulations have also played an important role. A variety of simulation tools such as PARAMICS (P. M. T. Simulation, 2009), CORSIM (CORSIM, 2009) and VISSIM (P. simulation VISSIM, 2009) etc have been developed to analyze transportation scenarios at the micro- and macro-scale levels. However, there was little effort in integrating communication techniques and scenarios in a realistic transportation simulation environment.

III. VANET SIMULATION PROBLEM

VANET integrates on the multiple ad-hoc networking technologies. In VANET helps in defining the safety measures in the vehicles, streaming communication between different vehicles, infotainment and telematics. Vehicular Ad-hoc Networks are expected to implement a variety of wireless technologies like Dedicated Short Range Communications (DSRC) which is a type of WiFi. Vehicular Ad-hoc Networks can be viewed as component of the Intelligent Transportation Systems (ITS).

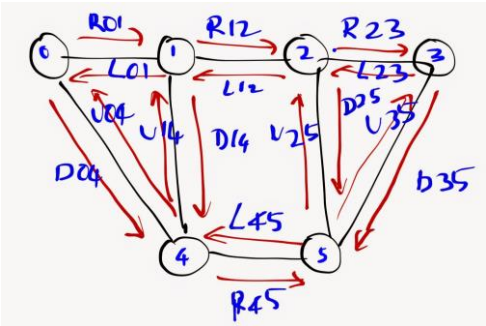

Fig. 2. My Own Road with Traffic Problems

The above diagram shows there are 6 junctions (0 to 5) and the Traffic signals are at 1,2,4 and 5. There are roads connecting the junctions. Each Road has two lanes named R for Right, L for Left, U for Up and D for down. R12 indicates a lane from 1 to 2 and L12 indicates 2 to 1.

A. Sumo

Simulation of Urban Mobility", or "SUMO" for short, is an open source, microscopic, multi-model traffic simulation. It allows to simulate how the given traffic demand that is consists of single vehicles moves through a given roadmap. The simulation allows addressing a large number of set of traffic management topics. It is purely microscopic in nature: each vehicle is modelled explicitly, has its own route, and moves individually through the network. After having generated a network, one could take the look at it with the help of SUMO-GUI, but no cars would be driving around. One must need some kind of description about the vehicles. We can it as his the traffic demand.The development of SUMO started in the year 2000. The major reason for the development of an open source, microscopic road traffic simulation was to support the traffic research community with a tool with the ability to implement and evaluate own algorithms. The tool has no need for regardingall the needed things for obtaining a complete traffic simulation such as implementing and/or setting up methods for dealing with road networks, demand, and traffic controls. By supplying such a tool, the DLR wanted to i) make the implemented algorithms more comparable by using a common architecture and model base, and ii) gain additional help from other contributors. Two major design goals are approached: the software shall be fast and it shall be portable. Due to this, the very first versions were developed to be run from the command line only - no graphical interface was supplied at first and all parameter had to be inserted by hand. This should increase the execution speed by leaving off slow visualization. Also, due to these goals, the software was split into several parts. Each of them has a certain purpose and must be run individually. This is something that makes SUMO different to other simulation packages where, for instance, the dynamical user assignment is made within the simulation itself, not via an external application like here. This split allows an easier extension of each of the applications within the package because each is smaller than a monolithic application that does everything. Also, it allows the usage of faster data structures, each adjusted to the current purpose, instead of using complicated and ballast-loaded ones. Still, this makes the usage of SUMO a little bit uncomfortable in comparison to other simulation packages. As there are still other things to do, we are not thinking of a redesign towards an integrated approach by now.A **SUMO network file** describes the traffic-related part of a map, the roads and intersections the simulated vehicles run along or across. At a coarse scale, a SUMO network is a directed graph.

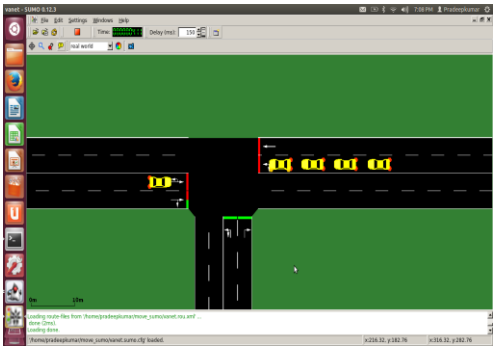

Fig. 3. Simulation for SUMO

B. Move

A key component for VANET simulations is a realistic vehicular mobility model that ensures conclusions drawn from simulation experiments will carry through to real deployments. However, VANET simulations raise many new questions about suitable levels of details in simulation models for nodes mobility. In VANET simulations, the mobility models used affect strongly the simulation output. The researchers need to decide what level of details are required for their simulations. In this chapter, the authors introduce a tool MOVE that allows users to rapidly generate realistic mobility models for VANET simulations. MOVE is built on

top of an open source micro-traffic simulator SUMO. The output of MOVE is a realistic mobility model and can be immediately used by popular network simulators such as ns-2 . The authors show that the simulation results obtained when using a realistic mobility model such as MOVE are significantly different from results based on the commonly used random waypoint model. In addition, the authors evaluate the effects of details of mobility models in three case studies of VANET.

C. Node

All nodes have at location (x- and y-coordinate, describing distance to the origin in meters) and an id for future reference. Thus our simple node file looks as follows.

```
<nodes>
<node id="1" x="-250.0" y="0.0" />
<node id="2" x="+250.0" y="0.0" />
<node id="3" x="+251.0" y="0.0" />
</nodes>
```

Fig. 3. Node Creation in Move

IV. EVALUATION

We evaluate the impact of mobility models generated by MOVE on the performance of ad-hoc routing protocol. We compare the performance of AODV when used with the random waypoint model to that using the MOVE mobility model. The simulation experiments were carried out in **NS-2 version 2.35 on UBUNTU 20** operating system. Each simulation lasts for 900 seconds. We generated scenarios for 150 nodes moving in an area of 4 square kilometers. The number of source nodes from 10 to 50, each of which is a CBR traffic source transmitting UDP packets of a size 64 bytes at the rate of 4 packets per second. All nodes use 802.11 MAC operating at 2Mbps. We used a path loss exponent 2.56 with standard deviation 4.0 based on real world measurement data from an inter-vehicle experiment.

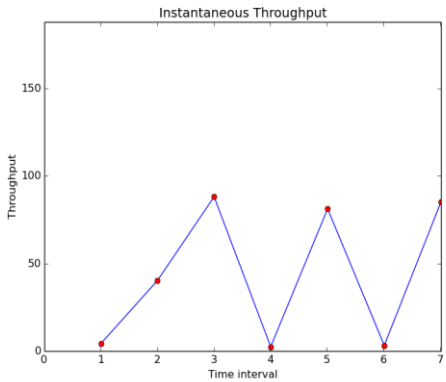

Fig. 4. Performance Results

Here the performance of the Packet Instantaneous throughput

1.00261	4.10974
2.00473	40.203
3.00628	88.1189
4.00641	2.37571
5.0128	81.2089
6.01384	3.11677
7.01836	85.318

Packet Delivery Ratio
GeneratedPackets = 1

ReceivedPackets = 56373

Packet Delivery Ratio = 5637300

Total Dropped Packets = 0

Each data point represents the average of six runs and the error bars represent the range of observed packet delivery ratios. Overall, the packet delivery ratios increase as the number of traffic sources increases, which suggest a higher density of nodes can increase the network performance as long as the increasing density does not create more radio interference. The packet delivery ratios when using MOVE mobility models are lower than when using Random Waypoint model and have larger variations. The larger variance in MOVE data points is possibly due to unstable network connectivity imposed by constrained node movements by roads and traffic control mechanisms.

V. CONCLUSION

One of the most important parameters in simulating ad-hoc networks is the node mobility. It is important to use a realistic mobility model so thatresults from the simulation correctly reflect the real-world performance of a VANET.By using SUMO and MOVE simulation software in Network Simulator -2,We gurantee that we can able to minimizing the Road Accidents and improving Road Safety to the users.

REFERENCES

[1] RaminKarimi, NorafidaIthnin ,ShukorAbdRazak and Sara Najafzadeh, “Non DTN Geographic Routing Protocols for Vehicular Ad Hoc Networks,”*International Journal of Computer Science Issues (IJCSI)*, vol. 8, Issue 5, no. 3, September 2011.

[2] Bijan Paul, Mohammed J. Islam, “Survey over VANET Routing Protocols for Vehicle to Vehicle Communication,”*IOSR Journal of Computer Engineering (IOSRJCE)*, ISSN: 2278-0661, ISBN: 2278-8727 vol. 7, Issue 5 (Nov-Dec. 2012), pp. 01-09.

[3] Vijayalaskhmi M., Avinash Patel, LinganagoudaKulkarni, “QoS Parameter Analysis on AODV and DSDV Protocols in a Wireless Network,” *International Journal of Communication Network & Security*, vol. 1, no. 1, 2011.

[4] Si Ho Cha1, Min-Woo Ryu and Kuk-Hyun Cho, "A Survey of Greedy Routing Protocols for Vehicular Ad Hoc Networks," *Smart Computing Review*, vol. 2, no. 2, April 2012.

[5] M. W. Ryu, S. H. Cha, J. G. Koh, S. Kang and K. H. Cho, “Position-based routing algorithm for improving”.

[6] OPNET Simulator. http://www.opnet.com/.Pamramics: Microscopic traffic Simulation. http://www.paramics-online.com/

[7] Pamramics: Microscopic traffic Simulation. http://www.paramics-online.com/.Ye, Deborah Estrin, and Ramesh Govindan. Effects of detail in wireless network simulation. In Proc. Of Communication Networks and Distributed Systems Modeling and Simulation Conference, January 2001.

[8] F. K. Karnadi, Z. H. Mo, and K. c. Lan, "Rapid generation of realistic mobility models for vanet," in IEEE WCNC, 2007, pp. 2506–2511

[9] reliability of inter-vehicle communication,"Transactions on Internet and Information Systems (TIIS), vol. 5, no. 8, Aug. 2011. urlhttp://freepatentsonline.com/article/KSII-Transactions-Internet-Information-Systems/272246267.html.

[10] James. JongHyukPark, Victor C.M. Leung, Cho-Li. Wang and TaeshikShon, "Future Information technology, Applications, and Services", FutureTechSpringer,vol. 1, pp. 82-98, 2012, urlhttp://books.google.com/books?id=pggzUBASE4IC&printsec=copyright#v=onepage&q&f=false.

[11] Akhtar Husain, Ram Shringar Raw, Brajesh Kumar and AmitDoegar, "Performance Comparison of Topology and Position Based Routing Protocols in Vehicular Network Environments", International Journal of Wireless & Mobile Networks (IJWMN), vol. 3, no. 4, August 2011.